Vacuolar Protein Sorting in Yeast: Characterization of Mutants and Identification of a Protein Required for Vacuole Biogenesis

Thesis by

Lois Margaret Banta

In Partial Fulfillment of the Requirements

for the Degree of

Doctor of Philosophy

California Institute of Technology

Pasadena, California

1990

(Submitted May 25, 1990)

Acknowledgements

First, I would like to recognize Jane Robinson for her major contribution to this project; without her isolation and characterization of the *vpt* mutants, none of the rest of this would have been possible. I am grateful to Mike Clark and all the members of the Emr lab, especially Dan Klionsky, Bruce Horazdovsky, Paul Herman, Tom Vida, Elliot Altman and Editte Gharakhanian, for answering an endless stream of questions. I would also like to acknowledge Cathy Blagg, Nancy King and Renee Thorf for typing the thesis and Jean Edens for all her work on the electron microscopic analysis. I am especially indebted to Scott for taking me in and for his support and inspiration over the years; I couldn't have asked for a better advisor. It's been a real pleasure to be in his lab. The tutelage of Saul Roseman and Maria Kukuruzinska played a major role in my decision to go into research; I appreciate their patience and everything I learned from them. Thanks to the National Science Foundation, General Electric, the National Institutes of Health, Scott, and Caltech itself for financing my education, and to my friends for keeping me sane here. Finally, I wish to thank my parents for sparking and supporting my interest in science and especially my husband, Silvio Eberhardt, for all his understanding and encouragement in the past 5.5 years.

Abstract

The lysosome-like vacuole of the yeast *Saccharomyces cerevisiae* is an acidic compartment containing a number of hydrolytic glycoproteins including carboxypeptidase Y (CPY), proteinase A (PrA) and proteinase B (PrB). A gene fusion-based selection scheme was utilized to isolate ~600 mutants defective in the localization and processing of vacuolar proteins. These *v*acuolar *p*rotein *s*orting (*vps*) mutants define >33 complementation groups and exhibit hybrid protein-independent defects in the sorting of CPY, PrA, and PrB. Light and electron microscopic analyses of the vacuole morphology revealed three distinct classes of *vps* mutants. The class A mutants (26 complementation groups) contain 1-3 large vacuoles that resemble those of the parental strain. One class A mutant is sensitive to low pH and exhibits a defect in vacuole acidification. Consistent with a role for vacuolar pH in protein sorting, perturbation of vacuole acidification resulted in the missorting and secretion of CPY and PrA in wild-type cells. Mutants in the three class B complementation groups exhibit a fragmented vacuole morphology. The class C *vps* mutants (four complementation groups) lack any compartment resembling a wild-type vacuole, but accumulate vesicles and other membranous structures. Many class C strains exhibit genetically linked defects including temperature-sensitivity and sensitivity to osmotic stress. Unlike other *vps* mutants, these mutants secrete up to 50% of a vacuolar membrane marker enzyme. The gene defined by one class C mutant, *vps33*, has been cloned. The predicted *VPS33* gene product is hydrophilic and shares sequence similarity with a family of ATP-binding proteins. Disruption of *VPS33* is not lethal but results in temperature-sensitive growth. Vps33p-specific antisera recognize a cytosolic protein of ~75 kD. One temperature-sensitive *vps33* mutant carrying a missense mutation contains apparently normal vacuoles at the permissive temperature, but lacks vacuoles specifically in the bud at the

nonpermissive temperature. We propose that the abnormalities in vacuole morphology and inheritance in *vps33* mutants are a consequence of a primary defect in Golgi-to-vacuole protein delivery. A second *VPS* gene, *VPS28*, has also ben cloned. Our data suggest that the *VPS28* gene product only indirectly affects vacuole protein sorting, but may function in a late protein modification process.

Table of Contents

Chapter 1

Introduction

The Secretory Pathway

Eukaryotic cells are distinguished by their set of discrete membrane-enclosed compartments with distinct functions and compositions. The secretory pathway mediates the modification, processing, and localization of proteins destined for a subset of these organelles, including the endoplasmic reticulum (ER), the Golgi complex, and the lysosome, as well as the plasma membrane. A hydrophobic signal sequence, often found at the amino terminus of secretory proteins, targets the proteins for entry into the secretory pathway (165). The signal recognition particle (SRP) interacts with this signal sequence shortly after it emerges from the ribosome (203). SRP, comprised of six protein subunits (72, 68, 54, 19, 14 and 9 kD) (202) and a 7SL RNA molecule (206), has three distinct activities. Signal recognition occurs when the 54 kD subunit binds the signal sequence (94,97,177). The 68 kD and 72 kD polypeptides mediate the cotranslational translocation across the ER membrane (177,204). Finally, the 9 kD and 14 kD subunits are involved in a transient arrest of chain elongation which occurs after the SRP interacts with the signal peptide (176,205). The arrest is not required for protein translocation, but may help in holding the precursors in an unfolded state in the cytoplasm (176). A second protein complex, the SRP receptor (46) or docking protein (121), mediates the interaction of the SRP-ribosome complex with the ER membrane. The 72 kD subunit of the SRP receptor is an integral membrane protein with an amino-terminal hydrophobic domain anchored in the ER and a large cytoplasmic domain (100); a 30 kD subunit has also been identified (183). The SRP receptor displaces SRP from the ribosome, releasing the elongation arrest so that translocation can proceed (45,47). Recently, an ER transmembrane protein has been identified that appears to be part of a putative translocation tunnel (58,95). *In vitro* reconstitution experiments have revealed that posttranslational translocation requires ATP hydrolysis

(56,207). At least part of this requirement may be attributed to an ATP-dependent unfolding reaction mediated by members of the 70 kD heat shock protein family (21). Translocation is also dependent on GTP (217); this nucleotide is necessary for the SRP receptor-catalyzed displacement of SRP from the ribosome (24).

Once translocation has taken place, some signal peptides are cleaved by the multisubunit ER complex signal peptidase (34). An initial glycosyl modification event, in which core oligosaccharides of the form $Glc_3Man_9(GlcNAC)_2$ are transferred from a lipid donor to acceptor asparagine residues in the context Asn-X-Ser/Thr, occurs within the lumen of the ER (90). Trimming of the glucose and mannose residues and fatty acylation of certain proteins also take place in this compartment. Finally, protein folding and assembly of multimeric complexes appear to occur in the ER, and misfolded or unassembled proteins often do not exit the ER (reviewed in 157).

Some secretory proteins reside in the ER, where they perform functions such as the ER-mediated protein modification events just mentioned. At least some mammalian proteins destined for retention within the ER contain the sequence Lys-Asp-Glu-Leu (KDEL) at their carboxy termini. This sequence is sufficient to cause the accumulation in the ER of a normally secreted protein (125). Other, viral proteins that remain in the ER lack this sequence, but have other defined sequences necessary for ER localization, indicating that multiple signals for ER retention exist (131,146). Recent experiments suggest that resident ER proteins may exit the ER and be retrieved from a post-ER compartment (141).

Secretory proteins that leave the ER are thought to utilize vesicular transport en route to the Golgi complex, where more extensive modification and protein sorting take place. The movement of proteins from the ER to the Golgi requires energy (74). Resident Golgi proteins mediate the addition of N-

acetylglucosamine (GlcNAC), galactose, sialic acid and fucose residues (90). The glycoprotein processing enzymes can be separated on sucrose density gradients; this fractionation and the ordering of modification events have been used to define operationally subcompartments within the Golgi through which secretory proteins sequentially pass. These compartments are called the ***cis***, ***medial***, and ***trans*** Golgi, and the *trans*-Golgi network (TGN) (31,35). Transport of proteins through the Golgi complex is also vesicle-mediated. This process has been reconstituted *in vitro* and extensively studied by Rothman and colleagues (e.g., 5,6).

The Golgi complex is also the site of protein sorting, as proteins destined for the lysosome or retention within the Golgi itself are separated from those to be secreted. At present, it appears that much of the protein secretion may occur by a default mechanism (19). Proteins containing specific signals for delivery to the lysosome, for example, are sorted within the Golgi (see below), while proteins lacking any targeting information probably utilize a bulk-flow pathway to the cell surface (212). However, in addition to constitutive secretion, a second, regulated mechanism also exists in certain cell types. In this pathway, proteins are concentrated in specialized organelles called secretory granules. These granules accumulate in the cytoplasm until a specific stimulus causes them to release their contents at the cell surface. The constitutive and regulated pathways can coexist in the same cell, and secretory granule proteins are diverted into the constitutive pathway if the regulated pathway is perturbed (reviewed in 19).

Lysosomal Protein Targeting

The lysosome is an acidic organelle, surrounded by a single membrane bilayer. This compartment is involved in intracellular turnover and the digestion of biological macromolecules brought into the cell by endocytosis (69). The pH of

macrophage lysosomes was determined to be ~4.8, based on the pH-dependent fluorescence of fluorescein isothiocyanate-labeled dextran in living cells (40,135,187). This acidification is generated by the activity of a proton-translocating ATPase (120). Lysosomes contain a variety of hydrolytic enzymes including proteases, ribonucleases, phosphatases, lipases and glycosidases (69). Many lysosomal enzymes, such as acid phosphatase, β-hexosaminidase, α-glucosidase and cathepsin D, are synthesized as larger precursor proteins (61,101). These proenzymes are processed to generate the mature enzyme upon arrival in the lysosome (69). In the case of cathepsin D, the proenzyme may be inactive until its maturation in the lysosome (92). Most lysosomal hydrolases have a pH optimum of 4.5 to 5.5, so that full activity is dependent upon proper localization in the lysosome (120).

As mentioned above, lysosomal proteins are sorted from other secretory proteins at the level of the Golgi. The targeting of many of these enzymes to the lysosome is mediated by a specific oligosaccharide-linked marker, mannose 6-phosphate (Man-6-P), and receptors that recognize this signal. The initial glycosylation events, including transfer of the core oligosaccharide and the removal of three glucose and one mannose residue, occur as described above for other secretory proteins. The addition of Man-6-P to this chain occurs in a post-ER compartment (49,93,144) and involves the action of two enzymes. In the first step, N-acetylglucosamine 1-phosphate is transferred by the enzyme UDP-N-acetylglucosamine:lysosomal enzyme N-acetylglucosamine-1-phosphotransferase (phosphotransferase) from the nucleotide sugar UDP-GlcNAC to the 6-hydroxyl group of selected mannose residues to form a phosphodiester intermediate (63,149). Studies with the partially purified phosphotransferase demonstrated that the enzyme exhibited a much higher affinity (>100-fold) for lysosomal enzymes as compared to nonlysosomal glycoproteins containing high-

mannose oligosaccharide units (150,199). Deglycosylated lysosomal proteins were able to act as specific inhibitors of the phosphorylation of intact lysosomal enzymes, indicating that the protein alone was sufficient for recognition by the phosphotransferase (98). However, no consensus sequence for phosphorylation is apparent in the lysosomal enzymes sequenced thus far, and, since heat-denatured proteins do not function as acceptor molecules, it is likely that protein conformation plays a role in recognition (93,150). The second step in the formation of the Man-6-P modification is the removal of the GlcNAC residue to generate the phosphomonoester (191,198). The enzyme that catalyzes this reaction, N-acetylglucosamine 1-phosphodiester α-N-acetylglucosaminidase, has also been purified (192). This enzyme appears to reside in a compartment that is distinct from that of the phosphotransferase (49,93,141).

Two different receptors recognize the Man-6-P signal. The first to be identified and isolated was the 215 kD, cation-independent transmembrane glycoprotein called CI-MPR (166,168). More recently, it was noted that certain cell lines lacked this receptor, although a portion of the lysosomal enzymes carrying Man-6-P appeared to be localized properly (38). These observations led to the isolation of a second receptor which also recognizes the Man-6-P marker. This receptor, CD-MPR, has a monomer molecular mass of 46 kD and is dependent on divalent cations for maximal ligand affinity (66,67). Although both receptors function in lysosomal enzyme targeting, it appears that the CD-MPR is less efficient than the CI-MPR, since CI-MPR is able to compensate for the loss of CD-MPR while CD-MPR can only partially substitute for CI-MPR loss (93). One study suggested that the relative affinities of the two receptors may vary with the pH of the compartment where ligand binding occurs (68). Other differences in the function of the receptors are discussed below.

Isolation and sequencing of the cDNA clones for each of the receptors

revealed that the two proteins share some structural features. Both receptors contain a single transmembrane domain, a lumenal amino terminus, a cytoplasmic carboxy-terminal domain, and a signal sequence for ER translocation (25,106,107,138,145). Although the other three domains have no obvious sequence similarities, the lumenal domains of the two receptors share sequence homology. The bovine CI-MPR extracytoplasmic domain consists of 15 repeated conserved regions of ~145 amino acids each (106,107), while the corresponding region of the bovine CD-MPR is homologous to a single repeat unit (25). The sequence of the human CI-MPR shows extensive homology with the bovine CI-MPR within the lumenal domain and also reveals that the human CI-MPR is identical with the insulin-like growth factor II receptor (138). The biological significance of this observation is not yet yet clear.

A number of diseases are attributable to a deficiency in one or more lysosomal enzyme activities. The reduced activities of these proteins lead to an accumulation of their substrates. Many of these disorders, including Tay-Sachs' disease, are caused by the complete absence, reduced synthesis, increased instability or reduced activity of a particular lysosomal protein. Other conditions, including the well-characterized mucolipidosis III (ML-III or pseudo-Hurler polydystrophy) and mucolipidosis II (ML-II or I-cell disease), are due to a more general defect in the targeting of several lysosomal proteins (91,182). ML-II and ML-III are inherited in an autosomal recessive fashion. ML-III patients typically exhibit mild mental retardation and short stature, but survive to adulthood. The electrophoretic mobilities of a number of lysosomal enzymes are altered, and fibroblasts from these patients contain numerous inclusions. Decreased intracellular levels of certain lysosomal enzyme activities are observed, while increased levels of these activities are found in body fluids. ML-II is biochemically similar to ML-III, but the more severe symptoms lead to death by

age six years (70,130). Preliminary characterization of the lysosomal hydrolases from ML-II patients indicated that phosphorylation was undetectable, suggesting that a deficiency in the phosphotransferase activity was responsible (62). More recent studies have demonstrated that fibroblasts from ML-III patients have some residual lysosomal enzyme activity and that these cell lines can be placed into at least two complementation groups, based on their specific defects (70,91). In one group of fibroblasts, the phosphotransferase exhibits a defect in the ability to recognize lysosomal proteins, although the catalytic activity of the enzyme toward exogenous substrates is normal. In the other group, the recognition function is intact, but the catalytic activity is impaired (99,105,193). Interestingly, the levels of lysosomal enzyme activities in some tissues other than fibroblasts from I-cell patients are normal, despite a lack of detectable phosphotransferase activity, suggesting that in certain organs, a Man-6-P-independent recognition system may exist (111,139,200).

Certain enzyme activities are found at normal levels in I-cell fibroblasts (85,130). Two of these enzymes, β-glucocerebrosidase and acetyl-CoA:α-glucosaminidase N-acetyltransferase, are tightly associated with the lysosomal membrane, while a third, acid phosphatase, is synthesized and transported as a transmembrane protein to the lysosome, where it is released by proteolytic cleavage into the lumen (201). These observations indicate that the targeting of these lysosomal membrane proteins (LMP's) is independent of the Man-6-P marker (201). More recently, a number of lysosomal membrane antigens have been identified (20,71,102). The function of these proteins is as yet unknown, although some of them are closely related to one another (71). These proteins do not appear to be phosphorylated or contain Man-6-P (93), and at least three have been shown to utilize a transport mechanism that is independent of N-linked carbohydrates (8). Thus, it appears that the pathway for delivery of LMP's is

distinct from the Man-6-P recognition system used by most soluble lysosomal hydrolases.

Intracellular Trafficking of Lysosomal Proteins and Endocytosis

As discussed earlier, subcompartments of the Golgi have been functionally defined based on the distribution of modifying enzymes and the vectorial transport of proteins through the complex. The addition of the Man-6-P recognition signal is generally agreed to occur in a post-ER compartment, but the site of interaction of Man-6-P-containing proteins with MPR's has been much more controversial. Early immunolocalization studies by Brown and Farquhar suggested that MPR's were concentrated in the *cis* (early) Golgi cisternae in several cell types (16,18). Based on these observations, these authors proposed that lysosomal proteins were sorted from secretory proteins at the *cis* Golgi (16). Other experiments, however, indicated that, in other cell types, MPR's were found predominantly in the TGN (18,43,44). Furthermore, at least some lysosomal proteins carry terminal glycosyl modifications such as galactose and sialic acid residues (36). The glycosyl transferases responsible for these processing events are found in the *trans* Golgi and the TGN, indicating that the lysosomal proteins in question pass through the entire Golgi en route to the lysosome.

From the Golgi, lysosomal proteins bound to MPR's appear to travel via coated vesicles (15,43,174,196) to a prelysosomal compartment, the endosome. Since this organelle is also labeled by endocytic tracers, it appears to serve as an intermediate in the endocytic pathway as well (see below) (17,52). High concentrations of MPR's are observed by immunocytochemistry in these endosomes, while much lower levels are seen in lysosomes (17,42-44,52). On the basis of these data, the endosome is proposed to be the site of discharge of lysosomal proteins from MPR's (44,52). From the endosome, the enzymes continue

on to the lysosome. The route for this transport is not well defined; it may involve vesicle carriers or a gradual transformation of the endosome into a lysosome (196). At the same time, the MPR's rapidly recycle back to the Golgi to perform another round of transport. Brown *et al.* have demonstrated that coated vesicles serve as the carriers for this recycling, which is triggered by ligand dissociation (14,17). This shuttling from Golgi to endosome does not occur in I-cell fibroblasts, which lack ligand (15). However, in other studies, MPR recycling between the endosome and the Golgi or the cell surface (see below) was constitutive and did not require ligand binding (12,30,76,143). The basis for these conflicting observations is not entirely clear (12,30,76,143). Recycling between the endosome and the TGN has been reconstituted *in vitro* and requires GTP hydrolysis (48).

It is presumed that the acidic environment of the endosome (120,187) induces the separation of ligands from their receptors (93,196). Both CI-MPR and CD-MPR release ligand below pH 5.5 (37,66,167); the pH of the endosome is ~5.0 (187). A number of experiments have demonstrated that weak bases such as ammonium chloride or chloroquine, which raise the pH of acidic organelles, result in an accumulation of MPR's at the endosome and a depletion of free receptors, thus impairing receptor recycling (14,50). Furthermore, mutant Chinese hamster ovary cells with defects in endosomal, but not lysosomal, acidification exhibit pleiotropic defects including secretion of lysosomal proteins (153,154,156). This phenotype is also seen in mutants with defective MPR's (152) or in cells treated with ammonium chloride or chloroquine (61,126). These data are consistent with an obligatory role for endosomal acidification in proper lysosomal protein targeting.

Lysosomes also serve as the terminal destination for endocytic traffic from the cell surface. This pathway not only mediates the internalization of exogenous

ligands (see below), but also acts as an alternate route for some lysosomal protein delivery. CI-MPR is found at the plasma membrane as well as within the Golgi and endosomal compartments (42-44,52,168), and a small fraction of the Man-6-P-containing lysosomal enzymes is secreted to the cell surface before delivery to the lysosome (92). The recapture and internalization of these proteins by MPR's function as a salvage pathway in fibroblasts and account for only 12% of the total lysosomal enzyme delivery in these cells (194). Addition of antibodies against the CI-MPR to the medium of fibroblasts inhibits by 95% the retrieval of lysosomal proteins from the cell surface and results in a loss of receptors (195). This loss correlates with an increase in the secretion of lysosomal enzyme precursors. These data indicate that the internal CI-MPR's and those at the plasma membrane are in dynamic equilibrium (39,76,195). Mutations in the carboxy-terminal cytoplasmic tail of the CI-MPR differentially alter endocytosis and the delivery of newly synthesized lysosomal proteins, indicating that different domains of the tail region are required for the two processes (108). As mentioned above, the CI-MPR has recently been shown to be identical to the receptor for insulin-like growth factor II; thus this receptor also mediates the endocytosis of extracellular IGF-II.

The intracellular site to which the cell surface MPR's return was determined by examining the new glycosyl modifications which occurred after internalization. These studies revealed that the surface receptors are transported to the TGN and recycle through other Golgi compartments less frequently (30,76). Thus, it appears that at least some cell surface MPR's return to the TGN and mix with the intracellular receptor pool after discharging their ligands in the endosome. A small fraction (~3-10%) of the 46 kD CD-MPR is also found at the cell surface. Although these receptors are in equilibrium with the internal pool of CD-MPR's, they do not appear to mediate the endocytosis of Man-6-P-containing ligands at the cell surface. The reason for this difference between the CI-MPR

and the CD-MPR is unclear at the present (178).

The route followed by membrane proteins en route to the lysosome has also been analyzed. Lysosomal membrane components, plasma membrane proteins, and soluble lysosomal hydrolases exhibit the same kinetics of transport through the Golgi and were shown by immunolocalization to be present in the same Golgi cisternae. Thus, these three classes of proteins utilize the same Golgi pathway and are sorted from one another in a post-Golgi compartment, possibly the TGN (51). The kinetics of delivery to the lysosome suggest that most LMP's are transported directly to their final destination, rather than being ferried to the plasma membrane and retrieved (51). These data are consistent with the observations that, in many cell types, LMP's are not detected at the cell surface (44,93). However, in chicken fibroblasts, small quantities of at least one LMP are found on the cell surface, and this protein has been shown to recycle continuously between the plasma membrane and the lysosomes via endosomes (103,104). The human lysosomal acid phosphatase also recycles from the endosome to the plasma membrane a number of times before arriving at its final destination (13).

Endocytosis is the process by which extracellular fluids and particles, including nutrients, hormones, growth factors and antibodies, are brought into the cell. Exogenous ligands internalized by fluid-phase or receptor-mediated endocytosis are transported via clathrin coated vesicles to the endosome, also called the compartment of uncoupling of receptor and ligand (CURL), receptosomes, or endocytic vesicles. As mentioned above, these compartments are acidic, and this low pH triggers the dissociation of ligand and receptor. Membrane and receptors are recycled from the endosome to the cell surface, while the lysosome serves as the terminal destination for the endocytosed ligands (41, reviewed in 120). Internalization of a lysosomal protein by MPR has been shown to follow a similar route (216). The transfer of endocytosed ligands from

endosomes to lysosomes has recently been reconstituted *in vitro* (124). Griffiths *et al.* have shown that the endosomal compartment labeled with the endocytic marker α_2-macroglobulin-gold also contains MPR and at least one LMP (52). Geuze *et al.* have also demonstrated the colocalization of an endocytic marker, CI-MPR, and an LMP (44). Together, these observations define a specific compartment which is shared by the endocytic and lysosomal biosynthetic targeting pathways. Soluble as well as membrane lysosomal proteins traveling from the TGN to the lysosome apparently transit this organelle, which also serves as the site of dissociation of MPR and ligand. However, another study has demonstrated a colocalization of an endocytic marker and secretory proteins in the TGN. These authors suggested that multiple recycling pathways for endocytosed receptors may exist (181). Schmid *et al.* have extended these studies by separating two distinct, but kinetically related, subpopulations of endosomes using free-flow electrophoresis. "Early" endosomes were the compartments first encountered by endocytic tracers and represent the major site of receptor and membrane recycling. The more acidic "late" lysosome (173) contained endocytic label only after a longer incubation and presumably represents a prelysosomal compartment. Interestingly, the polypeptide compositions of the two endosomal subpopulations differ in part from one another and from that of the plasma membrane, indicating that these compartments are not derived entirely from internalized cell surface material and may have discrete biosynthetic origins (172).

Yeast Secretory Pathway

Like other eukaryotes, the yeast ***Saccharomyces cerevisiae*** has a complex set of organelles that constitute the secretory pathway. As is true in mammalian cells, proteins destined for compartments including the ER, Golgi, plasma

membrane, periplasm and vacuole enter the secretory pathway at the level of the ER. Thus far, the yeast equivalents of the SRP and the docking protein/SRP receptor have not been unequivocally identified. However, an essential yeast gene with homology to the 54 kD subunit of mammalian SRP has recently been cloned (54). Furthermore, three mutants defective in protein translocation have been isolated (26,158). The gene products defined by these mutations appear to be membrane-associated and genetic evidence suggests that they may act together to facilitate translocation (28,158). Recent work has demonstrated that the heat shock response is essential for translocation into the ER as well as across mitochondrial membranes in yeast. Mutants were constructed that lacked the *SSA* genes encoding members of the yeast 70 kD heat shock protein (hsp70) family, but which expressed the *SSA*1 gene when induced with galactose. Upon depletion of the *SSA*1 gene product, precursor forms of a mitochondrial protein and a normally secreted protein accumulated. These precursors were found in the cytoplasm, indicating that translocation into the respective compartments had not occurred (27). Depletion of the hsp70 also led to defects in protein translocation *in vitro* (27); independent experiments showed that ER protein translocation was stimulated by members of this hsp family (21).

At least one protein destined for retention within the ER contains a carboxy-terminal HDEL signal (the yeast equivalent of KDEL); addition of this sequence to the normally secreted protein invertase (Inv) is sufficient to cause the Inv to remain in the ER (142). A mutant (*erd*1) defective in ER retention had been isolated. *erd*1 strains secrete an endogenous ER protein and exhibit defects in the Golgi-mediated modification of glycoproteins (see below). However, no gross morphological abnormalities were observed in these cells. The *ERD*1 gene is not essential and encodes a predicted integral membrane protein (57). Proteins not retained within the ER are transported to the Golgi complex, where they undergo

sorting and targeting to their final destinations. The signals for retention of resident Golgi proteins have not yet been well characterized.

The yeast secretory pathway also mediates the glycosylation of secretory proteins. Within the ER lumen, $Glc_3Man_9(GlcNAc)_2$ moieties are transferred as units from the lipid donor dolichol-pyrophosphate to selected asparagine residues on the peptide backbone. The first processing events, in which three glucose and one mannose residue are removed, also occur at the level of the ER. The subsequent modification events differ in yeast relative to mammalian cells, although the initial addition of core oligosaccharide seems to be analogous. Upon transport to the Golgi, the oligosaccharide chains are elongated by the stepwise addition of mannose residues. Secreted proteins may be hyperglycosylated with >50 mannoses, while vacuolar proteins such as carboxypeptidase Y (CPY) typically contain approximately twelve mannose residues per chain (96).

Protein secretion and cell surface growth in yeast are directed toward the bud portion of a dividing cell (185,186). The isolation of conditional mutants defective in protein secretion has allowed a detailed analysis of this process in yeast. These *sec* mutants, comprising at least 23 complementation groups, rapidly cease dividing and accumulate normally secreted proteins intracellularly at the nonpermissive temperature (132,133). Many of these strains exhibit a temperature-dependent exaggeration of secretory organelles including ER (e.g., *sec*18), vesicles (*sec*1) or novel structures called Berkeley bodies (*sec*7) (133). Characterization of the morphology of and the extent of glycosylation in double *sec* mutants allowed the epistatic relationships between these mutations to be determined (134). Recently, ER-to-Golgi transport in yeast has been reconstituted *in vitro*; this transport is dependent on energy, cytosol, and at least one *SEC* gene product (4,164). Complementation of the *sec* mutations *in vitro* should allow purification of the proteins involved in this intercompartmental

transport.

Targeting and Processing of Vacuolar Proteins

The yeast vacuole shares characteristics with the mammalian lysosome, as well as with plant vacuoles (see below). Like lysosomes, the vacuole is an acidic compartment (127,147) containing a number of hydrolytic enzymes (1,80,215). Some of these hydrolases, such as CPY, proteinase A (PrA), and proteinase B (PrB) are soluble components of the vacuole, while others, including α-mannosidase, dipeptidylaminopeptidase B (DPAP-B), and alkaline phosphatase (ALP) are associated with the vacuole membrane.

The targeting of CPY to the vacuole has been especially well studied. This protein is translocated into the ER, where it undergoes proteolytic removal of an amino-terminal signal sequence and the addition of core oligosaccharide to generate a 67 kD ER (p1) form (10,77). Passage of p1 CPY from the ER through the Golgi complex results in additional glycosyl modification; the 69 kD Golgi-modified form of CPY is called p2 CPY. *sec* mutants which block protein secretion at the level of the ER (*sec*18) or the Golgi (*sec*7), but not secretory vesicles (*sec*1), accumulate the corresponding precursor forms of CPY at the nonpermissive temperature (179). Based in part on this observation, the sorting of CPY from nonvacuolar secretory proteins bound for the periplasm or plasma membrane is presumed to take place at the Golgi. Although the exact mechanism of this process is as yet poorly defined, it is clear that glycosyl modification is not required for proper sorting of CPY to the vacuole. In cells labeled in the presence of tunicamycin, which inhibits the addition of N-linked oligosaccharide, CPY is localized properly (60,175). Likewise, the transport of PrA and ALP to the vacuole also occurs properly in the presence of tunicamycin (23,86,116). These observations indicate that, unlike the targeting of some lysosomal proteins,

vacuolar protein sorting is not determined by the presence of an oligosaccharide-linked phosphate moiety (175).

Upon arrival at the vacuole, CPY undergoes a maturation event in which an amino-terminal propeptide of ~8 kD is proteolytically removed to generate the mature active enzyme (59). This processing step is dependent on the presence of a second vacuolar protease, the *PEP4* gene product (65) and exhibits a half-time of approximately six minutes (59). A third vacuolar protease, PrB appears to be involved in the maturation of CPY *in vitro* (59,118), although in the absence of PrB activity *in vivo*, mature active CPY is formed (65).

The sequence determinants within CPY responsible for proper localization to the vacuole were mapped using two different strategies. In the first, various portions of the gene encoding CPY, *PRC*1 (180), were fused in frame to the *SUC*2 gene, which encodes Inv. By analyzing the location of the resulting hybrid proteins, it was found that the amino-terminal 50 amino acids of CPY were sufficient to direct delivery of enzymatically active Inv to the vacuole. Deletion of this putative vacuolar targeting signal from wild-type CPY resulted in missorting to the cell surface (77). In the second approach, deletion mutations in the portion of the *PRC*1 gene which encodes the propeptide segment of CPY were found to cause the mislocalization and secretion of the p2 form of CPY. Mutagenesis of this domain (amino acids 24-31) identified single amino acid changes that resulted in a similar defect in vacuolar targeting (162,190). Secretion of the mislocalized CPY precursor was blocked in a *sec* mutant (*sec*1) that accumulates secretory vesicles (190).

The processing and localization determinants of other vacuolar proteins have also been analyzed recently. Proteinase A, the product of the *PEP4* gene (2,218), is similar to CPY in that it contains an amino-terminal signal sequence (2), undergoes a similar pattern of ER- and Golgi-mediated glycosylation, and is

synthesized as an inactive precursor (116). The deduced amino acid sequence of PrA shows homology with mammalian aspartyl proteases, including human lysosomal cathepsin D (2,218). A propeptide of 76 amino acids (2) contains sufficient information to target PrA-Inv hybrid proteins to the vacuole (86), and the half-time of maturation is six minutes, identical to that for CPY (59,86). These observations suggest that PrA and CPY are likely to share a common delivery pathway, although the primary sequences of the sorting signals in the two proteins contain no obvious similarities.

As mentioned above, the maturation of CPY is dependent on the presence of functional PrA, the product of the *PEP4* gene (65). Other vacuolar hydrolases, including PrB and ALP, are also dependent on PrA for activation (65,79); in the absence of functional PrA, precursor forms of these proteins accumulate in the vacuole (87,117). A model in which a pH-dependent auto-activation of proPrA leads to the activation of other proteases has been proposed (2,218). However, recent findings with a strain carrying a deletion in the *VAT2* gene, which encodes one subunit of the vacuolar H^+-translocating ATPase (see below) do not support this model. The vacuoles in these cells are not acidified, yet the majority of PrA was found in the mature form, indicating that vacuole acidification is not required for zymogen activation (C. Yamashiro and T. Stevens, personal communication).

PrB is a subtilisin-like protease encoded by the *PRB1* gene (122). Like PrA and CPY, PrB is synthesized as a precursor protein, traverses the secretory pathway en route to the vacuole, and exhibits kinetics of maturation similar to those seen for proCPY (116,123). However, a more detailed analysis revealed that the processing of proPrB to the mature form is more complex than that of CPY or PrA and takes place in three steps. An amino-terminal propeptide of 280 amino acids is removed before the protein exits the ER (119,122,123); the resulting intermediate form undergoes two independent cleavage events at the carboxy

terminus to generate the mature active enzyme (119,123).

The nonspecific repressible alkaline phosphatase (ALP) is encoded by the *PHO8* gene. This protein has recently been shown to be anchored in the vacuolar membrane by an amino-terminal hydrophobic domain which also appears to function as an internal uncleaved signal sequence (87). The vacuolar sorting information in ALP resides within the cytoplasmic amino terminus and/or this transmembrane domain (88). ALP is synthesized as an inactive precursor; cleavage of a carboxy-terminal propeptide releases the mature enzyme (87). In contrast to two other vacuolar membrane enzymes, α-mannosidase and DPAP-B (see below), activation of ALP is dependent on *PEP4* function (65).

α-mannosidase is the classic marker enzyme for vacuolar membranes, although recent solubilization studies indicate that the protein may be only peripherally associated with the vacuolar membrane (219). α-mannosidase activity is found within the vacuolar lumen; however, the apparent lack of any signal sequence, transmembrane domain, or N-linked glycosylation suggests that this protein may not transit the secretory pathway en route to the vacuole. On the basis of these observations, it has been proposed that α-mannosidase may be translocated directly across the vacuole membrane from the cytoplasm (220). A similar secretory pathway-independent mechanism for the export of the yeast pheromone a-factor across the plasma membrane has recently been suggested (114).

Dipeptidylaminopeptidase B (DPAP-B) is an integral membrane protein which resides in the vacuolar membrane. Unlike α-mannosidase, DPAP-B contains a single potential transmembrane domain, is glycosylated, and therefore appears to utilize the early stages of the secretory pathway. Indeed, immunolocalization studies have shown that DPAP-B is localized properly to the vacuole in *sec*1 mutants, but accumulates in nonvacuolar compartments in *sec*18 or *sec*7 mutant

cells. Like ALP, DPAP-B is predicted to have a type II orientation in the membrane, with a short cytoplasmic amino terminus and a large lumenal carboxy terminus separated by the single transmembrane domain (155).

As mentioned above, mutations in the vacuolar localization determinant in CPY result in secretion of the Golgi-modified precursor form of CPY; this secretion is blocked in *sec*1 mutants at the nonpermissive temperature (77,190). In addition, Stevens and colleagues have demonstrated that overproduction of either CPY or PrA (expressed from a multicopy plasmid) also causes secretion of these proteins (159,180). Although this secretion is dependent on *SEC*1, it is interesting to note that the secreted proteins do not undergo the extensive glycosylation characteristic of normally secreted proteins such as Inv (159,180). These data indicate that in yeast, as is the case in mammalian cells, secretion appears to be the default fate of proteins which enter the secretory pathway lacking additional targeting information. In addition, the observed overproduction-induced secretion suggests that excess levels of vacuolar proteins might lead to the saturation of a putative vacuolar sorting receptor or other recognition machinery, and that this saturation of such a limiting component results in missorting (180). However, so far there is no direct genetic or biochemical evidence for the existence of a receptor for vacuolar proteins (89). Furthermore, although the similar kinetics of processing of CPY and PrA suggest that these two proteins utilize a common delivery pathway, overproduction of CPY does not cause the secretion of PrA (180), nor is CPY mislocalized in the presence of excess PrA (159). Thus, if a specific vacuolar sorting and recognition system does exist, there may be different receptors for these two proteins.

The finding that improperly targeted or overproduced CPY is secreted (180,190) has allowed the isolation of a number of mutants defective in the vacuolar localization of CPY. The Emr lab selection for vacuolar protein

*t*argeting (*vpt*) mutants made use of *PRC1-SUC2* gene fusions, encoding CPY-Inv hybrid proteins that were diverted to the vacuole in wild-type cells (see above). Mutants were selected that "mislocalized" the hybrid proteins to the cell surface and therefore contained periplasmic Inv activity. The mutants that were originally isolated define eight complementation groups and exhibit hybrid protein-independent missorting of precursor CPY to the cell surface (7). The isolation and characterization of ~500 more *vpt* mutants, comprising >25 additional complementation groups, are detailed in Chapters 2 and 3.

A second selection scheme, employed by Stevens and colleagues, took advantage of the conversion of mislocalized (periplasmic) precursor CPY to an enzymatically active form by an unknown protease (180). CPY activated in the periplasm by this protease, or vacuolar CPY activated by PrA in wild-type cells, catalyzes the peptide bond cleavage of the N-blocked dipeptide N-CBZ-L-phenyalanyl-L-leucine and thereby liberates leucine. *pep4* leucine auxotrophs secreting proCPY were selected for their ability to grow on a medium containing the dipeptide as the sole leucine source. The *v*acuolar *p*rotein *l*ocalization (*vpl*) mutants thus isolated define at least 19 complementation groups and exhibit sorting defects for PrA as well as CPY, although glycosylation and secretion of Inv appear to be normal in these strains (160,161).

Interestingly, the vacuole membrane marker α-mannosidase does not apear to be present at the cell surface in most of the *vpt* and *vpl* mutants, indicating that this protein is not subject to the vacuole protein sorting defects resulting from many of these mutations (7,160; see Chapter 2). It has recently been shown that the integral membrane protein ALP is less sensitive than CPY or PrA to the targeting defects exhibited by some of the *vpt* mutants or to the perturbation of vacuolar acidification, which also leads to the missorting and secretion of precursor forms of CPY and PrA (87, see Chapter 3). Together, these

observations suggest that vacuole membrane enzymes, like lysosomal membrane proteins, utilize a transport mechanism which is at least in part distinct from that for soluble hydrolases.

Another group of mutants, the *pep* mutants, were originally identified as having reduced levels of many vacuolar activities, including those of CPY, PrA and/or PrB (78). The *pep* mutations define 16 complementation groups. Stevens and colleagues have recently demonstrated that, with the exception of *pep4* mutants, all of these strains exhibit defects in the localization of CPY and PrA. Extensive overlap between the *vpl*, *vpt* and *pep* complementation groups exists (161, see Chapter 2).

Vacuolar Acidification and Storage of Metabolites

As mentioned above, the yeast vacuole shares many characteristics with plant vacuoles. Early studies implicated the vacuole in the storage of basic amino acids, ions and polyphosphates (112,113). Analysis of the amino acid pools in yeast vacuoles showed that basic amino acids, especially arginine, accumulate specifically in this organelle, while glutamate, the most abundant amino acid in yeast cells, is almost absent from the vacuole (214). By differential extraction of the vacuolar and cytosolic pools of amino acids, Anraku and coworkers have shown that the cytosolic pool remains relatively constant, while the content of the vacuolar pool fluctuates greatly under various growth conditions. Histidine and lysine in the growth medium cause a substantial increase in the vacuolar content of these amino acids. Inclusion of arginine in the medium also causes an accumulation of arginine in the vacuole; this amino acid is released upon nitrogen starvation (83). These observations are consistent with a role for the vacuole in the storage of nutrient reserves, since arginine serves as a major source of nitrogen. The mechanism of basic amino acid uptake has also been studied in some

detail. *In vitro* experiments indicated that this transport is driven by a proton motive force generated by the H^+-translocating ATPase of vacuolar membranes (see below) (136). Seven independent H^+/amino acid antiport systems and an arginine/histidine exchange transport system have been identified in purified vacuole membrane vesicles (170,171). In an effort to uncover mutants defective in the specific lysine transport system, Kitamoto *et al.* screened for strains sensitive to lysine in the medium. A mutant (*slp*1) containing smaller than normal vacuolar pools of lysine, arginine, and histidine has been isolated. The *slp*1 mutation results in an altered vacuole morphology in which many small vesicles but no large vacuoles are present (84). Thus, it seems likely that this mutant exhibits lysine-sensitive growth because it lacks a compartment in which to accumulate the excess levels of this amino acid. The *slp*1 mutant is allelic to a mutant defective in vacuolar protein sorting, *vpt33* (see Chapter 4).

Basic amino acids are sequestered in the vacuole against a large concentration gradient. In cells grown with arginine as the nitrogen source, the concentration of arginine in the vacuole is over 20 times greater than in the cytoplasm (72). Although the mechanism of this retention is not entirely clear, Durr *et al.* have proposed that the arginine is trapped in the vacuole by being bound to polyphosphate (32). Early studies had demonstrated that the vacuole contains a large insoluble pool of polyphosphate (73,189); this pool increases approximately threefold when cells are grown on arginine (32). However, Dürr *et al.* (32) have also shown that yeast cells are able to accumulate and mobilize arginine and polyphosphate independent of one another. For example, arginine is sequestered in vacuoles even when cells are starved for phosphate, indicating that a polyphosphate-independent means of concentrating this amino acid in the vacuole must also exist. It is interesting to note that a mutant, *end*1, which appears to lack vacuoles (see below), stores almost no arginine or polyphosphate

and grows poorly when starved of these substances (211). These data support the idea that the vacuole serves as the major cellular repository for nutrient reserves.

The yeast vacuole also appears to be involved in Ca^{2+} homeostasis. Under standard growth conditions, the majority of the cellular Ca^{2+} is sequestered in the vacuole, as determined by differential extraction from the cytoplasmic and vacuolar pools. An increase in the medium Ca^{2+} concentration resulted in a corresponding rise in the vacuolar Ca^{2+} content, while the cytoplasmic concentration was relatively unchanged (33,137a). Like basic amino acid transport, Ca^{2+} uptake by the vacuole appears to be driven by the electrochemical potential difference of protons across the vacuole membrane (137). A more general role for the vacuole in ion storage is suggested by the finding that vacuole membranes contain a membrane potential-dependent cation channel which conducts K^+, Cs^+, Na^+, and Li^+ (197).

Vacuolar functions have been implicated in protein turnover during starvation, which in turn mobilizes amino acids for reutilizaiton. Rates of basal protein degradation increase several fold when cells enter stationary phase or are starved for nitrogen (3). These changes correlate with an increase in the levels of vacuolar proteinases under these conditions (1,55,80,169) and mutants deficient in PrA and PrB have much lower rates of protein degradation during starvation (115,184). Protein turnover also increases dramatically under conditions which induce sporulation (9). The function of at least one vacuolar proteinase appears to be essential in this process, since diploids homozygous for the *pep4-3* mutation fail to sporulate (222).

In plant cells, the vacuole plays an important role in turgor and osmoregulation (11,64,221). The high concentration of amino acids and polyphosphate in the yeast vacuole might act in an osmoregulatory capacity, although there is little direct evidence for such a function (see Chapter 3). The

plant vacuole is also important in pH homeostasis; a decrease in external pH results in a lowered vacuolar pH, while the cytoplasmic pH remains constant (11). Relatively little is known about the role of the yeast vacuole in pH regulation, although vacuole acidification itself has been more extensively studied. Anraku and colleagues have identified a Mg^{2+}-dependent H^+-translocating ATPase activity in the membrane of purified intact vacuoles (81). The purified enzyme complex contains as many as eight different types of subunits (82,188). This multienzyme complex consists of both peripheral and integral membrane subunits and shares similarities in composition with vacuolar H^+-ATPases from both plant and animal cells (82). The vacuolar ATPase uses the energy of ATP hydrolysis to pump protons into the vacuole, creating an acidic pH within the organelle (81). The resulting proton motive force drives the transport of basic amino acids and Ca^{2+} into the vacuole (136,137). The pH of the vacuole has been measured using ^{31}P-NMR spectroscopy as well as flow cytometry (based on the pH-dependent fluorescence of 6-carboxyfluorescein). Both these methods gave similar values, 6.2 (flow cytometry) or 6.5-6.8 (^{31}P-NMR), for the pH of the vacuole (127,147). This is somewhat higher than the pH reported for lysosomes (see above). A mutant defective in vacuole acidification (*vph*1) was isolated by screening mutagenized yeast cells labeled with 6-carboxyfluorescein using fluorescence ratio microscopy. Cells carrying the *vph*1 mutation have a vacuolar pH of 6.9 and exhibit no vacuolar accumulation of quinacrine (147), a dye which accumulates in wild-type vacuoles in a pH-dependent manner (208). A second mutant strain, carrying a deletion of the *PEP*12 gene, also fails to accumulate quinacrine, but the vacuolar pH is nearly normal (6.3). This *pep*12 mutant is postulated to have a partial defect in H^+ transport into the vacuole, which could inhibit the uptake of quinacrine without drastically altering the steady-state vacuolar pH (147). At least two mutants originally selected for defects in

vacuolar protein sorting (see above) also fail to accumulate quinacrine in the vacuole. *vpl3* and *vpl6* cells contain diminished levels of two subunits of the H^+ ATPase in their vacuole membranes. The mutations apparently cause defects in ATPase assembly, since wild-type amounts of the proteins are seen in whole cell extracts from these mutants (163). One of the mutants, *vpl6*, falls into the same complementation group as *pep12* and a third mutant, *vpt13*, which also exhibits a defect in quinacrine accumulation and extreme sensitivity to low pH (161, see Chapter 3).

To assess directly the importance of vacuolar acidification and the vacuolar H^+-ATPase in cellular functions, several groups have recently begun cloning and disrupting the genes encoding the ATPase subunits. The deduced amino acid sequence of the *VAT2* gene, encoding the 57 kD subunit of the catalytic portion, shares extensive sequence similarity with the sequences of the *Neurospora* and *Arabidopsis* 57 kD vacuolar ATPase subunits (128,162). Cells carrying null mutations in *VAT2* are viable, although they exhibit the expected defects in vaucole acidification, including a failure to accumulate quinacrine in the vacuole (129,162). These observations indicate that vacuole acidification is not essential for vegetative growth. This is consistent with earlier findings that mutants deficient in multiple vacuolar hydrolases (78) and even strains lacking any organelle resembling a wild-type vacuole (84, see Chapter 3) are able to grow and divide. Thus far, no vacuolar functions have been found which are required for vegetative growth (89). Vacuole acidification does, however, appear to be important for the proper delivery of proteins to the vacuole. Perturbation of the vacuolar pH by the weak base ammonium acetate, inhibition of the vacuolar H^+-ATPase (see Chapter 3), or disruption of the *VAT2* gene (162) results in the missorting of PrA and CPY.

Endocytosis and Vacuole Biogenesis

As discussed above, mammalian cells contain compartments which appear to be shared by the lysosomal targeting and endocytic pathways. Although endocytosis in yeast has not been as well studied, various experiments have demonstrated the internalization of vesicular stomatitis virus and Semliki Forest virus into yeast spheroplasts (109), as well as the uptake of α-amylase (110), lucifer yellow (LY) (151) and the peptide pheromone α-factor (75) by whole cells. Lucifer yellow appears to be internalized by fluid-phase endocytosis (151), while α-factor uptake is believed to occur by a receptor-mediated mechanism (75). Both events take place in a time-, temperature-, and energy-dependent manner (22,151). Fluid-phase endocytosis apparently utilizes at least the late steps of the secretory pathway. *sec* mutants which accumulate secretory vesicles are defective in the uptake of LY (151) and α-amylase (110), as are some mutants blocked at the level of the ER or the Golgi (151). As in mammalian cells, the vacuole (lysosome) serves as the destination for the yeast endocytic traffic studied thus far. Internalized LY and viruses accumulate in the vacuole, while α-factor is degraded inside the cell in a *PEP4*-dependent manner (29,75), suggesting that this event is vacuole-mediated. A mutant (*end*1) has been isolated which is defective in the accumulation of LY (22). *end*1 cells have an altered morphology in which no large vacuolar structure is observed (22). These mutants also missort vacuolar hydrolases including CPY, PrA, and PrB and exhibit defects in gluconeogenic growth (29). Consistent with these observations, *end*1 mutants internalize α-factor but are unable to degrade it (29), suggesting that the primary defect in these cells is in vacuole biogenesis rather than endocytosis itself. Indeed, *end*1 mutants fall into the same complementation group as several other mutants described above, including *vpt*11, *vpl*9 and *pep*5 (29,161, see Chapter 2). The *END*1 gene encodes a hydrophilic protein which shares sequence similarity

with a number of ATP-binding proteins (29). Given the observations that coated vesicles appear to be involved in endocytosis and lysosomal protein targeting in mammalian cells, it is interesting to note that clathrin does not seem to be required for vacuolar protein sorting. Cells in which the clathrin heavy chain gene has been deleted localize CPY properly to the vacuole and take up α-factor at 50% of the normal rate (140).

Vacuole morphology and inheritance have been the subjects of a number of recent studies. The vacuole is a prominent organelle occupying as much as 20-25% of the cell volume (113). This compartment is very dynamic, as its structure varies depending on the growth conditions and the methods used in preparing the cells (148). While wild-type cells appear to contain one or a few vacuoles, certain conditions, including the disruption of microtubules, deletion of the clathrin heavy chain gene, or certain mutations result in apparent vacuole fragmentation (53,140, see Chapter 3). Early experiments using synchronized cells suggested that vacuole transmittal upon budding was achieved by fragmentation of the large vacuole in the mother cell followed by distribution of the small vacuoles between mother and daughter cells and coalescence to form a single large vacuole in each cell (112,213). However, a more recent study using asynchronous cultures has indicated that a major large vacuole was the most common morphology in both the mother and daughter cells at all stages of the cell cycle (208). The majority of buds contained a vacuole very early after budding, when the bud was less than half the size of the mother cell. These experiments also suggested that the bud receives some fraction of its contents from the mother cell (208). Transfer of contents between the parental vacuoles and the vacuole in the emerging bud in a zygote has also been observed (209). These authors postulated that this transfer might be mediated by vesicles or tubular structures. A mutant, *vac1*, defective in the segregation of vacuolar material from the mother cell to the bud has recently

been isolated. Although *vac1* mother cells contain vacuoles, the buds appear to receive little or no vacuolar contents from the mother and presumably form vacuoles by some process other than direct inheritance (210).

Conclusions

In summary, the yeast vacuole is a dynamic organelle with a complex composition. The involvement of this organelle in the regulation of a number of cellular processes indicates that it is more than just a "dumping ground" for macromolecules which are no longer needed by the cell. The synthesis of vacuolar hydrolases as inactive zymogens and their sequestration in the vacuole ensures that the protein degradation events that they mediate are confined to the vacuole. Indeed, inhibitors of the activities of PrA and PrB are found in the cytoplasm (1). Control of proteolytic activity appears to be at least somewhat temporally, as well as spatially, controlled, since the vacuolar hydrolases are induced under conditions such as entry into stationary phase or starvation. The function of the yeast vacuole in the storage of nutrient reserves and ions is well documented; roles in pH homeostasis and osmoregulation are also possible. The extensive overlap between mutants with defects in vacuolar hydrolase activities, vacuolar protein sorting, vacuolar acidification, endocytosis, and lysine storage emphasizes that these functions are all interrelated (89). The protein constituents that form the vacuolar structure also define its characteristic activities and properties; thus, the proper targeting of these proteins is an essential aspect of vacuolar function.

Literature Cited

1. Achstetter, T., and D. H. Wolf. 1985. Proteinases, proteolysis and biological control in the yeast *Saccharomyces cerevisiae*. Yeast **1**:139-157.

2. Ammerer, G., C. P. Hunter, J. H. Rothman, G. C. Saari, L. A. Valls, and T. H. Stevens. 1986. *PEP4* gene of *Saccharomyces cerevisiae* encodes proteinase A, a vacuolar enzyme required for processing of vacuolar precursors. Mol. Cell. Biol. **6**:2490-2499.

3. Bakalkin, G. Y., S. L. Kalnov, A. S. Zubatov, and V. N. Luzikov. 1976. Degradation of total cell protein at different stages of *Saccharomyces cerevisiae* yeast growth. FEBS Lett. **63**:218-221.

4. Baker, D., L. Hicke, M. Rexach, M. Schleyer, and R. Schekman. 1988. Reconstitution of *SEC* gene product-dependent intercompartmental protein transport. Cell **54**:335-344.

5. Balch, W. E., W. G. Dunphy, W. A. Braell, and J. E. Rothman. 1984. Reconstitution of the transport of protein between successive compartments of the Golgi measured by the coupled incorporation of N-acetylglucosamine. Cell **39**:405-416.

6. Balch, W. E., B. S. Glick, and J. E. Rothman. 1984. Sequential intermediates in the pathway of intercompartmental transport in a cell-free system. Cell **39**:525-536.

7. Bankaitis, V. A., L. M. Johnson, and S. D. Emr. 1986. Isolation of yeast mutants defective in protein targeting to the vacuole. Proc. Natl. Acad. Sci. USA **83**:9075-9079.

8. Barriocanal, J. G., J. S. Bonifacino, L. Yuan, and I. V. Sandoval. 1986. Biosynthesis, glycosylation, movement through the Golgi system, and transport to lysosomes by an N-linked carbohydrate-independent mechanism of three lysosomal integral membrane proteins. J. Biol. Chem. **261**:16755-16763.

9. Betz, H., and U. Weiser. 1976. Protein degradation and proteinases during yeast sporulation. Eur. J. Biochem. **62**:65-76.

10. Blachly-Dyson, E., and T. H. Stevens. 1987. Yeast carboxypeptidase Y can be translocated and glycosylated without its amino-terminal signal sequence. J. Cell. Biol. **104**:1183-1191.

11. Boller, T., and A. Wiemken. 1986. Dynamics of vacuolar compartmentation. Ann. Rev. Plant Physiol. **37**:137-164.

12. Braulke, T., C. Gartung, A. Hasilik, and K. von Figura. 1987. Is movement of mannose 6-phosphate-specific receptor triggered by binding of lysosomal enzymes? J. Cell Biol. **104**:1735-1742.

13. Braun, M., A. Waheed, and K. von Figura. 1989. Lysosomal acid phosphatase is transported to lysosomes via the cell surface. EMBO J. **8**:3633-3640.

14. Brown, W. J., E. Constantinescu, and M. G. Farquhar. 1984. Redistribution of mannose 6-phosphate receptors induced by tunicamycin and chloroquine. J. Cell Biol. **99**:320-326.

15. Brown, W. J., and M. G. Farquhar. 1984. Accumulation of coated vesicles bearing mannose 6-phosphate receptors for lysosomal enzymes in the Golgi region of I-cell fibroblasts. Proc. Natl. Acad. Sci. USA **81**:5135-5139.

16. Brown, W. J., and M. G. Farquhar. 1984. The mannose 6-phosphate receptor for lysosomal enzymes is concentrated in *cis* Golgi cisternae. Cell **36**:295-307.

17. Brown, W. J., J. Goodhouse, and M. G. Farquhar. 1986. Mannose 6-phosphate receptors for lysosomal enzymes cycle between the Golgi complex and endosomes. J. Cell Biol. **103**:1235-1247.

18. Brown, W. J., and M. G. Farquhar. 1987. The distribution of 215-kilodalton mannose 6-phosphate receptors within cis (heavy) and trans (light) Golgi subfractions varies in different cell types. Proc. Natl. Acad. Sci. USA **84**:9001-9005.

19. Burgess, T. L., and R. B. Kelly. 1987. Constitutive and regulated secretion of proteins. Ann. Rev. Cell Biol. **3**:243-293.

20. Chen, J. W., T. L. Murphy, M. C. Willingham, I. Pastan, and J. T. August. 1985. Identification of two lysosomal membrane glycoproteins. J. Cell Biol. **101**:85-95.

21. Chirico, W. J., M. G. Waters, and G. Blobel. 1988. 70K heat shock related proteins stimulate protein translocation into microsomes. Nature **332**:805-810.

22. Chvatchko, Y., I. Howald, and H. Riezman. 1986. Two yeast mutants defective in endocytosis are defective in pheromone response. Cell **46**:355-364.

23. Clark, D. W., J. S. Tkacz, and J. O. Lampen. 1982. Asparagine-linked carbohydrate does not determine the cellular location of yeast vacuolar nonspecific alkaline phosphatase. J. Bacteriol. **152**:865-873.

24. Connolly, T., and R. Gilmore. 1989. The signal recognition particle receptor mediates the GTP-dependent displacement of SRP from the signal sequence of the nascent polypeptide. Cell **57**:599-610.

25. Dahms, N. M., P. Lobel, J. Breitmeyer, J. M. Chirgwin, and S. Kornfeld. 1987. 46 kd mannose 6-phosphate receptor: Cloning, expression, and homology to the 215 kd mannose 6-phosphate receptor. Cell **50:**181-192.

26. Deshaies, R. J., and R. Schekman. 1987. A yeast mutant defective at an early stage in import of secretory protein precursors into the endoplasmic reticulum. J. Cell Biol. **105:**633-645.

27. Deshaies, R. J., B. D. Koch, M. Werner-Washburne, E. A. Craig, and R. Schekman. 1988. A subfamily of stress proteins facilitates translocation of secretory and mitochondrial precursor polypeptides. Nature **332:**800-805.

28. Deshaies, R. J., and R. Schekman. 1989. *SEC*62 encodes a putative membrane protein required for protein translocation into the yeast endoplasmic reticulum. J. Cell Biol. **109:**2653-2664.

29. Dulic, V., and H. Riezman. 1989. Characterization of the *END*1 gene required for vacuole biogenesis and gluconeogenic growth of budding yeast. EMBO J. **8:**1349-1359.

30. Duncan, J. R., and S. Kornfeld. 1988. Intracellular movement of two mannose 6-phosphate receptors: Return to the Golgi apparatus. J. Cell Biol. **106:**617-628.

31. Dunphy, W. G., and J. E. Rothman. 1985. Compartmental organization of the Golgi stack. Cell **42:**13-21.

32. Durr, M., K. Urech, T. Boller, A. Wiemken, J. Schwenke, and M. Nagy. 1979. Sequestration of arginine by polyphosphate in vacuoles of yeast (*Saccharomyces cerevisiae*). Arch. Microbiol. **121:**169-175.

33. Eilam, Y., H. Lavi, and N. Grossowicz. 1985. Cytoplasmic Ca^{2+} homeostasis maintained by a vacuolar Ca^{2+} transport system in the yeast *Saccharomyces cerevisiae*. J. Gen. Microbiol. **131:**623-629.

34. Evans, E. A., R. Gilmore, and G. Blobel. 1986. Purification of microsomal signal peptidase as a complex. Proc. Natl. Acad. Sci. USA **83**:581-585.

35. Farquhar, M. G. 1985. Progress in unraveling pathways of Golgi traffic. Ann. Rev. Cell Biol. **1**:447-488.

36. Fedde, K. N., and W. S. Sly. 1985. Ricin-binding properties of acid hydrolases from isolated lysosomes implies prior processing by terminal transferases of the trans-Golgi apparatus. Biochem. Biophys. Res. Commun. **133**:614-620.

37. Fisher, H. D., A. Gonzalez-Noriega, and W. S. Sly. 1980. β-glucuronidase binding to human fibroblast membrane receptors. J. Biol. Chem. **255**:5069-5074.

38. Gabel, C. A., D. E. Goldberg, and S. Kornfeld. 1983. Identification and characterization of cells deficient in the mannose 6-phosphate receptor: Evidence for an alternate pathway for lysosomal enzyme targeting. Proc. Natl. Acad. Sci. USA **80**:775-779.

39. Gartung, C., T. Braulke, A. Hasilik, and K. von Figura. 1985. Internalization of blocking antibodies against mannose 6-phosphate specific receptors. EMBO J. **4**:1725-1730.

40. Geisow, M. J., P. D. Hart, and M. R. Young. 1981. Temporal changes of lysosome and phagosome pH during phagolysosome formation in macrophages: Studies by fluorescence spectroscopy. J. Cell Biol. **89**:645-652.

41. Geuze, H. J., J. W. Slot, G. J. A. M. Strous, H. F. Lodish, and A. L. Schwartz. 1983. Intracellular site of asialoglycoprotein receptor-ligand uncoupling: Double-label immunoelectron microscopy during receptor-mediated endocytosis. Cell **32**:277-287.

42. Geuze, H. J., J. W. Slot, G. J. A. M. Strous, A. Hasilik, and K. von Figura. 1984. Ultrastructural localization of the mannose 6-phosphate receptor in rat liver. J. Cell Biol. **98**:2047-2054.

43. Geuze, H. J., J. W. Slot, G. J. A. M. Strous, A. Hasilik, and K. von Figura. 1985. Possible pathways for lysosomal enzyme delivery. J. Cell Biol. **101**:2253-2262.

44. Geuze, H. J., W. Stoorvogel, G. J. Strous, J. W. Slot, J. E. Bleekemolen, and I. Mellman. 1988. Sorting of mannose 6-phosphate receptors and lysosomal membrane proteins in endocytic vesicles. J. Cell Biol. **107**:2491-2501.

45. Gilmore, R., G. Blobel, and P. Walter. 1982. Protein translocation across the endoplasmic reticulum. I. Detection in the microsomal membrane of a receptor for the signal recognition particle. J. Cell Biol. **95**:463-469.

46. Gilmore, R., P. Walter, and G. Blobel. 1982. Protein translocation across the endoplasmic reticulum. II. Isolation and characterization of the signal recognition particle receptor. J. Cell Biol. **95**:470-477.

47. Gilmore, R., and G. Blobel. 1983. Transient involvement of signal recognition particle and its receptor in the microsomal membrane prior to protein translocation. Cell **35**:677-685.

48. Goda, Y., and S. R. Pfeffer. 1988. Selective recycling of the mannose 6-phosphate/IGF-II receptor to the *trans*-Golgi network in vitro. Cell **55**:309-320.

49. Goldberg, D. E., and S. Kornfeld. 1983. Evidence for extensive subcellular organization of asparagine-linked oligosaccharide processing and lysosomal enzyme phosphorylation. J. Biol. Chem. **258**:3159-3165.

50. Gonzalez-Noriega, A., J. H. Grubb, V. Talkad, and W. S. Sly. 1980. Chloroquine inhibits lysosomal enzyme pinocytosis and enhances lysosomal enzyme secretion by impairing receptor recycling. J. Cell Biol. **85**:839-852.

51. Green, S. A., K.-P. Zimmer, G. Griffiths, and I. Mellman. 1987. Kinetics of intracellular transport and sorting of lysosomal membrane and plasma membrane proteins. J. Cell Biol. **105**:1227-1240.

52. Griffiths, G., B. Hoflack, K. Simons, I. Mellman, and S. Kornfeld. 1988. The mannose 6-phosphate receptor and the biogenesis of lysosomes. Cell **52**:329-341.

53. Guthrie, B., and W. Wickner. 1988. Yeast vacuoles fragment when microtubules are disrupted. J. Cell Biol. **107**:115-120.

54. Hann, B. C., M. A. Poritz, and P. Walter. 1989. *Saccharomyces cerevisiae* and *Schizosaccharomyces pombe* contain a homologue to the 54 kD subunit of the signal recognition particle that in *S. cerevisiae* is essential for growth. J. Cell Biol. **109**:3223-3230.

55. Hansen, R. J., R. L. Switzer, H. Hinze, and H. Holzer. 1977. Effects of glucose and nitrogen source on the levels of proteinases, peptidases, and proteinase inhibitors in yeast. Biochim. Biophys. Acta. **496**:103-114.

56. Hansen, W., P. D. Garcia, and P. Walter. 1986. In vitro protein translocation across the yeast endoplasmic reticulum: ATP-dependent posttranslational translocation of the prepro-α factor. Cell **45**:397-406.

57. Hardwick, K. G., M. J. Lewis, J. Semenza, N. Dean, and H. R. B. Pelham. 1990. *ERD1*, a yeast gene required for the retention of luminal endoplasmic reticulum proteins, affects glycoprotein processing in the Golgi apparatus. EMBO J. **9**:623-630.

58. Hartmann, E., M. Wiedmann, and T. A. Rapoport. 1989. A membrane component of the endoplasmic reticulum that may be essential for protein translocation. EMBO J. **8**:2225-2229.

59. Hasilik, A., and W. Tanner. 1978. Biosynthesis of the vacuolar yeast glycoprotein carboxypeptidase Y. Conversion of precursor into the enzyme. Eur. J. Biochem. **85**:599-608.

60. Hasilik, A., and W. Tanner. 1978. Carbohydrate moiety of carboxypeptidase Y and perturbation of its biosynthesis. Eur. J. Biochem. **91**:567-575.

61. Hasilik, A., and E. F. Neufeld. 1980. Biosynthesis of lysosomal enzymes in fibroblasts. Synthesis as precursors of higher molecular weight. J. Biol. Chem. **255**:4937-4945.

62. Hasilik, A., and E. F. Neufeld. 1980. Biosynthesis of lysosomal enzymes in fibroblasts. Phosphorylation of mannose residues. J. Biol. Chem. **255**:4946-4950.

63. Hasilik, A., A. Waheed, and K. von Figura. 1981. Enzymatic phosphorylation of lysosomal enzymes in the presence of UDP-N-acetylglucosamine. Absence of the activity in I-cell fibroblasts. Biochem. Biophys. Res. Commun. **98**:761-767.

64. Hellebrust, J. A. 1976. Osmoregulation. Ann. Rev. Plant Physiol. **27**:485-505.

65. Hemmings, B. A., G. S. Zubenko, A. Hasilik, and E. W. Jones. 1981. Mutant defective in processing of an enzyme located in the lysosome-like vacuole of *Saccharomyces cerevisiae*. Proc. Natl. Acad. Sci. USA **78**:435-439.

66. Hoflack, B., and S. Kornfeld. 1985. Lysosomal enzyme binding to mouse $P388D_1$ macrophage membranes lacking the 215-kDa mannose 6-phosphate receptor: Evidence for the existence of a second mannose 6-phosphate receptor. Proc. Natl. Acad. Sci. USA **82:**4428-4432.

67. Hoflack, B., and S. Kornfeld. 1985. Purification and characterization of a cation-dependent mannose 6-phosphate receptor from murine $P388D_1$ macrophages and bovine liver. J. Biol. Chem. **260:**12008-12014.

68. Hoflack, B., K. Fujimoto, and S. Kornfeld. 1987. The interaction of phosphorylated oligosaccharides and lysosomal enzymes with bovine liver cation-dependent mannose 6-phosphate receptor. J. Biol. Chem. **262:**123-129.

69. Holtzman, E. 1989. Lysosomes. Plenum Press, New York.

70. Honey, N. K., O. T. Mueller, L. E. Little, A. L. Miller, and T. B. Shows. 1982. Mucolipidosis III is genetically heterogeneous. Proc. Natl. Acad. Sci. USA **79:**7420-7424.

71. Howe, C. L., B. L. Granger, M. Hull, S. A. Green, C. A. Gabel, A. Helenius, and I. Mellman. 1988. Derived protein sequence, oligosaccharides, and membrane insertion of the 120-kDa lysosomal membrane glycoprotein (lgp120): Identification of a highly conserved family of lysosomal membrane glycoproteins. Proc. Natl. Acad. Sci. USA **85:**7577-7581.

72. Huber-Walchli, V., and A. Wiemken. 1979. Differential extraction of soluble pools from the cytosol and the vacuoles of yeast (*Candida utilis*) using DEAE-dextran. Arch. Microbiol. **120:**141-149.

73. Indge, K. J. 1968. Polyphosphates of the yeast cell vacuole. J. Gen. Microbiol. **51:**447-455.

74. Jamieson, J. D., and G. E. Palade. 1968. Intracellular transport of secretory proteins in the pancreatic exocrine cell. IV. Metabolic requirements. J. Cell Biol. **39**:589-603.

75. Jenness, D. D., and P. Spatrick. 1986. Down regulation of the α-factor pheromone receptor in *S. cerevisiae*. Cell **46**:345-353.

76. Jin, M., G. G. Sahagian, and M. D. Snider. 1989. Transport of surface mannose 6-phosphate receptor to the Golgi complex in cultured human cells. J. Biol. Chem. **264**:7675-7680.

77. Johnson, L. M., V. A. Bankaitis, and S. D. Emr. 1987. Distinct sequence determinants direct intracellular sorting and modification of a yeast vacuolar protease. Cell **48**:875-885.

78. Jones, E. W. 1977. Proteinase mutants of *Saccharomyces cerevisiae*. Genetics **85**:23-33.

79. Jones, E. W., G. S. Zubenko, and R. R. Parker. 1982. *PEP4* gene function is required for expression of several vacuolar hydrolases in *Saccharomyces cerevisiae*. Genetics **102**:665-677.

80. Jones, E. W. 1984. The synthesis and function of proteases in *Saccharomyces*: Genetic approaches. Ann. Rev. Genet. **18**:233-270.

81. Kakinuma, Y., Y. Ohsumi, and H. Anraku. 1981. Properties of H^+-translocating adenosine triphosphatase in vacuolar membranes of *Saccharomyces cerevisiae*. J. Biol. Chem. **256**:10859-10863.

82. Kane, P. M., C. T. Yamashiro, and T. H. Stevens. 1989. Biochemical characterization of the yeast vacuolar H^+-ATPase. J. Biol. Chem. **264**:19236-19244.

83. Kitamoto, K., K. Yoshizawa, Y. Ohsumi, and Y. Anraku. 1988. Dynamic aspects of vacuolar and cytosolic amino acid pools of *Saccharomyces cerevisiae*. J. Bacteriol. **170**:2683-2686.

84. Kitamoto, K., K. Yoshizawa, Y. Ohsumi, and Y. Anraku. 1988. Mutants of *Saccharomyces cerevisiae* with defective vacuolar function. J. Bacteriol. **170**:2687-2691.

85. Klein, U., H. Kresse, and K. von Figura. 1978. Sanfilippo syndrome type C: Deficiency of acetyl-CoA: α-glucosaminide N-acetyltransferase in skin fibroblasts. Proc. Natl. Acad. Sci. USA **75**:5185-5189.

86. Klionsky, D. J., L. M. Banta, and S. D. Emr. 1988. Intracellular sorting and processing of a yeast vacuolar hydrolase: Proteinase A propeptide contains vacuolar targeting information. Mol. Cell. Biol. **8**:2105-2116.

87. Klionsky, D. J., and S. D. Emr. 1989. Membrane protein sorting: Biosynthesis, transport and processing of yeast vacuolar alkaline phosphatase. EMBO J. **8**:2241-2250.

88. Klionsky, D. J., and S. D. Emr. 1990. A new class of lysosomal/ vacuolar protein sorting signals. J. Biol. Chem. **265**:5349-5352.

89. Klionsky, D. J., P. K. Herman, and S. D. Emr. 1990. The fungal vacuole: Composition, function and biogenesis. Microbiol. Rev., in press.

90. Kornfeld, R., and S. Kornfeld. 1985. Assembly of asparagine-linked oligosaccharides. Ann. Rev. Biochem. **54**:631-664.

91. Kornfeld, S. 1986. Trafficking of lysosomal enzymes in normal and disease states. J. Clin. Invest. **77**:1-6.

92. Kornfeld, S. 1987. Trafficking of lysosomal enzymes. FASEB J. **1**:462-468.

93. Kornfeld, S., and I. Mellman. 1989. The biogenesis of lysosomes. Ann. Rev. Cell Biol. **5**:483-525.

94. Krieg, U. C., P. Walter, and A. E. Johnson. 1986. Photocrosslinking of the signal sequence of nascent preprolactin to the 54-kilodalton polypeptide of the signal recognition particle. Proc. Natl. Acad. Sci. USA **83**:8604-8608.

95. Krieg, U. C., A. E. Johnson, and P. Walter. 1989. Protein translocation across the endoplasmic reticulum membrane: Identification by photocross-linking of a 39 kD integral membrane glycoprotein as part of a putative translocation tunnel. J. Cell Biol. **109**:2033-2043.

96. Kukuruzinska, M. A., M. L. E. Bergh, and B. J. Jackson. 1987. Protein glycosylation in yeast. Ann. Rev. Biochem. **56**:915-944.

97. Kurzchalia, T. V., M. Weidmann, A. S. Girshovich, E. S. Bochkareva, H. Bielka, and T. A. Rapoport. 1986. The signal sequence of nascent preprolactin interacts with the 54K polypeptide of the signal recognition particle. Nature **320**:634-636.

98. Lang, L., M. Reitman, J. Tang, R. M. Roberts, and S. Kornfeld. 1984. Lysosomal enzyme phosphorylation. Recognition of a protein-dependent determinant allows specific phosphorylation of oligosaccharides present on lysosomal enzymes. J. Biol. Chem. **259**:14663-14671.

99. Lang, L., T. Takahashi, J. Tang, and S. Kornfeld. 1985. Lysosomal enzyme phosphorylation in human fibroblasts. Kinetic parameters offer a biochemical rationale for two distinct defects in the uridine diphospho-N-acetylglucosamine:lysosomal enzyme precursor N-acetylglusosamine-1-phosphotransferase. J. Clin. Invest. **76**:2191-2195.

100. Lauffer, L., P. D. Garcia, R. N. Harkins, L. Coussens, A. Allrich, and P. Walter. 1985. Topology of signal recognition particle receptor in endoplasmic reticulum membrane. Nature **318**:334-338.

101. Lemansky, P., V. Gieselmann, A. Hasilik, and K. von Figura. 1985. Synthesis and transport of lysosomal acid phosphatase in normal and I-cell fibroblasts. J. Biol. Chem. **260**:9023-9030.

102. Lewis, V., S. A. Green, M. Marsh, P. Vihko, A. Helenius, and I. Mellman. 1985. Glycoproteins of the lysosomal membrane. J. Cell Biol. **100**:1839-1847.

103. Lippincott-Schwartz, J., and D. M. Fambrough. 1986. Lysosomal membrane dynamics: Structure and interorganellar movement of a major lysosomal membrane glycoprotein. J. Cell Biol. **102**:1593-1605.

104. Lippincott-Schwartz, J., and D. M. Fambrough. 1987. Cycling of the integral membrane glycoprotein, LEP100, between plasma membrane and lysosomes: Kinetic and morphological analysis. Cell **49**:669-677.

105. Little, L. E., O. T. Mueller, N. K. Honey, T. B. Shows, and A. L. Miller. 1986. Heterogeneity of N-acetylglucosamine 1-phosphotransferase within mucolipidosis III. J. Biol. Chem. **261**:733-738.

106. Lobel, P., N. M. Dahms, J. Breitmeyer, J. M. Chirgwin, and S. Kornfeld. 1987. Cloning of the bovine 215-kDa cation-independent mannose 6-phosphate receptor. Proc. Natl. Acad. Sci. **84**:2233-2237.

107. Lobel, P., N. M. Dahms, and S. Kornfeld. 1988. Cloning and sequence analysis of the cation-independent mannose 6-phosphate receptor. J. Biol. Chem. **263**:2563-2570.

108. Lobel, P., K. Fujimoto, R. D. Ye, G. Griffiths, and S. Kornfeld. 1989. Mutations in the cytoplasmic domain of the 275 kD mannose 6-phosphate receptor differentially alter lysosomal enzyme sorting and endocytosis. Cell **57**:787-796.

109. Makarow, M. 1985. Endocytosis in *Saccharomyces cerevisiae*: Internalization of enveloped viruses into spheroplasts. EMBO J. **4**:1855-1860.

110. Makarow, M. 1985. Endocytosis in *Saccharomyces cerevisiae*: Internalization of α-amylase and fluorescent dextran into cells. EMBO J. **4**:1861-1866.

111. Martin, J. J., J. G. Leroy, M. van Eygen, and C. Ceuterick. 1984. I-cell disease. A further report on its pathology. Acta Neuropathol. **64**:234-242.

112. Matile, P., H. Moor, and C. F. Robinow. 1969. Yeast cytology. In A. H. Rose, and J. S. Harrison (Eds.), *The Yeasts*. Academic Press, London. pp. 219-302.

113. Matile, P. 1978. Biochemistry and function of vacuoles. Ann. Rev. Plant Physiol. **29**:193-213.

114. McGrath, J. P., and A. Varshavsky. 1989. The yeast *STE6* gene encodes a homologue of the mammalian multidrug resistance P-glycoprotein. Nature **340**:400-404.

115. Mechler, B., and D. H. Wolf. 1981. Analysis of proteinase A function in yeast. Eur. J. Biochem. **121**:47-52.

116. Mechler, B., M. Muller, H. Muller, F. Meussdoeffer, and D. H. Wolf. 1982. *In vivo* biosynthesis of the vacuolar proteinases A and B in the yeast *Saccharomyces cerevisiae*. J. Biol. Chem. **257**:11203-11206.

117. Mechler, B., B. Muller, H. Muller, and D. Wolf. 1982. *In vivo* biosynthesis of vacuolar proteinases in proteinase mutants of *Saccharomyces cerevisiae*. Biochem. Biophys. Res. Commun. **107**:770-778.

118. Mechler, B., H. Muller, and D. H. Wolf. 1987. Maturation of vacuolar (lysosomal) enzymes in yeast: Proteinase yscA and proteinase yscB are catalysts of the processing and activation event of carboxypeptidase yscY. EMBO J. **6**:2157-2163.

119. Mechler, B., H. Hirsch, H. Muller, and D. H. Wolf. 1988. Biogenesis of the yeast lysosome (vacuole): Biosynthesis and maturation of proteinase yscB. EMBO J. **7**:1705-1710.

120. Mellman, I., R. Fuchs, and A. Helenius. 1986. Acidification of the endocytic and exocytic pathways. Ann. Rev. Biochem. **55**:663-700.

121. Meyer, D. I., E. Krause, and B. Dobberstein. 1982. Secretory protein translocation across membranes — the role of the "docking protein." Nature **297**:647-650.

122. Moehle, C. M., R. Tizard, S. K. Lemmon, J. Smart, and E. W. Jones. 1987. Protease B of the lysosome-like vacuole of the yeast *Saccharomyces cerevisiae* is homologous to the subtilisin family of serine proteases. Mol. Cell. Biol. **7**:4390-4399.

123. Moehle, C. M., C. K. Dixon, and E. W. Jones. 1989. Processing pathway for protease B of *Saccharomyces cerevisiae*. J. Cell Biol. **108**:309-324.

124. Mullock, B. M., W. J. Branch, M. van Schaik, L. K. Gilbert, and J. P. Luzio. 1989. Reconstitution of an endosome-lysosome interaction in a cell-free system. J. Cell Biol. **108**:2093-2099.

125. Munro, S., and H. R. B. Pelham. 1987. A C-terminal signal prevents secretion of luminal ER proteins. Cell **48**:899-907.

126. Myerowitz, R., and E. F. Neufeld. 1981. Maturation of α-L-iduronidase in cultured human fibroblasts. J. Biol. Chem. **256**:3044-3048.

127. Navon, G., R. G. Shulman, T. Yamane, T. R. Eccleshall, K.-B. Lam, J. J. Baronofsky, and J. Marmur. 1979. Phosphorus-31 nuclear magnetic resonance studies of wild-type and glycolytic pathway mutants of *Saccharomyces cerevisiae*. Biochem. **18**:4487-4499.

128. Nelson, H., S. Mandiyan, and N. Nelson. 1989. A conserved gene encoding the 57- kDa subunit of the yeast vacuolar H^+-ATPase. J. Biol. Chem. **264**:1775-1778.

129. Nelson, H., and N. Nelson. 1990. Disruption of genes encoding subunits of yeast vacuolar H^+-ATPase causes conditional lethality. Proc. Natl. Acad. Sci. USA, in press.

130. Neufeld, E. F., and V. A. McKusick. 1983. Disorders of lysosomal enzyme synthesis and localization: I-cell disease and pseudo-Hurler polydystrophy. In J. B. Stansbury (Ed.), *The Metabolic Basis of Inherited Disease*, 5th Edition, McGraw-Hill Book Co., New York. pp. 778-787.

131. Nilsson, T., M. Jackson, and P. A. Peterson. 1989. Short cytoplasmic sequences serve as retention signals for transmembrane proteins in the endoplasmic reticulum. Cell **58**:707-718.

132. Novick, P., and R. Schekman. 1979. Secretion and cell-surface growth are blocked in a temperature-sensitive mutant of *Saccharomyces cerevisiae*. Proc. Natl. Acad. Sci. USA **76**:1858-1862.

133. Novick, P., C. Field, and R. Scheckman. 1980. Identification of 23 complementation groups required for posttranslational events in the yeast secretory pathway. Cell **21**:205-215.

134. Novick, P., S. Ferro, and R. Schekman. 1981. Order of events in the yeast secretory pathway. Cell **25**:461-469.

135. Ohkuma, S., and B. Poole. 1978. Fluorescence probe measurement of the intralysosomal pH in living cells and the perturbation of pH by various agents. Proc. Natl. Acad. Sci. USA **75**:3327-3331.

136. Ohsumi, Y., and Y. Anraku. 1981. Active transport of basic amino acids driven by a proton motive force in vacuolar membrane vesicles of *Saccharomyces cerevisiae*. J. Biol. Chem. **256**:2079-2082.

137. Ohsumi, Y., and Y. Anraku. 1983. Calcium transport driven by a proton motive force in vacuolar membrane vesicles of *Saccharomyces cerevisiae*. J. Biol. Chem. **258**:5614-5617.

137a. Ohsumi, Y., K. Kitamoto, and Y. Anraku. 1988. Changes induced in the permeability barrier of the yeast plasma membrane by cupric ion. J. Bacteriol. **170**:2676-2682.

138. Oshima, A., C. M. Nolan, J. W. Kyle, J. H. Grubb, and W. S. Sly. 1988. The human cation-independent mannose 6-phosphate receptor. Cloning and sequence of the full-length cDNA and expression of functional receptor in COS cells. J. Biol. Chem. **263**:2553-2562.

139. Owada, M., and E. F. Neufeld. 1982. Is there a mechanism for introducing acid hydrolases into liver lysosomes that is independent of mannose 6-phosphate recognition? Evidence from I-cell disease. Biochem. Biophys. Res. Commun. **105**:814-820.

140. Payne, G. S., D. Baker, E. van Tuinen, and R. Schekman. 1988. Protein transport to the vacuole and receptor-mediated endocytosis by clatharin heavy chain-deficient yeast. J. Cell Biol. **106**:1453-1461.

141. Pelham, H. R. B. 1988. Evidence that luminal ER proteins are sorted from secreted proteins in a post-ER compartment. EMBO J. **7**:913-918.

142. Pelham, H. R. B., K. G. Hardwick, and M. J. Lewis. 1988. Sorting of soluble ER proteins in yeast. EMBO J. **7**:1757-1762.

143. Pfeffer, S. R. 1987. The endosomal concentration of a mannose 6-phosphate receptor is unchanged in the absence of ligand synthesis. J. Cell Biol. **105**:229-234.

144. Pohlmann, R., A. Waheed A. Hasilik, and K. von Figura. 1982. Synthesis of phosphorylated recognition marker in lysosomal enzymes is located in the *cis* part of the Golgi apparatus. J. Biol. Chem. **257**:5323-5325.

145. Pohlmann, R., G. Nagel, B. Schmidt, M. Stein, G. Lorkowski, C. Krentler, J. Cully, H. E. Meyer, K. H. Grzeschik, G. Mersmann, A. Hasilik, and K. von Figura. 1987. Cloning of a cDNA encoding the human cation-dependent mannose 6-phosphate-specific receptor. Proc. Natl. Acad. Sci. USA **84**:5575-5579.

146. Poruchynsky, M. S., and P. H. Atkinson. 1988. Primary sequence domains required for the retention of rotavirus VP7 in the endoplasmic reticulum. J. Cell Biol. **107**:1697-1706.

147. Preston, R. A., R. F. Murphy, and E. W. Jones. 1989. Assay of vacuolar pH in yeast and identification of acidification-defective mutants. Proc. Natl. Acad. Sci. USA **86**:7027-7031.

148. Pringle, J. R., R. A. Preston, A. E. M. Adams, T. Stearns, D. G. Drubin, B. K. Haarer, and E. W. Jones. 1989. Fluorescence microscopy methods for yeast. Meth. Cell Biol. **31**:357-435.

149. Reitman, M. L., and S. Kornfeld. 1981. UDP-N-acetylglucosamine: glycoprotein N-acetylglucosamine-1-phosphotransferase. Proposed enzyme for the phosphorylation of the high mannose oligosaccharide units of lysosomal enzymes. J. Biol. Chem. **256**:4275-4281.

150. Reitman, M. L., and S. Kornfeld. 1981. Lysosomal enzyme targeting. N-acetylglucosaminylphosphotransferase selectively phosphorylates native lysosomal enzymes. J. Biol. Chem. **256**:11977-11980.

151. Riezman, H. 1985. Endocytosis in yeast: Several of the yeast secretory mutants are defective in endocytosis. Cell **40**:1001-1009.

152. Robbins, A. R., and R. Myerowitz. 1981. The mannose 6-phosphate receptor of Chinese hamster ovary cells. Compartmentalization of acid hydrolases in mutants with altered receptors. J. Biol. Chem. **256**:10623-10627.

153. Robbins, A. R., S. S. Peng, and J. L. Marshall. 1983. Mutant Chinese hamster ovary cells pleiotropically defective in receptor-mediated endocytosis. J. Cell Biol. **97**:1064-1071.

154. Robbins, A. R., C. Oliver, J. L. Bateman, S. S. Krag, C. J. Galloway, and I. Mellman. 1984. A single mutation in Chinese hamster ovary cells impairs both Golgi and endosomal functions. J. Cell Biol. **99**:1296-1308.

155. Roberts, C. J., G. Pohlig, J. H. Rothman, and T. H. Stevens. 1989. Structure, biosynthesis, and localization of dipeptidyl aminopeptidase B, an integral membrane glycoprotein of the yeast vacuole. J. Cell Biol. **108**:1363-1373.

156. Roff, C. F., R. Fuchs, I. Mellman, and A. R. Robbins. 1986. Chinese hamster ovary cell mutants with temperature-sensitive defects in endocytosis. I. Loss of function on shifting to the nonpermissive temperature. J. Cell Biol. **103**:2283-2297.

157. Rose, J. K., and R. W. Doms. 1988. Regulation of protein export from the endoplasmic reticulum. Ann. Rev. Cell Biol. **4**:257-288.

158. Rothblatt, J. A., R. J. Deshaies, S. L. Sanders. G. Daum, and R. Schekman. 1989. Multiple genes are required for proper insertion of secretory proteins into the endoplasmic reticulum in yeast. J. Cell Biol. **109**:2641-2652.

159. Rothman, J. H., C. P. Hunter, L. A. Valls, and T. H. Stevens. 1986. Overproduction-induced mislocalization of a yeast vacuolar protein allows isolation of its structural gene. Proc. Natl. Acad. Sci. USA **83**:3248-3252.

160. Rothman, J. H., and T. H. Stevens. 1986. Protein sorting in yeast: Mutants defective in vacuole biogenesis mislocalize vacuolar proteins into the late secretory pathway. Cell **47**:1041-1051.

161. Rothman, J. H., I. Howald, and T. H. Stevens. 1989. Characterization of genes required for protein sorting and vacuolar function in the yeast *Saccharomyces cerevisiae*. EMBO J. **8**:2057-2065.

162. Rothman, J. H., C. T. Yamashiro, P. M. Kane, and T. H. Stevens. 1989. Protein targeting to the yeast vacuole. Trends Biochem. Sci. **14**:347-350.

163. Rothman, J. H., C. T. Yamashiro, C. K. Raymond, P. M. Kane, and T. H. Stevens. 1989. Acidification of the lysosome-like vacuole and the vacuolar H^+-ATPase are deficient in two yeast mutants that fail to sort vacuolar proteins. J. Cell Biol. **109**:93-100.

164. Ruohola, H., A. K. Kabcenell, and S. Ferro-Novick. 1988. Reconstitution of protein transport from the endoplasmic reticulum to the Golgi complex in yeast: The acceptor Golgi compartment is defective in the *sec*23 mutant. J. Cell Biol. **107**:1465-1476.

165. Sabatini, D. D., G. Kreibich, T. Morimoto, and M. Adesnik. 1982. Mechanisms for the incorporation of proteins in membranes and organelles. J. Cell Biol. **92**:1-22.

166. Sahagian, G. G., J. Distler, and G. W. Jourdian. 1981. Characterization of a membrane-associated receptor from bovine liver that binds phosphomannosyl residues of bovine testicular β-galactosidase. Proc. Natl. Acad. Sci. USA **78**:4289-4293.

167. Sahagian, G. G., J. J. Distler, and G. W. Jourdian. 1982. Membrane receptor for phosphomannosyl residues. Meth. Enzymol. **83**:392-396.

168. Sahagian, G. G., and E. F. Neufeld. 1983. Biosynthesis and turnover of the mannose 6-phosphate receptor in cultured Chinese hamster ovary cells. J. Biol. Chem. **258**:7121-7128.

169. Saheki, T., and H. Holzer. 1975. Proteolytic activities in yeast. Biochim. Biophys. Acta **384**:203-214.

170. Sato, T., Y. Ohsumi, and Y. Anraku. 1984. Substrate specificities of active transport systems for amino acids in vacuolar-membrane vesicles of *Saccharomyces cerevisiae*. J. Biol. Chem. **259**:11505-11508.

171. Sato, T., Y. Ohsumi, and Y. Anraku. 1984. An arginine/histidine exchange transport system in vacuolar-membrane vesicles of *Saccharomyces cerevisiae*. J. Biol. Chem. **259**:11509-11511.

172. Schmid, S. L., R. Fuchs, P. Male, and I. Mellman. 1988. Two distinct subpopulations of endosomes involved in membrane recycling and transport to lysosomes. Cell **52**:73-83.

173. Schmid, S., R. Fuchs, M. Kielian, A. Helenius, and I. Mellman. 1989. Acidification of endosome subpopulations in wild-type Chinese hamster ovary cells and temperature-sensitive acidification-defective mutants. J. Cell Biol. **108**:1291-1300.

174. Schulze-Lohoff, E., A. Hasilik, and K. von Figura. 1985. Cathepsin D precursors in clatharin-coated organelles from human fibroblasts. J. Cell. Biol. **101**:824-829.

175. Schwaiger, H., A. Hasilik, K. von Figura, A. Wiemken, and W. Tanner. 1982. Carbohydrate-free carboxypeptidase Y is transferred into the lysosome-like yeast vacuole. Biochem. Biophys. Res. Commun. **104**:950-956.

176. Siegel, V., and P. Walter. 1985. Elongation arrest is not a prerequisite for protein translocation across the microsomal membrane. J. Cell Biol. **100**:1913-1921.

177. Siegel, V., and P. Walter. 1988. Each of the activities of signal recognition particle (SRP) is contained within a distinct domain: Analysis of biochemical mutants of SRP. Cell **52**:39-49.

178. Stein, M., J. E. Zijderhand-Bleekemolen, H. Geuze, A. Hasilik, and K. von Figura. 1987. M_r 46,000 mannose 6-phosphate specific receptor: Its role in targeting of lysosomal enzymes. EMBO J **6**:2677-2681.

179. Stevens, T., B. Esmon, and R. Schekman. 1982. Early stages in the yeast secretory pathway are required for transport of carboxypeptidase Y to the vacuole. Cell **30**:439-448.

180. Stevens, T. H., J. H. Rothman, G. S. Payne, and R. Schekman. 1986. Gene dosage-dependent secretion of yeast vacuolar carboxypeptidase Y. J. Cell Biol. **102**:1551-1557.

181. Stoorvogel, W., H. J. Geuze, J. M. Griffith, and G. J. Strous. 1988. The pathways of endocytosed transferrin and secretory protein are connected in the *trans*-Golgi reticulum. J. Cell Biol. **106**:1821-1829.

182. Tager, J. M. 1985. Biosynthesis and deficiency of lysosomal enzymes. Trends Biochem. Sci. **10**:324-326.

183. Tajima, S., L. Lauffer, V. L. Rath, and P. Walter. 1986. The signal recognition particle receptor is a complex that contains two distinct polypeptide chains. J. Cell Biol. **103**:1167-1178.

184. Teichert, U., B. Mechler, H. Muller, and D. H. Wolf. 1989. Lysosomal (vacuolar) proteinases of yeast are essential catalysts for protein degradation, differentiation, and cell survival. J. Biol. Chem. **264**:16037-16045.

185. Tkacz, J. S., and J. O. Lampen. 1972. Wall replication in *Saccharomyces* species: Use of fluorescein-conjugated concanavalin A to reveal the site of mannan insertion. J. Gen. Microbiol. **72**:243-247.

186. Tkacz, J. S., and J. O. Lampen. 1973. Surface distribution of invertase on growing *Saccharomyces* cells. J. Bacteriol. **113**:1073-1075.

187. Tycko, B., and F. R. Maxfield. 1982. Rapid acidification of endocytic vesicles containing α_2 macroglobulin. Cell **28**:643-651.

188. Uchida, E., Y. Ohsumi, and Y. Anraku. 1985. Purification and properties of H^+-translocating, Mg^{2+}-adenosine triphosphatase from vacuolar membranes of *Saccharomyces cerevisiae*. J. Biol. Chem. **260**:1090-1095.

189. Urech, K., M. Durr, T. Boller, A. Wiemken, and J. Schwencke. 1978. Localization of polyphosphate in vacuoles of *Saccharomyces cerevisiae*. Arch. Microbiol. **116**:275-278.

190. Valls, L. A., C. P. Hunter, J. H. Rothman, and T. H. Stevens. 1987. Protein sorting in yeast: The localization determinant of yeast vacuolar carboxypeptidase Y resides in the propeptide. Cell **48**:887-897.

191. Varki, A., and S. Kornfeld. 1980. Identification of a rat liver α-N-acetylglucosaminyl phosphodiesterase capable of removing "blocking" α-N-acetylglucosamine residues from phosphorylated high mannose oligosaccharides of lysosomal enzymes. J. Biol. Chem. **255**:8398-8401.

192. Varki, A., and S. Kornfeld. 1981. Purification and characterization of rat liver α-N-acetylglucosaminyl phosphodiesterase. J. Biol. Chem. **256**:9937-9943.

193. Varki, A. P., M. L. Reitman, and S. Kornfeld. 1981. Identification of a variant of mucolipidosis III (pseudo-Hurler polydystrophy): A catalytically active N-acetylglucosaminylphosphotransferase that fails to phosphorylate lysosomal enzymes. Proc. Natl. Acad. Sci. USA **78**:7773-7777.

194. Vladutiu, G. D., and M. C. Rattazzi. 1979. Excretion-reuptake route of β-hexosaminidase in normal and I-cell disease cultured fibroblasts. J. Clin. Invest. **63**:595-601.

195. von Figura, K., V. Gieselmann, and A. Hasilik. 1984. Antibody to mannose 6-phosphate specific receptor induces receptor deficiency in human fibroblasts. EMBO J. **3**:1281-1286.

196. von Figura, K., and A. Hasilik. 1986. Lysosomal enzymes and their receptors. Ann. Rev. Biochem. **55**:167-193.

197. Wada, Y., Y. Ohsumi, M. Tanifuji, M. Kasai, and Y. Anraku. 1987. Vacuolar ion channel of the yeast, *Saccharomyces cerevisiae*. J. Biol. Chem. **262**:17260-17263.

198. Waheed, A., A. Hasilik, and K. von Figura. 1981. Processing of the phosphorylated recognition marker in lysosomal enzymes. Characterization and partial purification of a microsomal α-N-acetylglucosaminyl phosphodiesterase. J. Biol. Chem. **256**:5717-5721.

199. Waheed, A., A. Hasilik, and K. von Figura. 1982. UDP-N-acetylglucosamine:lysosomal enzyme precursor N-acetylglucosamine-1-phosphotransferase. Partial purification and characterization of the rat liver Golgi enzyme. J. Biol. Chem. 257:12322-12331.

200. Waheed, A., R. Pohlmann, A. Hasilik, K. von Figura, A. van Elsen, and J. G. Leroy. 1982. Deficiency of UDP-N-acetylglusoamine: lysosomal enzyme N-acetylglucosamine-1-phosphotranferase in organs of I-cell patients. Biochem. Biophys. Res. Commun. **105**:1052-1058.

201. Waheed, A., S. Gottschalk, A. Hille, C. Krentler, R. Pohlmann, T. Braulke, H. Hauser, H. Geuze, and K. von Figura. 1988. Human lysosomal acid phosphatase is transported as a transmembrane protein to lysosomes in transfected baby hamster kidney cells. EMBO J. **7**:2351-2358.

202. Walter, P., and G. Blobel. 1980. Purification of a membrane-associated protein complex required for protein translocation across the endoplasmic reticulum. Proc. Natl. Acad. Sci. USA **77**:7112-7116.

203. Walter, P., I. Ibrahimi, and G. Blobel. 1981. Translocation of proteins across the endoplasmic reticulum. I. Signal recognition particle (SRP) binds to in vitro-assembled polysomes synthesizing secretory protein. J. Cell Biol. **91**:545-550.

204. Walter, P., and G. Blobel. 1981. Translocation of proteins across the endoplasmic reticulum. II. Signal recognition particle (SRP) mediates the selective binding to microsomal membranes of in vitro-assembled polysomes synthesizing secretory protein. J. Cell Biol. **91**:551-556.

205. Walter, P., and G. Blobel. 1981. Translocation of proteins across the endoplasmic reticulum. III. Signal recognition particle (SRP) causes signal sequence-dependent and site-specific arrest of chain elongation that is released by microsomal membranes. J. Cell Biol. **91**:557-561.

206. Walter, P., and G. Blobel. 1982. Signal recognition particle contains a 7S RNA essential for protein translocation across the endoplasmic reticulum. Nature **299**:691-698.

207. Waters, M. G., and G. Blobel. 1986. Secretory protein translocation in a yeast cell-free system can occur posttranslationally and requires ATP hydrolysis. J. Cell Biol. **102**:1543-1550.

208. Weisman, L. S., R. Bacallao, and W. Wickner. 1987. Multiple methods of visualizing the yeast vacuole permit evaluation of its morphology and inheritance during the cell cycle. J. Cell Biol. **105**:1539-1547.

209. Weisman, L. S., and W. Wickner. 1988. Intervacuole exchange in the yeast zygote: A new pathway in organelle communication. Science **241**:589-591.

210. Weisman, L. S., S. D. Emr, and W. Wickner. 1990. Mutants of *Saccharomyces cerevisiae* that block intervacuole vesicular traffic and vacuole division and segregation. Proc. Natl. Acad. Sci. USA **87**:1076-1080.

211. Westenberg, B., T. Boller, and A. Wiemken. 1989. Lack of arginine- and polyphosphate-storage pools in a vacuole-deficient mutant (end1) of *Saccharomyces cerevisiae*. FEBS Lett. **254**:133-136.

212. Wieland, F. T., M. L. Gleason, T. A. Serafini, and J. E. Rothman. 1987. The rate of bulk flow from the endoplasmic reticulum to the cell surface. Cell **50**:289-300.

213. Wiemken, A., P. Matile, and H. Moor. 1970. Vacuolar dynamics in synchronously budding yeast. Arch. Microbiol. **70**:89-103.

214. Wiemken, A., and M. Durr. 1974. Characterization of amino acid pools in the vacuolar compartment of *Saccharomyces cerevisiae*. Arch. Microbiol. **101**:45-57.

215. Wiemken, A., M. Schellenberg, and K. Urech. 1979. Vacuoles: The sole compartments of digestive enzymes in yeast (*Saccharomyces cerevisiae*)? Arch. Microbiol. **123**:23-35.

216. Willingham, M. C., I. H. Pastan, G. G. Sahagian, G. W. Jourdian, and E. F. Neufeld. 1981. Morphologic study of the internalization of a lysosomal enzyme by the mannose 6-phosphate receptor in cultured Chinese hamster ovary cells. Proc. Natl. Acad. Sci. USA **78**:6967-6971.

217. Wilson, C., T. Connolly, T. Morrison, and R. Gilmore. 1988. Integration of membrane proteins into the endoplasmic reticulum requires GTP. J. Cell Biol. **107**:69-77.

218. Woolford, C. A., L. B. Daniels, F. J. Park, E. W. Jones, J. N. van Arsdell, and M. A. Innis. 1986. The *PEP4* gene encodes an aspartyl protease implicated in the posttranslational regulation of *Saccharomyces cerevisiae* vacuolar hydrolases. Mol. Cell. Biol. **6**:2500-2510.

219. Yoshihisa, T., Y. Ohsumi, and Y. Anraku. 1988. Solubilization and purification of α-mannosidase, a marker enzyme of vacuolar membranes in *Saccharomyces cerevisiae*. J. Biol. Chem. **263**:5158-5163.

220. Yoshihisa, T., and Y. Anraku. 1989. Nucleotide sequence of *AMS*1, the structure gene of vacuolar α-mannosidase of *Saccharomyces cerevisiae*. Biochem. Biophys. Res. Commun. **163**:908-915.

221. Zimmerman, U. 1978. Physics of turgor- and osmoregulation. Ann. Rev. Plant Physiol. **29**:121-148.

222. Zubenko, G. S., and E. W. Jones. 1981. Protein degradation, meiosis and sporulation in proteinase-deficient mutants of *Saccharomyces cerevisiae*. Genetics **97**:45-64.

Chapter 2

Protein Sorting in *Saccharomyces cerevisiae*: Isolation of Mutants Defective in the Delivery and Processing of Multiple Vacuolar Hydrolases

Jane S. Robinson, Daniel J. Klionsky, Lois M. Banta and Scott D. Emr

Molecular and Cellular Biology **8**:4936-4948 (1988)

This paper was the result of a collaborative effort. Jane Robinson isolated the *vpt* mutants and performed the cell fractionation and genetic analyses. Daniel Klionsky assisted with the immunoprecipitation experiments. I carried out the quantitative assays for enzyme activity (i.e., the data presented in Tables 1 and 2).

ABSTRACT

Using a selection for spontaneous mutants that "mislocalize" a vacuolar carboxypeptidase Y-Invertase (CPY-Inv) fusion protein to the cell surface, vacuolar protein targeting (*vpt*) mutants in twenty-five new *vpt* complementation groups have been identified. Additional alleles in each of the eight previously identified *vpt* complementation groups (*vpt*1-8) were also obtained. Representative alleles from each of the 33 *vpt* complementation groups (*vpt*1-*vpt*33) have been shown to exhibit defects in the sorting of several native vacuolar proteins including the soluble hydrolases CPY, Proteinase A (PrA), and Proteinase B (PrB). Protein secretion, however, appears to be unaffected in the *vpt* mutants. Eighteen of the 33 complementation groups were found to contain mutant alleles that lead to extreme defects in the processing and/or sorting of each of these three soluble proteases. Indeed, most of these mutants missort and secrete more than 75% of CPY. The lack of significant leakage of cytosolic markers from the *vpt* mutant cells indicates that the vacuolar protein sorting defects associated with these mutants do not result from cell lysis. In addition, the observation that the precursor rather than the mature forms of CPY, PrA, and PrB are secreted from the *vpt* mutants is consistent with mislocalization occurring at a stage after Golgi-specific modification, but prior to final vacuolar sorting of these enzymes. Vacuolar membrane protein sorting appears to be unaffected in the great majority of the *vpt* mutants. However, a subset of the *vpt* mutants (*vpt*11, 16, 18, and 33) was found to exhibit defects in the sorting of a vacuolar membrane marker enzyme, α-mannosidase. Up to 50% of the α-mannosidase enzyme activity was found to be mislocalized to the cell surface in these *vpt* mutants. Seven of the *vpt* complementation groups (*vpt*3, 11, 15, 16, 18, 29, and 33) contain alleles that lead to a conditional lethal phenotype, temperature sensitive (*ts*) for vegetative cell growth. This *ts* phenotype has been shown to be recessive and to cosegregate with the vacuolar protein sorting defect in each case. Tetrad analysis has shown that *vpt*3 maps to chromosome 15R, and *vpt*15 maps to chromosome 2R. Intercrosses with other mutants

that exhibit defects in vacuolar protein sorting or function (*vpl*, *sec*, *pep*, and *end* mutants) have revealed several overlaps among these different sets of genes. Together, these data indicate that more than 50 gene products are involved, directly or indirectly, in the processes of vacuolar protein sorting.

INTRODUCTION

A basic and fundamental question in biology is that of how a cell is constructed spatially from the information encoded by its genes and from maternally inherited cues and structures. This spatially segregated cellular organization is critical for normal cell functioning. To understand the process, it is important to know not only how the cytoskeletal elements fit together and define the overall shape and structure of the cell, but also how proteins, structural and otherwise, find their way to appropriate locations within the cell. An analysis of the assembly and maintenance of each organelle individually could provide a view of the mechanism underlying the cellular construction process.

Protein sorting to mammalian lysosomes represents one of the best characterized protein delivery pathways (21,40). Much is known about the route followed by lysosomal enzymes, and a few components of the sorting machinery have been characterized at the biochemical and molecular levels. However, this is a complex process and we still lack a detailed understanding of the molecular mechanisms underlying this sorting pathway. We have chosen to work on protein sorting to the yeast equivalent of the mammalian lysosome, the vacuole. The yeast *Saccharomyces cerevisiae* is the organism of choice because we wish to take a genetic approach to solving the vacuolar protein targeting problem. The vacuole is an acidic compartment involved in amino acid and inorganic ion storage, as well as various degradative and nutrient recycling functions, especially under starvation conditions (22,46). It contains a variety of hydrolytic enzymes including the soluble glycoproteins carboxypeptidase Y (CPY), proteinase A (PrA), and proteinase B (PrB); and several membrane-bound enzymes including an α-mannosidase, a proton-translocating ATPase, dipeptidylaminopeptidase B, and several permeases (46,48).

Vacuolar proteins transit along with proteins destined for secretion through the early stages of the secretory pathway (41). The transport of the lumenal enzymes CPY and PrA has been studied in the greatest detail (19,20,38,41). Each is synthesized

initially as an inactive preproenzyme that is translocated into the lumen of the ER where the transient N-terminal signal peptide is removed and the proteins are modified with N-linked core oligosaccharide (13). These intermediate precursor forms are referred to as p1CPY and p1PrA. The p1 forms are then delivered to the Golgi complex where further glycosyl modifications convert them to larger p2 forms. At this stage, it is presumed that proteins on their way to the vacuole are sorted from other secretory proteins destined for secretion or assembly into the plasma membrane (10,12,41). Vesicular carriers are presumed to mediate Golgi-vacuole transfer of these enzymes. At present there is no evidence concerning the existence of an intermediate compartment, between the Golgi and the vacuole in yeast, analogous to the endosomal compartment detected in mammalian cells. Just prior to, or more likely, upon arrival in the vacuole, the p2 forms of CPY and PrA are proteolytically cleaved to their mature forms (mCPY and mPrA) (23,24). This proteolytic maturation is dependent on the presence of active vacuolar PrA, and involves the removal of N-terminal pro-segments from each protein (14). Similarly, other vacuolar enzymes such as PrB also appear to be made and transported in precursor form and to undergo PrA-dependent proteolytic maturation in the vacuole (23,25; C. Moehle and E. Jones, personal communication).

The observations that mutations in the CPY vacuole sorting signal or high gene dosage-induced overproduction of CPY and PrA lead to missorting and secretion of these proteins indicate that a failure to sort vacuolar proteins results in their delivery to the cell surface (16,42,44). This rationale was used by Rothman and Stevens to identify mutants defective in vacuolar protein sorting by isolating yeast strains that secrete CPY (37). Through this approach, they identified mutants that were assigned to 8 complementation groups (referred to as *vpl* for vacuolar protein localization defective mutants). Independently, we employed a gene fusion-based selection scheme to isolate mutants defective in vacuolar protein targeting (*vpt*) (2). Using this approach, mutants defective in the vacuolar sorting of a carboxypeptidase Y-invertase hybrid protein (CPY-

Inv433) (16) were selected. Eight *vpt* complementation groups were identified and shown to missort and secrete the CPY-Inv hybrid protein as well as wild-type CPY protein (2). The advantages of the invertase fusion approach include the following: 1) the identification of mutants is not dependent on their secretion of active CPY, 2) the gene fusion approach in theory could be applied to any vacuolar protein whether its biochemical activity was known or not, and 3) the absence or presence of external invertase activity can be easily assayed and powerful genetic selection procedures have been developed that demand the presence of external invertase activity.

In this work, we have greatly extended the gene fusion approach to isolate and biochemically characterize some 500 new *vpt* mutants. Here we describe the genetic and biochemical analysis of these vacuolar protein targeting mutants. Our results indicate that many different gene functions participate in the events associated with normal vacuolar protein sorting. This process is likely to involve several distinct steps including the selective recognition of vacuolar proteins, their packaging into transport vesicles, delivery of these vesicles to the correct target organelle, recognition and fusion with the target, release of the vacuolar proteins and recycling of transport components for additional rounds of protein sorting.

MATERIALS AND METHODS

Yeast strains. *Saccharomyces cerevisiae* strains SEY6210 (*MATα leu2-3,112 ura3-52 his3-Δ200 trp1-Δ901 lys2-801 suc2-Δ9 GAL*) and SEY6211 (*MATα leu2-3,112 ura3-52 his3-Δ200 trp1-Δ901 ade2-101 suc2-Δ9 GAL*) were constructed by standard genetic methods (39). Both strains contain a complete deletion (*suc2-Δ9*) of the chromosomal copy of *SUC2* and contain no other unlinked invertase structural genes (8). SEY6210 and SEY6211 were transformed to uracil independence with either of two CPY-Inv fusion encoding plasmids, pCYI-50 and pCYI-433 (16). *vpt* mutant alleles *vpt1-1* through *vpt8-1* (2) in the SEY2101 (*MATα ura3-52 leu2-3,112, suc2-Δ9 ade2-101*) (8) strain background were used for complementation tests with new *vpt* mutants isolated in strain SEY6210

(this work). They were also crossed with SEY6210 to give *MATα lys2-801 vpt1-1* through *vpt8-1* strains for crossing with new *vpt* mutants isolated from SEY6211.

Media and genetic methods. YPD, minimal yeast media, sporulation media and Bromocresol purple (BCP) indicator plates were prepared as described (39). The BCP plates contained 2% sucrose as the sole carbon source, and were spread with 0.2 mg Antimycin A in 95% ethanol just before use (2). Wickerham's minimal medium (45), modified as described in (16), was used for cell growth before and during labeling with $Na^{35}SO_4$ (ICN). Standard genetic methods (39) were used throughout. Replica plating to test phenotypes of segregants, etc., was done with a 48-pronged replicator, using dilution in sterile 96-well microtiter dishes (26). Rapid complementation analysis was carried out by using the pronged replicator to transfer arrays of 48 new *vpt* mutants to microtiter dishes containing *vpt* tester strains of the opposite mating type suspended in liquid YPD. Mating and diploid growth were allowed to occur in the wells for two days at 26°C. Replicas were then made to minimal media, supplemented to select for diploids. The resulting diploid patches were transferred without dilution to YP fructose and assayed for external invertase activity using a rapid filter replica assay method (16,20) to score complementation.

Enzyme assays. The procedures and unit definitions used for assays of yeast enzymes have already been described as follows: invertase and α-glucosidase (16), carboxypeptidase Y (42), proteinase A (1), α-mannosidase (30) and glyceraldehyde-3-phosphate dehydrogenase (4,47).

Labeling, fractionation and immunoprecipitation. Spheroplasts were prepared and labeled using a modification of the method described (34). Cells were grown to mid-log phase in Wickerham's minimal medium (16) supplemented with 0.2% yeast extract. Four OD_{600} units of cells were then centrifuged and resuspended in 0.1 M Tris SO_4 pH 9.4, 10 mM DTT and incubated at 30°C for 5 min, centrifuged again and resuspended in Wickerham's minimal medium adjusted to pH 7.4, containing 1.3 M sorbitol. Lyticase was

added to final activity of 30 units/OD and the cultures were incubated at 30° for 20 min to remove the cell wall. Spheroplasts were pelleted, resuspended in Wickerham's minimal medium containing 1.3 M sorbitol, and labeled with Tran^{35}S label (0.2 mCi/ml) for 20 min at 30°C. Chase was initiated by the addition of methionine (50 µg/ml final concentration). The labeled culture was separated into spheroplast (intracellular) and medium (extracellular) fractions. To examine proteins in the media fraction, cells were grown and labeled as described (16). The whole cells were then separated from the medium fraction by centrifugation, precipitated with 5% TCA, resuspended in loading buffer and run on 10% SDS polyacrylamide gels. Antisera to PrA, CPY, and Inv were prepared as described in (19).

Materials: Lyticase was from Enzogenetics, Tran^{35}S-label was from ICN Radiochemicals and all other chemicals were from Sigma Chemical Co. Antiserum to PrB was a gift from C. Moehle and E. Jones.

RESULTS

Isolation of 25 new *vpt* complementation groups. Previously, we observed that short amino-terminal domains of CPY sequence, when fused to mature enzymatically active invertase, can quantitatively divert delivery of this normally secreted enzyme to the yeast vacuole (16). Yeast cells require external invertase activity to grow on sucrose as a sole fermentable carbon source, so we could exploit the sorting behavior of the CPY-Inv hybrid protein to select mutants that "missort" and secrete the fusion protein. Yeast strains deleted for all endogenous genes encoding invertase (*Δsuc*) but containing a low copy number (*CENIV, ARSI*) plasmid encoding an appropriate CPY-Inv hybrid protein as their only source of invertase activity can not grow on sucrose because all the invertase activity is sequestered in the vacuole (Fig. 1). Suc^+ derivatives of such cells can be isolated simply by selecting for growth on sucrose media. Based on earlier results, many of these mutants were expected to also mislocalize the native vacuolar enzyme CPY, because targeting of the fusion proteins to the vacuole is dependent on the presence of the CPY vacuolar sorting signal at the amino-terminal end of the CPY-Inv hybrid proteins (16). In the present study, we decided to select such mutants using two different CPY-Inv hybrid proteins, CPY-Inv50 (encoded by plasmid pCYI-50) and CPY-Inv433 (encoded by plasmid pCYI-433) (Fig. 1). These gene fusions are composed of the coding sequence for the N-terminal 50 and 433 amino acids of proCPY, respectively, fused in frame to a truncated form of the *SUC2* gene carried on the *E. coli-S. cerevisiae* shuttle vector pSEYC306 (16). This modified *SUC2* gene lacks its 5' regulatory sequences and the coding sequence for its amino terminal signal peptide (16; Fig. 1). These two fusions are glycosylated to different extents during their passage to the yeast vacuole. Based on this, we reasoned that they may not follow precisely the same route to the vacuole and therefore, one might expect to obtain a broader spectrum of sorting defective mutants using both of these fusions rather than confining the study to only one or the other.

Suc$^+$ mutant strains were isolated from the *Δsuc2* strains SEY6210 and SEY6211, harboring either pCYI-50 or pCYI-433. To select Suc$^+$ mutants, single colonies of the 4 parental strains were plated on YP media with sucrose as the sole carbon source, antimycin A as an inhibitor of respiration, and BCP (Bromocresol purple) as a pH indicator, which turns yellow when sucrose is being fermented. Only one spontaneous mutant derived from each parental colony was picked to ensure that each mutation event was independent. 505 Suc$^+$ mutants were obtained and characterized, 241 *MATa* Suc$^+$ "*vpt*" mutants (isolated from SEY6211) and 264 *MATα* Suc$^+$ "*vpt*" mutants (from SEY6210). We confirmed that these *vpt* mutants secreted the CPY-Inv hybrid protein by carrying out a rapid filter assay for external invertase activity. This assay involves patching the mutants on YP fructose plates, incubating at 26°C for 24-36 h, then making replicas onto Whatman #1 filters pre-soaked in an invertase assay solution (16,20). External invertase reacts with the assay mixture to produce a red spot at the position of the appropriate cell patch. The presence of internal invertase activity can be confirmed by exposing the cell patches to chloroform vapor, which lyses the yeast cells, prior to transfer onto the assay filter. This simple method permitted us to get an initial indication of the extent of the mislocalization defect for each new *vpt* mutant. All of the *vpt* mutants were found to express external invertase activity by this assay. In the parental control strains, all of the invertase activity was internal as determined by the assay.

The invertase filter assay was also used to determine whether the *vpt* mutations were dominant or recessive in diploids derived by backcrossing each of the *vpt* mutants to the appropriate parent strain (SEY6210 or SEY6211). Recessive *vpt* mutants were then intercrossed, diploids were isolated and the filter assay was used to assign the *MATa* *vpt* x *MATα* *vpt* diploids to complementation groups (Fig. 2). Complementing pairs of recessive *vpt* mutants exhibited no external invertase activity (white patch on invertase filter assays), whereas noncomplementing pairs of *vpt* mutants gave rise to red patches

on the filters corresponding to the secretion of invertase activity. In general, the assay gave unambiguous results as shown in Fig. 2. Of the 505 new *vpt* mutants, 17 were found to contain mutations that led to a dominant Suc^+ phenotype. The remaining 488 mutants were recessive. Of these, 184 (84 *MATa* and 100 *MATα*) could be assigned to the previously identified *vpt* complementation groups, *vpt*1 through *vpt*8 (2). The remaining *MATa* *vpt* mutants were systematically crossed with new *MATα* *vpt* mutants until they could be assigned to new complementation groups (arbitrarily defined as containing one *MATa* and one *MATα* allele). Twenty-five new *vpt* complementation groups were identified (*vpt*9-*vpt*33) (Table 1). This left 21 recessive *MATa* *vpt* mutants and 36 recessive *MATα* *vpt* mutants that had been crossed with at least one allele from each of the 33 *vpt* complementation groups, and had in addition been crossed with all the remaining unassigned *vpt* mutants of the opposite mating type. All 21 unassigned *MATa* mutants complemented each of the remaining 36 unassigned *MATα* *vpt* mutants. We did not construct *MATa* and *MATα* alleles of each of these 57 unassigned *vpt* mutants and continue the complementation analysis further.

Because the *vpt* mutants were selected as spontaneous events, we expected that they would correspond to single site mutations. To obtain further support for this, many of the *vpt* mutants (*vpt* 3, 4, 7, 9, 11, 14, 15, 16, 18, 29, and 33) were crossed with parental *VPT* strains and subjected to tetrad analysis. For each mutant tested, the *vpt* defect as well as all the other markers scored in the cross segregated with the expected 2:2 Mendelian inheritance pattern of simple single locus mutations. This confirmed that these *vpt* mutants represent single site changes and further indicated that the genetic defects associated with these mutants do not result in any gross mating or chromosomal abnormalities. In the course of these analyses we noticed that two of the *vpt* mutants appeared to be linked to auxotrophic markers heterozygous in the crosses. The segregation data for *vpt*3 and *ade*2 (17 PD: 1 T: 0 NPD) indicated that *vpt*3 was linked to *ade*2. The approximate map distance (calculated as described in 39) between *ade*2 and

vpt3 is ~2.8 centimorgans. This locates the *VPT3* locus on the right arm of chromosome 15 where *ADE2* has been mapped (27). Another of the *vpt* mutants, *vpt15*, appears to be linked to *lys2* (17 PD:5 T:0 NPD), in this case less tightly (~11.4 centimorgans). The *LYS2* gene has been mapped to the right arm of chromosome 2 (27).

Mislocalization of vacuolar enzymes in the *vpt* mutants. At least one mutant from each of the 33 *vpt* complementation groups was subjected to a series of enzyme assays to quantitate the extent of the mislocalization defect and to test if mislocalization of the CPY-Inv fusion protein was due to cell lysis.

The extent of "mislocalization" of the CPY-invertase hybrid protein was determined for several alleles of each complementation group by assaying external invertase (in whole cells) as well as total invertase (in lysed cells) and then calculating the percent of invertase activity that is secreted (16). The results obtained for a representative *vpt* mutant allele from each complementation group are presented in Table 1. In most cases other alleles from the same complementation group secreted the CPY-Inv hybrid protein to a similar extent. Two to five alleles from each *vpt* complementation group were assayed. The alleles for which assay data are shown in Table 1 were used in all subsequent analyses.

The most obvious unrelated defect that might lead to the apparent secretion of vacuolar proteins is cell lysis. For this reason, assays of a cytoplasmic marker enzyme, glyceraldehyde-3-phosphate dehydrogenase (G3PDH), were carried out to determine if any of the *vpt* mutants exhibit significant levels of external G3PDH activity. In no case was there evidence of significant leakage of this cytoplasmic marker enzyme into an extracellular fraction. Furthermore, the level of cell-associated G3PDH activity detected after detergent lysis of *vpt* mutant cells was similar to that detected in the parental strains (SEY6210, SEY6211) (Table 1). In addition, the mutants were tested for the presence of external α-glucosidase, another cytoplasmic enzyme. Again no evidence for lysis was found (data not shown). As discussed below, the *vpt* mutants secrete

precursor forms of the vacuolar proteins and not the mature forms as would be expected if cell lysis were responsible for the observed secretion.

As an initial crude test to determine if the new *vpt* mutants also secrete CPY, we assayed CPY enzyme activity in each mutant. Since CPY is normally processed from the inactive p2 zymogen to the mature active form inside the vacuole, it is expected that if CPY is missorted into the media, it will not become activated or will be activated poorly (41,42). Thus, the more extreme the *vpt* mislocalization defect, the lower the cell-associated CPY activity is expected to be relative to the parental strains SEY6210 and SEY6211. As shown in Table 1, CPY activity levels ranged from 2% of parental activity in *vpt5* up to 82% in *vpt23*. It can be seen that CPY activity levels are inversely proportional to the level of CPY-Inv secreted from most of the *vpt* mutants (Table 2). For example, some mutants such as *vpt5* and *vpt33* are very defective by both criteria, whereas others, including *vpt2* and *vpt20*, do not show major defects by either assay. This result indicates that the behavior of the CPY-Inv hybrid protein in the *vpt* mutants accurately reflects the effect these mutations have on CPY activity and presumably on its localization.

The availability of PrA-Inv hybrid proteins that are efficiently targeted to the vacuole (Fig. 1; 19,20), offered a simple way for us to test the effect of *vpt* mutations on the localization of another protein that is found in the vacuole in wild-type yeast. To this end, the representative *vpt* alleles were cured of the plasmids encoding CPY-Inv fusions and retransformed with a vector (pP4I-404) encoding a fusion protein, PrA-Inv404, consisting of the N-terminal 404 amino acids of PrA fused to mature active invertase. The hybrid protein expressed by pP4I-404 is delivered efficiently to the vacuole in *VPT* yeast (19). Invertase assays showed that in most of the *vpt* mutants significant amounts of PrA-Inv hybrid protein were secreted instead of being targeted to the vacuole (Table 1). The most severe *vpt* mutants, as estimated by the reduction in CPY activity levels and secretion of the CPY-Inv hybrid proteins, were also the mutants

that exhibited the largest defects in PrA-Inv sorting (Table 1). It is possible that both PrA and CPY use a common delivery pathway.

We were also interested in determining if, in addition to the sorting of soluble vacuolar hydrolases, sorting of vacuolar membrane proteins was affected in any of the *vpt* mutants. One vacuolar membrane enzyme that has been well characterized is α-mannosidase. This enzyme is not dependent on PrA processing for its activation (18), and thus would be expected to remain active even when mislocalized (to the cell surface, for example). The *vpt* mutants were tested for the presence of cell surface α-mannosidase activity by assaying whole as well as detergent-lysed cells. The only *vpt* mutants that showed significant levels of external cell-associated α-mannosidase activity were *vpt*10, 11, 15, 16, 18, 27, and 33 (Table 1). It is interesting to note that these mutants, with the exception of *vpt*10 and *vpt*27, are severely defective by several other criteria, including CPY and PrA mislocalization (Fig. 5), and the possession of additional phenotypes such as temperature sensitivity (Table 1) and abnormal vacuolar morphology (3). All of the representative *vpt* alleles shown in Table I were non-temperature-sensitive alleles. To further address the α-mannosidase localization defect, we also assayed the potentially more severe *ts* alleles of each complementation group for which they were available (*vpt* 11, 15, 16, 18 and 33). Interestingly, we observed as much as 40-50% of the α-mannosidase activity at the cell surface in some *ts* alleles of *vpt*11, 16, 18, and 33 even when grown at the permissive growth temperature (25°C). No evidence for cell lysis of the *ts* alleles was obtained.

We suspected that some of the *vpt* mutants might secrete an altered spectrum of proteins as compared to wild-type, *VPT* yeast for two reasons. First, since secretory and vacuolar proteins transit together through portions of the secretory pathway (41), some gene products affecting the delivery of molecules to the vacuole might also affect the transport of other molecules destined for secretion. Thus, if the *vpt* mutations affect the secretion pathway, some extracellular proteins might be missing or reduced in the

medium isolated from certain of the *vpt* mutant strains. Second, and conversely, additional protein species may accumulate in the growth medium, since the *vpt* mutants were selected for their ability to secrete vacuolar contents. To address these questions, we examined the secretion of radioactively labeled proteins by some *vpt* mutants into the growth medium. Cells were labeled with $^{35}SO_4$ for 20 min and then chased for 20 min in the presence of excess unlabeled SO_4. Media proteins were precipitated in TCA, resolved by SDS-Page, and examined by autoradiography (Fig. 4). No striking differences between the media fractions isolated from wild-type or *vpt* mutant cells were observed. Comparable amounts of a similar set of proteins were observed in extracts from both wild-type and *vpt* mutant cells. Two of the mutants (*vpt7* and *vpt11*) exhibited an extra protein band in addition to the set observed in *VPT* yeast (Fig. 4). We have not determined if either of these new bands corresponds to a known vacuolar protein. Based on their apparent molecular weights, these proteins are not CPY or PrA. Because we analyzed the media from pulse-labeled cells, we can also infer that the rate of normal protein secretion is not grossly altered in the *vpt* mutants. The lack of new media proteins corresponding to CPY or PrA is probably due to the instability of these mislocalized proteins (41,2) as well as their relatively low abundance as compared to the media proteins observed under these experimental conditions.

In addition, many of the mutants were transformed with an invertase-encoding plasmid (pRB58) and tested for normal invertase secretion (assay and calculations as described; 28). The *vpt* mutants were found to secrete invertase at the same levels as wild-type *VPT* yeast. This provides further evidence that the *vpt* mutants carry out secretion normally.

vpt mutants exhibit defects in the sorting and processing of several vacuolar proteins. To directly assess the extent of the sorting defect in the various *vpt* mutants, we labeled and fractionated *vpt* mutant cells. Antisera directed against CPY, PrA, and PrB were used to detect the amount and form of these different vacuolar proteins in

each cell fraction. Initially, cells were labelled and fractionated into media, periplasm, and spheroplast fractions, with subsequent immunoprecipitation by anti-CPY and anti-PrA antisera. These data (not shown) allowed us to categorize the *vpt* mutants based on the severity of their CPY and PrA localization and processing defects. However, we noticed that during the fractionation, presumably because of the incubation time required to remove the cell wall enzymatically, some fraction of these proteins was being degraded or modified. To avoid this, we converted the mutant cells to spheroplasts prior to labeling and fractionation. In this way we were able to look at mislocalization by simply isolating spheroplast (pellet) and media fractions by centrifugation. The media fraction corresponds to all material secreted from the cells, including those proteins normally retained in the periplasm. A further advantage of labeling spheroplasts is that because lysed spheroplasts do not incorporate the label, it reduces the background of labeled vacuolar proteins in the media resulting from cell lysis during spheroplast preparation. To confirm that the spheroplast labeling technique does not alter normal protein secretion or protein sorting to the vacuole, we initially analyzed the modification and processing of the secreted enzyme, invertase, and the vacuolar proteins, CPY and PrA, in spheroplasts prepared from a wild-type strain. As can be seen in Figs. 3 and 5, both protein secretion and vacuolar protein sorting and processing appear to be normal. Indeed, we observed that the level of protein expression as well as the kinetics of protein modification and delivery also appear to be normal in the spheroplast labeling technique (16,20). This argues that secretory protein traffic occurs normally in yeast spheroplasts.

Wild-type and *vpt* mutant spheroplasts were labeled with ^{35}S methionine for 20 min and chased with cold methionine for 30 min. Supernatant (external) and pellet (internal) fractions were immunoprecipitated with anti-CPY antisera. We observed two significant effects of the *vpt* mutants on the biogenesis of the vacuolar protein carboxypeptidase Y (Fig. 5). First, processing was altered; 14 of the mutants exhibited no mature CPY at all (*vpt*1, 3, 4, 5, 6, 7, 11, 15, 16, 17, 18, 29, 30, 33), and an additional 5 *vpt* mutants

processed less than 30% of CPY to the mature form (*vpt*8, 9, 13, 19, 26). Second, missorting and secretion of CPY were observed. Two of the *vpt* mutants (*vpt*15 and *vpt*29) secreted more than 95% of CPY into the periplasmic/medium fraction. An additional 12 *vpt* mutants (*vpt*1, 3, 4, 5, 6, 7, 11, 16, 17, 18, 30, 33) were almost as defective, they secreted between 60% and 80% of CPY (Fig. 5). These 14 most defective mutants exhibited a complete defect in maturation of the small amount of CPY that remained associated with the spheroplast fraction, as discussed above, indicating that the accumulated proCPY is not being sorted to the vacuole, or possibly that the vacuole of these mutants is so defective that it is not competent for the processing of proCPY. Many of the remaining *vpt* mutants exhibited less severe defects in the sorting of the CPY protein. In these mutants, a substantial portion of CPY remained spheroplast-associated and was processed to the mature active enzyme, indicating that some of the proCPY is being sorted correctly to the vacuole (Fig. 5).

To determine if this protein sorting defect is specific for CPY or extends to other vacuolar proteins, we examined sorting and processing of two additional vacuolar proteins, PrA and PrB, in the *vpt* mutants. Relative to CPY, lower levels of both PrA and PrB were secreted by the *vpt* mutants. However, we noted that the extent of the defect in maturation of these proteins paralleled that observed for CPY in each of the *vpt* mutants (Figs. 5 and 6). The simple absence of CPY in the vacuole cannot explain the accumulation of precursor forms of PrA and PrB as maturation of these proteases is not dependent on CPY function. This suggested that the defect in vacuolar sorting of PrA and PrB may be similar to that observed for CPY, but that secretion of the missorted PrA and PrB is blocked. We reasoned that the reduced level of proPrA and proPrB in the media fraction might be due to a reduced rate in secretion of these missorted proteins. To address this possibility, we extended the length of the chase period from 30' to 90', otherwise performing the fractionation and immunoprecipitation as described above. When this experiment was carried out on *vpt*5, *vpt*11, and *vpt*15, no

increases in the media levels of proPrA or proPrB were observed after this extended chase period (data not shown). We also observed in this experiment that no additional processing of the proPrA and proPrB occurred during the chase.

An alternative explanation is that the lack of these proteins in the media fraction might not be due to a block in secretion of the mislocalized zymogens, but rather to the specific or nonspecific association of these proteins with the spheroplast membrane surface. To test this possibility, we treated the labeled spheroplasts with 500 μg per ml of proteinase K for 30 min at 0°C to determine if any of the cell-associated proPrA and proPrB was accessible to the exogenously added protease. Several *vpt* mutants (*vpt5*, 17, and 26) were analyzed in this way and in each case, PrA and PrB were unaffected by the added proteinase K. As expected, secreted CPY was degraded under these conditions. Both PrA and PrB were, however, subject to degradation if the detergent, Triton X-100 (1%) was added prior to protease addition. Taken together, these experiments indicate that proPrA and proPrB accumulate in some intracellular compartment. The present data do not rule out the vacuole as the site in which these proteins reside, however the lack of processing of the accumulated proteins suggests that this may not be case. This lack of processing does not eliminate the vacuole as the site of accumulation of PrA and PrB because of the observation that in missense PrA mutants, CPY activity is normal but PrA activity is decreased (24).

Several *vpt* mutants are temperature-sensitive for growth. It is not clear if vacuolar protein sorting is essential for yeast cell growth. The *pep4* mutants (49) are defective in enzyme activities of many soluble vacuolar hydrolases, yet they grow normally at all temperatures. We selected our mutants at 26° to allow us to score for potential temperature-conditional phenotypes. Thus, after the mutants had been selected for their ability to grow on sucrose media at 26°C, they were tested for their ability to grow at 37° on YPD. Of the 505 mutants isolated, 23 (approximately 5%) were temperature-sensitive (*ts*) for growth at 37° (i.e., they did not form colonies at 37°). As

shown in Table 1, these *ts* mutants belong to six *vpt* complementation groups (*vpt*11, 15, 16, 18, 29, and 33). In addition, one allele of *vpt*3 had a partial *ts* phenotype (very small colonies at 37°). Genetic crosses and tetrad analysis were used to confirm that in each case the *ts* phenotype cosegregated with the *vpt* protein sorting defect. One *ts* allele from each complementation group was crossed to the parent strain (SEY6210 or SEY6211), sporulated, and subjected to tetrad dissection. Ten or more tetrads were examined for each cross (an example of the cosegregating phenotypes is shown in Fig. 7). The remaining *ts* alleles in a given complementation group were inferred to be linked to the appropriate *vpt* locus by complementation testing at 37°. It is interesting to note that of the *vpt* complementation groups that contain *ts* alleles (not including *vpt*3), 22 out of 50 total alleles (i.e., 44%) in these complementation groups are *ts*. Thus, the *ts* alleles are not scattered at random throughout the total set of *vpt* complementation groups. In addition, the complementation groups which possess *ts* alleles all tend to exhibit more severe defects by several criteria. These defects include missorting of vacuolar proteins, sensitivity to high osmotic pressure, and inability to assemble morphologically normal vacuoles (3).

As described above, the *ts vpt* mutants exhibit a vacuolar protein sorting defect at the permissive growth temperature. We examined the *ts* alleles at restrictive temperature to see if the transport defect was exaggerated further and thereby might explain their inviability at 37°. The mutants were preincubated for 60 min at 37°, then labeled for 20 min with $^{35}SO_4$ and chased for 20 min, both at 37°. Immunoprecipitation with CPY antibody showed that there is no apparent difference in CPY processing or secretion at the restrictive temperature (not shown), but it should be noted that all of these *ts vpt* mutants exhibit extreme defects in vacuolar protein sorting even at the permissive temperature. Since the *ts vpt* mutants secrete invertase at 37°C, secretion apparently is not blocked at this temperature (see below). Because the defect in CPY sorting and processing is nearly complete even at the permissive growth temperature, the

absence of growth at the nonpermissive temperature may be explained either by appearance of a more complete sorting defect at the high temperature which alters the sorting of additional vacuolar proteins and possibly also affects secreted proteins that are essential for growth. Alternately, it may be that the combined stress of growth at high temperature together with a defect in vacuolar protein sorting may in an additive fashion prevent cell growth at 37°C. For example, it is possible that a loss of vacuole protein localization at high temperature may result in a block in secretion or endocytosis, or both, since these defects have been shown to be lethal (28,36). To address these questions, the *ts vpt* mutants were tested in several ways for possible secretory or endocytic defects. First, the *ts vpt* mutants were transformed with a plasmid, pRB58 carrying the entire wild-type structural gene and regulatory sequences of *SUC2*, and tested for invertase secretion at restrictive and permissive temperatures. For the restrictive temperature experiment, cells were shifted to 37° for 60 or 120 min prior to the assay. Activities in whole cells and lysed cells were measured and compared to determine the percent of invertase secreted (28). The mutants tested were not found to be significantly different from the parent strain, SEY6210, harboring the same *SUC2* plasmid (data not shown). This implies that the *ts vpt* mutants do not exhibit an invertase secretion defect at 37°. Second, the *ts vpt* mutants were tested for genetic overlap with the temperature-sensitive secretion-defective mutants, *sec*1-23 (28) and *sec*53 (11). The *sec* mutants are defective for the secretion of invertase at 37°C and are blocked for transport at various stages of the secretory pathway in yeast (29). *sec* x *vpt* diploids were selected and tested for complementation of the temperature sensitivity at 37°C. In each case complementation was observed, implying that there is no genetic overlap between these two sets of mutants. The *ts vpt* mutants were also crossed with the *ts* endocytosis-defective mutant, *end*1 (6). Diploids were again tested for *ts* growth defects. It was found that *vpt*11 did not complement *end*1, implying that these two mutants are allelic to one another. This genetic overlap raises the possibility that some

of the *vpt* mutants may have a defect in endocytosis, possibly at the restrictive temperature as discussed above.

Overlap between the *vpt* and *vpl* mutants. Independent of our *vpt* mutant screen, Rothman and Stevens have also isolated mutants defective in *v*acuolar *p*rotein *l*ocalization, *vpl*1-*vpl*8 (37). Recently, they have extended this work and selected new *vpl* mutants and assigned them to 11 new *vpl* complementation groups (T. Stevens, personal communication). Intercrosses of the *vpt* mutants with all the *vpl* mutants allowed us to determine the overlap between these two sets of presumably related mutants. Each of the *vpl* mutants (*vpl*1-19) was crossed with our Suc$^-$ parental strain, diploids were selected and sporulated, and Suc$^-$ *vpl* segregants were identified. These *Δsuc vpl* mutants were then crossed to representative *vpt* mutant alleles from each complementation group, harboring the CPY-Inv433 hybrid protein encoding plasmid. Mislocalization of the hybrid protein from the diploids was scored by invertase filter assays. The results of these complementation studies are shown in Table 3. We observed that twelve of the thirty-three *vpt* mutants overlapped with *vpl* complementation groups. This overlap was confined in most cases, to *vpt* complementation groups with the less severe vacuolar protein localization defects (see Tables 1 and 3). At present, we do not have an explanation for this observation. Differences in the selection schemes used or in the starting strains may in part have affected the final set of mutants obtained. Rothman and Stevens (unpublished data) have employed another complementation assay technique and have independently confirmed each of these results. To avoid future confusion regarding these two classes of mutants, we have decided to use the general term *vps* for "*v*acuolar *p*rotein *s*orting" to describe both classes of mutants (Table 3).

Some differences were seen between *vpl* and *vpt* mutants in terms of levels of missorting of vacuolar proteins. For example, *vpt5* and *vpl5* are in the same complementation group (*vps5*). The *vpl5* allele analyzed by Rothman and Stevens showed a weaker protein sorting defect for CPY and PrA than did *vpt5* (2,37; Fig. 5). This result

may indicate allele differences. However, since the two mutations are in unrelated genetic backgrounds, the discrepancy also could be due to strain background differences.

Some members of another class of mutants, the *pep* mutants, may also affect vacuolar protein sorting (17). Complementation analysis has shown that there is genetic overlap between small subsets of the *pep*, *vpt* and *vpl* mutants (T. Stevens and E. Jones, personal communication).

DISCUSSION

In an effort to identify additional mutants exhibiting novel defects in vacuolar protein sorting and to develop an appreciation for the number of gene functions that may contribute to this process, we have exploited a CPY-Inv fusion-based selection scheme (2) to isolate more than 500 new *vpt* mutants. The mutants have been assigned to some 33 different complementation groups, seven of which contain *ts* alleles. Even though this is an unexpectedly large number of complementation groups, our data suggest that many additional gene functions are likely to influence the vacuolar protein delivery pathway. Several of the newly isolated *vpt* mutants could not be assigned to any of these 33 complementation groups. In addition, genetic comparison of the *vpt* mutants with similar mutants from other labs (*sec*, *pep*, *vpl*, *end*; 6, 11, 17, 28, 37) affecting secretory protein delivery or processing, indicates that although there is overlap among some of these different sets of mutants, more than 50 gene functions are implicated in the vacuolar protein sorting process.

This large number of genes can be interpreted to indicate that vacuolar protein sorting is a very complex process involving a series of distinct and precisely controlled sorting events. These include translocation into ER, sorting to and through the Golgi complex, separation from proteins destined for secretion or Golgi retention, and selective delivery to the vacuole, possibly via an intermediate endosome-like compartment. Because each of these steps is likely to be catalyzed by proteins that are

re-used through several rounds of protein transfer, any mutations that affect their level of expression, stability, activity or ability to recycle back to the appropriate compartment of action may lead to sorting defects. Alternatively, the large number of mutants identified may suggest that many unrelated physiological and cellular defects can interfere with vacuolar protein sorting by indirectly influencing the process. That the former argument (that the *vpt* mutations cause specific changes in the targeting machinery) may indeed be the case for the more severe *vpt* mutants, is supported by the following observations. 1) All of the late-acting *sec* mutants, which exhibit major defects in protein secretion, do not alter the delivery or maturation of CPY (41). 2) Yeast strains deleted for the gene encoding the clathrin heavy chain do not exhibit defects in vacuolar protein biogenesis, even though the growth rate and intracellular morphology of these mutants is dramatically different from that of wild-type cells (31,32). 3) Cell fractionation and enzyme assay data rule out the release of vacuolar proteins as a consequence of yeast cell lysis. 4) Though many of the *vpt* mutants exhibit major defects in the targeting and maturation of vacuolar proteins, protein secretion as well as many other cell functions, including cell division, mating, and respiratory growth, remain largely unaffected. Direct evidence concerning the specificity of the events affected by the *vpt* mutants will depend on the identification of the various *vpt* gene products, their site of action in the cell, and their individual biochemical activities.

Several observations led us to suspect that if vacuolar enzymes were not efficiently targeted to the vacuole, they would appear in the medium. Both CPY and PrA travel through the initial part of the secretory pathway (19,41), so it can be postulated that if CPY or PrA fail to be diverted to the vacuole at the appropriate step, they might continue to be carried through the secretory pathway and end up at the cell surface. Indeed, much evidence has accumulated suggesting that many proteins are secreted by a default mechanism, while vacuolar and lysosomal enzymes must be actively sorted away from these proteins (5,33). In addition, gene dosage-induced overproduction of CPY or

PrA, or mutational changes in the vacuolar sorting signals of these proteins, lead to their missorting and secretion (16,19,42,44), suggesting that if the vacuolar targeting apparatus is overloaded or unable to recognize vacuolar proteins, the default reaction for these proteins is secretion. A similar overproduction-induced mislocalization phenotype has been observed for the vacuolar CPY-Inv and PrA-Inv hybrid proteins (2,19). Finally, an initial set of vacuolar protein mislocalization mutants which missort and secrete vacuolar enzymes had already been obtained by this scheme (2,37).

The *vpt* mutants were selected on the basis of their ability to missort and secrete a hybrid vacuolar protein, CPY-Inv. The sorting of the artificial hybrid protein, CPY-Inv, fairly accurately reflects the sorting of the native CPY protein. Several lines of evidence support this conclusion. CPY-Inv hybrid proteins, carrying the CPY sorting signal, are very efficiently localized to the vacuole, as is true for native CPY (16,19). Mutants selected as defective in the vacuolar sorting of CPY-Inv hybrid proteins (*vpt*), also exhibit similar defects in the sorting of wild-type CPY (2). Enzyme assay data from this work, and (2), demonstrate that the extent of mislocalization of both the CPY-Inv hybrid proteins and native CPY protein correlate closely in each of the *vpt* mutants (2; Table 2). The *vpt* mutants genetically overlap with the *vpl* mutants, which were selected by an independent scheme for defects in CPY sorting (37; Table 3).

The observation that CPY-Inv hybrid proteins appear to accurately mimic the sorting and transport of native vacuolar CPY protein, provided us with a convenient scheme for the rapid selection and genetic classification of the vacuolar protein targeting (*vpt*) mutants. This approach also offers the advantage that it can be generally applied to the study of other gene products independent of any knowledge of their biochemical activity (7,8,15).

It is of interest to note that though the extent of the sorting defects seen in different *vpt* mutants may vary, each mutant individually appears to exhibit qualitatively similar defects in the sorting/processing of the three proteins analyzed; CPY, PrA, and

PrB. Though the *vpt* mutants do not secrete the same level of proCPY, proPrA, and proPrB, they all appear to exhibit similar proteolytic processing defects for each of these proteins (Figs. 5 and 6). The *vpt* mutants cause significantly higher levels of proCPY to be mislocalized to the media than observed for either proPrA or proPrB. Most of the *vpt* mutants secrete p2 CPY forms, indicating that this protein passes correctly through the Golgi complex. Although some level of secretion of proPrA and proPrB is observed in many of the *vpt* mutants, the bulk of each of these precursor proteins appears to accumulate in an intracellular compartment distinct from the vacuole. They remain associated with the spheroplast cell fraction and are not degraded when extracellular proteases are added to the labeled spheroplasts. The proteins accumulate in their precursor forms, even though in many *vpt* mutants, mature forms are also present, indicating that the vacuoles of these mutants are still competent for precursor maturation (Figs. 5 and 6). We do not know where in the cells the precursors accumulate nor why they are not secreted like proCPY. The PrA-Inv hybrid protein is efficiently secreted by many of the vpt mutants (Table 1 and Fig. 5) suggesting that PrA itself is missorted in the mutants but cannot transit through later stages of the secretory pathway as efficiently as the PrA-Inv hybrid protein (invertase is normally secreted by yeast and may facilitate transit of the PrA-Inv hybrid). proPrA and proPrB may associate specifically or nonspecifically with some component of an intracellular membrane or they may be diverted into a compartment that does not communicate with the cell surface. The vacuolar protein sorting signals in both proCPY and proPrA have been identified but they appear to share no significant primary sequence similarities (16,20,44) and therefore may be recognized by different carrier systems.

Given the extreme sorting/processing defects seen for proCPY, proPrA, and proPrB in most of the *vpt* mutants, one might expect that all protein traffic to the vacuole would be altered. We have found, however that the great majority of the *vpt* mutants continue to assemble morphologically normal vacuoles (3). Indeed, when we assayed for

the location of the vacuolar membrane marker enzyme, α-mannosidase, we found that it was not mislocalized to the cell surface in most of the *vpt* mutants. Vacuoles isolated from two of these mutants (*vpt3* and *vpt4*) retained normal levels of this enzyme activity (2). However, a small subset of the *vpt* mutants does exhibit significant defects in the sorting of α-mannosidase activity. Alleles of *vpt*11, 16, 18, and 33 secrete up to 50% of their α-mannosidase activity to the cell surface. Interestingly, this same set of *vpt* mutants also exhibits other phenotypes that are consistent with these mutants having defects in both lumenal and membrane vacuolar protein sorting. These phenotypes include absence of a detectable vacuole in the mutant cells using light or electron microscopy, and accumulation of novel membrane-enclosed structures that may correspond to intermediates in vacuole membrane biogenesis (3).

An important unresolved question regarding protein sorting to mammalian lysosomes or to the yeast vacuole is whether lumenal proteins transit together with integral membrane proteins and if so, does a common sorting apparatus participate in directing delivery of these two distinct sets of proteins? In the case of I-cell disease, many lysosomal lumenal enzymes are missorted; however, certain membrane proteins clearly continue to be faithfully sorted to the vacuole (35,40,43). Our results indicate that at least some vacuolar membrane proteins may share a common sorting step or compartment with soluble vacuolar proteins en route to the vacuole. Clearly, however, other sorting events appear to be specific for each set of proteins. In most of the mutants, α-mannosidase is sorted to the vacuole in a *vpt*-independent manner.

A useful observation is that 7 of the *vpt* complementation groups have alleles exhibiting a temperature-sensitive growth defect (on YPD at 37°C). In each case, this *ts* growth defect has been shown to be genetically linked to the *vpt* phenotype. It is probably not coincidental that these mutants all exhibit interesting additional vacuole-related defects. These *ts vpt* mutants can be divided into three groups on the basis of their additional phenotypes and characteristics. 1) *vpt15* and *vpt29*; these two

complementation groups have the most severe localization defect for CPY and PrA (Fig. 5). In addition, they both exhibit abnormal morphologies, including the accumulation of vesicular and Golgi-related structures, and apparently enlarged vacuoles relative to *VPT* yeast (3). 2) *vpt*11, 16, 18, and 33; these four *vpt* mutants also exhibit severe defects in the sorting of CPY, and show the accumulation of most of their PrA in precursor form, indicating that it probably also does not reach the vacuole. These mutants exhibit the most striking structural defects of any of the *vpt* mutants, since they do not contain a morphologically identifiable vacuole. 3) *vpt3*; this mutant has one *ts* allele, and is moderately defective in CPY and PrA localization, as assessed by immunoprecipitation (Fig. 5). The *vpt3* mutant is interesting morphologically because it appears to contain highly fragmented vacuoles (3).

A surprising finding concerning the *ts vpt* mutants was that none of them exhibits a more severe sorting or vacuole morphology defect at the non-permissive temperature than observed at the permissive temperature, 26°C. The *ts vpt* mutants also did not show any apparent defects in the secretion of wild-type invertase at 37°C. Thus, in the absence of any additional detectable phenotypes at 37°C apart from the actual death of the cells, it seems possible that certain vacuole functions may only be required for growth at high temperature, and these functions are missing in the *ts vpt* mutants.

One of the *vpt* mutants (*vpt*11) was found to be allelic to the *ts* endocytosis defective mutant, *end*1 (6). This observation is interesting because it provides the first genetic evidence for a link between the endocytotic and biosynthetic delivery routes to the yeast vacuole. The result is not unexpected because some mutants defective in the secretory pathway (*sec*) are also defective in endocytosis (36), and, as discussed above, early stages of vacuolar protein targeting are *sec*-dependent (41). Clearly, it will be of interest to address the endocytic competence of the *vpt* mutants.

We have identified many new genes whose products are involved in the process of vacuolar protein targeting. We expect that many of the gene products act directly in

targeting and transport of molecules to the yeast vacuole. More detailed information about how the vacuolar targeting pathway operates is anticipated upon cloning of the *VPT* genes and detailed biochemical characterization of the gene products.

ACKNOWLEDGEMENTS

We would like to thank John DeModena for excellent technical assistance, and Cathy Elkins for her patience in typing the manuscript. We are grateful to Elizabeth Jones and Charles Moehle for their generous gift of anti-PrB antisera, and to Howard Riezman, Joel Rothman and Tom Stevens for communicating their results prior to publication. In addition, we wish to thank David Bedwell, Paul Herman and Tom Vida for critical reading of the manuscript and valuable discussions during the course of the work. This study was supported by Public Health Service grant GM-32703 from the National Institutes of Health to S.D.E. J.S.R. was supported by graduate fellowships from the Lucy Mason Clark fund and the Markey Charitable Trust fund, L.M.B. was supported by graduate fellowships from the National Science Foundation and General Electric, D.J.K. was supported by a research fellowship from the Helen Hay Whitney Foundation, and S.D.E. is an NSF Presidential Young Investigator supported by National Science Foundation grant DCB-8451633.

LITERATURE CITED

1. Ammerer, G., C. P. Hunter, J. H. Rothman, G. C. Saari, L. A. Valls, and T. H. Stevens. 1986. *PEP4* gene of *Saccharomyces cerevisiae* encodes Proteinase A, a vacuolar enzyme required for processing of vacuolar precursors. Mol. Cell. Biol. 6:2490-2499.

2. Bankaitis, V. A., L. M. Johnson, and S. D. Emr. 1986. Isolation of yeast mutants defective in protein targeting to the vacuole. Proc. Natl. Acad. Sci. USA 83:9075-9079.

3. Banta, L. M., J. S. Robinson, D. J. Klionsky, and S. D. Emr. 1988. Organelle assembly in yeast: Characterization of yeast mutants defective in vacuolar biogenesis and protein sorting. J. Cell. Biol., submitted.

4. Bernstein, M., W. Hoffman, G., Ammerer, and R. Schekman. 1985. Characterization of a gene product (Sec53p) required for protein assembly in the yeast endoplasmic reticulum. J. Cell Biol. 101:2374-2382.

5. Burgess, T. L. and R. B. Kelly. 1987. Constitutive and regulated secretion of proteins. Ann. Rev. Cell Biol. 3:243-293.

6. Chvatcho, Y., I. Howald, and H. Riezman. 1986. Two yeast mutants defective in endocytosis are defective in phenemone response. Cell 46:355-364.

7. Douglas, M. G., B. L. Geller, and S. D. Emr. 1984. Intracellular targeting and import of an F_1-ATPase β-subunit-β-galactosidase hybrid protein into yeast mitochondria. Proc. Natl. Acad. Sci. USA 81:3983-3987.

8. Emr, S. D., R. Schekman, M. C. Flessel, and J. Thorner. 1983. An MFα1-SUC2 (α-factor invertase) gene fusion for study of protein localization and gene expression in yeast. Proc. Natl. Acad. Sci. USA 80:7080-7084.

9. Esmon, P. C., B. E. Esmon, T. E. Schaer, A. Taylor, and R. Schekman. 1987. Structure, assembly, and secretion of octameric invertase. J. Biol. Chem. 262:4387-4394.

10. Farquhar, M. G. and G. E. Palade. The Golgi apparatus (complex)-(1954-1981)-from artifact to center stage. J. Cell. Biol. **81**:77s-103s.

11. Ferro-Novick, S., P. Novick, C. Field, and R. Schekman. 1984. Yeast secretory mutants that block the formation of active cell surface enzymes. J. Cell. Biol. **98**:35-43.

12. Griffiths, F. and K. Simons. 1986. The *trans* Golgi network: Sorting at the exit site of the Golgi complex. Science **234**:438-443.

13. Hasilik, A. and W. Tanner. 1978. Biosynthesis of the vacuolar yeast glycoprotein carboxypeptidase Y. Eur. J. Biochem. **85**:599-608.

14. Hemmings, B. A., G. S. Zubenko, A. Hasilik and E. W. Jones. 1981. Mutant defective in processing of an enzyme located in the lysosome-like vacuole of *Saccharomyces cerevisiae*. Proc. Natl. Acad. Sci. USA **78**:435-439.

15. Hoffmann, W. 1987. *CAN1-SUC2* gene fusion studies in *Saccharomyces cerevisiae*. Mol. Gen. Genet. 210:277-281.

16. Johnson, L. M., V. A. Bankaitis, and S. D. Emr. 1987. Distinct sequence determinants direct intracellular sorting and modification of a yeast vacuolar protease. Cell **48**:875-885.

17. Jones, E. W. 1977. Proteinase mutants of *Saccharomyces cerevisiae*. Genetics **85**:23-33.

18. Jones, E. W., G. S. Zubenko, and R. R. Parker. 1982. *PEP4* gene function is required for expression of several vacuolar hydrolases in *Saccharomyces cerevisiae*. Genetics 102:665-677.

19. Klionsky, D. J., L. M. Banta, J. S. Robinson, and S. D. Emr. (1988). Vacuolar protein targeting and organelle biogenesis in yeast. Molec. Biol. of Organelle Assembly, in press.

20. **Klionsky, D. J., L. M. Banta and S. D. Emr.** 1988. Intracellular sorting and processing of a yeast vacuolar hydrolase: ProteinaseA propeptide contains vacuolar targeting information. Mol. Cell. Biol. **8**:2105-2116.

21. **Kornfeld, S.** (1986). Trafficking of lysosomal enzymes in normal and diseased states. J. Clin. Invest. **77**:1-6.

22. **Matile, P., H. Moor, and C. F. Robinow.** 1969. Yeast cytology. In *The Yeasts*. A. H. Rose and J. S. Harrison, eds., Academic Press, London. pp. 219-302.

23. **Mechler, B., M. Müller, H. Müller, F. Meussdoerffer, and D. H. Wolf.** 1982. *In vivo* biosynthesis of the vacuolar proteinases A and B in the yeast *Saccharomyces cerevisiae*. J. Biol. Chem. **257**:11203-11206.

24. **Mechler, B., H. Müller and D. H. Wolf.** 1987. Maturation of vacuolar (lysosomal) enzymes in yeast: Proteinase yscA and proteinase yscB are catalysts of the processing and activation event of carboxypeptidase yscY. EMBO **6**:2157-2163.

25. **Mechler, B., H. H. Hirsch, H. Muller and D. H. Wolf.** 1988. Biogenesis of the yeast lysosome (vacuole): biosynthesis and maturation of proteinase yscB. EMBO **7**:1705-1710.

26. **Moir, D., S. Stewart, B. Osmond, and D. Botstein.** 1982. Cold-sensitive cell-division-cycle mutants of yeast: Isolation, properties and pseudoreversion studies. Genetics **100**:547-563.

27. **Mortimer, R. K. and D. C. Hawthorne.** 1986. Genetic mapping in *Saccharomyces*. Genetics **53**:165-173

28. **Novick, P., C. Field, and R. Schekman.** 1980. Identification of 23 complementation groups required for post-translational events in the yeast secretory pathway. Cell **21**:205-215.

29. **Novick, P., S. Ferro, and R. Schekman.** 1981. Order of events in the yeast secretory pathway. Cell **25**:461-469.

30. **Opheim, D. J.** 1978. α-D-mannosidase of *Saccharomyces cerevisiae*, characterization and modulation of activity. Biochim. Biophys. Acta. **524**:121-130.

31. **Payne, G. S., T. B. Hasson, M. S. Hasson, and R. Schekman.** 1987. Genetic and biochemical characterization of clathrin-deficent *Saccharomyces cerivisiae*. Mol. Cell Biol. **7**:3888-3898.

32. **Payne, G. S., D. Baker, E. van Tuinen, and R. Schekman.** 1988. Protein transport to the vacuole and receptor-mediated endocytosis by clathrin heavy chain-deficient yeast. J. Cell. Biol. **106**:1453-1461.

33. **Pfeffer, S. R., J. E. Rothman.** 1987. Biosynthetic protein transport and sorting by the endoplasmic reticulum and Golgi. Ann. Rev. Biochem. **56**:829-852.

34. **Reid, G. A.** 1983. Pulse labeling of yeast cells and spheroplasts. Meth. Enzymol. **97**:324-329.

35. **Reitman, M. L., A. Varki, and S. Kornfeld.** 1981. Fibroblasts from patients with I-cell disease and pseudo-Hurler polydystrophy are deficient in uridine 5'-diphosphate-N-acetylglucosamine:glycoprotein N-acetylglucosaminylphospho-transferase activity. J. Clin. Invest. **67**:1574-1579.

36. **Riezman, H.** 1985. Endocytosis in yeast: Several of the yeast secretory mutants are defective in endocytosis. Cell **40**:1001-1009.

37. **Rothman, J. H., and T. H. Stevens.** 1986. Protein sorting in yeast: Mutants defective in vacuole biogenesis mislocalize vacuolar proteins into the late secretory pathway. Cell **47**:1041-1051.

38. **Rothman, J. H., and T. H. Stevens.** 1988. Protein sorting and biogenesis of the lysosome-like vacuole in yeast. In: *Protein Transfer and Organelle Biogenesis*, R. C. Das and P. W. Robins, Eds. In press.

39. **Sherman, F., G. R. Fink, and C. W. Lawrence.** 1979. Methods in yeast genetics: A laboratory manual. Cold Spring Harbor Laboratory, Cold Spring Harbor, NY.

40. **Sly, W. S., and Fischer, H. D.** 1982. The phosphomannosyl recognition system for intracellular and intercellular transport of lysosomal enzymes. J. Cell Biochem. **18**:67-85.

41. **Stevens, T., B. Esmon, and R. Schekman.** 1982. Early stages in the yeast secretory pathway are required for transport of carboxypeptidase Y to the vacuole. Cell **30**:439-448.

42. **Stevens, T. H., J. H. Rothman, G. S. Payne, and R. Schekman.** 1986. Gene dosage-dependent secretion of yeast vacuolar carboxypeptidase Y. J. Cell. Biol. **102**:1551-1557.

43. **Tager, J. M.** 1985. Biosynthesis and deficiency of lysosomal enzymes. Trends Biochem. Sci. **10**:324-326.

44. **Valls, L. A., C. P. Hunter, J. H. Rothman, and T. H. Stevens.** 1987. Protein sorting in yeast: the localization determinant of yeast vacuolar carboxypeptidase Y resides in the propeptide. Cell **48**:887-897.

45. **Wickerham, L. J.** 1946. A critical evaluation of the nitrogen assimilation tests commonly used in the classification of yeasts. J. Bacteriol. **52**:293-301.

46. **Wiemken, A., M. Schellenberg, and K. Urech.** 1979. Vacuoles: the sole compartments of digestive enzymes in yeast (*Saccharomyces cerevisiae*)? Arch. Microbiol. **123**:23-35.

47. **Worthington Biochemical Co.** 1972. Worthington Enzyme Manual. Worthington Biochemical Corporation, Freehold, New Jersey.

48. **Yoshihisa, T., Y. Otsumi, and Y. Anraku.** 1988. Solubilization and purification of vacuolar membranes in *Saccharomyces cerevisiae*. J. Biol. Chem. **263**:5158-5163.

49. Zubenko, G. S., F. J. Park, and E. W. Jones. 1983. Mutations in *PEP4* locus of *Saccharomyces cerevisiae* block final step in maturation of two vacuolar hydrolases. Proc. Natl. Acad. Sci. USA 80:510-514.

TABLE 1. The *vpt* mutants were assigned to 33 complementation groups on the basis of standard complementation analysis. Also shown is the number of *ts vpt* mutants in each of the 7 complementation groups that have *ts* alleles. Invertase assays were performed on several alles of each complementation group. Whole cells were assayed for external invertase activity, and lysed cells were assayed for total invertase activity. The percentage of external invertase activity was calculated for each mutant allele. A strongly defective allele (high % Inv out) was chosen for further analysis. Levels of other enzyme activities secreted by, or associated with, these representative alleles are presented.

Complementation groups	Total # of alleles	*ts* alleles	CPY-Inv (% secreted)	CPY (% of parent)	Pra-Inv (% secreted)	G3PDH (% external)	α Mannosidase (% external)
vpt1	46	-	85	10	45	5	<5
vpt2	29	-	25	65	N.D.	N.D.	N.D.
vpt3	11	1	80	10	75	<5	<5
vpt4	15	-	75	5	65	<5	<5
vpt5	9	-	100	<5	65	<5	5
vpt6	6	-	70	5	45	<5	<5
vpt7	32	-	90	30	55	<5	10
vpt8	33	-	65	25	65	<5	<5
vpt9	20	-	65	35	55	<5	<5
vpt10	29	-	50	30	35	<5	20
vpt11	8	2	90	10	60	<5	25
vpt12	3	-	65	70	55	<5	<5
vpt13	26	-	100	25	110	<5	10
vpt14	8	-	50	45	35	<5	15
vpt15	14	8	80	25	65	5	20
vpt16	5	2	75	10	60	<5	30
vpt17	40	-	80	20	65	<5	<5
vpt18	8	3	100	30	90	<5	30
vpt19	16	-	80	20	100	<5	<5
vpt20	5	-	35	75	30	5	5
vpt21	2	-	85	45	105	<5	5
vpt22	4	-	35	50	25	<5	<5
vpt23	4	-	25	80	30	<5	<5
vpt24	8	-	40	50	50	<5	10
vpt25	4	-	35	50	30	5	<5
vpt26	4	-	95	15	70	<5	15
vpt27	9	-	40	40	40	<5	20
vpt28	7	-	35	65	40	<5	5
vpt29	8	2	70	15	90	<5	10
vpt30	4	-	60	40	70	<5	5
vpt31	2	-	15	65	30	<5	5
vpt32	5	-	35	55	35	<5	5
vpt33	7	5	90	10	85	<5	20
VPT+	-	-	5	100	5	<5	<5

TABLE 2. Grouping of *vpt* mutants based on severity of CPY and CPY-Inv fusion localization defects. Percentage of CPY enzyme activity has been broken into four levels across the horizontal axis, and % of CPY-Inv hybrid protein secreted has been divided likewise along the vertical axis. The 33 *vpt* complementation group numbers are shown in the appropriate boxes. *vpt* mutants that show severe mislocalization and/or processing defects for both CPY and PrA as shown by cell fractionation and immunoprecipitation of these proteins (Fig. 5) have been typed in outline form.

% of CPY-Inv Activity Secreted	CPY Activity (% of Parent)			
	<15%	15-30%	30-50%	>50%
>90%	5,26, 33	7,13, 18		
65-90%	1,3,4, 6,11,16	15,17, 19,29	21	
40-65%		8,10	9,30, 14,24	12
<40%			27	2,20,22, 23,25,28 31,32

TABLE 3. Summary of complementation analysis between *vpt* and *vpl* mutants. The *vpt* mutants were crossed with the *vpl* mutants (that had been made Δ*suc2* by crossing with SEY6210) and tested for their ability to complement the CPY-Inv433 sorting defect. Extensive overlap was seen and it is proposed that to avoid confusion in the future these strains should be referred to as *vps* mutants (for vacuolar protein sorting) and the numbers should be as listed in the table (also, Rothman and Stevens, in preparation).

vpt mutants	*vpl* mutants	Common complementation group name
vpt26	*vpl1*	*vps1*
-	*vpl2*	*vps2*
vpt17	*vpl3*	*vps3*
vpt10	*vpl4*	*vps4*
vpt5	*vpl5*	*vps5*
vpt13	*vpl6*	*vps6*
-	*vpl7*	*vps7*
vpt8	*vpl8*	*vps8*
vpt9	-	*vps9*
vpt1	-	*vps10*
vpt11	*vpl9*	*vps11*
vpt12	-	*vps12*
vpt2	-	*vps13*
vpt14	-	*vps14*
vpt15	-	*vps15*
vpt16	-	*vps16*
vpt3	-	*vps17*
vpt18	-	*vps18*
vpt19	-	*vps19*
vpt20	*vpl10*	*vps20*
vpt21	-	*vps21*
vpt22	*vpl14*	*vps22*
vpt23	*vpl15*	*vps23*
vpt24	-	*vps24*
vpt25	*vpl12*	*vps25*
vpt4	-	*vps26*
vpt27	-	*vps27*
vpt28	*vpl13*	*vps28*
vpt6	-	*vps29*
vpt30	-	*vps30*
vpt31	-	*vps31*
vpt32	-	*vps32*
vpt33	-	*vps33*
vpt29	-	*vps34*
vpt7		*vps35*
-	*vpl11*	*vps36*
-	*vpl16*	*vps37*
-	*vpl17*	*vps38*
-	*vpl18*	*vps39*
-	*vpl19*	*vps40*

FIG. 1. Selection scheme for *vpt* mutants.

A. *PRC1-SUC2* gene fusions encoding CPY-Inv hybrid proteins. At the top is a schematic representation of the gene encoding CPY (*PRC1*). The signal sequence is indicated by a solid black box, the pro-segment by hatched lines and the mature sequences by dots (16). The positions of the oligosaccharide addition sites are indicated by tadpoles. The two fusions of *PRC1* sequences to *SUC2* used to select *vpt* mutants are shown below. The 50 amino acid fusion receives extensive glycosyl modification whereas the 433 amino acid fusion does not become hyperglycosylated.

B. The gene encoding PrA (*PEP4*) and below a representation of the *PEP4-SUC2* gene fusion tested for its localization in the *vpt* mutants (Table 1).

C. A simple diagram showing the vacuolar protein delivery route followed by the CPY-invertase hybrid protein (C-I). The *vpt* mutants were selected for their mislocalization of some or all of this C-1 hybrid protein to the cell surface. For some of the *vpt* mutants secretion of the mislocalized C-I has been shown to be dependent on *SEC1* gene function, indicating that delivery to the surface is mediated by secretory vesicles (2).

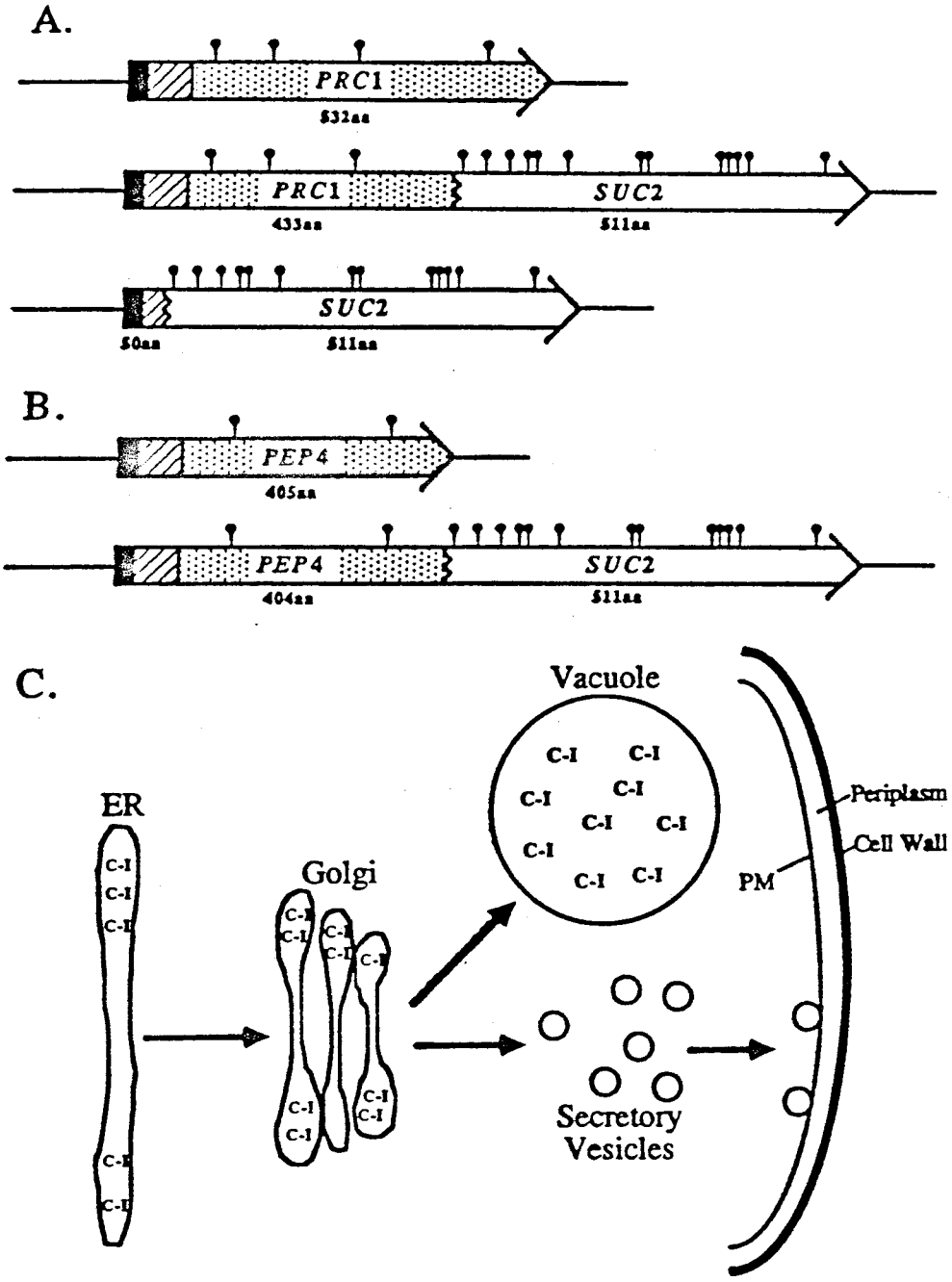
A.
PRC1
532aa
PRC1
SUC2
433aa
511aa
SUC2
50aa
511aa
B.
PEP4
405aa
PEP4
SUC2
404aa
511aa
C.
Vacuole
C-I
ER
Golgi
Periplasm
Cell Wall
PM
Secretory
Vesicles

FIG. 2. Complementation analysis of *vpt* mutants. Diploids were constructed by crossing *vpt* α *lys2* with *vpt* a *ade2* mutants and selecting $Ade^{+}Lys^{+}$ diploids on minimal media. These diploids were patched in an array on YP fructose and screened by invertase filter assay. Noncomplementation is seen as a red spot indicating secretion of the CPY-Inv hybrid protein, while complementation is observed as no reaction (white).

Secreted Inv Activity
(Intact Cells)

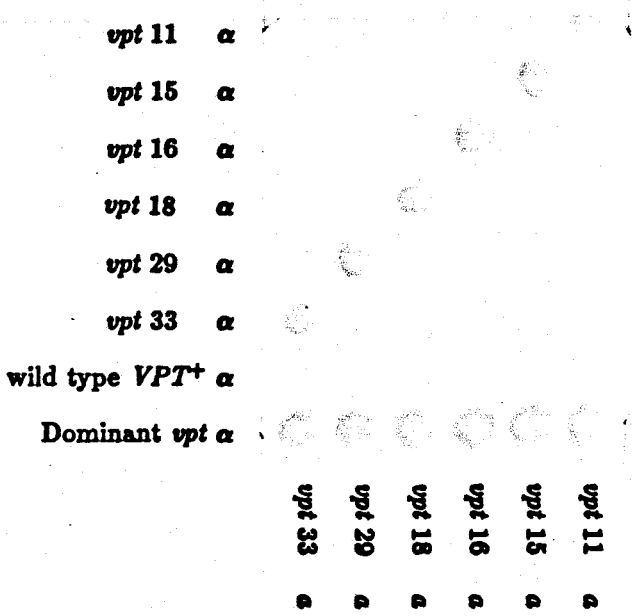

FIG. 3. Immunoprecipitation of invertase from labeled spheroplasts. The *VPT* yeast strain SEY6211, containing the invertase encoding plasmid, pRB58, was derepressed by growth in 0.1% glucose for 30 min, converted to spheroplasts and labeled for 5 min with ^{35}S-methionine. Chase with cold methionine was for 0', 3' or 7' as indicated. Spheroplasts were separated into pellet (I) and supernatant (E) fractions by centrifugation, and immunoprecipitated with invertase antisera. The core glycosylated invertase found in the E.R. migrates as a set of bands that are converted to a heterogeneous mixture of highly glycosylated molecules in the Golgi prior to secretion from the cell.

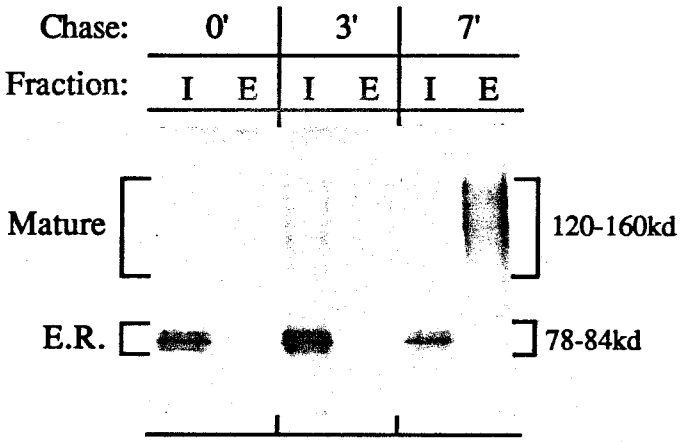
Chase:
0'
3'
7'
Fraction:
I E I E I E
Mature
120-160kd
E.R.
78-84kd

FIG. 4. Proteins secreted from wild-type and *vpt* mutant strains. Strains were labeled with $^{35}SO_4$ for 20 min and chased for 20 min with $(NH_4)_2SO_4$ (1 mM). Cells were removed by centrifugation. The supernatant (medium) proteins were precipitated with TCA and run on a 10% polyacrylamide gel. Size standards are as indicated.

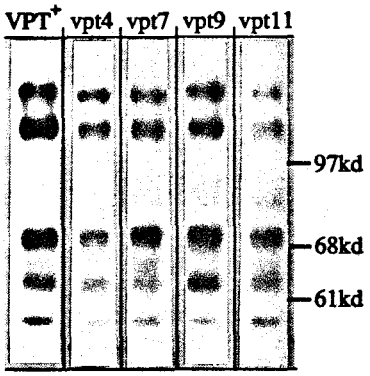
VPT+
vpt4
vpt7
vpt9
vpt11
97kd
68kd
61kd

FIG. 5. Immunoprecipitation of carboxypeptidase Y and proteinase A in wild-type (SEY6210 and SEY6211) and *vpt* mutant yeast strains. Spheroplasts were labeled (as described in Materials and Methods) and chased for the times indicated. The spheroplast pellet makes up the internal (I) fraction and the supernatant constitutes the external (E) fraction in each case. Immunoprecipitations were carried out using CPY or PrA antisera. Densitometer tracings were used to calculate the approximate percentages of CPY and PrA in the internal and external fractions for each mutant shown. The *vpt* mutants with similar phenotypes to those shown are listed. *vpt*1, 3, 4, 6, 7, and 30 have phenotypes that range between those shown for *vpt*5 and *vpt*17. The migration positions of precursor and mature forms of CPY and PrA and their approximate molecular weights are indicated. For many of the mutants a protein form intermediate in size between p2 CPY and mature CPY was immunoprecipitated by anti-CPY antisera. This band migrated at approximately the same position as p1 CPY on our gels. The p1 and p2 forms of PrA could not be resolved under the gel conditions used.

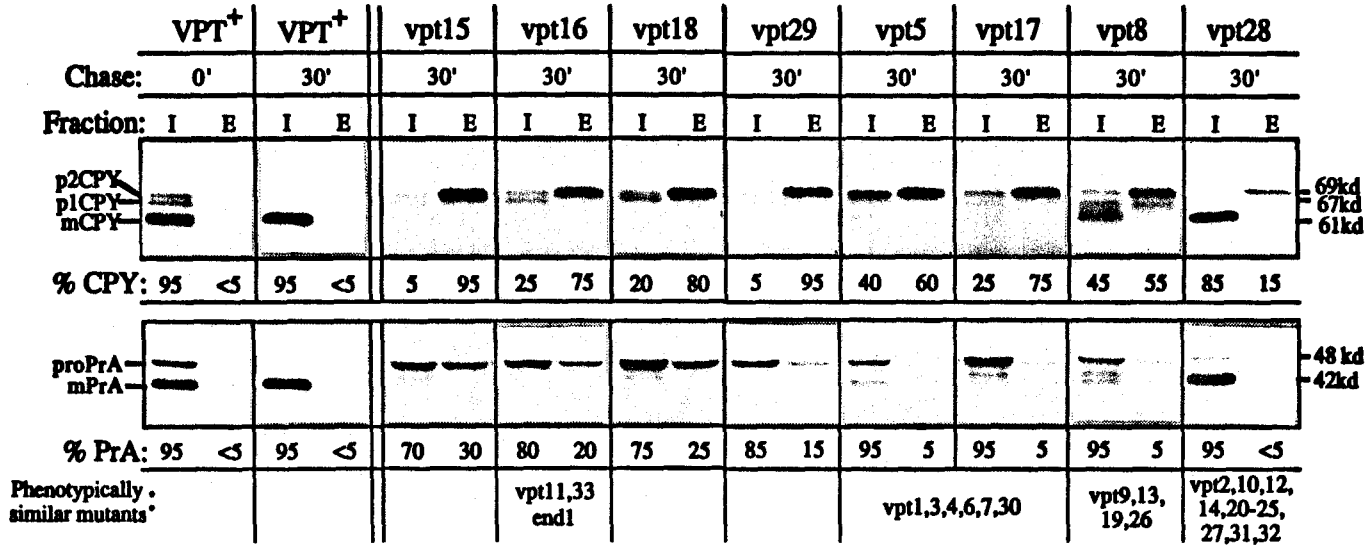
VPT+
VPT+
vpt15
vpt16
vpt18
vpt29
vpt5
vpt17
vpt8
vpt28
Chase: 0' 30' 30' 30' 30' 30' 30' 30' 30' 30'
Fraction: I E I E I E I E I E I E I E I E I E I E
p2CPY
p1CPY
mCPY
69kd
67kd
61kd
% CPY: 95 <5 95 <5 5 95 25 75 20 80 5 95 40 60 25 75 45 55 85 15
proPrA
mPrA
48 kd
42kd
% PrA: 95 <5 95 <5 70 30 80 20 75 25 85 15 95 5 95 5 95 5 95 <5
Phenotypically similar mutants*
vpt11,33 end1
vpt1,3,4,6,7,30
vpt9,13, 19,26
vpt2,10,12, 14,20-25, 27,31,32

FIG. 6. Immunoprecipitation of Proteinase B in wild-type (SEY6210 and SEY6211) and *vpt* mutant yeast strains. Spheroplasts were labeled as described in Materials and Methods and chased for the times indicated. I = internal (spheroplast-pellet fraction) and E = external (supernatant fraction). Proteinase B antiserum was used for the immunoprecipitations. The migration positions of precursor and mature forms of PrB and their approximate molecular weights are indicated. Note the extra band at 0', presumably an intermediate in PrB maturation.

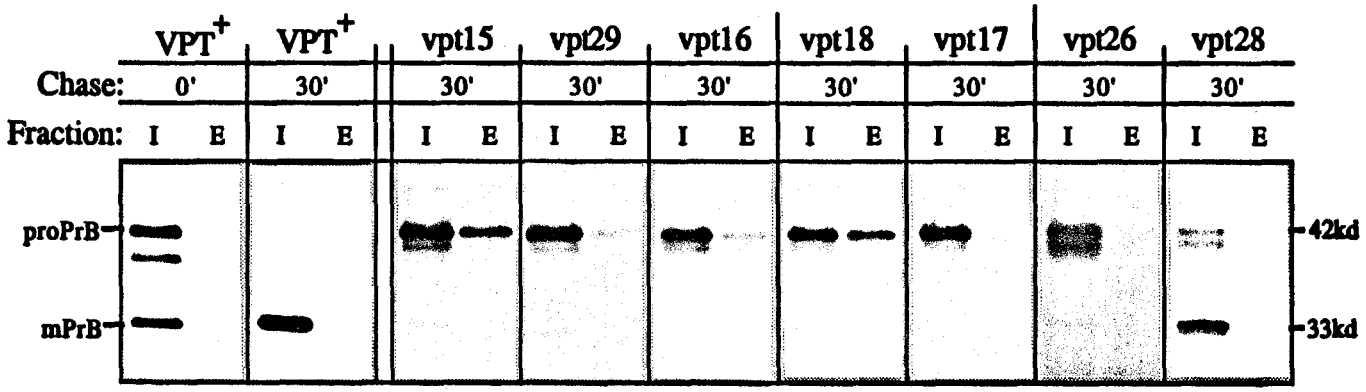
VPT+
VPT+
vpt15
vpt29
vpt16
vpt18
vpt17
vpt26
vpt28
Chase:
0'
30'
30'
30'
30'
30'
30'
30'
30'
Fraction:
I E I E I E I E I E I E I E I E I E
proPrB
mPrB
42kd
33kd

FIG. 7. Demonstration that the temperature-sensitive growth phenotype and the *vpt* mislocalization phenotype cosegregate in four representative tetrads from a cross of a *ts* allele of *vpt*16 with SEY6210. The filter assay of the lysed segregant patches shows that each spore has invertase activity. Below, the invertase filter assay of intact segregant patches shows that the ability to secrete invertase activity (i.e., the CPY-Inv hybrid protein) segregates 2:2. Similar cosegregation of the *ts* and *vpt* defects was also seen for *vpt*3, 11, 15, 18, 29 and 33. In each case at least 10 tetrads were analyzed.

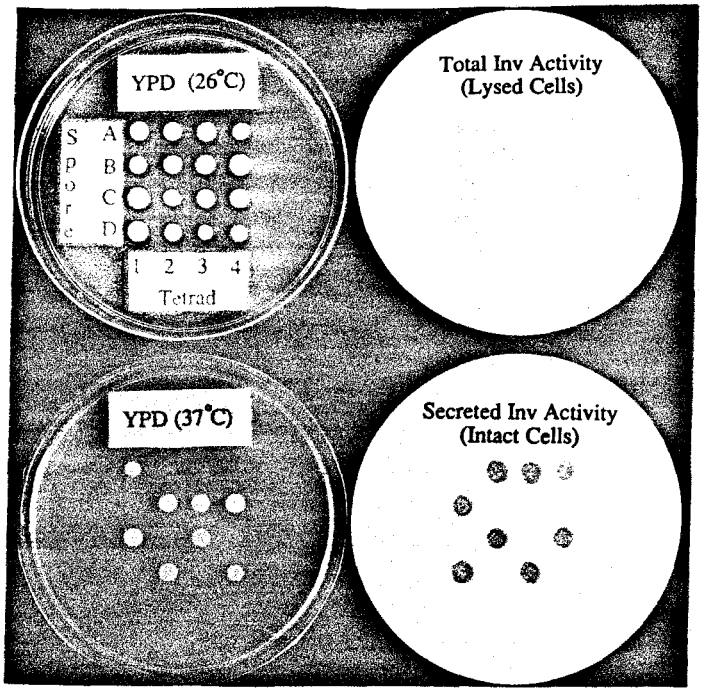
YPD (26°C)
Spore
A
B
C
D
1 2 3 4
Tetrad
YPD (37°C)
Total Inv Activity
(Lysed Cells)
Secreted Inv Activity
(Intact Cells)

Chapter 3

Organelle Assembly in Yeast: Characterization of Yeast Mutants Defective in Vacuolar Biogenesis and Protein Sorting

Lois M. Banta, Jane S. Robinson, Daniel J. Klionsky and Scott D. Emr

Journal of Cell Biology **107**:1369-1383 (1988)

ABSTRACT

Yeast *v*acuole *p*rotein *t*argeting (*vpt*) mutants exhibit defects in the sorting and processing of multiple vacuolar hydrolases. In order to evaluate the impact these *vpt* mutations have on the biogenesis and functioning of the lysosome-like vacuole, we have employed light and electron microscopic techniques to analyze the vacuolar morphology in the mutants. These observations have permitted us to assign the *vpt* mutants to three distinct classes. The class A *vpt* mutants (26 complementation groups) contain 1-3 large vacuoles that are morphologically indistinguishable from those in the parental strain, suggesting that only a subset of the proteins destined for delivery to this compartment is mislocalized. One class A mutant (*vpt*13) is very sensitive to low pH and exhibits a defect in vacuole acidification. Consistent with a potential role for vacuolar pH in protein sorting, we found that bafilomycin A_1, a specific inhibitor of the vacuolar ATPase, as well as the weak base ammonium acetate and the proton ionophore carbonyl cyanide m-chlorophenylhydrazone, collapse the pH gradient across the vacuolar membrane and cause the missorting and secretion of two vacuolar hydrolases in wild-type cells. Mutants in the three class B *vpt* complementation groups exhibit a fragmented vacuole morphology. In these mutants, no large normal vacuoles are observed. Instead, many (20-40) smaller vacuole-like organelles accumulate. The class C *vpt* mutants, which constitute four complementation groups, exhibit extreme defects in vacuole biogenesis. The mutants lack any organelle resembling a normal vacuole, but accumulate other organelles, including vesicles, multilamellar membrane structures, and Golgi-related structures. Heterozygous class C zygotes reassemble normal vacuoles rapidly, indicating that some of the accumulated aberrant structures may be intermediates in vacuole formation. These class C mutants also exhibit sensitivity to osmotic stress, suggesting an osmoregulatory role for the vacuole. The *vpt* mutants should provide insights into

the normal physiological role of the vacuole, as well as allowing identification of components required for vacuole protein sorting and/or vacuole assembly.

INTRODUCTION

Eukaryotic cells are distinguished by their several discrete membrane-enclosed organelles. Each of these subcellular compartments has unique structural and functional characteristics which are conferred in large part by the distinct set of proteins that constitutes that organelle. Thus, accurate sorting and trafficking of proteins from their site of synthesis in the cytoplasm to their correct non-cytoplasmic destinations are essential for maintaining the functional and structural identity of each organelle.

In mammalian cells, the secretory pathway has been shown to mediate the modification, processing, and delivery of proteins destined for a variety of intracellular and extracellular compartments. Proteins destined for secretion, assembly into the plasma membrane, delivery to lysosomes, or retention within endoplasmic reticulum (ER)[1] and Golgi compartments transit through all or a portion of the secretory pathway (11). Presently, available data are consistent with a model in which much of protein secretion occurs via a default mechanism (5). Proteins competent for entry into the ER but lacking any additional sorting information passively transit from the ER to the Golgi complex and then are secreted via a nonspecific bulk flow mechanism (58). However, proteins that depart from this pathway, such as lysosomal enzymes, contain additional sorting signals that permit specific recognition, modification, and subsequent delivery of these proteins from late Golgi compartments to the lysosome (53).

In the yeast *Saccharomyces cerevisiae* most protein secretion also appears to occur via a constitutive default pathway (55). However, like mammalian lysosomal enzymes, proteins destined for the yeast vacuole depend on the

[1]Abbreviations used in this paper: Bb, Berkeley body; CCCP, carbonyl cyanide m-chlorophenylhydrazone; CPY, carboxypeptidase Y; ER, endoplasmic reticulum; FD, FITC-conjugated dextran; Inv, invertase; PrA, proteinase A; PrB, proteinase B.

presence of additional protein sorting information (21,25,56). The yeast vacuole is a prominent intracellular organelle which shares functional characteristics with both mammalian lysosomes and plant central vacuoles. This organelle is believed to play an important role in the storage of amino acids and other small molecules (30). Like mammalian lysosomes, the yeast vacuole is an acidic compartment and contains a number of hydrolytic enzymes (33,59). Certain of these hydrolases, including the glycoproteins proteinase A (PrA), proteinase B (PrB) and carboxypeptidase Y (CPY) have been shown to be synthesized at the level of the ER as inactive precursors. These proenzymes transit through the Golgi complex and are sorted to the vacuole, where they are processed to the mature active enzymes (16,19,32,54). Sequence determinants have been defined within proCPY and proPrA that are necessary and sufficient to target these proteins to the vacuole (21,25,56). Mutational alterations in the proCPY sorting signal lead to missorting and secretion of the precursor form of this enzyme. Although the sorting signals in proCPY and proPrA lack any obvious primary sequence similarity, it is presumed that a common cellular protein sorting apparatus mediates specific recognition and subsequent vacuolar localization of these enzymes. Each undergoes a similar set of compartment-specific modifications, and the kinetics for vacuolar delivery of both proteins are essentially the same (25). It seems likely that many soluble vacuolar proteins are segregated to this compartment via the same targeting mechanism.

In an effort to identify components of the vacuolar protein sorting apparatus, we recently isolated a number of mutants that exhibit defects in the proper localization and processing of several vacuolar proteins. These vacuolar protein targeting (*vpt*) mutants were identified using a gene fusion-based selection scheme. In wild-type cells, proCPY sequences fused to the gene for the normally-secreted enzyme invertase (Inv) contain sufficient sorting information to divert

delivery of enzymatically-active Inv to the yeast vacuole (2,21). Mutants have been selected that missort and secrete such CPY-Inv hybrid proteins. The approximately 600 mutants isolated thus far have been assigned to more than 33 complementation groups. The mutants exhibit hybrid protein-independent defects in the sorting of normal vacuolar enzymes including CPY, PrA and PrB (46). Upon missorting, the precursor forms of these proteins are secreted, presumably because the selective vacuole protein delivery pathway is defective and the proteins then follow the default secretion pathway (2).

Given this large number of potential gene products that can influence the vacuolar protein sorting process, it seemed likely that mutations in at least some of these genes might also affect biogenesis of a normal vacuole. Specifically, some of the proteins that are mislocalized in the *vpt* mutants may be essential in defining important structural and functional characteristics of this organelle. In addition, one might expect that lipid and protein constituents of the vacuole membrane would transit together with soluble vacuolar enzymes via a common vesicle carrier. Defects in vacuole membrane assembly therefore might also be expected in certain of the *vpt* mutants. In order to address these questions, we have assessed the vacuolar as well as other organellar morphologies in each of the *vpt* mutants. Using both light and electron microscopic techniques, we found that mutants in most of the *vpt* complementation groups still assembled morphologically normal vacuoles. However, mutants in three complementation groups accumulated what appeared to be multiple small vacuoles. Cells in four other *vpt* complementation groups exhibited extreme defects in vacuole biogenesis; these mutants accumulated vesicles and membrane-enclosed compartments that bore no resemblance to a normal vacuole. In addition, certain of the *vpt* mutants exhibited other phenotypes such as sensitivity to low pH or to

osmotic stress. These observations provide insights into the mechanism(s) of vacuole biogenesis as well as the normal physiological role of this organelle.

MATERIALS AND METHODS

Strains and Media. Mutants were isolated as described (46) from parental strains SEY6210 *MATα ura3-52 leu2-3,112 his3-Δ200 trp* 1-Δ901 *lys2-801 suc-Δ9* and SEY6211 *MATα ura3-52 leu2-3,112 his3-Δ200 trp1-Δ901 ade2-101 suc2-Δ9*. Other strains used were HMSF1 *MATα sec1-1* (37), SEY5078 *MATα sec7-1 suc2-Δ9 leu2-3,112 ura3-52* (this study), and SEY5186 *MATα sec18-1 leu2-3,112 ura3-52* (this study). Cells were grown on standard YPD or SD (synthetic miminal, supplemented as necessary) media (49). *ade2* strains were scored for the presence of red pigment after growth for 3-5 days on both standard YPD (containing 2% glucose) and YPD containing 8% glucose. Sensitivity to low pH was assessed on YPD adjusted to pH 3.5, 3.0, or 2.5 with 6N HCl. Sensitivity to high osmotic pressure was determined on YPD containing 1.0 or 1.5 M NaCl, 1 M KCl or 2.5 M glycerol (osmosity approximately 1.7S). As noted previously by Singh (51), certain batches of hypertonic media stored more than a few days inhibited growth of the wild-type strains; therefore it was important to test the media with a strain known to be resistant to the osmotic conditions present.

Genetic crosses, sporulation of diploids, and dissection of tetrads were performed as described by Sherman *et al.* (49).

Labeling of Cells with Fluorescent Dyes. All manipulations were performed at room temperature unless otherwise noted. Cells were labeled in the presence of FITC-dextran (FD) as described by Makarow (27), with the following modifications. Cells (5 ml) were grown in YPD to early log phase (1-2 x 10^7 cells/ml), centrifuged for 5 min in an IEC clinical centrifuge, and washed once in YPD, pH 4.5. The cell pellet was resuspended to a concentration of 1.5 x 10^8 cells/ml in YPD, pH 4.5 containing 100 mg/ml 70S FD, and incubated for 90 min at 37°C (or 25°C for temperature-sensitive strains) on a rotary shaker. The cells were centrifuged for 2 min at 6000 rpm in a Savant microcentrifuge, washed twice

in PBS (10 mM Na-phosphate, pH 7.4, 140 mM NaCl) and resuspended in 0.4 ml PBS. The resuspended cells were mixed with low melting point agarose (0.5% final concentration) at 37°C, mounted on glass slides, covered with a cover slip which was sealed with nail polish, and observed immediately. Alternatively, cells were labeled with FITC as described previously (41). Cells (2×10^7) were resuspended in 1 ml YPD containing 50 mM Na-citrate, pH 5.5, and 10 µg/ml FITC in DMSO. After a 10 min incubation at 25°C with shaking, cells were centrifuged, washed once, and resuspended in 0.1 ml 100 mM K-phosphate, pH 7.5 containing 2% glucose. Cells were mounted as above.

For quinacrine labeling, cells were grown as described above and quinacrine was added to a final concentration of 175 µM in YPD, pH 7.6. After a 5 min incubation at 30°C, cells were centrifuged and mounted as above without washing. Ammonium acetate (200 mM final concentration) was added to the incubation mix where indicated (57).

For observation of the *ade2* endogenous fluorophore, cells were grown as described by Weisman *et al.* (57) and mounted as for FD.

Microscopy. Cells were observed using a Zeiss microscope, with a 100X oil-immersion objective, equipped for Nomarski optics and epifluorescence. Fluorescence filters used were Zeiss BP450-490 (excitation), FT510 (beam splitter), and BP520-560 (emission barrier). All fluorescent images were photographed for 40-60s using Kodak Tri-X Pan ASA400 film, increased to ASA1600 by using Diafine developer.

Electron Microscopy. Cells were prepared using a modification of the procedure of Byers and Goetsch (6). Cells (100 ml) were grown in synthetic minimal medium to an OD_{600} of approximately 0.3, shifted to YPD medium and allowed to grow for one generation. The cells were harvested by centrifugation (5 min in an IEC clinical centrifuge), washed in dH_2O and fixed for 2 h at room

temperature in 2 ml of 0.1 M Na-cacodylate, pH 6.8, 5 mM $CaCl_2$ (Buffer A) containing 3% gluteraldehyde. The fixed cells were washed once in 100 mM Tris-HCl, pH 8.0, 25 mM dithiothreitol, 5 mM Na_2-EDTA, 1.2 M sorbitol and then incubated in the same buffer for 10 min at 30°C. To remove cell walls, the cells were centrifuged, washed once with 1 ml 0.1 M K-phosphate (adjusted to pH 5.8 with citric acid) containing 1.2 M sorbitol and resuspended in 0.5 ml of the same buffer containing 0.05 ml β-glucuronidase type H-2 and 2.5 mg zymolyase. This cell suspension was incubated for 2 h at 30°C. The spheroplasts were centrifuged and washed in 1 ml buffer A. Temperature-sensitive (*ts*) strains were shifted to 37°C for 3 h prior to harvesting and were fixed at 37°C for analysis at the nonpermissive temperature; the rest of the procedure was identical to that for non-*ts* strains. The reduced osmium-thiocarbohydrazide-reduced osmium membrane-enhancement staining technique was adapted from Willingham and Rutherford (60). Spheroplasts prepared as described above were resuspended in 0.5 ml 1% OsO_4, 1% K-ferrocyanide in buffer A and incubated for 30 min at room temperature. After 4 washes in dH_2O (1 ml each), the cells were resuspended in 1% thiocarbohydrazide, incubated for 5 min at room temperature and washed again four times in dH_2O. The cells were stained with 1% OsO_4, 1% K-ferrocyanide in buffer A for 3 min at room temperature and washed in dH_2O as before. The samples were dehydrated through an ethanol series and embedded in LRWhite, which was allowed to polymerize for 3 days at 4°C with exposure to UV light. Thin sections were collected on 200-mesh copper grids, stained for 30-45 s with lead citrate (42), and observed on a Phillips 420 transmission electron microscope.

Immunoprecipitations. Immunoprecipitations on labeled spheroplasts (46) were performed as described previously (25).

Materials. Bafilomycin A_1 was the generous gift of K. Altendorf. Tran ^{35}S-label was purchased from ICN Radiochemicals, Irvine, CA. Gluteraldehyde, OsO_4, thiocarbohydrazide and K-ferrocyanide were purchased from Polysciences, Inc., Warrington, PA. Zymolyase was purchased from Seikagaku Kogyo Co., Ltd., Japan, and low melting point agarose was purchased from Bethesda Research Labs, Inc., Gaithersburg, MD. Diafine developer was the product of Acufine, Chicago, IL. LRWhite embedding resin was purchased from Ted Pella Co., Tustin, CA. FD (70S), FITC, quinacrine, β-glucuronidase (type H-2), and all other chemicals not listed above were purchased from Sigma Chemical Co., St. Louis, MO.

RESULTS

Vacuole Morphology in vpt Mutants

We have employed light and fluorescence microscopy to determine the state of the vacuole in multiple *vpt* alleles from each of 33 complementation groups. In a wild-type strain grown in rich medium, yeast vacuoles occupy approximately 20% of the yeast cell volume and can often be visualized in the light microscope using Nomarski optics. However, small vacuoles can not be visualized by this technique and some cells do not appear to have any vacuole when observed by Nomarski optics (57). Therefore, in order to visualize even small vacuoles, we have taken advantage of a number of fluorescent dyes that specifically accumulate in this organelle.

FITC-dextran (FD) as well as FITC[2] by itself have been used to label yeast vacuoles (27,41). In wild-type cells, the vacuole appeared as a single large fluorescent spot or 2-3 spots of approximately equal size under the labeling conditions used (Fig. 1a). A large vacuole was also visible in these cells using Nomarski optics. Unexpectedly, when the *vpt* mutants were examined using this dye, most of the mutants (26 complementation groups, see Table I) exhibited a vacuolar morphology indistinguishable from that of the parental strains (Fig. 1b). We have grouped these mutants together and refer to them as class A *vpt* mutants. The remaining 7 complementation groups exhibited an altered vacuolar morphology. In 3 of the groups (*vpt3*, *5* and 26), cells had multiple smaller organelles which were visible using Nomarski optics and which stained with FITC (Fig. 1c). This group of mutants has been designated class B. The remaining 4 *vpt*

[2]While these studies were in progress, Preston *et al.* reported that the vacuolar staining associated with FD was in fact due to nonendocytic uptake of FITC and other contaminating impurities in the FD (41). We have repeated the vacuole labeling experiments in a few of the *vpt* mutants using FITC and have observed vacuolar morphologies similar to those reported here for FD.

complementation groups (*vpt*11, 16, 18, and 33) had no intracellular structures which stained in the presence of FD. When observed by Nomarski optics, cells in these complementation groups appeared to have rough surfaces, and no vacuoles were visible (Fig. 1d). We have defined this group of mutants as class C *vpt* mutants (Table I). These observations have been confirmed using two other fluorescent dyes that also accumulate in yeast vacuoles (see below).

Class A vpt Mutants Exhibit Wild-Type Vacuole Morphology

We have studied the *vpt* mutants exhibiting each of the three vacuolar morphologies in more detail. In *ade2* strains of *S. cerevisiae*, an endogenous fluorophore accumulates in the vacuole and can be visualized using fluorescence microscopy (57). By this method, the parental strains and the class A *vpt* mutants had vacuolar morphologies identical to those observed using FD (Fig. 1e, f).

Like mammalian lysosomes (38), yeast vacuoles have an acidid pH (33) and can be labeled by dyes, such as quinacrine (1,57), chloroquine (26) and neutral red (20,34), which accumulate in a pH-dependent manner. These weak bases are presumed to diffuse through membranes and accumulate in acidic compartments (9). The vacuole morphology of wild-type cells as observed using quinacrine was identical to that seen with FD or the *ade2* endogenous dye (Fig. 2a, 4a). Most of the class A *vpt* mutants also contained 1-3 large vacuoles which accumulated quinacrine, although in many cases, the fluorescence was less intense than that in the parental strain (not shown). Multiple alleles of 3 complementation groups (*vpt*10, 13 and 24), exhibited very little or no vacuolar staining with quinacrine, although vacuoles were clearly visible by Nomarski optics in these cells (Fig. 2e). These *vpt* mutants, which had morphologically normal vacuoles but exhibited no pH-dependent accumulation of dye, might carry mutations which affect vacuole acidification. In plant cells, the vacuole plays an important role in pH homeostasis; a decrease in external pH results in a lowered vacuolar pH, while the

cytoplasmic pH remains constant (3). We reasoned that mutants defective in vacuole acidification might also exhibit defects in the regulation of intracellular pH. In order to address this issue, we tested whether any of the *vpt* mutants were sensitive to low pH. Growth was assayed on YPD media adjusted to pH 3.5, 3.0 or 2.5. The parental strains grew, although more slowly than on standard YPD, under these conditions. Strains in one complementation group, *vpt13*, were found to be extremely sensitive to low pH. Fourteen of 21 *vpt13* alleles were unable to grow at pH 3.5, and 19 alleles of *vpt13* were inhibited for growth at pH 3.0 (Fig. 3a). Some alleles of other *vpt* mutants were also weakly sensitive to low pH (data not shown).

The existence of *vpt* mutants that exhibited possible defects in vacuole acidification led us to investigate the role of vaucolar pH in the localization of proteins to the vacuole in wild-type cells. The vacuolar membrane contains a proton-translocating Mg^{++}-dependent ATPase which produces a proton gradient across the vacuolar membrane and acidifies the interior of the vacuole (24). The drug bafilomycin A_1 has been shown to be a specific inhibitor of the vacuolar membrane proton-translocating ATPase of *Neurospora crassa* (4). When wild-type yeast cells were treated with 10 μM bafilomycin A_1 for 10 min prior to staining with quinacrine, no vacuolar fluorescence was observed (Fig. 4b). The inhibition of the pH-dependent quinacrine staining in these cells indicates that bafilomycin eliminates the pH gradient across the yeast vacuolar membrane, presumably by inhibiting the vacuolar membrane ATPase. In order to assess the role of the pH of the yeast vacuole in vacuolar protein localization, we next examined the effect of bafilomycin on the sorting and processing of vacuolar hydrolases. Spheroplasts were pretreated with bafilomycin (10 μM final concentration) for 10 min, radioactively labeled, and separated into intracellular and extracellular fractions prior to immunoprecipitation with CPY- and PrA-specific antisera. As shown in

Fig. 4c, in the absence of bafilomycin all of the CPY and PrA was processed to the mature enzyme form and remained associated with the yeast spheroplast fraction (lanes 1 and 2), indicating that these enzymes had been delivered to the vacuole (46,59). In contrast, in the presence of bafilomycin, approximately 50% of the CPY was present in the proenzyme form, and most of this proCPY was secreted into the extracellular fraction (Fig. 4c, lanes 3 and 4). Bafilomycin caused a similar defect in the processing and targeting of PrA. Other agents known to raise vacuolar pH, including the weak base ammonium acetate (200-400 mM) (57) and the proton ionophore carbonyl cyanide m-chlorophenylhydrazone (CCCP; 40 μM) also caused the mislocalization of CPY and PrA (data not shown). Significantly, protein traffic to the cell surface was not disrupted under these conditions, and the concentration of bafilomycin used in these experiments did not inhibit yeast cell growth. Together these data indicate that vacuole pH plays a role in the efficient delivery and maturation of at least some vacuolar hydrolases.

We next examined the class A *vpt* mutants by transmission electron microscopy, using a technique that results in enhanced staining of biomembranes and structures containing glycomolecules (see Materials and Methods). As seen in Fig. 5a, the vacuole stained as a large electron-dense compartment using this procedure. Thin sections of wild-type cells typically contained one large or 2-3 smaller vacuoles per cell. Other intracellular structures such as the nucleus, mitochondria and ER were also readily visible. The majority of the class A *vpt* strains, such as the ones shown in Fig. 5b and c, exhibited typical wild-type morphology. In thin sections of both wild-type and class A strains, we often observed an apparent substructure within the vacuole that did not stain like the rest of the vacuole and remained electron transparent (e.g., see Fig. 5b). The significance of this structure is unclear, although it may represent the polyphosphate precipitate often observed in freeze-etched yeast cells (30).

Electron microscopic analysis also revealed that certain class A *vpt* mutants accumulated aberrant structures in addition to the normal vacuole. Mutants in two complementation groups, *vpt15* and *vpt29*, contained organelles similar to those seen in yeast protein secretion (*sec*) mutants (37), including vesicles and Berkeley bodies (Bbs, structures presumably related to the Golgi complex; see reference 36). The electron micrographs in Fig. 6 show typical *vpt15* and *vpt29* cells and, for comparison, a *sec1* strain (accumulates vesicles), a *sec18* strain (accumulates ER), and a *sec7* strain (accumulates Bbs), prepared using the membrane enhancement technique. The vacuoles in these *vpt15* and *vpt29* cells were abnormally large and occasionally contained inclusions (Fig. 6c). This aberrant morphology was seen in every *vpt15* and *vpt29* allele examined. *vpt13* and *vpt26* cells also occasionally contained vesicles and Bbs (not shown).

In two complementation groups, *vpt7* and *vpt28*, stacks of lamellae and reticular membrane arrays were observed at a high frequency (Fig. 7). These organelles were more prevalent in *vpt7* and *vpt28* than in the parental strain (i.e., 0.8-1.0 structure per cell section versus 0.4 for the parent in 30-50 sections examined for each strain). These structures, which were usually not associated with any other organelle, are likely to correspond to exaggerated Golgi complexes. Finally, cells in one class A mutant, *vpt12*, accumulated vesicles similar to those seen in the class C mutants (see below).

Class B vpt Mutants Exhibit an Altered Vacuole Morphology

Unlike the class A *vpt* mutants, cells in the three class B complementation groups (*vpt3, 5, 26*) contained multiple compartments that stained in the presence of FD and were visible using Nomarski optics (Fig. 1c). These small "vacuoles" also accumulated the *ade2* endogenous fluorophore (Fig. 1g). In order to determine whether these organelles had the lowered pH characteristic of wild-type vacuoles, we tested their ability to accumulate quinacrine. As shown in

Fig. 2c, the structures in the class B *vpt* mutants stained with quinacrine, suggesting that these compartments had a pH similar to that of the vacuole in the parental strain. This hypothesis was further tested by labeling with quinacrine in the presence of ammonium acetate (57). Under these conditions, no fluorescent staining was observed in the parental strain or the class B *vpt* mutant (Fig. 2b,d). This supports the hypothesis that the fluorescent staining observed in class B cells is due to the acidic pH of the compartments stained rather than to some non-specific accumulation of dye.

The class B *vpt* mutants were also examined at the ultrastructural level to confirm the multiple-vacuole morphology observed by light and fluorescence microscopy. As seen in Fig. 5d, a representative class B *vpt5* mutant allele contained multiple small organelles that stained like wild-type vacuoles. The number of vacuoles per cell section was quantitated for *vpt5* and for the parental strain (using 30-40 cell sections per strain). The average number of vacuole-like structures per cell section for the class B *vpt* was 5.7, while the number for the wild-type strain was 1.8. Seventy-one percent of the class B cells, as compared to 16% of the parental cells, had 3 or more vacuoles. On the basis of the size of the vacuoles and the thickness of the sections, we have calculated that an average class B cell contains approximately 35 of these small vacuoles, while wild-type cells contain 1-4 vacuoles per cell. Representatives of the other two class B complementation groups (*vpt3* and *vpt26*) exhibited similar vacuolar morphologies when observed by electron microscopy.

Yeast which carry a mutation in the β-tubulin gene (*tub2*) or which have been treated with microtubule-disrupting drugs have a fragmented vacuole phenotype similar to that of the class B *vpt* mutants (15). We examined representative alleles of each complementation group by immunofluorescence,

using anti-tubulin antibodies. No evidence of abnormal microtubule structures in any of the *vpt* mutants was observed (data not shown).

Class C vpt Mutants are Defective in Vacuole Assembly

Cells in four *vpt* complementation groups (*vpt*11, 16, 18, and 33) lacked any intracellular structures which stained in the presence of FD (Fig. 1d). This phenotype was not simply due to an inability to sequester FITC in the vacuole; these mutants also failed to accumulate quinacrine or the *ade2* endogenous fluorophore (Fig. 1h). The *ade2* dye is produced when a purine biosynthetic intermediate concentrates in the vacuole and undergoes oxidation and polymerization to produce a naturally-fluorescent red pigment (23,50). As a result, *ade2* mutant yeast exhibit a red colony color when supplied with limiting amounts of adenine. All class A and class B *ade2 vpt* mutants grown under conditions of limiting adenine were red. However, several *ade2* alleles in each of the class C complementation groups were white. This phenotype was shown to be genetically linked to the *vpt* defect (see below). These observations suggest that in the absence of a functional vacuole, the purine biosynthetic intermediate is unable to undergo the reactions necessary to form the red color. We do not know whether the precursor accumulates in the cytoplasm or in other intracellular compartments, or whether it is secreted from the cell.

By electron microscopy, all class C mutants examined (at least 2 alleles of each of the 4 complementation groups) exhibited the same morphology (Fig. 8a-c). Even at high magnification, these mutants appeared to lack any structure exhibiting the characteristic staining properties of a wild-type vacuole. Ultrastructural analysis also revealed that the class C *vpt* mutants accumulated a variety of novel membrane-enclosed organelles, including vesicles and Bbs. Figures 8d and 8e show higher-magnification views of some of the structures that were exaggerated in these cells. The vesicles that accumulated in these mutants

(Fig. 8d) were enclosed by a membrane bilayer and were approximately 80 nm in diameter. In comparison, the vesicles that accumulate in the secretory mutant *sec*1 at the nonpermissive temperature are ~100 nm in diameter and have a very different appearance from the vesicles seen in class C *vpt* mutants (37; see Fig. 6f). As shown in Fig. 8e, class C mutants also accumulated large, multilamellar, membrane-enclosed structures. Somewhat surprisingly, these structures were electron transparent, suggesting that they do not contain significant amounts of glycoproteins or sugars.

Several of the *vpt* complementation groups contain temperature-sensitive (*ts*) alleles (46). Four of these groups (*vpt*11, 16, 18 and 33) are class C, one (*vpt*3) is class B and two (*vpt*15 and *vpt*29) are class A. These two class A mutants contained vacuoles but also accumulated organelles similar to those seen in the class C mutants (see above). We have examined the morphology of these conditional lethal strains at both the permissive (25°C) and the nonpermissive (37°C) temperature. Surprisingly, the vacuolar morphology of each of the *ts* strains examined was identical at 25°C and 37°C; aberrant organelles accumulated to the same extent at either temperature.

The existence of mutants in several complementation groups that lacked any apparent vacuole allowed us to begin to analyze the requirements for vacuole biogenesis *in vivo*. If a vacuole can be formed via a *de novo* synthetic pathway, diploids made by mating two class C mutants from different complementation groups should contain a normal vacuole. If, however, a pre-existing normal template vacuole is necessary to direct synthesis of the new organelle, diploids heterozygous for two class C mutations may be incapable of generating a vacuole despite the presence of both wild-type gene products. When we examined diploids made by crossing a *ts vpt*11 allele with a *ts vpt*18 allele, we observed that the diploid: 1) was temperature-resistant, 2) was competent to sort vacuolar proteins,

and 3) contained a normal-appearing vacuole which stained with FITC. Homozygous diploids made by crossing two *ts* alleles of the same class C complementation group exhibited typical class C morphology and were *ts*, as expected. Furthermore, when the mating pairs were examined within 4-6 hours of mixing, heterozygous class C zygotes were observed which clearly contained a vacuole in each of the conjugating cells, as well as in the diploid bud emerging from the zygote (Fig. 9). Ultrastructural analysis confirmed the presence of vacuoles in these heterozygous mating pairs (not shown). These observations suggest that vacuole biogenesis can occur *de novo* in the absence of a normal template organelle. This assembly is rapid, occurring within one generation after conjugation. We cannot at present, however, exclude the possibility that the class C mutants contain tiny degenerate vacuole forms that are capable of functioning as templates or targets for new vacuolar protein and membrane delivery.

Class C Mutants are Defective in Several Vacuolar Functions

The vacuole has been implicated in a number of diverse cellular functions in wild-type cells, including osmoregulation (29), storage of amino acid reserves (30), endocytosis (43), and adaptation to adverse growth conditions (48). Like mammalian lysosomes and plant vacuoles (10,28), the yeast vacuole may also mediate the normal intracellular turnover of macromolecules. Protein degradation increases dramatically during sporulation, and mutants lacking proteinase A or proteinase B activity are partially or completely defective in sporulation (22). We postulated that the class C *vpt* mutants, which exhibited extreme aberrations in vacuole assembly and morphology, might be defective in other cellular functions that may be vacuole related.

If the vacuole is required for adaptation to a change in external osmosity, one might expect that cells that lack a vacuole would be unable to survive in the presence of even a small increase in ionic or osmotic pressure. We assessed the

growth of representative *vpt* alleles on YPD medium supplemented with 1.0 M or 1.5 M NaCl, 1.0 M KCl, or 2.5 M glycerol. None of the class C mutants was able to survive, although the parental strains grew under these conditions (Fig. 3b). In addition, *vpt*15, 26 and 29 were somewhat sensitive to the presence of 1.0 M NaCl or 2.5 M glycerol and were completely unable to grow on YPD medium containing 1.5 M NaCl. None of the other *vpt* mutants was sensitive to any of the osmotic stress conditions tested.

The class C mutants also exhibited other physiological defects, including: 1) poor growth on nonfermentable carbon sources such as glycerol or lactate; 2) poor growth in minimal media containing proline as the sole nitrogen source; 3) poor sporulation of homozygous diploids; and 4) low frequencies of DNA transformation. Furthermore, the class C *vpt* mutants contained smaller pools of basic amino acids than the class A or class B *vpt* mutants, as judged by a filter assay for basic amino acids (8) (data not shown). Other cellular functions in the class C mutants, however, appeared to be normal. Based on the ultrastructural analysis, these mutants exhibited wild-type morphology of organelles such as the nuclei and mitochondria (e.g., see Fig. 8b). The microtubules in these mutants appeared normal, as judged by immunofluorescence. Protein secretion also appeared to be unaffected in the class C as well as the other *vpt* mutants (36).

All vpt Phenotypes Cosegregate in Genetic Crosses

If the pleiotropic phenotypes discussed above all result from the *vpt* mutation in question, each of the phenotypes should cosegregate in genetic crosses of the mutants with wild-type cells. To confirm this, representative *vpt* mutants were back-crossed to the parental strain of the opposite mating type, the diploids were sporulated and tetrads were dissected. In this way, the vacuole morphology associated with each of the class B and class C *vpt* mutants was shown to cosegregate with the *vpt* defect (data not shown). The segregation of each of the

other phenotypes associated with the class C mutants was also examined. In crosses between *ts* class C mutants and parental strains, all phenotypes showed the expected 2:2 segregation pattern. In each cross, the temperature sensitivity, osmotic sensitivity and block in *ade2* red pigment formation all cosegregated with the vacuole protein sorting defect. The results of a typical tetrad analysis for a *ts* class C mutant, *vpt16*, are shown in Fig. 10. Similar tetrad analyses also demonstrated that the low pH sensitivity exhibited by *vpt13* cosegregated with the *vpt* sorting defect (data not shown).

DISCUSSION

We have analyzed in detail the morphology and growth properties of a number of mutants defective in vacuole protein targeting. Three distinct vacuolar morphologies associated with the *vpt* mutants have been observed. The class A mutants, constituting 26 complementation groups, resembled the wild-type parent strains in that they had one or a few large vacuoles which were easily observed using light and fluorescence microscopy (Fig. 1a,b). A second class of mutants, Class B, consisted of three complementation groups and was characterized by an altered morphology in which the vacuole was highly fragmented (Fig. 1c). Mutants in the four class C complementation groups had no discernible vacuoles (Fig. 1d), but accumulated small vesicles and other novel membrane-enclosed structures throughout the cytoplasm (Fig. 8).

The majority of class A *vpt* mutants showed no apparent abnormalities in the vacuole itself or in other cellular features, as determined by electron microscopic analysis. In these mutants, at least some proteins presumably must continue to be properly targeted to the vacuole. Consistent with this idea, many of the class A *vpt* mutants mislocalize only a small fraction of CPY, PrA, PrB, or a CPY-Inv hybrid protein that contains vacuolar sorting information (46). It is possible that these mutants define functions which are only peripherally involved in vacuole protein targeting. However, other class A *vpt* mutants (*vpt*1, 4, 6, 7, 15, 17, 29, 30) exhibit gross defects in the localization and processing of vacuolar proteins, secreting as much as 70-100% of the CPY (46). These class A mutants still contain intact vacuoles and secrete <5% of the activity of a vacuolar membrane marker enzyme, α-mannosidase, suggesting that different pathways may exist for the sorting of soluble and membrane vacuolar proteins (see below).

Mutants in one of the class A complementation groups, *vpt*13, exhibited extreme sensitivity to low pH (Fig. 3a), suggesting that these cells may be unable

to regulate their intracellular pH. The *vpt*13 mutants were also defective in the pH-dependent accumulation of quinacrine in the vacuole (Fig. 2e). In mammalian cells, endosomal acidity has been implicated in the proper localization of proteins to this organelle. Compounds such as amines that raise intralysosomal and endosomal pH (40) cause lysosomal enzymes to be secreted. The increase in pH appears to inhibit the uncoupling of lysosomal enzymes from their receptor carrier(s), resulting in a saturation of the available receptor sites (13). Furthermore, mammalian cell mutants have been described which appear to be defective in acidification of the endosome; these mutants secrete increased amounts of lysosomal hydrolases (45). In yeast, vacuolar pH may also play an important role in vacuole protein targeting. Treatment of wild-type yeast cells with ammonium acetate, the proton ionophore CCCP, or bafilomycin A_1, a drug which specifically inhibits the vacuolar ATPase, resulted in a block in the pH-dependent accumulation of quinacrine in the vacuole as well as the missorting of CPY and PrA (Fig. 4). Therefore, it seems likely that one or more of the *VPT* genes (e.g., *VPT*13) encode subunits of the vacuolar Mg^{++}-ATPase or other proteins involved in maintaining the vacuolar (or prevacuolar/endosomal) pH. Indeed, Stevens and coworkers (personal communication) have recently obtained data indicating that *vpt*13 mutants exhibit levels of vacuolar ATPase activity that are tenfold lower than those in wild-type strains.

Unlike the class A *vpt*s, the class B mutants exhibited gross aberrations in vacuolar structure. The many small vacuole-like compartments observed in class B *vpt* mutants may represent the accumulation of an intermediate in vacuolar biogenesis or alternatively, fragmentation of a larger vacuole. These mutants might lack a vacuolar surface molecule which promotes fusion of small "pre-vacuolar" compartments to form a large vacuole. Alternatively, the gene products defined by the mutants could encode cellular constituents required to

maintain the structural integrity of the organelle. These mutants also raise the issue of what exactly constitutes a vacuole. The organelles observed in the class B *vpt* mutants accumulated the dyes used to stain wild-type vacuoles and apparently had a similar acidic pH, as determined by the pH-dependent quinacrine staining (Fig. 2). However, the "vacuole" structures that accumulated in these mutants presumably are not recognized as valid destinations for certain vacuolar proteins, since the vast majority of PrA and CPY expressed in these mutants remains unprocessed and much is secreted (46).

The class C *vpt* mutants exhibited the most extreme defects in vacuole asembly among the *vpt* mutants isolated thus far. Many of these cells appeared to be essentially devoid of any organelles that resembled a vacuole, based on the criteria of size, shape and histochemical staining properties of normal vacuoles (Fig. 1d). The observation that these cells are viable despite the absence of a vacuole indicates that many vacuolar functions may not be necessary under optimal growth conditions. Many of the class C mutants, however, are temperature-sensitive for growth (46). The block in growth at 37°C exhibited by these mutants may indicate a requirement for a specific vacuolar function, or more likely, the cumulative effect of the loss of several vacuolar functions combined with the stress of growth at a temperature significantly above the preferred growth temperature of the organism.

The class C *vpt* mutants also exhibited an exaggeration of other organelles including Bbs, which are presumably related to Golgi structures and represent an intermediate compartment of the secretory pathway (36). The accumulation of Golgi-like structures or Bbs observed in these and certain other *vpt* mutants is consistent with a backup of vacuole proteins at the Golgi, the site of segregation for these proteins (54). In addition, the cytoplasm in these cells was filled with vesicles and complex lamellar arrays that might represent remnant vacuolar

material or intermediates in vacuole biogenesis (Fig. 8). Several scenarios could account for the accumulation of organelles in these mutants. The gene products defined by the class C *vpt* mutants might correspond to essential components of a vacuolar protein sorting apparatus or to structural proteins of the vacuole itself. Alternatively, the class C *VPT* gene products might be involved in the regulation of organelle biogenesis, a process about which very little is known. Like its mammalian counterpart, the yeast vacuole may play an important role in the intracellular turnover of macromolecules. Perhaps in the class C mutants, organelles and membrane fragments accumulate because the cells lack a vacuole to perform this digestive function. The vesicles observed in these *vpt* mutants might represent intermediates in endocytic traffic that, in the absence of a vacuole, have no suitable target destination. On the other hand, the structures which accumulate in the class C mutants might represent actual intermediates in vacuole biogenesis. However, because these organelles are present at both permissive and nonpermissive growth temperatures, we are at present unable to test whether they correspond to actual reversible intermediates in the vacuole assembly pathway or are dead-end, nonreversible compartments. Additional experiments, such as immunoelectron microscopy or purification of the vesicles, will be required to address the nature of the content of these structures and their likely origin.

In plant cells, the large central vacuole plays an important role in regulating cell turgor pressure (3,18,61). Although not as extensively studied, it is possible that the vacuole may have a similar osmoregulatory function in yeast. High concentrations of solutes such as polyphosphates are stored in the yeast vacuole as osmotically inactive aggregates or polymers that could be converted into osmotically active forms by enzymatic digestion of the polymers. Large pools of sugars and basic amino acids (especially arginine) may also be present

(29). Mutants in the four class C complementation groups were sensitive to osmotic stress (Fig. 3b). Perhaps these cells are unable to accumulate the compounds normally used to generate high internal osmotic pressures. Alternatively, the osmotic-sensitive phenotype may not be directly related to vacuolar function. A number of seemingly diverse mutants, including nonsense suppressors, plasma membrane ATPase mutants and actin mutants are sensitive to osmotic stress (31,35,51). Singh and Sherman have suggested that, like *ts* mutations, alterations in a variety of essential proteins may make cells unusually sensitive to stressful growth conditions, in this case hypertonicity (52). Two class A *vpt* mutants (*vpt*15, 29) were partially inhibited for growth in the presence of hypertonic stress. The vacuoles in these strains were abnormally large and occasionally appeared to contain inclusions. Like class C *vpt* mutants, cells in these groups accumulated vesicles and Bbs (Fig. 6), and many of these strains are *ts* for growth. Furthermore, these mutants are severely defective in the processing and sorting of CPY and PrA (46). On the basis of the class C-like phenotypes exhibited by *vpt*15 and *vpt*29, we propose that these mutants may represent an intermediate between the class A and class C morphologies.

The class C *vpt* mutants are among the most defective in targeting CPY, PrA and PrB to the vacuole (46). Unlike other *vpt* mutants, however, the class C mutants secrete 30-50% of the vacuolar membrane marker enzyme, α-mannosidase (46), indicating that the sorting defect in these mutants extends to membrane, as well as lumenal, proteins. Taken together, the data suggest that different recognition systems may participate in the sorting of soluble vacuole proteins, such as CPY and PrA, and vacuole membrane proteins (e.g., α-mannosidase). However, both sets of proteins may transit via common carrier vesicles or other intermediate compartments en route to the vacuole. According to such a model, the class C *vpt* mutants might affect protein sorting at the level

of the common compartment. In contrast, the defects observed in many of the class A mutants, which mislocalize only a subset of the vacuole proteins, are likely to affect more specific components in the pathway, such as protein receptors.

A set of *v*acuolar *p*rotein *l*ocalization (*vpl*) mutants similar to those described here has been isolated by selecting for the presence of active CPY in the periplasm (47). Some of these mutants also exhibit aberrant organelles such as Bbs and multivesicular bodies in addition to a normal vacuole. Complementation analysis has revealed that several of the *vpl* mutations are allelic to various *vpt* mutations. However, none of the *vpl* mutants exhibits the extreme defects in vacuole biogenesis seen in the class C *vpt* mutants (46,47; J. Rothman and T. Stevens, personal communication).

Two mutants which are defective in the accumulation of an endocytic marker, lucifer yellow carbohydrazide, and in pheromone response have been described by Chvatchko *et al.*, (7). One of these mutants, *end*1, has a morphology similar to that of the class C *vpt* mutants in that it lacks a vacuole and accumulates many small vesicles in the cytoplasm. This mutant is also defective in CPY processing (44) and sorting (46). Like the class C *vpt* mutants, *end*1 grows poorly on glycerol (V. Dulic and H. Riezman, personal communication) and is unable to grow under conditions of osmotic stress or high temperature. Complementation analysis has demonstrated that *end*1 is allelic to *vpt*11 (46; V. Dulic and H. Riezman, personal communication). This finding suggests that the vacuolar protein sorting and endocytic pathways may converge and that some gene functions may be common to both pathways. Geuze *et al.*, have suggested that lysosomal enzymes are directed to lysosome via a prelysosomal compartment which is also the site of uncoupling of endocytosed ligands and receptors (12). More recently, Griffiths *et al.* have identified a compartment in rat kidney cells

which, by immunolocalization studies, appears to be shared by the lysosomal targeting and endocytic pathways (14).

The extreme defects in vacuole biogenesis, aberrations in vacuolar and cellular morphology, and increased sensitivity to suboptimal growth conditions observed in certain of the *vpt* mutants suggest strongly that vacuole structure and/or function are impaired in these strains. However, functions such as secretion and microtubule assembly appear to be normal in all of the *vpt* mutants (46). Although the class C *vpt* mutants, as well as *vpt15* and *vpt29*, accumulate organelles resembling those seen in certain *sec* mutants, complementation analysis has shown that these *vpt* mutants and the *sec* mutants are not allelic (46). Other yeast mutations have been described which result in *vpt*-like morphological defects. A *ts* mutation in the single yeast actin gene (*act1*) leads to an accumulation of Bbs and vesicles similar to that seen in *vpt15* and *vpt29* (35); however, complementation analysis indicates that none of the *ts vpt* mutants is allelic to *act1* (unpublished results). Likewise, although a deletion of the clathrin heavy chain gene in yeast causes severe morphological and growth defects, these cells continue to sort vacuolar proteins properly (39). A recently isolated mutant, *slp1*, exhibits a *vpt*-like morphology in that it lacks a central vacuole but contains many small vesicles thoughout the cytoplasm (24a). We have not yet been able to test the allelism of this mutation with any of the *vpt* mutations.

The class B and C *vpt* mutants, which exhibit altered vacuolar morphologies, may define functions required for specific stages of vacuole biogenesis. These mutants may be especially useful for *in vitro* studies directed at reconstituting different steps in vacuole assembly. Molecular cloning of the *VPT* genes and characterization of the encoded gene products, coupled with the development of an *in vitro* system in which these gene products can be assayed, should help elucidate the roles these proteins play in vacuolar function, protein targeting, and organelle biogenesis.

ACKNOWLEDGEMENTS

We would like to thank Jean Edens for invaluable assistance with the electron microscopy, Michael W. Clark for the membrane-enhancement technique protocol and advice on the fluorescence microscopy, and Paul Herman for helpful discussions and assistance with the zygote experiments. We also thank K. Altendorf for the gift of bafilomycin A_1, Cathy Elkins for typing the manuscript, and Joel Rothman, Tom Stevens, Barry Bowman, and Howard Riezman for communicating their results prior to publication. This study was supported by Public Health Service grant GM-32703 from the National Institutes of Health to S.D.E. L.M.B. was supported by graduate fellowships from the National Science Foundation and General Electric. J.S.R. was supported by graduate fellowships from the Evelyn Sharp Foundation, the Lucy Mason Clark fund, and the Markey Charitable Trust Fund. D.J.K. was supported by a research fellowship from the Helen Hay Whitney Foundation. S.D.E. is an NSF Presidential Young Investigator supported by National Science Foundation grant DCB-8451633.

LITERATURE CITED

1. Allison, A. C., and M. R. Young. 1969. Vital staining and fluorescence microscopy of lysosomes. In J. T. Dingle, and H. B. Fell (Ed.), *Lysosomes in Biology and Pathology*. Vol. 2. North Holland, Amsterdam. pp. 600-628.
2. Bankaitis, V. A., L. M. Johnson, and S. D. Emr. 1986. Isolation of yeast mutants defective in protein targeting to the vacuole. Proc. Natl. Acad. Sci. USA 83: 9075-9079.
3. Boller, T., and A. Wiemken. 1986. Dynamics of vacuolar compartmentation. Ann. Rev. Plant Physiol. 37: 137-164.
4. Bowman, E. J., A. Siebers, and K. Altendorf. 1988. Bafilomycins: a new class of inhibitors of membrane ATPases from microorganisms, animal cells, and plant cells. Proc. Natl. Acad. Sci. USA 85:7972-7976.
5. Burgess, T. L., and R. B. Kelly. 1987. Constitutive and regulated secretion of proteins. Ann. Rev. Cell Biol. 3: 243-293.
6. Byers, B., and L. Goetsch. 1975. The behavior of spindles and spindle plaques in the cell cycle and conjugation of *Saccharomyces cerevisiae*. J. Bacteriol. 124: 511-523.
7. Chvatchko, Y., I. Howald, and H. Riezman. 1986. Two yeast mutants defective in endocytosis are defective in pheromone response. Cell 46: 355-364.
8. Cramer, C. L., and R. H. Davis. 1979. Screening for amino acid pool mutants of *Neurospora* and yeasts: replica-printing technique. J. Bacteriol. 137: 1437-1438.
9. DeDuve, C., T. DeBarsy, B. Poole, A. Trouet, P. Tulkens, and F. van Hoof. 1974. Lysosomotropic agents. Biochem. Pharm. 23: 2495-2531.

10. Ericsson, J. L. E. 1969. Mechanism of cellular autophagy. In J. T. Dingle, and H. B. Fell (Ed.), *Lysosomes in Biology and Pathology*. Vol. 2. North Holland, Amsterdam. pp. 345-394.

11. Farquhar, M. G. 1985. Progression in unraveling pathways of Golgi traffic. Ann. Rev. Cell Biol. 1: 447-488.

12. Geuze, H. J., J. W. Slot, G. J. A. M. Strous, A. Hasilik, and K. von Figura. 1985. Possible pathways for lysosomal enzyme delivery. J. Cell Biol. 101: 2253-2262.

13. Gonzalez-Noriega, A., J. H. Grubb, V. Talkad, and W. S. Sly. 1980. Chloroquine inhibits lysosomal enzyme pinocytosis and enhances lysosomal enzyme secretion by impairing receptor recycling. J. Cell. Biol. 85: 839-852.

14. Griffiths, G., B. Hoflack, K. Simons, I. Mellman, and S. Kornfeld. 1988. The mannose-6-phosphate receptor and the biogenesis of lysosomes. Cell 52: 329-341.

15. Guthrie, B., and W. Wickner. 1988. Yeast vacuoles fragment when microtubules are disrupted. J. Cell. Biol. 107: 115-120.

16. Hasilik, A., and W. Tanner. 1978. Biosynthesis of the vacuolar yeast glycoprotein carboxypeptidase Y. Conversion of precursor into the enzyme. Eur. J. Biochem. 85: 599-608.

17. Hay, R., P. Böhni, and S. Gasser. 1984. How mitochondria import proteins. Biochim. Biophys. Acta. 779: 65-87.

18. Hellebust, J. A. 1976. Osmoregulation. Ann. Rev. Plant Physiol. 27: 485-505.

19. Hemmings, B. A., G. S. Zubenko, A. Hasilik, and E. W. Jones. 1981. Mutant defective in processing of an enzyme located in the lysosome-like vacuole of *Saccharomyces cerevisiae*. Proc. Natl. Acad. Sci. USA 78: 435-439.

20. Indge, K. J. 1968. The isolation and properties of the yeast cell vacuole. J. Gen. Microbiol. 51: 441-446.

21. Johnson, L. M., V. A. Bankaitis, and S. D. Emr. 1987. Distinct sequence determinants direct intracellular sorting and modification of a yeast vacuolar protease. Cell 48: 875-885.

22. Jones, E. W. 1984. The synthesis and function of proteases in *Saccharomyces*: genetic approaches. Ann. Rev. Genet. 18: 233-270.

23. Jones, E. W., and G. R. Fink. 1982. Regulation of amino acid and nucleotide biosynthesis in yeast. In J. N. Strathern, E. W. Jones, and J. R. Broach (Ed.), *The Molecular Biology of the Yeast* Saccharomyces cerevisiae. *Metabolism and Gene Expression.* Cold Spring Harbor Laboratory. Cold Spring Harbor, New York. pp. 181-299.

24. Kakinuma, Y., Y. Ohsumi, and Y. Anraku. 1981. Properties of H^+-translocating adenosine triphosphatase in vacuolar membranes of *Saccharomyces cerevisiae*. J. Biol. Chem. 256: 10859-10863.

24a. Kitamoto, K., K. Yoshizawa, Y. Ohsumi, and Y. Anraku. 1988. Mutants of *Saccharomyces cerevisiae* with defective vacuolar function. J. Bacteriol. 170: 2687-2691.

25. Klionsky, D. J., L. M. Banta, and S. D. Emr. 1988. Intracellular sorting and processing of a yeast vacuolar hydrolase: the proteinase A propeptide contains vacuolar targeting information. Mol. Cell. Biol. 8: 2105-2116.

26. Lenz, A.-G., and H. Holzer. 1984. Effects of chloroquine on proteolytic processes and energy metbolism in yeast. Arch. Microiol. 137: 104-108.

27. Makarow, M. 1985. Endocytosis in *Saccharomyces cerevisiae*: internalization of α-amylase and fluorescent dextran into cells. EMBO J. 4: 1861-1866.

28. Matile, P. 1969. Plant lysosomes. In J. T. Dingle, and H. B. Fell (Ed.), *Lysosomes in Biology and Pathology.* Vol. 1 North Holland, Amsterdam. pp. 406-430.

29. Matile, P. 1978. Biochemistry and function of vacuoles. Ann. Rev. Plant Physiol. 29: 193-213.

30. Matile, P., H. Moor, and C. F. Robinow. 1969. Yeast cytology. In A. H. Rose, and J. S. Harrison (Ed.), *The Yeasts.* Academic Press, London. pp. 219-302.

31. McCusker, J. H., D. S. Perlin, and J. E. Haber. 1987. Pleiotropic plasma membrane ATPase mutations of *Saccharomyces cerevisiae.* Mol. Cell. Biol. 7: 4082-4088.

32. Mechler, B., M. Müller, H. Müller, F. Meussdoerffer, and D. H. Wolf. 1982. *In vivo* biosynthesis of the vacuolar proteinases A and B in the yeast *Saccharomyces cerevisiae.* J. Biol. Chem. 257:11203-11206.

33. Navon, G., R. G. Shulman, T. Yamane, T. R. Eccleshall, K.-B. Lam, J. J. Baronofsky, and J. Marmur. 1979. Phosphorus-31 nuclear magnetic resonance studies of wild-type and glycolytic pathway mutants of *Saccharomyces cerevisiae.* Biochemistry 18: 4487-4499.

34. Nishimura, M. 1982. pH in vacuoles isolated from castor bean endosperm. Plant Physiol. 70: 742-744.

35. Novick, P., and D. Botstein. 1985. Phenotypic analysis of temperature-sensitive yeast actin mutants. Cell 40: 405-416.

36. Novick, P., S. Ferro, and R. Schekman. 1981. Order of events in the yeast secretory pathway. Cell 25: 461-469.

37. Novick, P., C. Field, and R. Schekman. 1980. Identification of 23 complementation groups required for post-translational events in the yeast secretory pathway. Cell 21: 205-215.

38. Ohkuma, S., and B. Poole. 1978. Fluorescence probe measurement of the intralysosomal pH in living cells and the perturbation of pH by various agents. Proc. Natl. Acad. Sci. USA 75: 3327-3331.

39. Payne, G. S., T. B. Hasson, M. S. Hasson, and R. Schekman. 1987. Genetic and biochemical characterization of clathrin-deficient *Saccharomyces cerevisiae*. Mol. Cell. Biol. 7: 3888-3898.

40. Poole, B., and S. Ohkuma. 1981. Effect of weak bases on the intralysosomal pH in mouse peritoneal macrophages. J. Cell Biol. 90: 665-669.

41. Preston, R. A., R. F. Murphy, and E. W. Jones. 1987. Apparent endocytosis of fluorescein isothiocyanate-conjugated dextran by *Saccharomyces cerevisiae* reflects uptake of low molecular weight impurities, not dextran. J. Cell Biol. 105: 1981-1987.

42. Reynolds, E. S. 1963. The use of lead citrate at high pH as an electron-opaque stain in electron microscopy. J. Cell Biol. 17: 208-212.

43. Riezman, H. 1985. Endocytosis in yeast: several of the yeast secretory mutants are defective in endocytosis. Cell 40: 1001-1009.

44. Riezman, H., Y. Chvatchko, and V. Dulic. 1986. Endocytosis in yeast. Trends Biochem. Sci. 11: 325-328.

45. Robbins, A. R., S. S. Peng, and J. L. Marshall. 1983. Mutant Chinese hamster ovary cells pleiotropically defective in receptor-mediated endocytosis. J. Cell Biol. 96: 1064-1071.

46. Robinson, J. S., D. J. Klionsky, L. M. Banta, and S. D. Emr. 1988. Protein sorting in yeast: isolation of mutants defective in the processing and sorting of multiple vacuolar hydrolases. Mol. Cell. Biol. 8:4936-4948.

47. Rothman, J. H., and T. H. Stevens. 1986. Protein sorting in yeast: mutants defective in vacuole biogenesis mislocalize vacuolar proteins into the late secretory pathway. Cell 47: 1041-1051.

48. Schwencke, J. 1988. The vacuole, internal membranous systems and vesicles. In A. H. Rose, and J. S. Harrison (Ed.), *The Yeasts*. Academic Press, London, in press.

49. Sherman, F., G. R. Fink, and C. W. Lawrence. 1979. Methods in Yeast Genetics: A Laboratory Manual. Cold Spring Harbor Laboratory, Cold Spring Harbor, New York. 1-98.

50. Silver, J. M., and N. R. Eaton. 1969. Functional blocks of the *ad*1 and *ad*2 mutants of *Saccharomyces cerevisiae*. Biochem. Biophys. Res. Commun. 34: 301-305.

51. Singh, A. 1977. Nonsense suppressors of yeast cause osmotic-sensitive growth. Proc. Natl. Acad. Sci. USA 74: 305-309.

52. Singh, A., and F. Sherman. 1978. Deletions of the iso-1-cytochrome c and adjacent genes of yeast: discovery of the *osm*1 gene controlling osmotic sensitivity. Genetics 89: 653-665.

53. Sly, W. S., and H. D. Fischer. 1982. The phosphomannosyl recognition system for intracellular and intercellular transport of lysosomal enzymes. J. Cell. Biochem. 18: 67-85.

54. Stevens, T., B. Esmon, and R. Schekman. 1982. Early stages in the yeast secretory pathway are required for transport of carboxypeptidase Y to the vacuole. Cell 30: 439-448.

55. Stevens, T. H., J. H. Rothman, G. S. Payne, and R. Schekman. 1986. Gene dosage-dependent secretion of yeast vacuolar carboxypeptidase Y. J. Cell Biol. 102: 1551-1557.

56. Valls, L. A., C. P. Hunter, J. H. Rothman, and T. H. Stevens. 1987. Protein sorting in yeast: the localization determinant of yeast vacuolar carboxypeptidase Y resides in the propeptide. Cell 48: 887-897.

57. Weisman, L. S., R. Bacallao, and W. Wickner. 1987. Multiple methods of visualizing the yeast vacuole permit evaluation of its morphology and inheritance during the cell cycle. J. Cell Biol. 105: 1539-1547.

58. Wieland, F. T., M. L. Gleason, T. A. Serafini, and J. E. Rothman. 1987. The rate of bulk flow from the endoplasmic reticulum to the cell surface. Cell 50: 289-300.

59. Wiemken, A., M. Schellenberg, and K. Urech. 1979. Vacuoles: the sole compartments of digestive enzymes in yeast (*Saccharomyces cerevisiae*)? Arch. Microbiol. 123: 23-35.

60. Willingham, M. C., and A. V. Rutherford. 1984. The use of osmium-thiocarbohydrazide-osmium (OTO) and ferrocyanide-reduced osmium methods to enhance membrane contrast and preservation in cultured cells. J. Histochem. Cytochem. 32: 455-460.

61. Zimmermann, U. 1978. Physics of turgor- and osmoregulation. Ann. Rev. Plant Physiol. 29: 121-148.

Table I. Summary of *vpt* Mutant Phenotypes

	Abnormal Growth Phenotypes			
	Vacuole Morphology	Osmotic Sensitive	Low pH Sensitive	Aberrant Organelles Accumulated*
Class A: (*vpt*1,2,4,6,7,8, 9,10,12,13,14, 15,17,19,20,21, 22,23,24,25, 27,28,29,30, 31,32)	Wild-type vacuoles	*vpt*15,29	*vpt*13	*vpt* 15,29-Bbs, vesicles *vpt*7,28-"Golgi" *vpt*12-vesicles
Class B: (*vpt*3,5,26)	Fragmented vacuoles	*vpt*26		
Class C: (*vpt*11,16,18,33)	No vacuoles	*vpt*11,16,18,33		Multilamellar membrane structures, vesicles, Bbs

*Bbs - Berkeley bodies, presumably related to Golgi complexes (36).

Figure 1. Vacuole morphology in *vpt* mutants labeled with FITC or the *ade2* endogenous fluorophore. (A, B, C, and D) Nomarski (left) and fluorescence (right) photomicrographs of cells labeled in the presence of FD (see Materials and Methods). (E, F, G, and H) Nomarski (left) and fluorescence (right) photomicrographs of cells grown in SD containing limiting adenine (12 μg/ml) to allow production of the *ade2* fluorophore. In each cell, the fluorescent spot corresponds to the vacuole, which appears as a large circular indentation using Nomarski optics (arrows). (A and E) Wild-type vacuole morphology as seen in the parental strains SEY6210 (A) or SEY6211 (E). (B and F) Representative class A *vpt* mutants, *vpt10* (B) and *vpt29* (F), in which the vacuole morphology is indistinguishable from that of the parent. (C and G) The class B *vpt* mutants, *vpt5* (C) and *vpt3* (G) contain multiple small vacuoles. (D and H) Representative class C *vpt* mutants *vpt18* (D) and *vpt11* (H), which contain no structures that stain like vacuoles. The bar represents 10 μm.

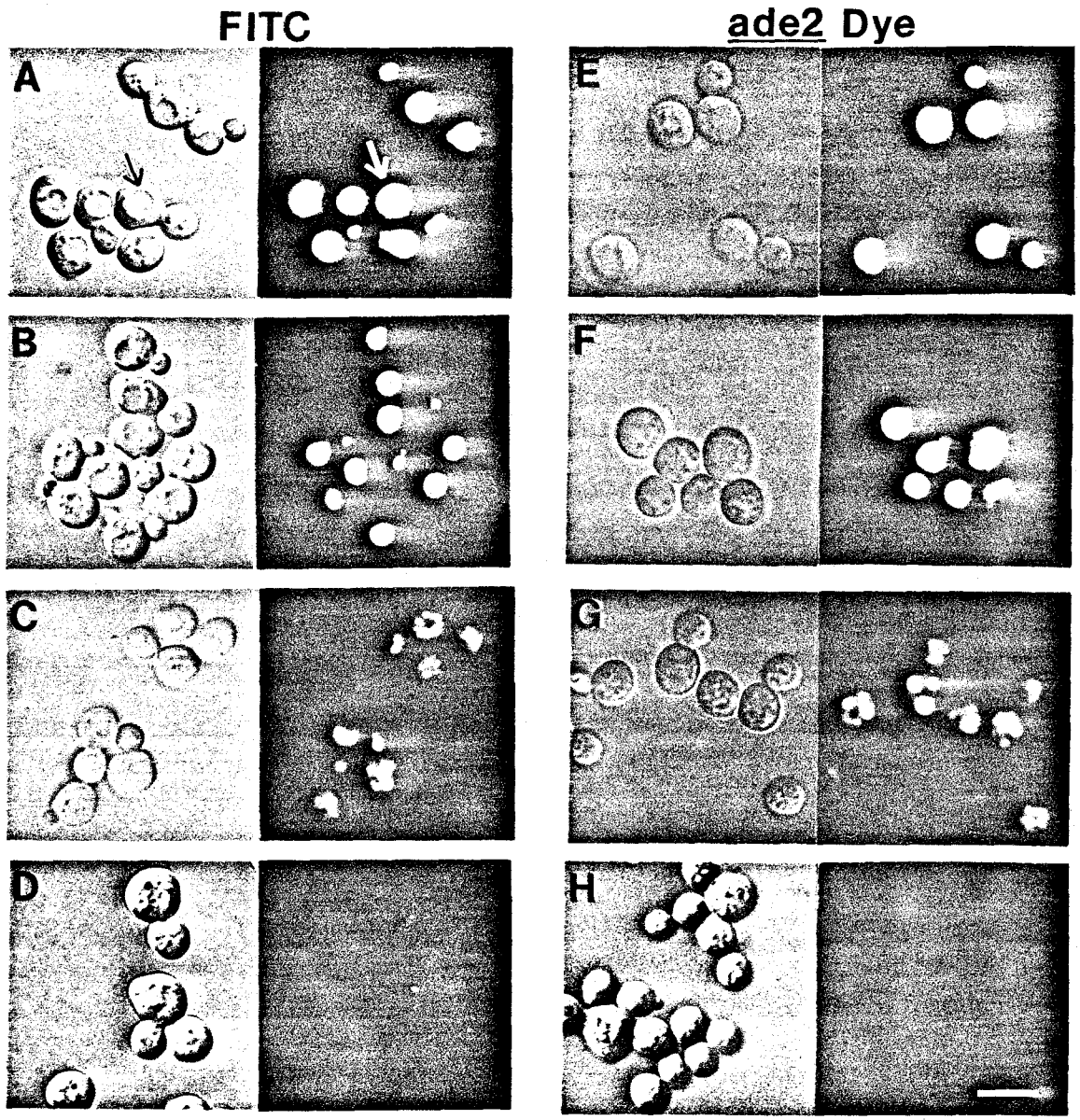
FITC
ade2 Dye
A
B
C
D
E
F
G
H

Figure 2. Quinacrine accumulation in the vacuoles of wild-type cells and *vpt* mutants. Cells were incubated in YPD, pH 7.6 containing 175 μM quinacrine for 5 min in the absence (A, C, and E) or presence (B and D) of 200 mM ammonium acetate. (A and B) Nomarski (left) and fluorescence (right) images of the parental strain SEY6210. (C and D) Nomarski (left) and fluorescence (right) images of *vpt5*, which exhibits a typical class B vacuole morphology. (E) *vpt13* exhibits no quinacrine staining (right), although vacuoles are clearly visible using Nomarski optics (left). The bar represents 10 μm.

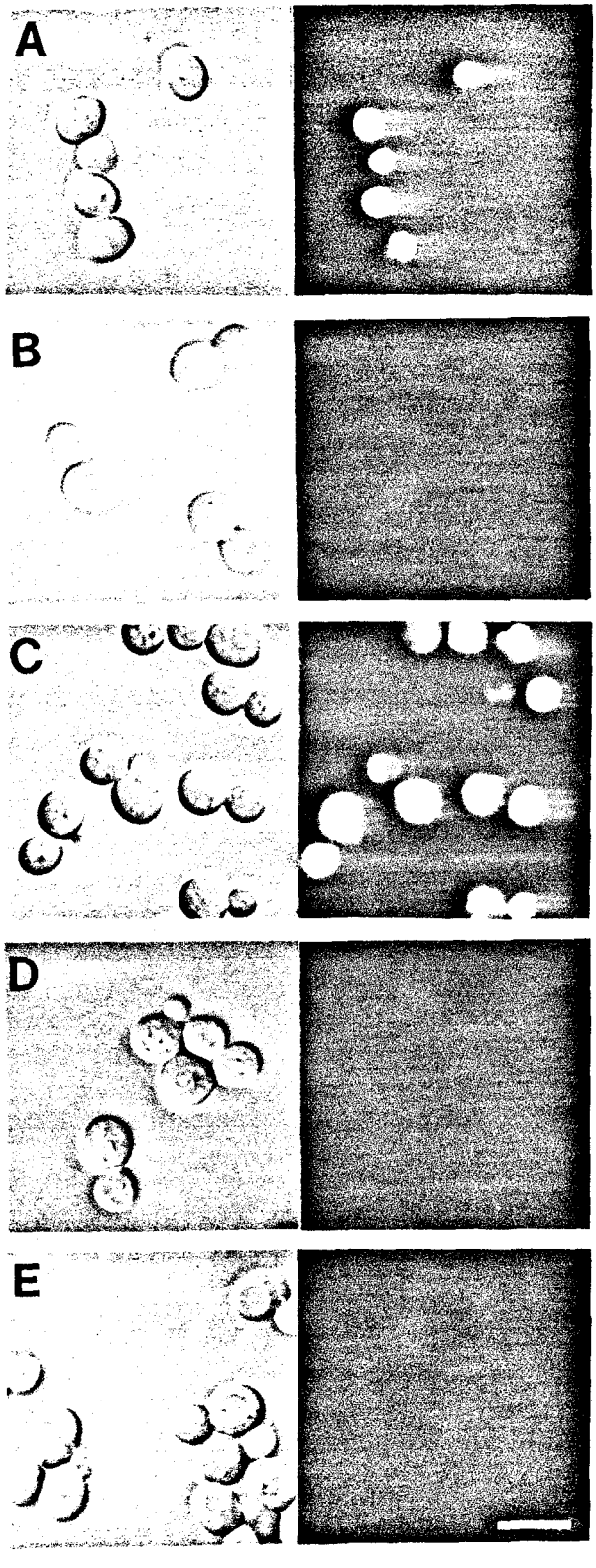
A
B
C
D
E

Figure 3. Growth defects associated with *vpt13* and the class C *vpt* mutants. (A) Three alleles of *vpt13* and the parental strain SEY6210 were streaked on YPD medium (left) or YPD medium adjusted to pH 3.0 with 6 N HCl (right). The plates were incubated at 30°C for 2 and 4 days, respectively. (B) A representative allele from each of the four class C *vpt* complementation groups was streaked on YPD medium (left) or YPD medium containing 1.5 M NaCl (right). The plates were incubated at 30°C for 2 and 5 days, respectively. The parental strain SEY6211 and a class A *vpt* mutant, *vpt1*, are shown for comparison.

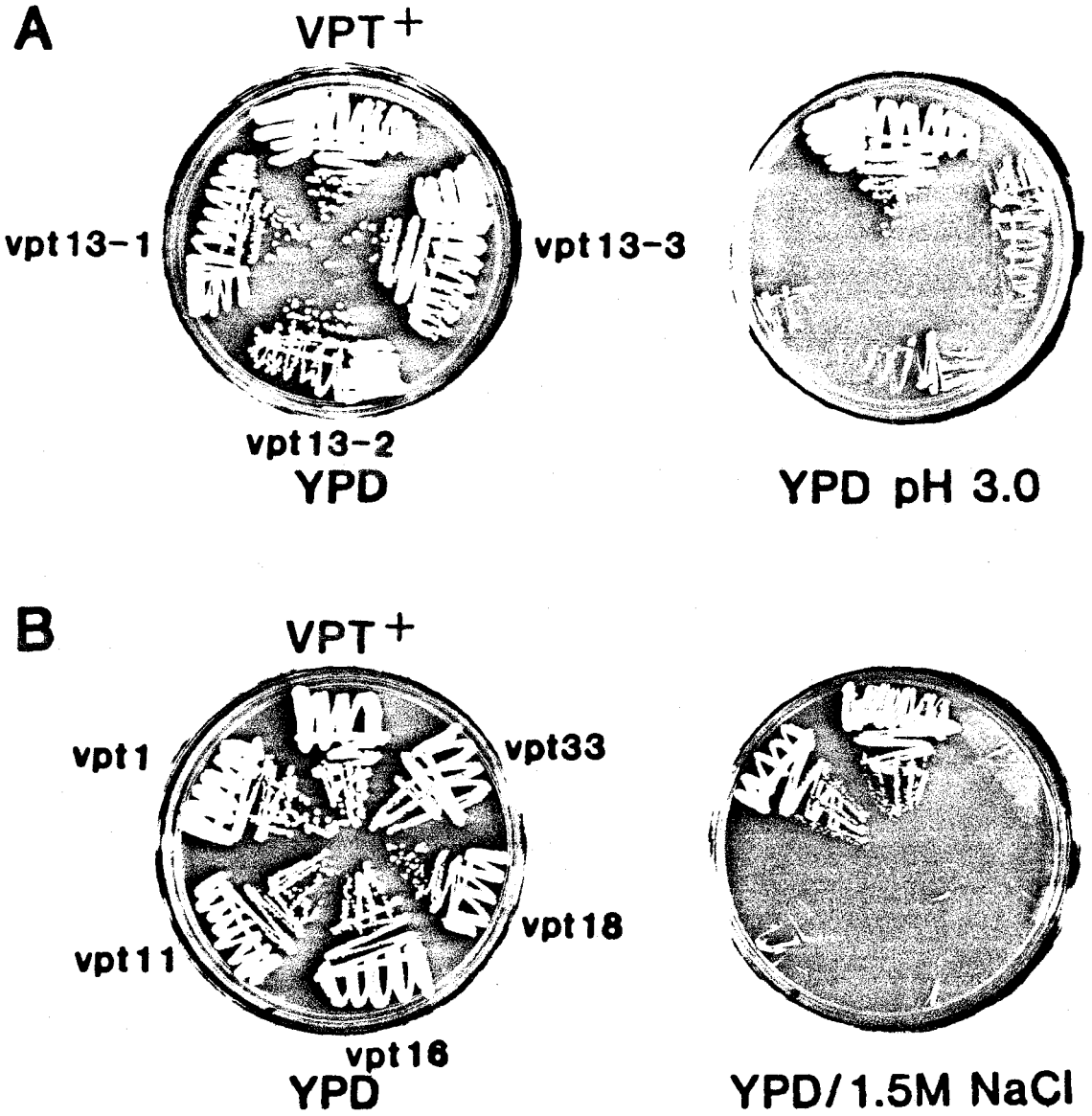
A
VPT+
vpt13-1
vpt13-3
vpt13-2
YPD
YPD pH 3.0
B
VPT+
vpt1
vpt33
vpt11
vpt18
vpt16
YPD
YPD/1.5M NaCl

Figure 4. Effect of bafilomycin on vacuole staining with quinacrine and on vacuolar protein sorting. (A and B) Nomarski (left) and fluorescence (right) images of parental strain SEY6210 stained with quinacrine. Cells (2.5×10^7 in 0.25 ml) were preincubated for 10 min at 25°C in YPD pH 7.6 in the absence (A) or presence (B) of 10 μM bafilomycin (in DMSO). An aliquot of cells (50 μl = 5×10^6 cells) from each sample was added to 400 μl of YPD pH 7.6 containing 200 μM quinacrine without (A) or with (B) 10 μM bafilomycin. Cells were incubated for 5 min at 30°C, resuspended and mounted as described in Materials and Methods. The bar represents 10 μm. (C) Strain SEY6210 was enzymatically converted to spheroplasts as described (46). Bafilomycin was added to 10 μM final concentration as indicated 10 min prior to the addition of radioactive label. Cells were labeled with Tran ^{35}S-label for 20 min at 30°C and chased for 30 min by the addition of 5 mM methionine. Cultures were then separated into (I) intracellular (spheroplast) and (E) extracellular (periplasm and media) fractions (46). Immunoprecipitations with antisera to CPY and PrA were performed as described (25). The predicted locations and approximate molecular sizes of the different forms of CPY and PrA are indicated (kD, kilodaltons). Increased concentrations (100 μM) of bafilomycin did not increase the amount of missorted precursor CPY or PrA. Importantly, bafilomycin had no effect on mitochondrial protein import (data not shown), which requires an electrochemical potential across the mitochondrial inner membrane (17).

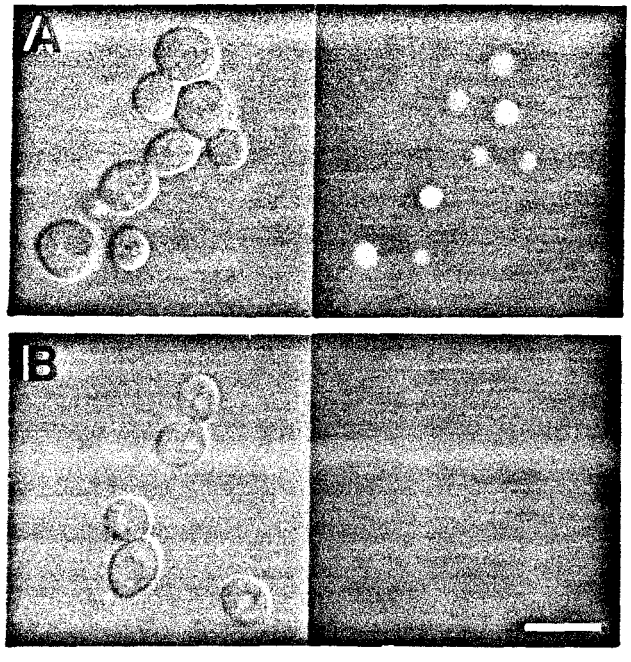
A
B

C:

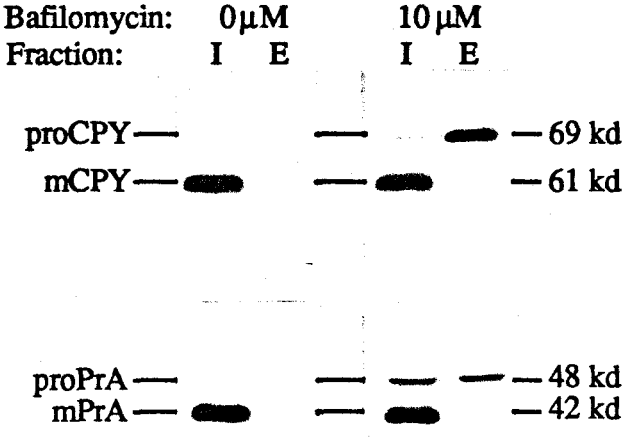
Bafilomycin: 0μM 10μM
Fraction: I E I E
proCPY
mCPY
69 kd
61 kd
proPrA
mPrA
48 kd
42 kd

Figure 5. Electron micrographs of cells exhibiting wild-type, class A, and class B vacuole morphologies. Cells were prepared using the reduced osmium-thiocarbohydrazide-reduced osmium membrane-enhancement technique as described in Materials and Methods. (A) Parental strain SEY6210. (B and C) Representative class A *vpt* mutants *vpt*17 (B) and *vpt*9 (C) also exhibit wild-type vacuolar and overall cellular morphology. (D) *vpt5*, a representative class B mutant, contains many small membrane-enclosed compartments which stain like wild-type vacuoles. V, vacuole; N, nucleus; M, mitochondrion; L, lipid droplet. Bar, 1 μm.

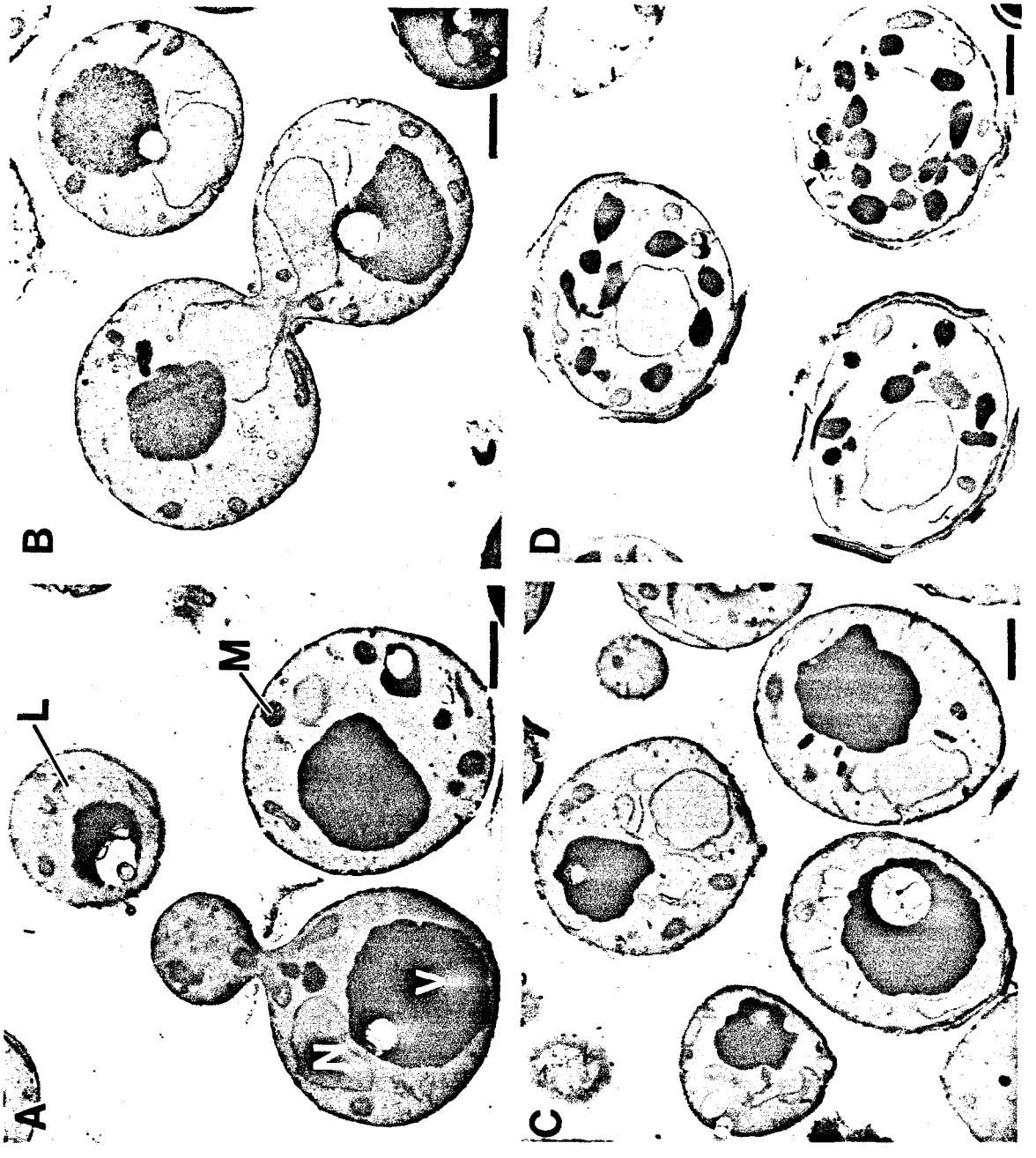
B
D
L
M
A
N
A
C

Figure 6. Electron micrographs of *vpt15* and *vpt29*, class A mutants which exhibit aberrant organelles similar to those seen in certain of the *sec* mutants. Cells were prepared as described in the legend to Fig. 5. (A and B) *vpt15* (A) and *vpt29* (B) cells contain Bbs (large arrows) and vesicles (small arrows) throughout the cytoplasm. (C) A typical *vpt15* cell, in which inclusions are seen in the vacuole. (D, E, and F) *sec* mutants (37) prepared using the membrane-enhancement technique, are shown for comparison. Each of the mutant strains was incubated at 37°C for 3 h prior to fixation. (D) Exaggerated tubular networks of membranes, presumably corresponding to ER, are clearly visible in this typical *sec18* cell. (E) Accumulated Bbs are seen in this high-magnification view of a portion of a representative *sec7* cell. (F) A high-magnification view of part of a *sec1* cell shows an accumulation of secretory vesicles. These vesicles have a different appearance than those seen in *vpt15* and *vpt29* (compare with A and B). The bar represents 0.5 μm in A, B, C, and D; in E and F the bar represents 0.1 μm.

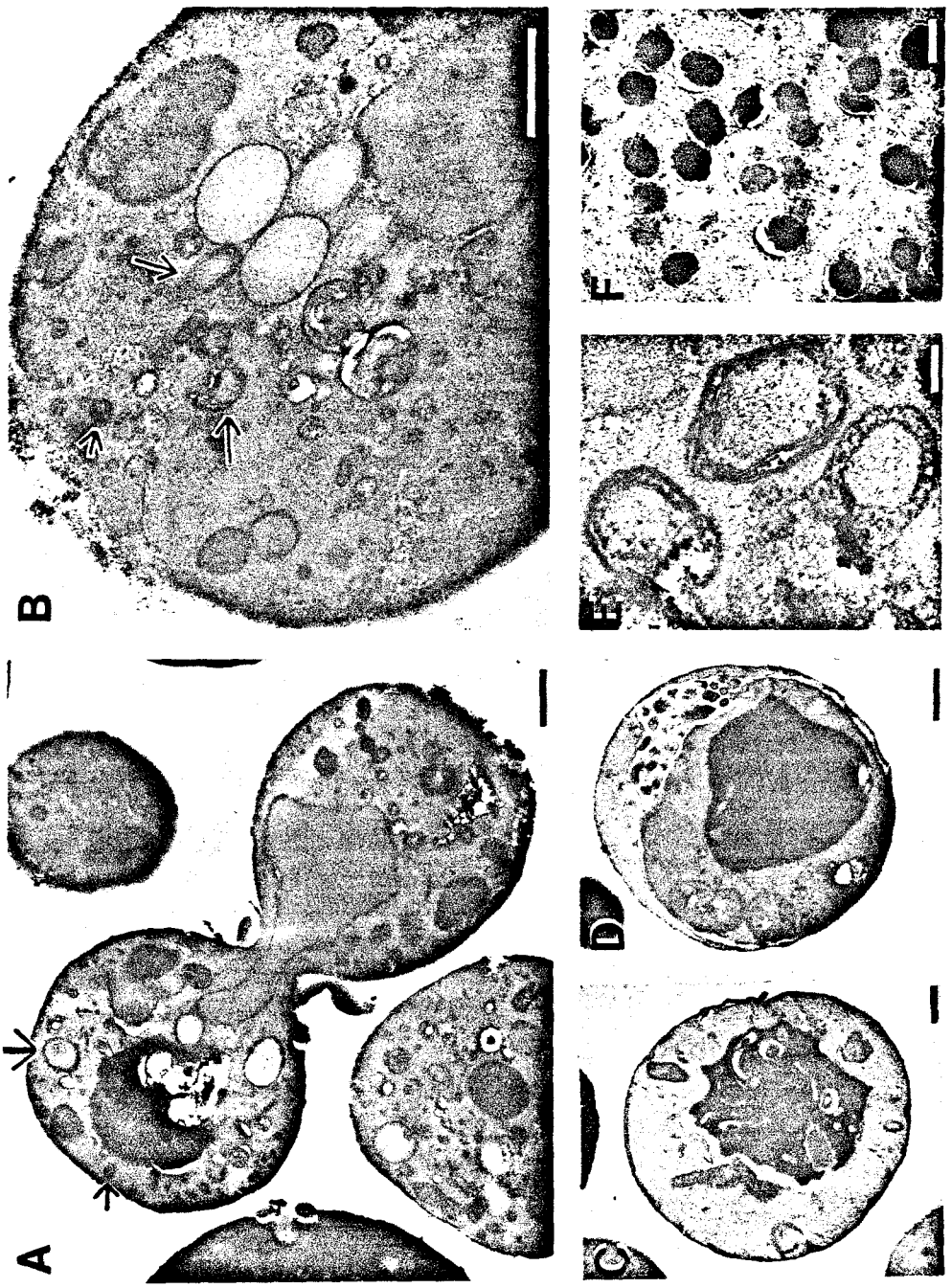
A
B
C
D
E
F

Figure 7. A gallery of electron micrographs of *vpt28* and *vpt7*, which accumulate Golgi-like structures (arrows). Cells were prepared as described in the legend to Fig. 5. View A shows *vpt7* cells; view B shows a *vpt28* cell. Panes C and D are high-magnification views of two Golgi-like structures representative of those seen in these mutants. The bar represents 1 μm in A and B; in C and D, the bar represents 0.2 μm.

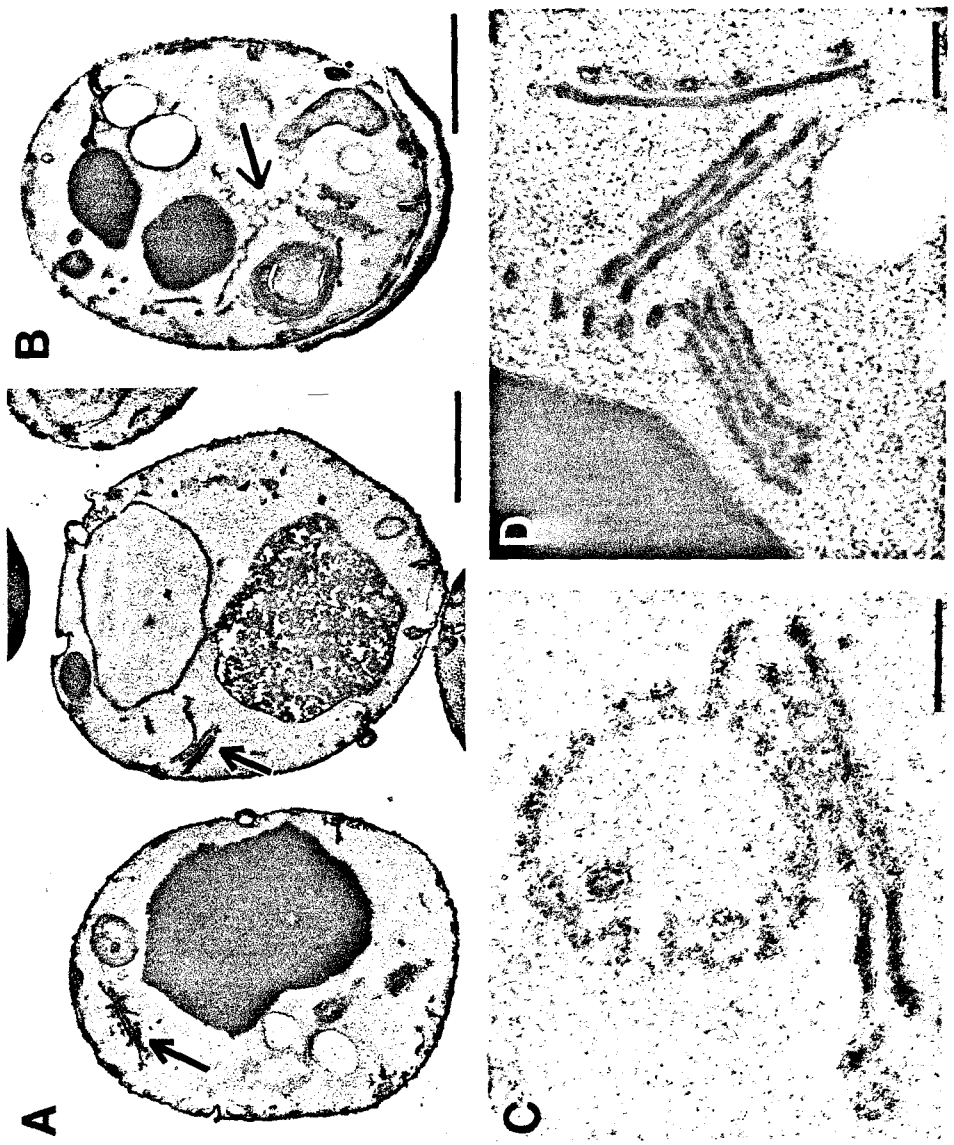
A
B
C
D

Figure 8. Electron micrographs of class C *vpt* mutants, which exhibit extreme defects in vacuole biogenesis. Cells were prepared as described in the legend to Fig. 5. (A, B, and C) Typical class C cells lack a discernible vacuole but accumulate aberrant organelles, including vesicles (small arrows), Bbs (large arrow), and large membranous structures (asterisk). (A) and (B) show *vpt*16 cells; (C) shows *vpt*11 cells. (D) shows a high-magnification view of the vesicles that accumulate in class C cells (compare with vesicles in *sec*1 mutant, Fig. 6f). Panel E shows a high-magnification view of the complex multilamellar arrays that accumulate in the cytoplasm in the class C *vpt* mutants. N, nucleus; L, lipid droplet; M, mitochondrion. The bar represents 0.5 μm in panels A, B, and C; in panels D and E, the bar represents 0.1 μm.

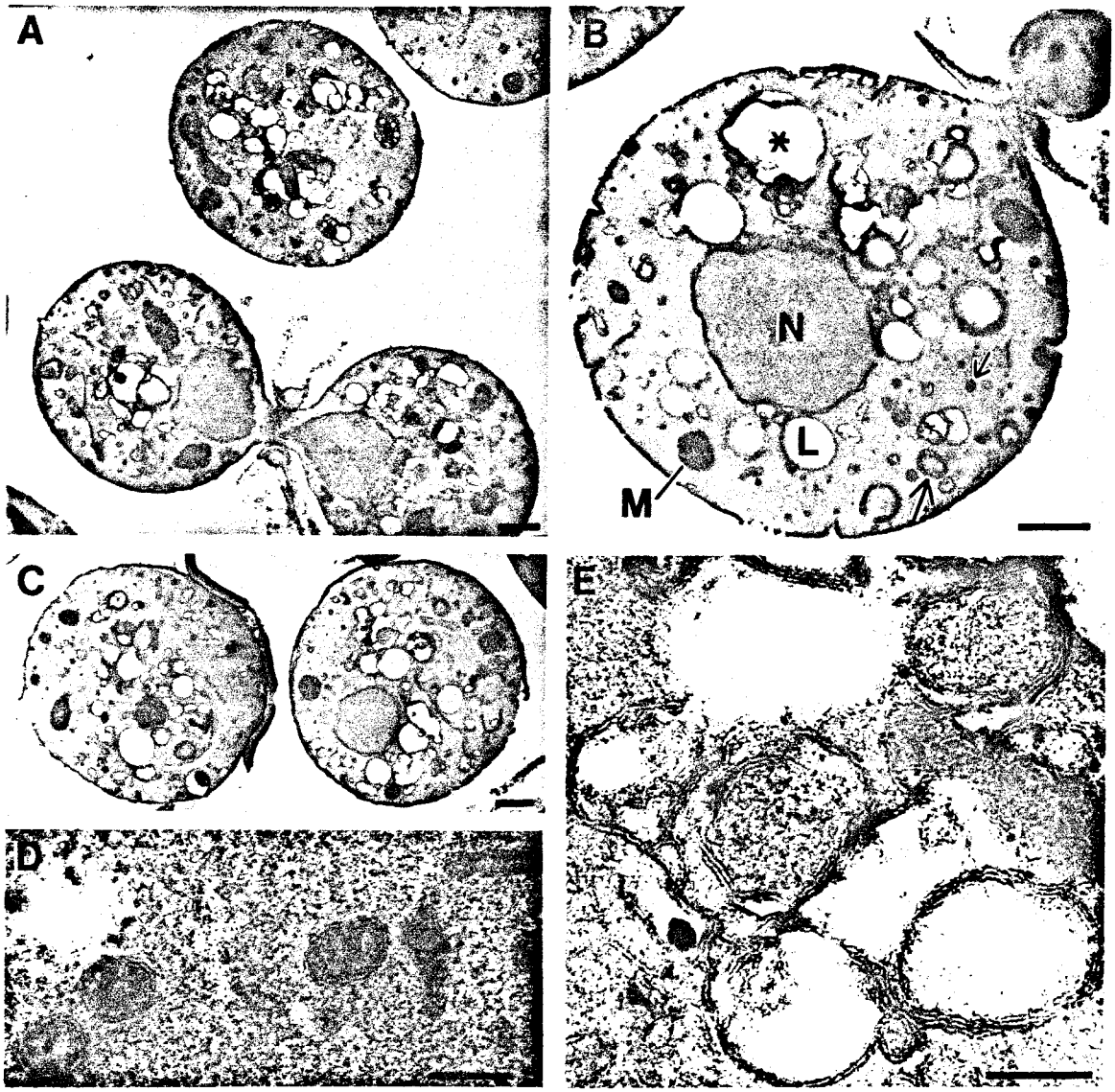
A
B
*
N
L
M
C
D
E

Figure 9. Heterozygous class C *vpt* zygotes form vacuoles within one generation after mating. (A) *vpt*18 (*MAT*α) and *vpt*33 (*MAT*a) cells were patched together on YPD medium and allowed to mate for 7 h at 25°C. Cells were scraped off the plate, resuspended in 1 ml YPD containing 50 mM Na-citrate, pH 5.5, and 1 µl of 10 mg/ml FITC was added. Cells were incubated for 10 min at 25°C, washed, and mounted as described in Materials and Methods. (B) Two *vpt*33 alleles were mated and stained as described for (A). The bar represents 10 µm.

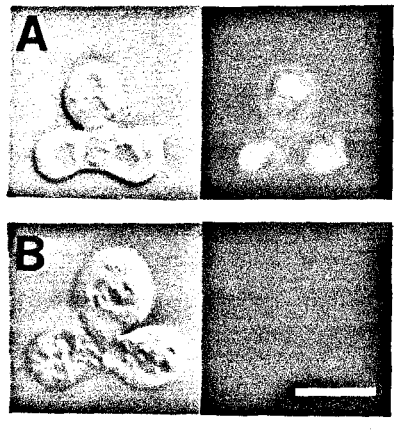
A
B

Figure 10. Cosegregation of the temperature-sensitive and osmotic-sensitive phenotypes in tetrads resulting from the sporulation of a *MAT*α *vpt*16/*MAT*a *VPT*$^+$ diploid. *vpt*16 was crossed with parental strain SEY6211 and diploids were selected. Diploids were sporulated and tetrads dissected as described in (49). Segregants were patched onto YPD medium and replica-plated onto YPD medium which was incubated at 25°C or 37°C or onto YPD medium containing 1.5 M NaCl (incubated at 25°C), as indicated. Segregants from four tetrads are shown. In each tetrad, the *ts* defect also was shown to be linked to the originally-selected *vpt* phenotype, secretion of the CPY-Inv hybrid protein (46).

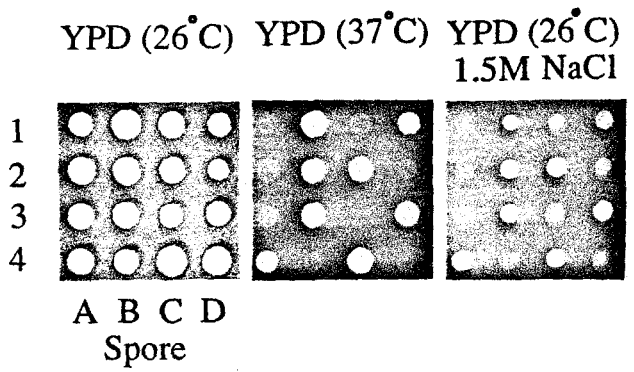
YPD (26°C)
YPD (37°C)
YPD (26°C)
1.5M NaCl
1
2
3
4
A B C D
Spore

Chapter 4

Characterization of the Yeast Vps33p, a Protein Required for Vacuolar Protein Sorting and Vacuole Biogenesis

Lois M. Banta, Thomas A. Vida, Paul K. Herman, and Scott D. Emr

Molecular and Cellular Biology, in press

ABSTRACT

vps33 mutants missort and secrete multiple vacuolar hydrolases and exhibit extreme defects in vacuolar morphology. Toward a molecular understanding of the role of the *VPS33* gene in vacuole biogenesis, we have cloned this gene from a yeast genomic library by complementation of a temperature-sensitive (*ts*) *vps33* mutation. Gene disruption has demonstrated that *VPS33* is not essential, but is required for growth at high temperature. At the permissive temperature, *vps33* null mutants exhibit defects in vacuolar protein localization and vacuole morphology similar to those seen in most of the original mutant stains. Sequence analysis reveals a putative open reading frame sufficient to encode a protein of 691 amino acids. Hydropathy analysis indicates that the deduced product of the *VPS33* gene is generally hydrophilic, contains no obvious signal sequence or transmembrane domains, and is therefore unlikely to enter the secretory pathway. Polyclonal antisera raised against TrpE-Vps33 fusion proteins recognize a protein in yeast of the expected molecular weight, ~75,000. In cell fractionation studies, Vps33p behaves as a cytosolic protein. The predicted *VPS33* gene product possesses sequence similarity with a number of ATPases and ATP-binding proteins specifically in their ATP-binding domains. One *vps33ts* mutant contains a missense mutation near this region of sequence similarity; the mutation results in a Leu→Pro substitution at position 646 in Vps33p. This *ts* mutant strain contains normal vacuoles at the permissive temperature, but lacks vacuoles specifically in the bud at the nonpermissive temperature. Our data suggest that Vps33p acts in the cytoplasm to facilitate Golgi-to-vacuole protein delivery. We propose that, as a consequence of the *vps33* protein sorting defects, abnormalities in vacuolar morphology and vacuole inheritance result.

INTRODUCTION

Eukaryotic cell lines contain a number of distinct membrane-enclosed organelles whose function and morphology are defined largely by the unique set of proteins residing within them. Thus, mutations that disrupt the accurate sorting of proteins to their correct intracellular locations might also affect the assembly and morphology of the target organelle. Conversely, abnormalities in organelle biogenesis may be manifest as protein trafficking or delivery defects.

In the yeast *Saccharomyces cerevisiae*, proteins destined for the lysosome-like vacuole traverse the secretory pathway en route to the vacuole. Soluble vacuolar proteins such as carboxypeptidase Y (CPY) and proteinase A (PrA) are synthesized as inactive precursors; upon delivery to the vacuole, these proenzymes undergo proteolytic processing to generate the mature active enzymes (14,15,25,48). We and others have recently isolated a number of mutants that exhibit defects in the proper localization and processing of multiple vacuolar hydrolases (1,39,41,42). These *v*acuolar *p*rotein *s*orting, or *vps*, mutants define more than 40 complementation groups. Morphological studies using both light and electron microscopy have revealed at least three distinct groups of *vps* mutants (2). The majority of the *vps* mutants (called class A *vps* mutants) contain morphologically wild-type vacuoles. A second class of mutants, class B, is characterized by an altered morphology in which the vacuole is highly fragmented. Mutants in four *vps* complementation groups exhibit the most extreme abnormalities in vacuole morphology. Electron microscopic analysis has revealed that these cells accumulate many small vesicles but lack any compartment that resembles a wild-type vacuole. This morphology has been designated class C (2).

The class C *vps* mutants exhibit extreme defects in the sorting and processing of soluble vacuolar proteins. In these strains, the Golgi-modified forms

of CPY, PrA, and proteinase B accumulate and are secreted. Little or no mature forms of these vacuolar enzymes can be detected in these mutants. Unlike other *vps* mutants, these class C strains also mislocalize as much as 50% of the activity of a vacuolar membrane enzyme, α-mannosidase (39). The class C *vps* mutants exhibit other genetically linked phenotypic defects including temperature-sensitive growth and sensitivity to osmotic stress. However, nonvacuolar functions such as secretion and microtubule assembly, as well as nuclear and mitochondrial structure, appear to be unaffected in these strains (2, 39).

In an effort to understand the molecular basis for the phenotypic defects exhibited by the class C *vps* mutants, we have examined in more detail the seven mutants comprising one of these class C complementation groups, *vps33*. We report here the cloning of the *VPS33* gene. This gene is not essential, but is required for growth at 37°C. The predicted *VPS33* gene product is a relatively hydrophilic protein of ~75 kd, which shares sequence similarity with a number of ATP-binding proteins. Cell fractionation studies indicate that Vps33p is soluble. We suggest that the *VPS33* gene product acts in the cytoplasm to facilitate Golgi-to-vacuole trafficking, thereby promoting vacuole assembly.

MATERIALS AND METHODS

Strains and Media. *Escherichia coli* strains MC1061 [F⁻ *araD139* Δ*(araABOIC-leu)7679* Δ*lacX74 galU galK rpsL hsdR strA*] (4), JM101 [*supE thi* Δ*(lac-proAB)* (F' *traD36 proAB lacI*^{q} *Z M15)*] (26), and DH1 [F⁻ *endA1 hsdR17 (rk*⁻ *mk*$^{+}$*) supE44 thi-1 recA1 gyrA96 relA1?*] (13) were used for cloning and TrpE-Vps33 fusion protein production. *E. coli* strain JF1754 (*hsdR metB leuB hisB lac gal*) (24) was used in screening plasmids pLB33-313 and pLB33-317. *E. coli* strain BW313 (Hfr KL16 PO/45[*lysA* (61-62)]*dut1 ung1 thi1 relA1*) (19A) was used in the oligonucleotide mutagenesis. *Saccharomyces cerevisiae* parental strains were SEY6210 (*MAT*α *ura3-52 leu2-3,112 his3-*Δ*200 trp1-*Δ*901 lys2-801 suc2-*Δ*9*) and SEY6211 (*MAT*a *ura3-52 leu2-3,112 his3-*Δ*200 trp1-*Δ*901 ade2-101 suc2-*Δ*9*) (39). *vps33* mutant strains SEY33-2, SEY33-4, and SEY33-5 are isogenic with SEY6210 and carry the *vps33-2*, *vps33-4*, and *vps33-5* mutations, respectively. SEY33-7, carrying the *vps33-7* allele, is isogenic with SEY6211. LBY317 carries a *vps33* null mutation and was derived from SEY6210 (see below). Bacterial strains were grown on standard media (27). Yeast strains were grown on standard yeast extract peptone dextrose (YPD) or synthetic dextrose (SD) (synthetic minimal, supplemented as necessary) media (46).

Materials. Restriction enzymes, T4 DNA ligase, Klenow enzyme and polyacrylamide gel electrophoresis (PAGE) supplies were purchased from Boehringer Mannheim Biochemicals (Indianapolis, IN). Mung bean nuclease and exonuclease III were the products of New England Biolabs (Beverly, MA). 5-Fluoroorotic acid was purchased form PCR, Inc. (Gainesville, FL). Isopropyl-β-D-thiogalactoside (I.P.T.G.), 5-bromo-4-chloro-3-indolyl-β-D-galactoside (X-gal), and Sequenase DNA Sequencing Kit were purchased from United States Biochemical Corp. (Cleveland, OH). Deoxynucleotides and Miniprep Kit Plus were the products of Pharmacia (Piscataway, NJ). Tran^{35}S label was the product of

ICN Radiochemicals (Irvine, CA). Multiprime DNA Labeling System, [α-^{35}S]dATP and [α-^{32}P]dCTP were purchased from Amersham (Arlington Heights, IL). Nitrocellulose and the Elutrap Electro-Separation Chamber were the products of Schleicher and Schuell (Keene, NH) and were used according to the manufacturer's instructions. Autofluor was purchased from National Diagnostics (Manville, NJ), Freund's complete and incomplete adjuvants were purchased from Gibco (Grand Island, NY), and dichlorocarboxyfluorescein diacetate (Cl_2CFDA) was purchased from Molecular Probes, Inc. (Eugene, OR). Antisera against CPY was from Klionsky *et al.* (19). All other chemicals were purchased from Sigma (St. Louis, MO) or other standard sources.

Genetic and DNA Manipulations. Standard recombinant DNA techniques were performed as described (22). Genetic crosses, sporulation of diploids, and dissection of tetrads were performed according to Sherman *et al.* (46). Yeast transformations were done using the lithium acetate method of Ito *et al.* (16), in the presence of 10 μg denatured salmon sperm carrier DNA.

Chromosomal DNA was isolated and Southern analysis was performed (22), using DNA fragments containing either the *HIS3* gene or the *VPS33* gene as a probe. Northern analysis (22) was carried out using the 1.1 kb *ClaI-SmaI VPS33* fragment as a probe and total RNA isolated as described by Eakle *et al.* (9). DNA probes were labeled using the Multiprime DNA Labeling System of Amersham (Arlington Heights, IL).

Vectors and Plasmid Constructions. ***E. coli*** plasmids pBluescript KS (+) and (-) are described in the Stratagene (La Jolla, CA) catalog. The yeast integrating vector pPHYI10 (*TRP1*, selectable marker) and the *E. coli*-yeast shuttle vectors pPHYC16 and pPHYC18 (*CEN4 ARS1 URA3*) will be described elsewhere (P. Herman, manuscript in preparation). The *E. coli*-yeast shuttle vector pSEY18 is a derivative of pSEY8 (11) in which the pUC8 polylinker has been replaced with the

polylinker of pUC18. The *HIS3* gene was isolated as a 1.75 kb *Bam*HI fragment from a plasmid kindly provided by E. Phizicky. The pATH vectors used in the TrpE-Vps33 fusion protein production have been previously described (6).

The 3.7 kb *Sal*I-*Xba*I fragment of *VPS33* (Fig. 2b) was subcloned into the pBluescript KS (+) and (-) vectors to generate pLB33-211 and pLB33-212, respectively. Plasmid pLB33-102, used in the integrative mapping experiment, was constucted by cloning the 5.3 kb *Sal*I-*Pvu*II fragment shown in Fig. 2b into the *Sal*I/*Sma*I sites of the yeast integrating vector pPHY110. Construction of pLB33-313, used in the disruption of *VPS33*, was achieved by digesting the plasmid pLB33-212 with *Eco*RI to remove the region shown in Fig. 2c, gel purifying the resulting linear DNA away from the two *Eco*RI fragments, blunting the ends with Klenow enzyme and inserting the *HIS3* gene as a blunted *Bam*HI fragment. Recombinant plasmids were selected directly for the presence of the *HIS3* gene in the *his*B bacterial strain JF1754 (24) on M63 minimal media lacking histidine (27). In a similar manner, the 2.1 kb *Hind*III-*Sma*I fragment indicated in Fig. 2c was removed and replaced with the *HIS3* gene to generate plasmid pLB33-317. Plasmid pLB33-221, carrying the *VPS33* gene on a multicopy (2μ) vector, was constructed by excising the *Sal*I-*Xba*I fragment from pLB33-21 (see below) as a *Sal*I-*Sac*I fragment (using the *Sac*I site in the polylinker) and ligating it to the *Sal*I/*Sac*I sites of the 2μ vector pSEY18. A truncated form of *VPS33*, encoding all but the carboxy-terminal 56 amino acids (aa) of Vps33p, was constructed by subcloning the 2.7 kb *Pst*I fragment (Fig. 2c) into the *Pst*I site of pBluescript KS (-), and then moving this fragment (as a *Bam*HI-*Sal*I fragment) into the corresponding sites in the *E. coli*-yeast shuttle vector pPHYC18 to construct pLB33-304. Plasmid pLB33-162 was constructed by cloning the 3.7 kb *Sal*I-*Xba*I fragment into the *E. coli*-yeast shuttle vector pPHYC16.

Cloning and Sequence Analysis of VPS33. Yeast strain SEY33-2 was grown

in YPD to an optical density at 600 nm of 0.5-1.0 and transformed at room temperature as described (16) with a yeast genomic library constructed by Rose *et al.* (40). The library contains inserts from a partial *Sau*3A digestion of *S. cerevisiae* genomic DNA carried on the *E. coli*-yeast shuttle vector YCp50 (*CEN4, ARS1 URA3*). Transformants were selected on SD lacking uracil at 25°C and replicated to YPD plates, which were incubated at the restrictive temperature, 37°C. Temperature resistant (*TR*) transformants were picked, restreaked, and cured of the plasmid by incubation on 5-fluroorotic acid plates (3). Complementing plasmid DNA (pLB33-6) was isolated and propagated in the bacterial strain MC1061. Plasmid DNA was transformed into SEY33-2, SEY33-5, and SEY33-7, and transformants were tested for temperature sensitivity (growth on YPD at 37°C), osmotic sensitivity (growth on YPD containing 1.5 M NaCl) (2), vacuolar protein sorting (39), and vacuole morphology (see below). The plasmid DNA was also subjected to restriction enzyme analysis. The restriction fragments shown in Fig. 2b were isolated from pLB33-6 and subcloned into the appropriate restriction sites within the polylinker of the *E. coli*-yeast shuttle vector pPHYC18 to generate plasmids pLB33-20 through pLB33-24. The plasmid pLB33-21 was digested with *Sal*I and *Kpn*I and exonucleaseIII was used (49) to generate deletions from the *Sal*I end of the insert. The ends were blunted using Mung Bean nuclease and Klenow enzyme and religated to generate deletion plasmids pLB33-41 and pLB33-42. The approximate endpoints of these deletions were determined by restriction analysis.

Two sets of nested deletion templates for sequencing were generated by deleting from the *Sal*I end of the insert in pLB33-212 and the *Xba*I end of the insert in pLB331-211, using exonucleaseIII (49). Deletions were also generated from the internal *Sma*I site in pLB33-211, and additional templates were constructed by cloning the 0.5 kb *Eco*RI fragment, the 1.5 kb *Cla*I-*Xba*I fragment,

the 0.4 kb *Pst*I-*Xba*I fragment, the 2.7 kb *Pst*I fragment, and the 1.4 kb *Hind*III fragment (Fig. 2c) into pBluescript KS (-). Single-stranded template DNA was prepared from these constructs (49) after infection with the helper phage VCSM13 (Stratagene, La Jolla, CA) and synthetic primers corresponding to the T3 or T7 promoter sequences were prepared by DNA synthesizer. The sequence of both strands of *VPS33* was determined using the dideoxy chain termination method (45).

DNA sequence and hydropathy analysis (20) were done using a program written by K. Eakle (unpublished). A DNA homology search was performed using the TFASTA algorithm and the GENEMBL databank. Additional homology searches using the GENBANK, EMBL, NBRF and SWISS-PROT protein databases and the FASTA program (35) were done on BIONET.

Oligonucleotide Mutagenesis of Lys^{494}*→Glu.* The 1.0 kb *Xho*I-*Xba*I fragment was subcloned into the pBluescript KS (-) vector to generate pLB33-213. This fragment was excised as a *Sac*I-*Kpn*I fragment and inserted into the corresponding restriction sites in the vector M13mp18. An oligonucleotide containing the desired nucleotide substitution (A at nucleotide 1880 to G) was synthesized and mutagenesis was performed as described (19A). Candidate mutants were screened by sequencing. The *Xho*I-*Xba*I fragment from a clone carrying the desired mutation was used to replace the corresponding wild-type fragment in pLB33-162, generating plasmid pLB33-166. The *Xho*I-*Xba*I fragment from pLB33-166 was reisolated and subcloned into pBluescript KS (-); sequencing confirmed that the fragment did indeed contain the single bp substitution. The *VPS33* gene carrying the mutated ATP-binding domain was excised from pLB33-166 as a *Sal*I-*Sac*I fragment (using the *Sac*I site in the polylinker) and inserted into the appropriate restriction sites of the 2μ vector pSEY18 to generate plasmid pLB33-266.

Mapping and Rescue of the vps33-4ts Allele. Recombinational rescue

analysis was carried out on SEY33-4 carrying the plasmid pLB33-23 or pLB33-24, described above. Additional plasmids were constructed by cloning the 2.1 kb *Sma*I-*Pvu*II fragment, the 2.3 kb *Sph*I-*Pvu*II fragment, and the 0.7 kb *Hind*III-*Sma*I fragment (Figs. 2b and c) into the appropriate restriction sites of pSEY18. In each case, the plasmid was transformed into SEY33-4 and the frequency of *TR* recombinants was scored.

The *vps33-4ts* mutation was rescued using double-stranded gap repair (32) as follows. The complete *VPS33* gene was subcloned as a 5.3 kb *Pvu*II-*Sal*I fragment into the *E. coli*-yeast shuttle vector pPHYC16, and the resulting plasmid (pLB33-160) was digested with *Xba*I and *Sma*I to generate a gapped linear plasmid. The linear plasmid was gel-purified away from the 0.5 kb *Sma*I-*Xba*I fragment. SEY33-4 was transformed with this plasmid and Ura^+ transformants were scored for temperature sensitivity. Plasmid DNA (designated pLB33-161) carrying the rescued *vps33-4ts* allele was purified. The *Sma*I-*Xba*I fragment carrying the mutation was isolated and subcloned into pBluescript KS (-). Double-stranded DNA was isolated using the Pharmacia Miniprep Kit Plus and sequenced. The *VPS33* gene carrying the *vps33-4ts* mutation was excised from pLB33-161 as a *Sal*I-*Sac*I fragment (using the *Sac*I site in the polylinker) and cloned into the 2μ vector pSEY18 to generate pLB33-271.

Antibody Production. *trpE-VPS33* gene fusions were constructed using the two fragments of the *VPS33* gene depicted in Fig. 2c. The 0.7 kb *Hind*III-*Sma*I fragment was isolated from pLB33-21, blunted using Klenow enzyme and ligated to the blunted *Sal*I site of the pATH3 vector to generate an in-frame fusion encoding amino acids 379-608 of Vps33p. The 0.5 kb *Eco*RI fragment was isolated and blunted as above and ligated into the *Sma*I site of the pATH2 vector to generate an in-frame fusion encoding amino acids 140-303 of Vps33p. Individual transformants were purified and the presence and orientation of the *VPS33*

sequence was confirmed by restriction analysis. Bacterial strains carrying candidate fusion constructs were assayed for the production of fusion protein (47). Whole cell lysates and insoluble fractions were prepared basically as described by Kleid *et al.* (18) (except that 2% Triton X-100 was used rather than 0.2% NP-40), and subjected to sodium-dodecyl-sulfate (SDS)-9% PAGE (21). Inducible fusion proteins of the expected molecular weights (62 kD and 55 kD) were the predominant bands visualized in the insoluble fractions upon Coomassie staining. The bands containing the fusion proteins were excised from Coomassie-stained preparative gels and electroluted from the gel slices using a Schleicher and Schuell (Keene, NH) Electro-Separation Chamber. Approximately 175 μg of each purified fusion protein, emulsified with Freund's complete adjuvant, was injected intramuscularly and subcutaneously into a young male New Zealand White rabbit. After 4 weeks, the rabbit was boosted with 25 μg of each fusion protein in an emulsion with Freund's incomplete adjuvant. Antisera were screened by immunoprecipitation. A titration curve was generated for these antisera to determine the amount needed for quantitative recovery of overproduced levels of Vps33p.

Immunoprecipitation. Cells were grown in SD media (46), supplemented with the appropriate amino acids. Whole cells (1.5 units at an optical density at 600 nm of 1.0) were collected by centrifugation. The cells were resuspended in 0.5 ml of the same media, and 125 μCi of Tran^{35}S label were added. The cells were labeled for 20 min with shaking at the appropriate temperature. A 30 min chase was initiated by the addition of methionine to a final concentration of 4 mM. The chase was terminated and cells were lysed and subjected to a single round of immunoprecipitation using antisera specific for Vps33p or CPY as described (9,19).

Cell Fractionation. Cells were grown in SD media (46) as above. Six units

of cells at an optical density at 600 nm of 1.0 were harvested by centrifugation and spheroplasted in the same media as described (39). Spheroplasts were labeled and chased as above. All subsequent manipulations were performed at 4°C. Labeled spheroplasts were pelleted at 1200 x g for 2 min. The spheroplasts were resuspended in 1 ml of lysis buffer (50 mM Tris-Cl, pH 7.5/1 mM EDTA/5 mM $MgCl_2$/1 mM phenylmethylsulfonyl fluoride/1 μM leupeptin/1 mM NaAzide/0.125 mg/ml α_2-macroglobulin) with varying concentrations of KCl as indicated and vortexed for 30 sec. Unlysed spheroplasts were removed by centrifugation at 500 x g for 2 min and subjected to a second round of lysis. Unlysed spheroplasts were removed as before, and the lysates were pooled and immediately centrifuged at 100,000 x g for 90 min. The pellet was rinsed gently with 1 ml of lysis buffer and resuspended in 1 ml of 0.5% SDS. Supernatant and pellet fractions were precipitated with trichloroacetic acid (5% final concentration) and immunoprecipitated.

Fluorescent Labeling of Cells and Microscopy. Cells were grown in YPD, labeled with Cl_2CFDA or fluorescein isothiocyanate (FITC) and observed as described previously (2,36,37).

RESULTS

Cloning and Genetic Analysis of the VPS33 Gene

The *VPS33* gene was cloned by complementation of the *vps33-2ts* mutation (in the Ura3$^-$ strain SEY33-2) with a yeast genomic library carried on the single copy vector YCp50 (40). Among 11,000 Ura$^+$ transformants, seven were temperature-resistant (*TR*). Upon curing these transformants of the plasmid, five remained *TR*, indicating that the temperature resistance was not dependent on the presence of the plasmid. The remaining two transformants were *ts* when cured, suggesting that the *TR* phenotype was indeed conferred by the plasmid. Restriction analysis of the purified plasmid from these two transformants revealed that the two complementing plasmids contained identical inserts. Retransformation of SEY33-2 and two other *vps33* strains demonstrated that this plasmid, designated pLB33-6, complemented all of the phenotypes associated with the *vps33* mutations, including temperature sensitivity (Fig. 1), mislocalization of vacuolar proteins (see Fig. 5), osmotic sensitivity, and the defect in vacuole biogenesis (data not shown).

A restriction map of the 12 kb insert in pLB33-6 is shown in Fig. 2a. Subcloning and complementation analysis (Fig. 2b) indicated that the complementing activity resided on a 3.7 kb *SalI-XbaI* fragment. Removal of as much as 1000 bp from the *SalI* end, using exonuclease III, did not destroy the ability to complement.

To confirm that this complementing ability was not due to suppression by another gene, we carried out integrative mapping studies with the clone. The complementing 5.3 kb *SalI-PvuII* fragment (Fig. 2b) was cloned into the integrating vector pPHY110, which carries the selectable marker *TRP1*. The resulting plasmid was linearized at the internal *XhoI* site to facilitate homologous recombination (31) and was transformed into a Trp1$^-$ strain harboring the *vps33-7ts* mutation.

Trp^+ *TR* transformants were crossed to the $Trp1^-$*VPS*$^+$ parental strain SEY6210. Tetrad analysis of the sporulated diploids showed the expected 2:2 Trp^+:Trp^- segregation pattern; all four spores in each of the 12 asci analyzed were *TR* and exhibited wild-type vacuolar morphology. Further analysis of 190 random spores also failed to uncover any *ts* segregants, while the Trp^+:Trp^- phenotype segregated 97:93. These observations demonstrated that the complementing clone is tightly linked to the *vps33* mutant locus.

The complementing *SalI-XbaI* fragment was also cloned into the 2μ (multicopy) vector pSEY18 to generate the plasmid pLB33-221. Yeast transformants harboring this plasmid overproduce the *VPS33* gene product ~20-fold (see below). Transformation of SEY33-7 or wild-type strains with pLB33-221 resulted in a Vps^+ phenotype, indicating that several-fold overproduction of the *VPS33* gene product is not detrimental to otherwise wild-type cells. We also transformed pLB33-221 into a representative allele of each of the other three class C complementation groups, *vps*11, 16, and 18. In no case did the plasmid suppress any of the defects associated with these mutations; thus, overproduction of Vps33p appears unable to rescue any of these phenotypically similar mutants.

VPS33 Sequence Analysis

The nucleotide sequence of *VPS33* was determined by sequencing a series of nested exonuclease III-generated deletion templates using the dideoxynucleotide chain termination method (45). The DNA sequence (Fig. 3) contains a single open reading frame (ORF) of 2073 bp, with the potential to encode a protein of 691 aa. Examination of the 5' noncoding sequences revealed a possible transcription initiation sequence, TATATTAA (30), at position -157 relative to the putative translational initiation codon. A consensus sequence for transcription termination, TAG....TAGT....TTTT (30) (underlined in Fig. 3), is found 147 bp downstream of the ORF stop codon TAA. Northern analysis was performed using

an internal fragment of *VPS33* as a probe to identify the *VPS33* transcript. Consistent with the ORF size predicted from the DNA sequence, a single RNA species of 2.2 kb was detected (data not shown).

The sequence of the predicted *VPS33* gene product was subjected to hydropathy analysis, according to the model of Kyte and Doolittle (20). The predicted Vps33 polypeptide is hydrophilic (26% charged amino acids), with no apparent hydrophobic domains that could span a membrane or function as a signal sequence (data not shown). A search for sequence homology using the GENEMBL data bank and the TFASTA algorithm (35) revealed that the 3' end of the *VPS33* gene (nucleotides 2307-2695) is identical to the sequence upstream of the yeast *COX8* gene, which encodes the cytochrome c oxidase subunit VIII. Furthermore, the published sequence of the *COX8* gene contains a short ORF 5' of the *COX8* coding region which corresponds to the last 55 codons of the *VPS33* ORF (34). From these results, we conclude that the *VPS33* gene lies next to the *COX8* gene in the yeast genome.

Further homology searches using the GENBANK, EMBL, NBRF, and SWISS-PROT protein databases uncovered no additional significant sequence similarities (35). However, a manual search of the predicted amino acid sequence revealed two regions of sequence similarity with a number of known and predicted ATP-binding proteins. As shown in Fig. 4, these two areas of similarity are conserved in a diverse assortment of ATPases and ATP-binding proteins, including the *E. coli* ATPase α- and β-subunits, myosin, and phosphofructokinase, and consensus sequences have been determined (51). The two domains are often separated by 60 to 100 aa and some proteins (e.g., myosin, phosphofructokinase) contain only one of the two regions. In Vps33p, the two regions are located at residues 480-498 and 661-679 (Fig. 3).

A number of studies suggest that these domains are directly involved in

nucleotide binding and/or enzyme function. The conserved lysine residue in adenylate kinase, marked with an asterisk in Fig. 4 (top panel), has been shown by affinity labeling and other experiments to interact with ATP (7,12,50). Mutagenesis of the corresponding lysine in the *E. coli* ATPase α-subunit severely impaired apparent ATP binding (38), while a change in the conserved lysine of the β-subunit resulted in a reduction in catalytic activity (33). Mutagenesis of the codons corresponding to Lys48 or Gly47 of the yeast *RAD3* gene, an essential gene required for DNA repair, resulted in the loss of the excision repair function, although not the essential function (29). To address the significance of this conserved domain in Vps33p function, we have used oligonucleotide-mediated site-directed mutagenesis to change the corresponding lysine in the predicted *VPS33* gene product, Lys^{494}, to glutamic acid. The plasmid pLB33-166, carrying the *VPS33-Glu494* gene was constructed as described in Materials and Methods and introduced into the *vps33* mutant strain SEY33-7. This plasmid was able to complement fully the defects in protein localization, vacuolar morphology, and growth at 37°C exhibited by SEY33-7 (data not shown). Similar results were obtained when this plasmid was used to transform a *vps33* null mutant (see below). To test the possibility that overexpresison of Vps33p-Glu494 could poison a given process within the cell, the mutant allele was subcloned into a 2μ vector and the resulting plasmid was used to transform wild-type and *vps33* mutant cells. None of these transformants exhibited any defect in protein localization or growth at 37°C, suggesting that the *VPS33-Glu494* allele is completely functional, even in high copy number (data not shown).

Disruption of VPS33

Disruption of the *VPS33* locus was accomplished using the one-step gene disruption technique (43) with two different constructions. In the first, the 700 bp *Eco*RI fragment shown in Fig. 2c was replaced with the *HIS3* gene. This disrupted

VPS33 construction was digested with *SalI* and *XbaI* and used to transform the parental *his3*-Δ200 diploid SEY6210/SEY6211. Two different resulting His^+ transformants were subjected to tetrad analysis. In each of the 10 asci examined, all spores were viable but a segregation pattern of 2 *ts* His^+:2 *TR* His^- spores was observed. Microscopic examination of the *ts* segregants streaked on YPD revealed that the cells doubled at most two times at 37°C. A second construction replaced the entire 2.1 kb *Hind*III-*Sma*I fragment (indicated in Fig. 2c) with the *HIS3* gene. This construction deleted all but the carboxy-terminal 250 bp of the putative *VPS33* ORF. Transformation of the haploid strain SEY6210 with the linear *Sal*I-*Xba*I fragment carrying this construction yielded *ts* His^+ tranformants. The *ts* phenotype of one such transformant, LBY317, is shown in Fig. 1. In liquid media, this strain doubles 1.5 times at 37°C and exhibits a terminal arrest phenotype in which, after 24 h at 37°C, approximately 50% of the cells contain a medium or large bud and an additional 20% contain two or more buds. Southern analysis of the chromosomal DNA from these disrupted strains confirmed the removal of the *VPS33* sequences and the integration of the *HIS3* gene at the *VPS33* locus as expected (data not shown). From these results, we conclude that *VPS33* is not essential at low temperature, but is required for growth at 37°C.

As expected, disruption of the *VPS33* gene also leads to the other phenotypic defects associated with the original mutant alleles. Strains harboring a disrupted *VPS33* gene exhibit extreme defects in vacuole morphology and in vacuole protein localization and processing at the permissive temperature (Fig. 5). The *vps33* null mutant strain LBY317 was radioactively labeled at 25°C for 20 min and chased for 30 min before immunoprecipitation with antisera specific for the vacuolar protease CPY. CPY is present almost exclusively in the precursor form in these cells (lane 2), while in wild-type cells labeled under identical conditions, 100% of the CPY is present in the mature vacuolar form

(lane 1). Previous characterization of the *vps* mutants has demonstrated that most of the precursor CPY is secreted from the cell, implying that a processing defect is indicative of missorting (39). The localization defect exhibited by the null mutant is completely complemented when the wild-type *VPS33* gene is present on a single copy vector (lane 3).

Identification of Vps33p

To identify the Vps33p, we overproduced the *VPS33* gene product as two different TrpE-Vps33 hybrid proteins in *E. coli* and raised antisera against the fusion proteins. Two coding fragments of the *VPS33* gene, from *Hin*dIII-*Sma*I and from *Eco*RI-*Eco*RI, were cloned into the appropriate pATH vectors (6) to generate in-frame fusions to the *trp*E gene of *E. coli*. These fragments, depicted in Fig. 2c by hashed boxes, encode 230 aa and 164 aa, respectively, of Vps33p. When these constructions were expressed in *E. coli*, hybrid proteins of the expected molecular weights (MW) were overproduced upon induction. Both overexpressed proteins were isolated and injected into a single rabbit as described in Materials and Methods. The resulting antisera were used in immunoprecipitation experiments to detect Vps33p. As shown in Fig. 6, lane 1, the antibodies recognize a single major species of the predicted MW, ~75,000, in radioactively labeled wild-type cells. This protein was ~20-fold more abundant when the *VPS33* gene was present on a multicopy plasmid (lane 2), and was not detected in the *vps33* null mutant (lane 5) or by the preimmune serum (lane 6). Pulse-chase analysis suggests that the turnover rate for Vps33p is relatively slow; after a 30 min or a 90 min chase, there is no significant difference in the amount of the protein produced from a multicopy plasmid. Comparison with CPY indicates that the *VPS33* gene product is present at very low levels in wild-type yeast cells. By densitometric quantitation, we estimate that the production of Vps33p from the multicopy plasmid is comparable to the level of expression of CPY from the chromosomal

locus (0.05-0.1% of the total cell protein). Cells were also labeled in the presence of tunicamycin, an inhibitor of N-linked glycosylation (10). As shown in Fig. 6 (lanes 3 and 4), the size of Vps33p was unaffected by the drug, indicating that none of the seven potential sites for N-linked carbohydrate addition (23) (Asn-X-Ser/Thr) is utilized.

The subcellular localization of Vps33p was examined by cellular fractionation and immunoprecipitation studies. Wild-type cells carrying *VPS33* on a multicopy plasmid were converted to spheroplasts, radioactively labeled, and osmotically lysed under a variety of conditions before being subjected to centrifugation at 100,000 x g for 90 min. These centrifugation conditions are sufficient to pellet membrane-associated proteins, including those associated with vesicles, while soluble proteins should remain in the supernatant fraction (28). The results of some representative experiments are shown in Fig. 7. As seen in lanes 1-8, Vps33p was found primarily in the supernatant fraction; this solubility was not affected by varying the salt concentration of the lysis buffer from 0 mM to 1 M KCl. Likewise, the localization of Vps33p was not altered by the inclusion of 0.3 M mannitol in the lysis buffer (28) (lanes 9-10) or by varying the pH (7.5 to 6.5 or 8.0) (44) (data not shown). These results suggest that the *VPS33* gene product resides in the cytoplasm and is not tightly associated with any membrane fraction. Vps33p expressed from the chromosomal *VPS33* locus, although considerably more difficult to detect, also behaved as a soluble cytosolic protein in cell fractionation studies (data not shown). By immunofluorescence studies, we have detected a weak background fluorescence that may be due to cytoplasmic staining (data not shown).

vps33 Mutant Strain SEY33-4 Exhibits a Bud Vacuole Defect

Wild-type vacuoles can be visualized in live cells using various dyes, including Cl_2CFDA (37) and FITC (36), that accumulate in this organelle. As

previously mentioned, most of the class C *vps* mutants exhibit extreme defects in vacuole morphology in that they contain no compartments that resemble wild-type vacuoles. Instead, they accumulate many small vesicles and other membranous structures (2). When these class C *vps* mutants are stained with Cl_2CFDA or FITC, only small speckles of fluorescence are detected. Two *vps33* mutant strains, SEY33-4 and SEY33-5, however, do not exhibit these gross abnormalities in their vacuole morphologies. Instead, they contain vacuoles that stain like those in wild-type cells. Unlike the other more extreme *vps33* mutants, these strains also are not sensitive to osmotic stress. Furthermore, SEY33-4 and SEY33-5 are only moderately defective in vacuole protein localization, missorting ~40% of the soluble vacuolar protease CPY. One of these strains, however, is temperature-sensitive for growth. This strain, SEY33-4, contains morphological wild-type vacuoles, as visualized using either Cl_2CFDA or FITC, in both the mother cell and the bud at 25°C, the permissive temperature (Fig. 8a,b). However, when the strain is shifted to the nonpermissive temperature (37°C) for 2 h, budding cells are observed in which the bud does not appear to have any stain (Fig. 8c,d). Incubation for longer times at 37°C results in fewer buds with detectable vacuole staining (Fig. 8e-j). By 6 h after the shift to 37°C, only a small fraction of the buds have vacuole fluorescence, and some unbudded cells exhibit a typical class C phenotype in that little or no vacuole fluorescence is visible (Fig. 8j). The wild-type parental strain SEY6210 is shown for comparison in Fig. 8k,l. Under identical staining conditions, bud vacuole fluorescence is clearly visible in these cells at 25°C (Fig. 8k) or after 6 at 37°C (Fig. 8l). The extent of the bud vacuole staining defect in SEY33-4 has been quantitated; the results are shown in Fig. 8. When SEY33-4 is grown at 25°C, 80% of the buds examined contained vacuole fluorescence. After 6 h at 37°C, only 14% of the buds exhibited vacuole staining. The vacuole protein sorting phenotype of SEY33-4 is also exacerbated by

exposure to 37°C. After 6 h at 37°C, ~70% of the CPY is mislocalized, as compared to 40% at 25°C (Fig. 9, compare lanes 2 and 6). The *ts* mutation and the bud vacuole defect in SEY33-4 are genetically linked to the vacuole protein localization defect (2,39) and each of the defects is completely complemented by the cloned *VPS33* gene.

The vps33-4ts Mutation Results in a Leu^{646}→Pro Change

The *ts* mutation in SEY33-4 was mapped using a strategy of recombinational rescue. Initially, SEY33-4 was transformed with the noncomplementing plasmids pLB33-23 or pLB33-24 (see Fig. 2b); transformants streaked on YPD plates were incubated at 37°C and the presence or absence of *TR* colonies were scored. Many *TR* recombinants were obtained from SEY33-4 harboring pLB33-23, indicating that the *ts* mutation likely lies 3' of the *Cla*I site within the ORF. Various fragments containing this region of the *VPS33* gene were subcloned into the multicopy vector pSEY18, and SEY33-4 transformants carrying these plasmids were again scored for the frequency at which *TR* revertants arose. The results of this analysis (data not shown) suggested that the *ts* mutation mapped to the 250 bp region between the *Sma*I site and the end of the ORF (see Fig. 2c). The chromosomal mutation was recovered by transforming SEY33-4 with a replicating plasmid carrying *VPS33* containing a double-stranded gap between the *Sma*I and the *Xba*I sites (32). Sequencing of the *Sma*I-*Xba*I fragment from the rescued plasmid revealed that a single bp change within the ORF, resulting in a leucine to proline change at residue 646, was responsible for the temperature sensitivity.

The predicted aa sequences of the wild-type *VPS33* gene product and the mutant Vps33p carrying the Leu^{646}→Pro alteration were subjected to Chou-Fasman analysis (5). The two-dimensional structures predicted for the two forms of the protein are shown in Fig. 10. The presence of proline at position 646 is

predicted to cause a structural change in the *VPS33* gene product, inserting a turn in a region that is expected to form a random coil in the wild-type protein.

The nature of the temperature sensitivity was examined by retransforming various wild-type and *vps33* strains with the *vps33* gene carrying the rescued *ts* mutation on single and multicopy vectors. Transformation of SEY33-4 with a second copy of the *ts* mutant allele resulted in a strain which grew slightly better at 37°C than did the original mutant. A null mutant carrying the *vps33-4* mutant allele on a single copy vector had a growth rate comparable to that of the original mutant allele. Both mutants exhibited wild-type growth at 37°C when the *ts* allele was present on a multicopy vector. Transformation of the wild-type strain SEY6210 with either the single or the multicopy construction did not affect its ability to grow at 37°C (Fig. 9a). Thus, the *ts* mutant allele *vps33-4* is recessive to the wild-type allele, even when overproduced. Furthermore, strains carrying the *vps33-4* mutant allele appear to exhibit a dosage-dependent growth phenotype; overexpression of the mutant allele results in complementation of the *ts* defect of the null mutant or SEY33-4. However, although the strains carrying multiple copies of *vps33-4* are *TR*, they still exhibit a partial Vps^- phenotype. Immunoprecipitation experiments indicated that 15% of the CPY is mislocalized in SEY33-4 carrying the *ts* allele on a multicopy plasmid (Fig. 9b). Together, our observations suggest that the *vps33-4* mutant allele encodes a partially functional protein, and that multiple copies of this protein can compensate for its diminished activity. The partial function of this Vps33-4p is unlikely to be a result of inactivation of the 45 aa following the changed residue, since a 3' truncation of the *VPS33* gene, lacking the coding sequence for the carboxy-terminal 56 aa, is unable to complement a *vps33* null mutation (data not shown).

DISCUSSION

VPS33, a gene required for vacuole protein sorting and normal vacuole formation, has been cloned and sequenced. Disruption of *VPS33* leads to a *ts* growth phenotype (Fig. 1), indicating that the gene is essential for growth only at elevated temperatures. At the permissive temperature, the null mutants are extremely defective in vacuolar protein sorting (Fig. 5) and lack any structure resembling a wild-type vacuole. These phenotypes are comparable to those exhibited by most of the original *vps33* mutants, implying that many of the originally isolated alleles may be null (complete loss of function) mutations. The temperature sensitivity of the null mutants likely reflects a requirement at 37°C for one or more vacuolar functions which cannot be provided by whatever vacuole remnants remain in these mutant cells.

The phenotypes exhibited by *vps33* mutants resemble those of the recently described mutant *slp1* (17). This mutant was originally selected for its sensitivity to lysine. The strain contains smaller than normal vacuolar pools of lysine, arginine, and histidine, and is characterized by pleiotropic defects including lowered activities of soluble vacuolar enzymes such as CPY and PrA and an aberrant morphology in which many small vesicles but no large vacuoles are observed. Complementation analysis revealed that the *slp1* and *vps33* mutants define a single complementation group (L. Banta, S. Emr, Y. Wada, and Y. Anraku, unpublished observations). Comparison of the restriction map and sequence of our *VPS33* clone and the recently cloned *SLP1* gene (50A) has demonstrated that the two genes are identical.

Antibodies raised against a TrpE-Vps33 fusion protein recognize a relatively rare protein in yeast (<0.01% of cell protein) of ~75 kd (Fig. 6). In cell fractionation experiments, Vps33p behaves as a soluble cytoplasmic protein under a variety of lysis conditions (Fig. 7). The hydrophilic nature of the predicted aa

sequence and the apparent lack of N-linked glycosylation (Fig. 6) are consistent with a cytoplasmic location for Vps33p.

The predicted aa sequence of Vps33p possesses two regions of similarity with a number of ATPases and ATP-binding proteins (Fig. 4). Mutagenesis of a highly conserved residue, Lys494, within one of these domains in Vps33p did not appear to inactivate *VPS33*, as assayed by the ability to complement a *vps33* mutation *in vivo*. However, the results of this single aa change do not rule out the possibility that Vps33p is able to bind ATP. The conserved lysine may not play as crucial a role in *VPS33* gene product function as it does in the other proteins mentioned above (see Results). Alternatively, the presence of this conserved domain may have an evolutionary basis, although it is not required for the current function of Vps33p. A second class C *vps* mutant, *vps11*, falls into the same complementation group as the mutant *end1* (8,39). The *END1* gene has been cloned and sequenced (8). This gene also shares sequence similarity with *VPS33* and the family of ATP-binding proteins throughout the two conserved domains. This observation raises the interesting possibility that ATP binding (and perhaps ATP hydrolysis) may play a role in vacuolar protein sorting and vacuole biogenesis. Further experiments, such as ATP-binding studies and affinity labeling, will be necessary to determine if Vps33p does indeed bind ATP.

One *vps33* mutant strain, SEY33-4, exhibits a particularly interesting temperature-conditional defect in vacuolar protein sorting and vacuole inheritance. At the permissive temperature, this *ts* strain mislocalizes 40% of the CPY but contains vacuoles that are apparently normal by a number of criteria. These vacuoles exhibit wild-type staining with a variety of dyes including quinacrine, a compound which accumulates in vacuoles in a pH-dependent manner (2, 53; L. Banta, unpublished observations). Unlike the more defective class C strains, SEY33-4 does not mislocalize the vacuolar membrane enzyme α-

mannosidase to the cell surface and is able to process 60% of the CPY to the mature form, indicating that the vacuoles in these cells are able to function as acceptor compartments for at least some vacuolar proteins. Upon incubation of SEY33-4 at 37°C, budding cells appear to lack vacuole staining selectively in the bud (Fig. 8) and the vacuolar protein sorting defect is exacerbated (Fig. 9). The *ts* defect in this strain is due to a single bp substitution which results in a leucine to proline change at position 646 in the *VPS33* gene product. This mutation is predicted to cause a structural change in the carboxy terminus of the protein (Fig. 10).

The bud vacuole defect and increase in protein missorting observed in SEY33-4 at the nonpermissive temperature suggest a number of possible roles for the wild-type Vps33p in vacuole biogenesis. For example, Vps33p may be required for: 1) vacuole segregation to the bud during cell division (52); 2) maintenance of normal vacuolar structure; or 3) sorting and delivery of vacuolar proteins between the Golgi and the vacuole. For the following reasons, we favor a model in which Vps33p acts primarily in Golgi-to-vacuole protein transport. The observation that Vps33p fractionates as a cytosolic protein suggests that this protein is not a structural component of the vacuole itself. In addition, the existence of SEY33-4 and a second *vps33* strain, SEY33-5, that mislocalize CPY yet contain apparently normal vacuoles at 25°C is inconsistent with a structural function for Vps33p in maintaining vacuole integrity. A primary role for Vps33p in vacuole inheritance also seems unlikely, given that SEY33-4 and SEY33-5 exhibit apparently normal vacuole segregation patterns during cell division at the permissive temperature. These observations suggest that the primary defect in these mutants lies in Golgi-to-vacuole trafficking. If Vps33p were directly involved in vacuole inheritance or vacuolar structure, mutants which clearly affect vacuole protein localization would also be expected to exhibit morphological abnormalities in the vacuole.

The simplest explanation for the extreme abnormalities in vacuole morphology exhibited by most of the *vps33* mutants is that, as a consequence of a primary defect in Golgi-to-vacuole protein transport, proteins necessary for vacuolar inheritance and/or structural stability are mislocalized. In strong *vps33* mutants, which exhibit partial missorting of a vacuolar membrane component as well as almost completely aberrant targeting of soluble hydrolases, vacuole assembly is severely impaired. The less defective mutant SEY33-4 appears to contain a partially functional Vps33p. The residual activity is sufficient to permit some Golgi-to-vacuole protein transport and thus the formation of nearly normal vacuoles. The lack of a vacuole in the bud at 37°C may reflect a more complete loss of function if, for example, the mutant protein is less stable at high temperature. We cannot exclude, however, the possibility that the *VPS33* gene product is bifunctional, with roles in both vacuole protein targeting and vacuole maintenance or segregation to emerging buds. In this scenario, the protein encoded by the *vps33-4* allele might be defective in only the former function at 25°C, but both functions at 37°C.

A possible role for Vps33p in Golgi-to-vacuole sorting is suggested by a recent observation that the protein is phosphorylated *in vivo* (P. Herman, J. Stack, and S. Emr, unpublished observations). Perhaps Vps33p undergoes a cycle of phosphorylation/dephosphorylation, which in turn regulates its activity in promoting Golgi-to-vacuole protein transport. Since this transport is assumed to be vesicle-mediated, the *VPS33* gene product could act at the level of vesicle formation, transport, or fusion with the target organelle. The accumulation of many small vesicles in *vps33* mutant cells (2) suggests that the defect in these strains may occur after vesicle formation. Using the probes developed in this study in conjunction with an *in vitro* assay for protein transport from the Golgi to the vacuole (T. Vida and S. Emr, manuscript in preparation), we hope to determine

the step(s) at which Vps33p acts, as well as the significance of the observed phosphorylation.

ACKNOWLEDGEMENTS

We wish to thank Raffi Aroian for the YCp50 library DNA, Dan Klionsky for many helpful discussions, and Elliot Altman, Editte Gharakhanian, and Bruce Horazdovsky for critically reading the manuscript. We also thank Yoh Wada and Yasuhiro Anraku for communicating results prior to publication. This work was supported by a National Science Foundation Presidential Young Investigator award (to S.D.E.). Partial support was also provided by General Electric (to L.M.B.) and the Natural Sciences and Engineering Research Council of Canada (to P.K.H.). T.A.V. is supported by a postdoctoral fellowship from the American Cancer Society.

LITERATURE CITED

1. Bankaitis, V. A., L. M. Johnson, and S. D. Emr. 1986. Isolation of yeast mutants defective in protein targeting to the vacuole. Proc. Natl. Acad. Sci. USA 83:9075-9079.

2. Banta, L. M., J. S. Robinson, D. J. Klionsky, and S. D. Emr. 1988. Organelle assembly in yeast: Characterization of yeast mutants defective in vacuole biogenesis and protein sorting. J. Cell Biol. 107:1369-1383.

3. Boeke, J. D., F. Lacroute, and G. R. Fink. 1987. 5-Fluoroorotic acid as a selective agent in yeast molecular genetics. Meth. Enzymol. 154:164-175.

4. Casadaban, M. J., and S. N. Cohen. 1980. Analysis of gene control signals by DNA fusion and cloning in *E. coli*. J. Mol. Biol. 138:179-207.

5. Chou, P. Y., and G. D. Fasman. 1978. Prediction of the secondary structure of proteins from their amino acid sequence. Adv. Enzymol. 47:45-148.

6. Dieckmann, C. L., and A. Tzagoloff. 1985. Assembly of the mitochondrial membrane system. *CBP6*, a yeast nuclear gene necessary for synthesis of cytochrome b. J. Biol. Chem. 260:1513-1520.

7. Dreusicke, D., and G. E. Schulz. 1986. The glycine-rich loop of adenylate kinase forms a giant anion hole. FEBS 208:301-304.

8. Dulic, V., and H. Riezman. 1989. Characterization of the *END*1 gene required for vacuole biogenesis and gluconeogenic growth of budding yeast. EMBO J. 8:1349-1359.

9. Eakle, K. A., M. Bernstein, and S. D. Emr. 1988. Characterization of a component of the yeast secretion machinery: Identification of the *SEC*18 gene product. Mol. Cell. Biol. 8:4098-4109.

10. Elbein, A. D. 1987. Inhibitors of the biosynthesis and processing of N-linked oligosaccharide chains. Ann. Rev. Biochem. 56:497-534.

11. Emr, S. D., A. Vassarotti, J. Garrett, B. L. Geller, M. Takeda, and M. G. Douglas. 1986. The amino terminus of the yeast F_1-ATPase β-subunit precursor functions as a mitochondrial import signal. J. Cell Biol. 102:523-533.

12. Fry, D. C., S. A. Kuby, and A. S. Mildvan. 1986. ATP-binding site of adenylate kinase: Mechanistic implications of its homology with *ras*-encoded p21, F_1-ATPase, and other nucleotide-binding proteins. Proc. Natl. Acad. Sci. USA 83:907-911.

13. Hanahan, D. 1983. Studies on the transformation of *Escherichia coli* with plasmids. J. Mol. Biol. 166:557-580.

14. Hasilik, A., and W. Tanner. 1978. Biosynthesis of the vacuolar yeast glycoprotein carboxypeptidase Y. Conversion of precursor into the enzyme. Eur. J. Biochem. 85:599-608.

15. Hemmings, B. A., G. S. Zubenko, A. Hasilik, and E. W. Jones. 1981. Mutant defective in processing of an enzyme located in the lysosome-like vacuole of *Saccharomyces cerevisiae*. Proc. Natl. Acad. Sci. USA 78:435-439.

16. Ito, H., Y. Fukada, K. Murata, and A. Kimura. 1983. Transformation of intact yeast cells treated with alkali cations. J. Bacteriol. 153:163-168.

17. Kitamoto, K., K. Yoshizawa, Y. Ohsumi, and Y. Anraku. 1988. Mutants of *Saccharomyces cerevisiae* with defective vacuolar function. J. Bacteriol. 170:2687-2691.

18. Kleid, D. G., D. Yansura, B. Small, D. Dowbenko, D. M. Moore, M. G. Grubman, P. D. McKercher, D. O. Morgan, B. H. Robertson, H. L. Bachrach. 1981. Cloned viral protein vaccine for foot-and-mouth disease: Responses in cattle and swine. Science 214:1125-1129.

19. Klionsky, D. J., L. M. Banta, and S. D. Emr. 1988. Intracellular sorting and processing of a yeast vacuolar hydrolase: Proteinase A propeptide contains vacuolar targeting information. Mol. Cell. Biol. 8:2105-2116.

19A. Kunkel, T. A., J. D. Roberts, and R. A. Zakour. 1987. Rapid and efficient site-specific mutagenesis without phenotypic selection. Meth. Enzymol. 154:367-382.

20. Kyte, J., and R. F. Doolittle. 1982. A simple method for displaying the hydropathic character of a protein. J. Mol. Biol. 157:105-132.

21. Laemmli, U. K., 1970. Cleavage of structural proteins during the assembly of the head of bacteriophage T4. Nature 277:680-685.

22. Maniatis, T., E. F. Fritsch, and J. Sambrook. 1982. Molecular cloning: A laboratory manual. Cold Spring Harbor Laboratory, Cold Spring Harbor, N.Y.

23. Marshall, R. D. 1972. Glycoproteins. Ann. Rev. Biochem. 41:673-702.

24. McNeil, J. B. and J. D. Friesen. 1981. Expression of the herpes simplex virus thymidine kinase gene in *Saccharomyces cerevisiae*. Mol. Gen. Genet. 184:386-393.

25. Mechler, B., M. Muller, H. Muller, M. Meusdoerffer, and D. H. Wolf. 1982. *In vivo* biosynthesis of the vacuolar proteinases A and B in the yeast *Saccharomyces cerevisiae*. J. Biol. Chem. 257:11203-11206.

26. Messing, J. 1979. Recombinant DNA technical bulletin. National Institutes of Health Publication No. 79-99. 2:43-48.

27. Miller, J. 1972. Experiments in molecular genetics. Cold Spring Harbor Laboratory, Cold Spring Harbor, N.Y.

28. Nakano, A., D. Brada, and R. Schekman. 1988. A membrane glycoprotein, Sec12p, required for protein transport from the endoplasmic reticulum to the Golgi apparatus in yeast. J. Cell. Biol. 107:851-863.

29. Naumovski, L., and E. C. Friedberg. 1986. Analysis of the essential and excision repair functions of the *RAD3* gene of *Saccharomyces cerevisiae* by mutagenesis. Mol. Cell. Biol. 6:1218-1227.

30. Oliver, S. G., and J. R. Warmington. 1989. Transcription. In A. H. Rose, and J. S. Harrison (Eds.), *The Yeasts*, Vol. 3, 2nd ed. Academic Press, London. pp. 117-160.

31. Orr-Weaver, T. L., J. W. Szostak, and R. J. Rothstein. 1981. Yeast transformation: A model system for the study of recombination. Proc. Natl. Acad. Sci. USA 78:6354-6358.

32. Orr-Weaver, T. L., J. W. Szostak, and R. J. Rothstein. 1983. Genetic applications of yeast transformation with linear and gapped plasmids. Meth. Enzymol. 101:228-245.

33. Parsonage, D., S. Wilke-Mounts, and A. E. Senior. 1987. Directed mutagenesis of the β-subunit of F_1-ATPase from *Escherichia coli*. J. Biol. Chem. 262:8022-8026.

34. Patterson, T. E., and R. O. Poyton. 1986. *COX8*, the structural gene for yeast cytochrome c oxidase subunit VIII. DNA sequence and gene disruption indicate that subunit VIII is required for maximal levels of cellular respiration and is derived from a precursor which is extended at both its NH_2 and COOH termini. J. Biol. Chem. 261:17192-17197.

35. Pearson, W. R., and D. J. Lipman. 1988. Improved tools for biological sequence analysis. Proc. Natl. Acad. Sci. USA 85:2444-2448.

36. Preston, R. A., R. F. Murphy, and E. W. Jones. 1987. Apparent endocytosis of fluorescein isothiocynate-conjugated dextran by *Saccharomyces cerevisiae* reflects uptake of low molecular weight impurities, not dextran. J. Cell Biol. 105:1981-1987.

37. Pringle, J. R., R. A. Preston, A. E. M. Adams, T. Stearns, D. G. Drubin, B. F. Haarer, and E. W. Jones. 1989. Fluorescence microscopy methods for yeast. Meth. Cell. Biol. 31:357-435.

38. Rao, R., J. Pagan, and A. E. Senior. 1988. Directed mutagenesis of the strongly conserved lysine 175 in the proposed nucleotide-binding domain of α-subunit from *Escherichia coli* F_1-ATPase. J. Biol. Chem. 263: 15957-15963.

39. Robinson, J. S., D. J. Klionsky, L. M. Banta, and S. D. Emr. 1988. Protein sorting in *Saccharomyces cerevisiae*: Isolation of mutants defective in the delivery and processing of multiple vacuolar hydrolases. Mol. Cell. Biol. 8:4936-4948.

40. Rose, M. D., P. Novick, J. H. Thomas, D. Botstein, and G. R. Fink. 1987. A *Saccharomyces cerevisiae* genomic plasmid bank based on a centromere-containing shuttle vector. Gene 60:237-243.

41. Rothman, J. H., and T. H. Stevens. 1986. Protein sorting in yeast: Mutants defective in vacuole biogenesis mislocalize vacuolar proteins into the late secretory pathway. Cell 47:1041-1051.

42. Rothman, J. H., I. Howald, and T. H. Stevens. 1989. Characterization of genes required for protein sorting and vacuolar function in the yeast *Saccharomyces cerevisiae*. EMBO J. 8:2057-2065.

43. Rothstein, R. J. 1983. One step gene disruption in yeast. Meth. Enzymol. 101:202-211.

44. Salminen, A., and P. J. Novick. 1989. The Sec15 protein responds to the function of the GTP binding protein, Sec4, to control vesicular traffic in yeast. J. Cell Biol. 109:1023-1036.

45. Sanger, F., S. Nicklen, and A. R. Coulson. 1977. DNA sequencing with chain-terminating inhibitors. Proc. Natl. Acad. Sci. USA 74:5463-5467.

46. Sherman, F., G. R. Fink, and C. W. Lawrence. 1979. Methods in yeast genetics: A laboratory manual. Cold Spring Harbor Laboratory, Cold Spring Harbor, N.Y.

47. Spindler, K. R., D. S. E. Rosser, and A. J. Berk. 1984. Analysis of adenovirus transforming proteins from early regions 1A and 1B with antisera to inducible fusion antigens in *Escherichia coli*. J. Virol. 49:132-141.

48. Stevens, T., B. Esmon, and R. Schekman. 1982. Early stages in the yeast secretory pathway are required for transport of carboxypeptidase Y to the vacuole. Cell 30:439-448.

49. Stratagene. 1988. Bluescript Exo/Mung DNA Sequencing System Instruction Manual. Stratagene. La Jolla, CA.

50. Tagaya, M., T. Yagami, and T. Fukui. 1987. Affinity labeling of adenylate kinase with adenosine diphosphopyridoxal. Presence of Lys21 in the ATP-binding site. J. Biol. Chem. 262:8257-8261.

50A. Wada, Y., K. Kitamoto, T. Kanbe, K. Tanaka, and Y. Anraku. 1990. *SLP1* gene of *Saccharomyces cerevisiae* is essential for vacuolar morphogenesis and function. Mol. Cell. Biol. 10:2214-2223.

51. Walker, J. E., M. Saraste, M. J. Runswick, and N. J. Gay. 1982. Distantly related sequences in the α- and β-subunits of ATP synthase, myosin, kinases and other ATP-requiring enzymes and a common nucleotide binding fold. EMBO J. 1:945-951.

52. Weisman, L. S., and W. Wickner. 1988. Intervacuole exchange in the yeast zygote: A new pathway in organelle communication. Science 241:589-591.

53. Weisman, L. S., R. Bacallao, and W. Wickner. 1987. Multiple methods of visualizing the yeast vacuole permit evaluation of its morphology and inheritance during the cell cycle. J. Cell Biol. 105:1539-1547.

54. Wilson, D. W., C. A. Wilcox, G. C. Flynn, E. Chen, W.-J. Kuang, W. J. Henzel, M. R. Block, A. Ullrich, and J. E. Rothman. 1989. A fusion protein required for vesicle-mediated transport in both mammalian cells and yeast. Nature 339:355-359.

Figure 1. Complementation of *vps33-2ts* by the cloned *VPS33* gene. The parental strain SEY6210, the SEY33-2 mutant strain without and with the complementing plasmid pLB33-21, and the isogenic *vps33* null mutant LBY317 were streaked on YPD solid media and incubated at 25°C or 37°C, as indicated.

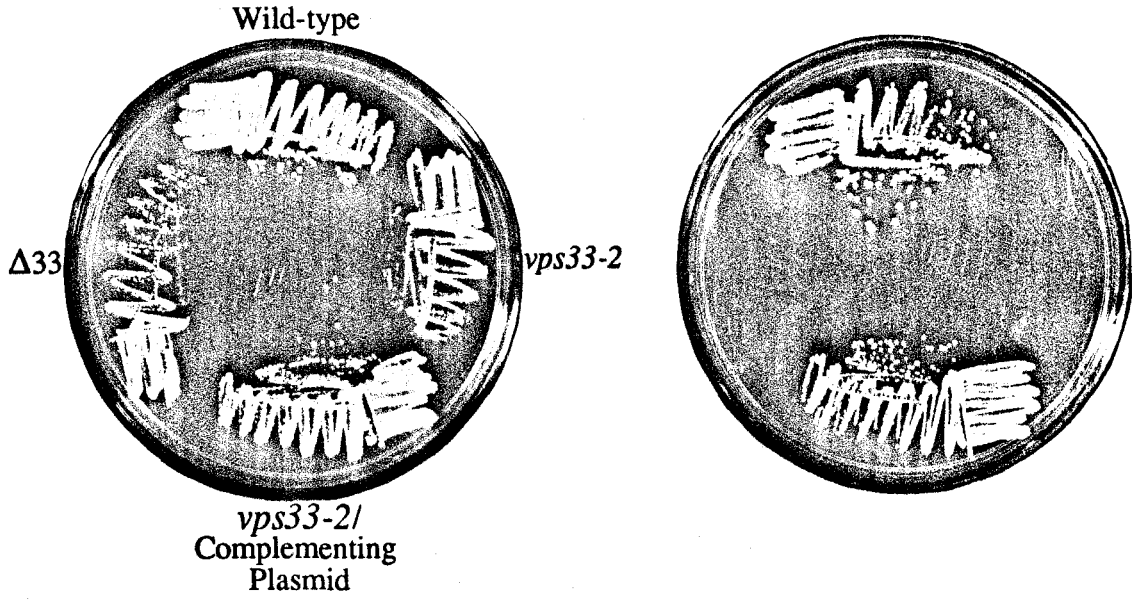
Wild-type
Δ33
vps33-2
vps33-2/
Complementing
Plasmid
25°C
37°C

Figure 2. (A) Restriction map of the entire 12 kb *VPS33* complementing clone. Restriction site abbreviations: B, *Bam*HI, C, *Cla*I; Pv, *Pvu*II; S, *Sal*I; Sa, *Sac*I: Sm, *Sma*I; Xb, *Xba*I; Xh; *Xho*I. (B) Complementation analysis of the *VPS33* subclones. Restriction fragments were cloned into pPHYC18 (*CEN4 ARS1 URA3*) to generate pLB33-20, pLB33-21, pLB33-22, pLB33-23 and pLB33-24. Plasmids pLB33-41 and pLB33-42 were the result of exonucleaseIII deletions from the *Sal*I end of the complementing fragment in pLB33-21 to yield the endpoints shown. The plasmids were transformed into SEY33-7 and Ura^+ transformants were tested for growth at 37°C. Vacuole morphology, as assessed by staining with Cl_2CFDA (see Materials and Methods), was also scored. A plus sign indicates that the transformants were *TR* and exhibited class A (wild-type) vacuole morphology; a minus sign indicates a *ts*, class C phenotype. (C) Fragments used for antibody production and gene disruption. The position of the ORF as determined by sequencing is shown. Plasmids pLB33-313 and pLB33-317, in which the *HIS3* gene replaced the indicated portions of *VPS33*, were used to generate *vps33* null mutants as described in the text. The fragments indicated by hashed boxes were used to generate in-frame *trpE-VPS33* gene fusions. The encoded hybrid proteins were used in antibody production as described in Materials and Methods. Additional restriction site abbreviations: H, *Hind*III; P, *Pst*I; R, *Eco*RI; Sp, *Sph*I.

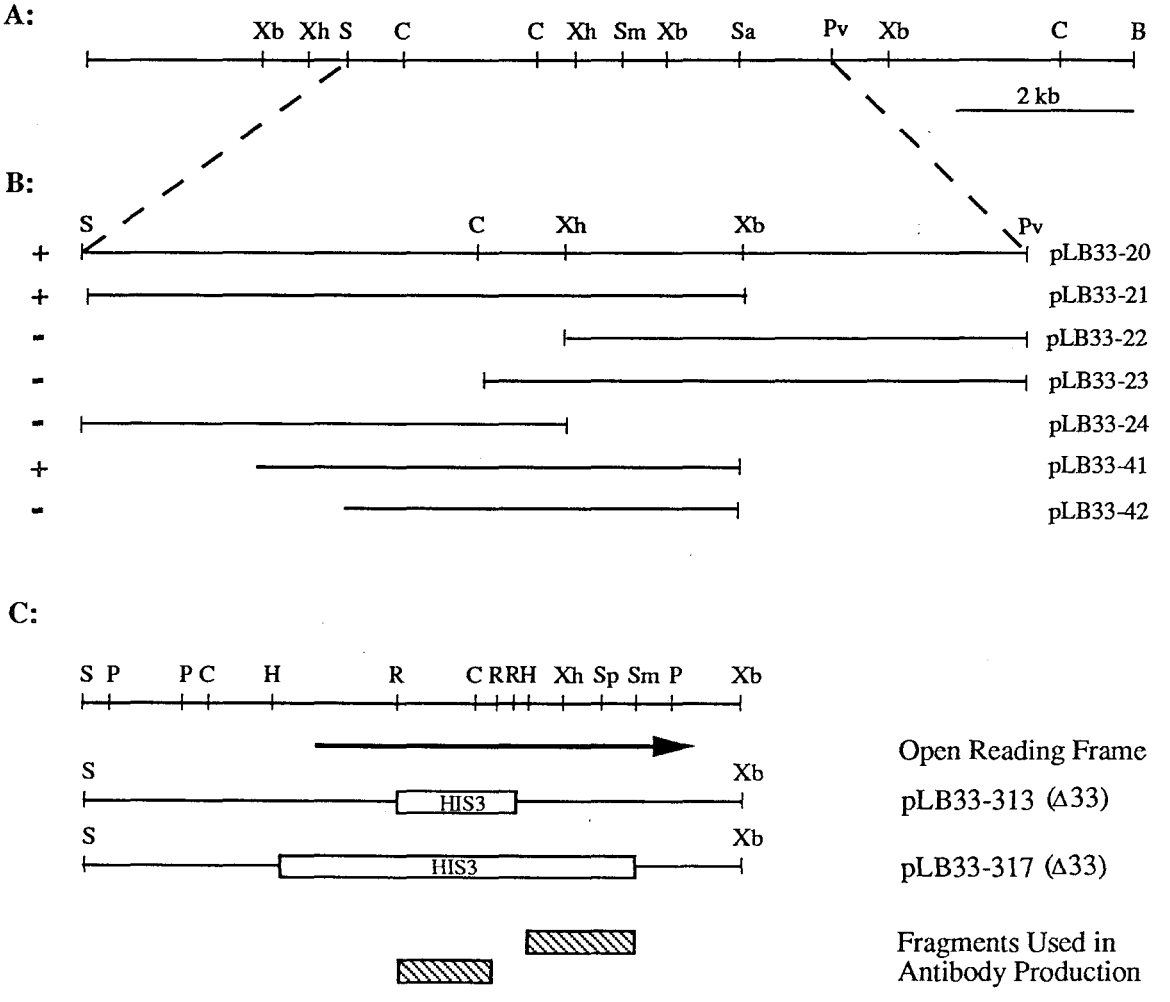
A:
Xb Xh S C C Xh Sm Xb Sa Pv Xb C B
2 kb
B:
S C Xh Xb Pv
+ pLB33-20
+ pLB33-21
- pLB33-22
- pLB33-23
- pLB33-24
+ pLB33-41
- pLB33-42
C:
S P P C H R C R R H Xh Sp Sm P Xb
Open Reading Frame
S Xb
HIS3
pLB33-313 (Δ33)
S Xb
HIS3
pLB33-317 (Δ33)
Fragments Used in Antibody Production

Figure 3. Sequence of *VPS33*. The nucleotide sequence and the deduced aa sequence of the ORF are shown. The putative transcription initiation and termination sequences are underlined. The regions which share sequence similarity with ATP-binding proteins are boxed. The T denoted with an * is replaced with a C in *vps33-4ts*.

```
   1  GTCAAGAAGC  GGGCTTGGCT  GCCATAATGG  AAGATTTAGA  TGTCGCAAAA  GTGGAATTAC  GTCATTTTGA  GAAAGCTTTT  AAAGGAATTG  CTAGGGGCAT  100
 101  TACTCCAGAA  ATGCTCTCTT  ATTATGAAGA  GTTTGCTCTA  AGAAGCGGTT  CATCTTCGTA  AGCTTGTTCA  TAGTCAATTC  TTTTCCTTTG  TGTGCTCAAT  200
 201  AATAGTAGAT  AGAAATTATA  CTGAACTCCG  GTCATTTTGT  ATAATATATT  AATCACTTCA  CACGAACATA  CATAAATAAA  ATATCATAAA  GGTTAGCAAA  300
 301  TTGGAACTAG  TTATATGTTA  ATTAGTTAAA  AGATAGAAAA  TTCGAGAAAG  GAAGAAAAAG  CTGATATTGC  CCATCTCCAA  CTTTATCAAA  TCATTTCACG  400

 401  ATG AAT AGA TTT TGG AAT ACT AAG AAA TTT TCA TTA ACA AAT GCC GAT GGA CTA TGT GCT ACC TTA AAT GAG ATA TCT CAA AAT GAT GAA  490
   1  Met Asn Arg Phe Trp Asn Thr Lys Lys Phe Ser Leu Thr Asn Ala Asp Gly Leu Cys Ala Thr Leu Asn Glu Ile Ser Gln Asn Asp Glu   30

 491  GTT CTT GTG GTT CAA CCA AGT GTA TTG CCA GTA CTC AAT AGT TTG CTA ACT TTC CAA GAT TTG ACT CAA TCA ACT CCT GTA AGG AAA ATT  580
  31  Val Leu Val Val Gln Pro Ser Val Leu Pro Val Leu Asn Ser Leu Leu Thr Phe Gln Asp Leu Thr Gln Ser Thr Pro Val Arg Lys Ile   60

 581  ACG TTA CTC GAT GAT CAG CTA AGT GAC GAT TTA CCG AGT GCC TTA GGC AGC GTT CCG CAA ATG GAT CTT ATT TTT CTT ATT GAT GTC AGA  670
  61  Thr Leu Leu Asp Asp Gln Leu Ser Asp Asp Leu Pro Ser Ala Leu Gly Ser Val Pro Gln Met Asp Leu Ile Phe Leu Ile Asp Val Arg   90

 671  ACA TCT CTC CGA CTC CCT CCA CAA CTG CTT GAT GCT GCT CAA AAG CAC AAT TTA TCA TCT TTG CAT ATA ATA TAC TGT CGA TGG AAA CCG  760
  91  Thr Ser Leu Arg Leu Pro Pro Gln Leu Leu Asp Ala Ala Gln Lys His Asn Leu Ser Ser Leu His Ile Ile Tyr Cys Arg Trp Lys Pro  120

 761   CT TTC CAA AAT ACT TTG GAG GAT ACA GAG CAA TGG CAA AAG GAT GGT TTC GAT TTG AAT TCA AAA AAA ACA CAT TTC CCT AAC GTC ATT  850
 121   er Phe Gln Asn Thr Leu Glu Asp Thr Glu Gln Trp Gln Lys Asp Gly Phe Asp Leu Asn Ser Lys Lys Thr His Phe Pro Asn Val Ile  150

 851   AA TCT CAG TTA AAG GAG CTA TCG AAC GAA TAT ACC CTT TAC CCT TGG GAT CTC TTG CCC TTC CCA CAG ATT GAT GAA AAT GTT CTA TTG  940
 151   lu Ser Gln Leu Lys Glu Leu Ser Asn Glu Tyr Thr Leu Tyr Pro Trp Asp Leu Leu Pro Phe Pro Gln Ile Asp Glu Asn Val Leu Leu  180

 941  ACT CAT TCC CTT TAT AAC ATG GAA AAT GTA AAC ATG TAT TAT CCC AAC TTA CGT TCT TTG CAG AGT GCC ACA GAG TCA ATA CTG GTT GAT 1030
 181  Thr His Ser Leu Tyr Asn Met Glu Asn Val Asn Met Tyr Tyr Pro Asn Leu Arg Ser Leu Gln Ser Ala Thr Glu Ser Ile Leu Val Asp  210

1031  GAT ATG GTC AAT TCG TTG CAG AGC TTG ATT TTT GAA ACT AAT AGT ATC ATA ACA AAT GTT GTG TCG ATA GGT AAT CTG TCT AAG AGA TGT 1120
 211  Asp Met Val Asn Ser Leu Gln Ser Leu Ile Phe Glu Thr Asn Ser Ile Ile Thr Asn Val Val Ser Ile Gly Asn Leu Ser Lys Arg Cys  240

1121  AGC CAT CTT TTG AAG AAA CGA ATC GAT GAG CAT CAA ACA GAG AAT GAT TTA TTC ATC AAG GGT ACG CTT TAT GGT GAA CGA ACC AAC TGT 1210
 241  Ser His Leu Leu Lys Lys Arg Ile Asp Glu His Gln Thr Glu Asn Asp Leu Phe Ile Lys Gly Thr Leu Tyr Gly Glu Arg Thr Asn Cys  270

1211  GGA CTA GAA ATG GAC TTG ATT ATC TTG GAA AGG AAT ACC GAT CCT ATA ACG CCA TTG TTG ACA CAA CTT ACG TAT GCA GGA ATA CTA GAT 1300
 271  Gly Leu Glu Met Asp Leu Ile Ile Leu Glu Arg Asn Thr Asp Pro Ile Thr Pro Leu Leu Thr Gln Leu Thr Tyr Ala Gly Ile Leu Asp  300

1301  GAT CTA TAT GAA TTC AAT TCT GGC ATA AAG ATA AAG GAG AAA GAC ATG AAC TTC AAT TAT AAG GAA GAT AAA ATA TGG AAT GAT TTG AAA 1390
 301  Asp Leu Tyr Glu Phe Asn Ser Gly Ile Lys Ile Lys Glu Lys Asp Met Asn Phe Asn Tyr Lys Glu Asp Lys Ile Trp Asn Asp Leu Lys  330

1391  TTT TTA AAT TTT GGG TCG ATT GGG CCG CAG TTA AAT AAA TTG GCA AAG GAA CTA CAA ACG CAA TAT GAT ACA AGG CAT AAA GCC GAG AGC 1480
 331  Phe Leu Asn Phe Gly Ser Ile Gly Pro Gln Leu Asn Lys Leu Ala Lys Glu Leu Gln Thr Gln Tyr Asp Thr Arg His Lys Ala Glu Ser  360

1481  GTA CAT GAA ATC AAA GAA TTC GTT GAT TCC TTA GGT TCT TTG CAA CAA AGG CAA GCT TTT TTG AAA AAT CAC ACA ACC TTA TCA TCC GAC 1570
 361  Val His Glu Ile Lys Glu Phe Val Asp Ser Leu Gly Ser Leu Gln Gln Arg Gln Ala Phe Leu Lys Asn His Thr Thr Leu Ser Ser Asp  390

1571  GTT TTG AAA GTG GTA GAG ACT GAA GAG TAC GGA TCT TTC AAT AAA ATC TTA GAG TTA GAG CTG GAA ATT TTG ATG GGA AAT ACA CTT AAT 1660
 391  Val Leu Lys Val Val Glu Thr Glu Glu Tyr Gly Ser Phe Asn Lys Ile Leu Glu Leu Glu Leu Glu Ile Leu Met Gly Asn Thr Leu Asn  420

1661  AAC GAC ATT GAA GAT ATT ATA CTC GAG TTG CAG TAC CAG TAC GAG GTT GAT CAA AAG AAG ATT CTC AGA TTA ATC TGT TTA TTG TCT CTT 1750
 421  Asn Asp Ile Glu Asp Ile Ile Leu Glu Leu Gln Tyr Gln Tyr Glu Val Asp Gln Lys Lys Ile Leu Arg Leu Ile Cys Leu Leu Ser Leu  450

1751  TGT AAA AAT TCA CTT CGA GAA AAG GAT TAT GAA TAT CTA AGA ACC TTT ATG ATC GAC TCT TGG GGC ATT GAA AAA TGC TTT CAA CTT GAA 1840
 451  Cys Lys Asn Ser Leu Arg Glu Lys Asp Tyr Glu Tyr Leu Arg Thr Phe Met Ile Asp Ser Trp Gly Ile Glu Lys Cys Phe Gln Leu Glu  480

1841  TCA TTG GCT GAG TTA GGA TTT TTC ACT AGC AAA ACG GGA AAA ACT GAT TTG CAT ATT ACA ACA AGT AAG TCA ACA AGA TTA CAG AAA GAA 1930
 481  Ser Leu Ala Glu Leu Gly Phe Phe Thr Ser Lys Thr Gly Lys Thr Asp Leu His Ile Thr Thr Ser Lys Ser Thr Arg Leu Gln Lys Glu  510

1931  TAC CGT TAT ATT TCA CAA TGG TTC AAT ACA GTA CCC ATA GAA GAC GAG CAT GCT GCC GAT AAA ATC ACA AAT GAG AAC GAT GAC TTC TCG 2020
 511  Tyr Arg Tyr Ile Ser Gln Trp Phe Asn Thr Val Pro Ile Glu Asp Glu His Ala Ala Asp Lys Ile Thr Asn Glu Asn Asp Asp Phe Ser  540

2021  GAA GCC ACT TTT GCT TAC AGT GGT GTA GTG CCC TTG ACA ATG AGA CTG GTT CAG ATG TTA TAT GAT AGG TCT ATC TTG TTC CAT AAT TAT 2110
 541  Glu Ala Thr Phe Ala Tyr Ser Gly Val Val Pro Leu Thr Met Arg Leu Val Gln Met Leu Tyr Asp Arg Ser Ile Leu Phe His Asn Tyr  570

2111  TCC TCG CAG CAG CCT TTT ATA CTG TCA AGA GAA CCT AGA GTT TCT CAA ACG GAG GAT TTA ATT GAA CAG TTA TAT GGA GAC TCA CAT GCG 2200
 571  Ser Ser Gln Gln Pro Phe Ile Leu Ser Arg Glu Pro Arg Val Ser Gln Thr Glu Asp Leu Ile Glu Gln Leu Tyr Gly Asp Ser His Ala  600

2201  ATC GAA GAG AGT ATA TGG GTC CCG GGA ACC ATT ACA AAA AAG ATC AAT GCA AGC ATC AAG AGC AAT AAT AGA CGG TCC ATA GAC GGA TCT 2290
 601  Ile Glu Glu Ser Ile Trp Val Pro Gly Thr Ile Thr Lys Lys Ile Asn Ala Ser Ile Lys Ser Asn Asn Arg Arg Ser Ile Asp Gly Ser  630

2291  AAT GGG ACA TTT CAT GCT GCA GAG GAT ATT GCA CTC GTA GTA TTC CTC GGA GGT GTA ACA ATG GGT GAA ATA GCT ATA ATG AAG CAT TTG 2380
 631  Asn Gly Thr Phe His Ala Ala Glu Asp Ile Ala Leu Val Val Phe Leu Gly Gly Val Thr Met Gly Glu Ile Ala Ile Met Lys His Leu  660

2381  CAA AAA ATA CTA GGT AAA AAA GGT ATC AAT AAA AGG TTT ATC ATC ATC GCC GAT GGC TTG ATC AAT GGC ACA AGG ATC ATG AAC TCT ATA 2470
 661  Gln Lys Ile Leu Gly Lys Lys Gly Ile Asn Lys Arg Phe Ile Ile Ile Ala Asp Gly Leu Ile Asn Gly Thr Arg Ile Met Asn Ser Ile  690

2471  TCT TAA      TTATTATATG  ATAGATTTGT  TAATTTTTTG  TATATGCAAA  TGTGCTTTTT  TTCACCAAAC  GGTTTGCACC  AATCATACGA  GAGAAGTGTT 2566
 691  Ser END 691
2567   CGGTGTTTAC  GGAAAAGCTA  GGGGACTAAG  AAAAATTGAA  AATAAAGGCT  GACAGCAGTA  GAAACCATTG  TGCTGGCTTA  GTGATTTATA  AGAATGGTTA 2666
2667   ATTAGTTTTG  TATCCTTTAA  TTTTCTAGA   2695
```

Figure 4. Comparison of the predicted Vps33p sequence with known and predicted ATP-binding proteins. The deduced aa sequence of Vps33p shares similarity with the proteins listed through the two domains shown. Residues which are highly conserved at a given position are shown in boldface and boxed, and a consensus sequence is indicated above each domain. The significance of the starred lysine in domain A is discussed in the text. In domain B, the * denote hydrophobic residues; this region is followed by an aspartic acid in one of the next three positions in each of the proteins listed (51). The sequences shown are taken from Walker *et al.* (51) (*E. coli* ATPase α- and β-subunits, adenylate kinase, rabbit myosin, phosphofructokinase, RecAp), Naumovski and Friedberg (29) (DnaBp, Rad3p), or Dulic and Riezman (8) (End1p). By analogy to the NSF protein of mammalian cells, with which it is functionally equivalent (54), the Sec18p of yeast (9) is also predicted to bind ATP. The abbreviations used are, PFK, phosphofructokinase; Adenyl. Kin., adenylate kinase.

Domain A:

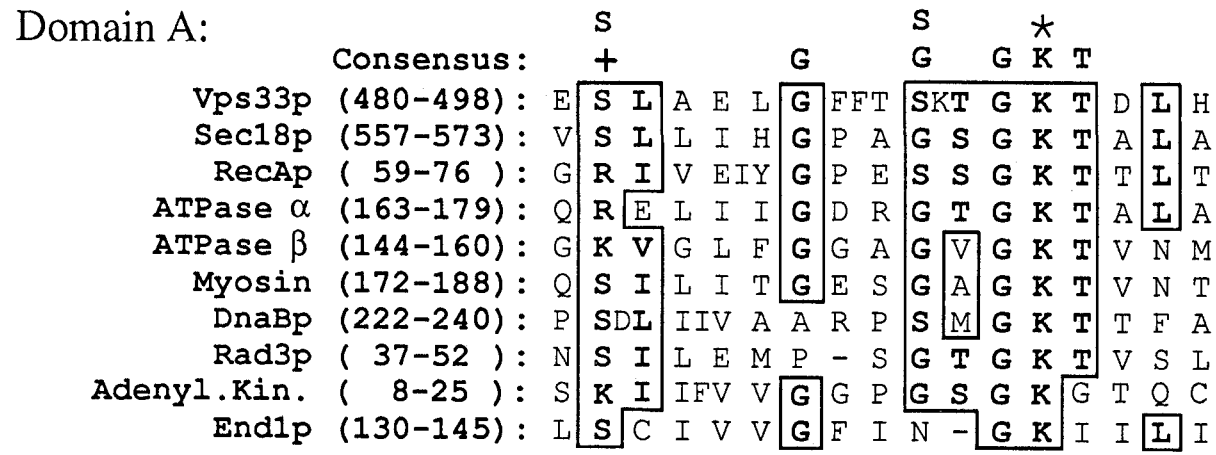

Domain B:

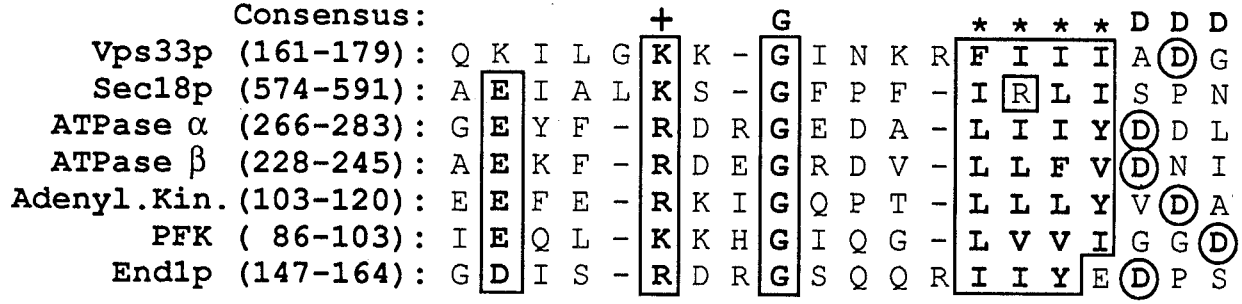

Figure 5. Processing of CPY in a *vps33* null mutant in the presence and absence of the cloned *VPS33* gene. Whole cells were labeled with Tran^{35}S-label for 20 min at 25°C, chased for 30 min by the additon of 4 mM methionine, and subjected to immunoprecipitation with CPY-specific antisera. The migration positions of precursor (pro) and mature (m) CPY are indicated. The isogenic strains used were: lane 1, *VPS*$^{+}$ (SEY6210); lane 2, *vps33* null mutant (LBY317) and lane 3, *vps33* null mutant carrying the cloned *VPS33* gene on a single copy plasmid (LBY317/pLB33-162).

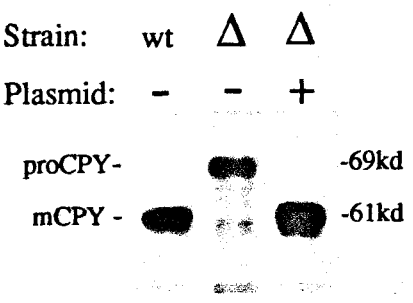
Strain: wt Δ Δ
Plasmid: - - +
proCPY-
mCPY -
-69kd
-61kd

Figure 6. Identification of the *VPS33* gene product. Spheroplasts (A) or whole cells (B) were labeled and chased as described in the legend to Fig. 5. Strains used were: parental strain SEY6210 (lane 1), SEY6210 carrying *VPS33* on the multicopy plasmid pLB33-221 (lanes 2, 3, 4 and 6), or the *vps33* null mutant LBY317 (lane 5). Tunicamycin was added to 20 μg/ml final concentration as indicated 15 min before the addition of the radioactive label. Immunoprecipitations were performed using the preimmune (lane 6) or Vps33p immune (lanes 1-5) sera. The migration positions for MW standards are indicated. In (A), the exposure time for lane 1 was twice as long as for lane 2.

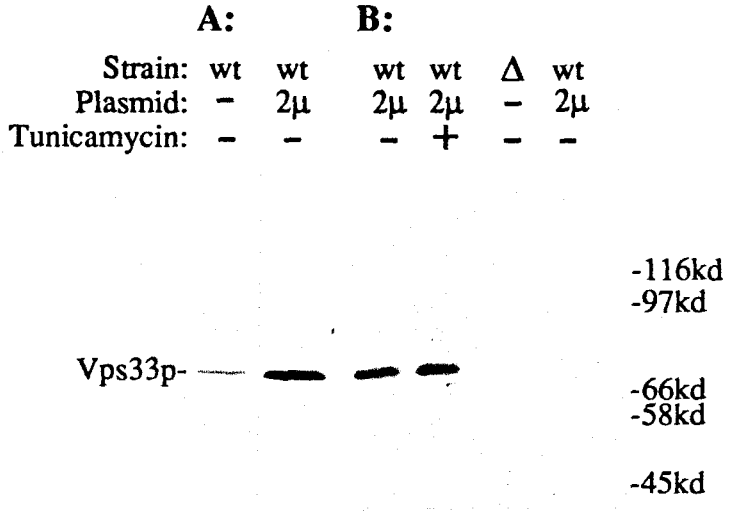
A:
B:
Strain: wt wt wt wt Δ wt
Plasmid: – 2μ 2μ 2μ – 2μ
Tunicamycin: – – – + – –
-116kd
-97kd
Vps33p-
-66kd
-58kd
-45kd

Figure 7. Subcellular fractionation of Vps33p. Strain SEY6210 carrying *VPS33* on the multicopy plasmid pLB33-221 was enzymatically converted to spheroplasts. Spheroplasts were labeled at 30°C for 20 min and chased for 30 min by the addition of 4 mM methionine. Labeled spheroplasts were pelleted and osmotically lysed as described in Material and Methods in lysis buffer containing the indicated concentration of KCl. For the samples in B, the buffer also contained 0.3 M mannitol. Unlysed cells were removed by centrifugation at 500 x g and the resulting lysate was centrifuged at 100,000 x g for 90 min at 4°C. The supernatant (S) and pellet (P) fractions were processed as described in Materials and Methods and immunoprecipitated with antisera to Vps33p.

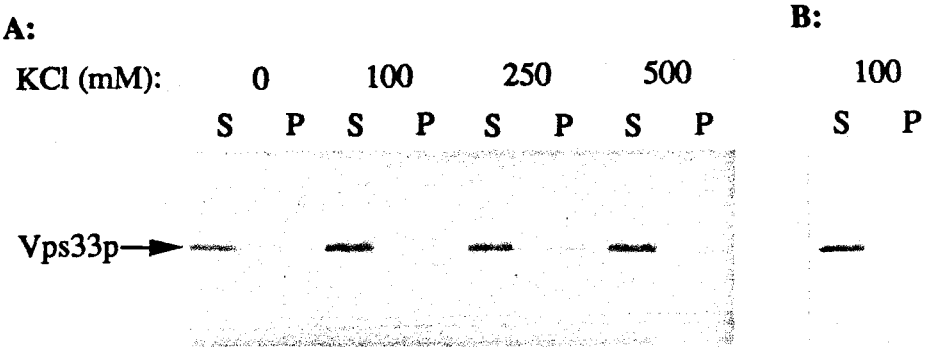
A:
B:
KCl (mM):
0
100
250
500
100
S P S P S P S P
S P
Vps33p

Figure 8. Mother and bud vacuole staining in SEY33-4. SEY33-4 was grown in YPD at 25°C (A and B) and shifted to 37°C for 2 h (C and D), 4 h (E and F), or 6 h (G-J) before harvesting. Also shown for comparison is the parental strain SEY6210 grown at 25°C (K) and shifted to 37°C for 6 h (L). Cells were stained with FITC as described in Materials and Methods and observed using Nomarski (left) or fluorescence (right) optics. The number of buds exhibiting vacuole fluorescence was quantitated and expressed as a percentage of the total number of large budded cells (n). Cells were grown at 25°C, incubated at 37°C for the indicated lengths of time, and stained with FITC as described above. Bar, 10 μm.

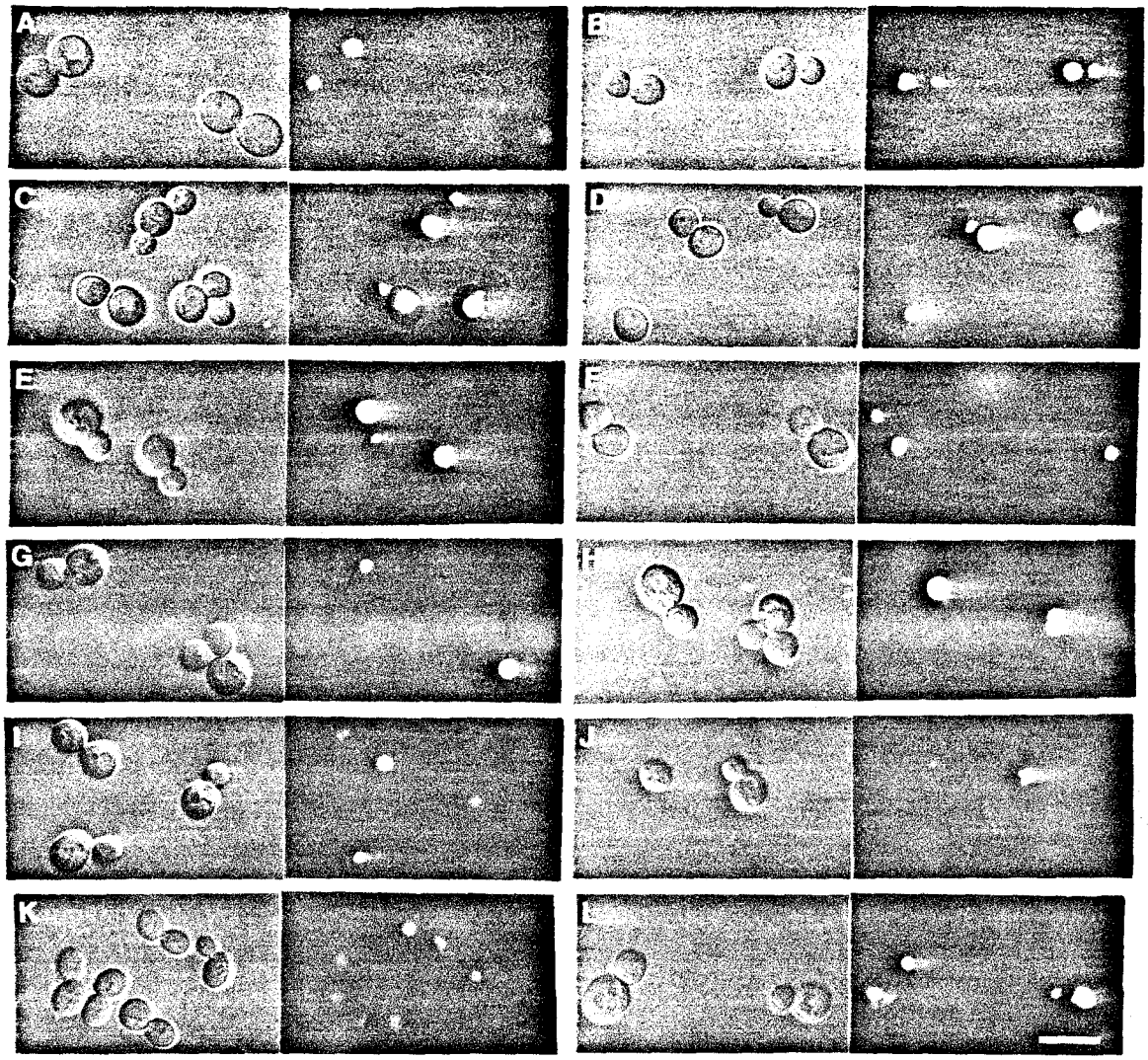

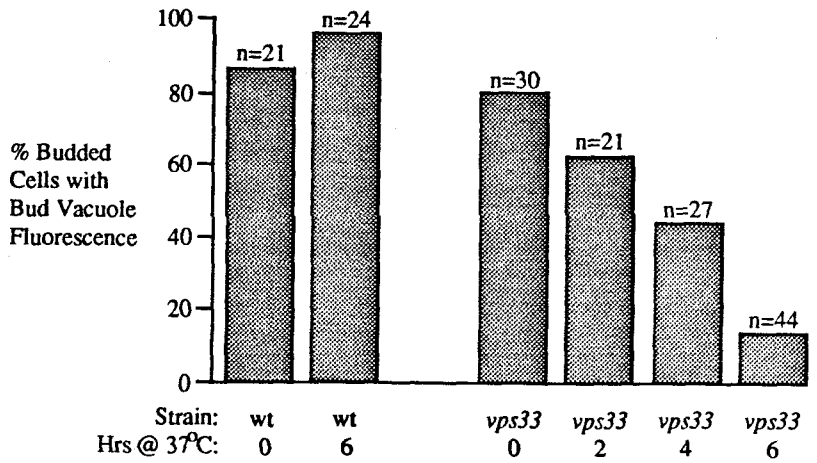
100
80
60
40
20
0
% Budded Cells with Bud Vacuole Fluorescence
n=21
n=24
n=30
n=21
n=27
n=44
Strain: wt wt vps33 vps33 vps33 vps33
Hrs @ 37°C: 0 6 0 2 4 6

Figure 9. Rescue of the SEY33-4 phenotypic defects by overexpression of the mutant allele. (A) The indicated strains were streaked on YPD solid media and incubated at 25°C or 37°C. 1, Parental strain SEY6210; 2, SEY33-4; 3, SEY33-4 carrying the plasmid pLB33-161 (*vps33-4ts* allele on a single copy vector); 4, SEY33-4 carrying the plasmid pLB33-271 (*vps33-4ts* allele on a multicopy vector); 5, SEY6210 carrying pLB33-271. (B) Whole cells were labeled and chased at 25°C (lanes 1-5) or 37°C (lane 6) and subjected to immunoprecipitation with CPY-specific antisera as described in the legend to Fig. 5. Lanes 1-5, strains listed above. Lane 6, SEY33-4 was grown at 25°C and shifted to 37°C for 5 h before radioactive labeling. Wild-type cells grown and labeled under these conditions contain CPY exclusively in the mature form (data not shown). The migration positions of precursor (pro) and mature (m) CPY are shown.

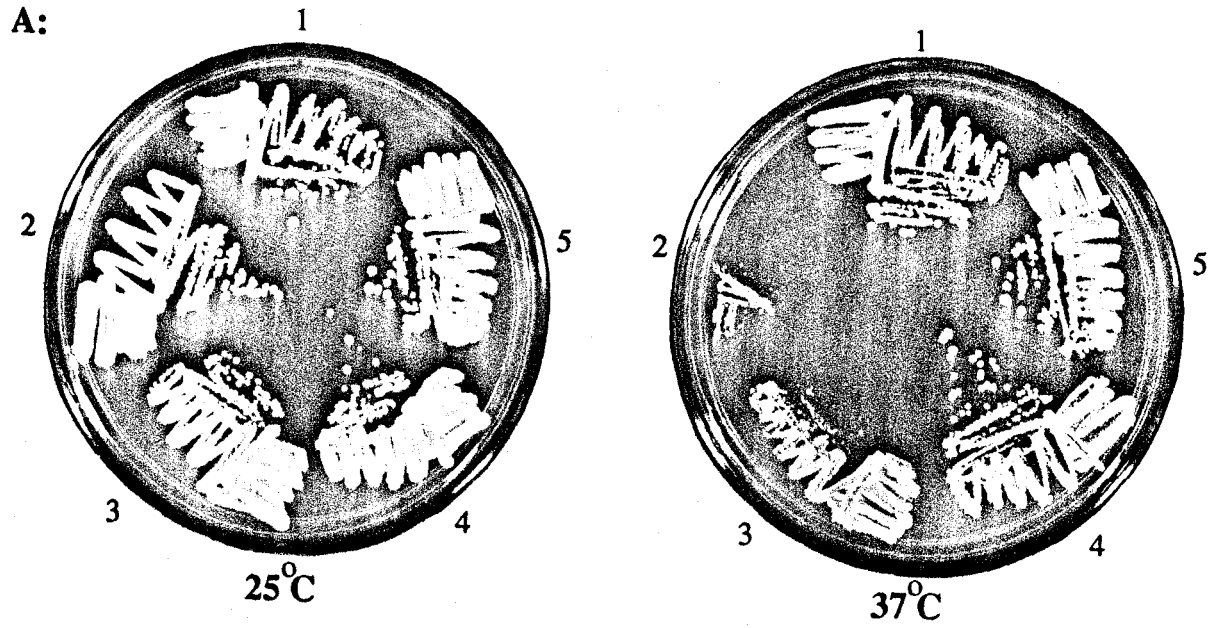
A:
1
2
3
4
5
25°C
1
2
3
4
5
37°C
B:
1 2 3 4 5
6
proCPY-
mCPY-
-69kd
-61kd

Figure 10. Predicted secondary structure of the carboxy terminal 50 aa of the wild-type Vps33p (left) and the Vps33-4p (right). The position of the leucine^{646}, which is replaced by proline in the mutant protein, is indicated. Secondary structures were predicted by the method of Chou and Fasman (5) and displayed graphically using the PlotStructure program of the University of Wisconsin Genetics Computer Group Sequence Analysis Software Package.

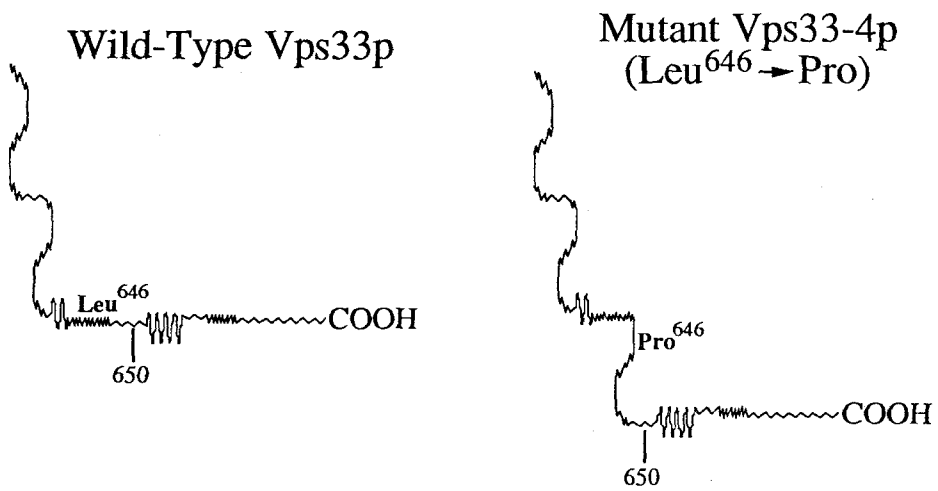
Wild-Type Vps33p
Leu646
650
COOH
Mutant Vps33-4p
(Leu646→Pro)
Pro646
650
COOH

Chapter 5

Cloning and Initial Characterization of a Gene, *VPS*28, Involved in Protein Modification and Vacuolar Protein Sorting

Lois M. Banta, Thomas A. Vida, and Scott D. Emr

This chapter represents preliminary work on this project, which will be continued by another member of the Emr lab.

ABSTRACT

*vps*28 mutant yeast contain morphologically wild-type vacuoles, but mislocalize and secrete a small fraction of the soluble vacuolar hydrolases carboxypeptidase Y (CPY), proteinase A, and proteinase B. These cells also appear to accumulate aberrant, possibly Golgi-related, structures. Consistent with this observation, the CPY in *vps*28 mutants exhibits an altered mobility which likely results from a defect in glycosyl modification as this protein transits the Golgi. The *VPS*28 gene has been cloned from a yeast genomic library, using a novel screen for complementation of the vacuolar protein localization defect. The complementing activity has been found to reside on a 4.2 kb DNA fragment. Integrative mapping has confirmed that this cloned DNA fragment is genetically linked to the *vps*28 mutant locus. Disruption of *VPS*28 does not appear to be lethal, but results in a vacuolar protein sorting defect comparable to that of the original mutants. We propose that the *VPS*28 gene product is involved in a late protein modification step; as a consequence of a primary defect in this process, *vps*28 mutants exhibit a modest missorting of vacuolar proteins.

INTRODUCTION

In eukaryotic cells, the secretory pathway mediates the modification, processing, and delivery of proteins destined for a variety of subcellular compartments including the plasma membrane, lysosomes, endoplasmic reticulum (ER) and Golgi. Proteins entering this pathway are translocated from their cytoplasmic site of synthesis across the ER, where initial N-linked glycosyl modifications take place. Those proteins not retained at the ER are transported to the Golgi complex, where they are separated and targeted to their final intracellular destinations. During transit through the Golgi complex, the oligosaccharide chains are further modified by a number of resident Golgi enzymes (8). The extent of N-linked modification is often used as a marker to monitor the progress of a substrate through the secretory pathway.

In the yeast *Saccharomyces cerevisiae*, proteins bound for the lysosome-like vacuole also traverse the secretory pathway en route to their final destination (27). Soluble vacuolar hydrolases such as carboxypeptidase Y (CPY), proteinase A (PrA), and proteinase B (PrB) are synthesized as inactive precursors; these proteins are proteolytically processed upon arrival at the vacuole to yield the mature active enzymes (10, 11, 18). The propeptides of CPY and PrA contain sequence determinants that function as vacuole-sorting signals (13, 15, 28).

We have isolated a number of mutants that exhibit defects in the proper localization and processing of several vacuolar proteins. These *v*acuolar *p*rotein *s*orting, or *vps*, mutants were identified using a gene fusion-based selection scheme in which the vacuole-targeting signal of CPY was fused to the entire coding region of the normally secreted protein invertase (Inv). In wild-type cells, the hybrid protein encoded by this gene fusion is diverted to the vacuole (13). Approximately 600 mutants were isolated in which various amounts of this CPY-Inv fusion protein were missorted to the cell surface (1, 22). These mutants,

defining >33 complementing groups, are also defective in the localization of wild-type CPY, PrA, and PrB.

Examination of the vacuole morphology in the *vps* mutants revealed that the majority of these strains (the class A mutants), including *vps*28 mutants, contain normal-looking vacuoles. Ultrastructural analysis suggested, however, that mutants in four of these class A complementation groups accumulate aberrant organelles such as vesicles or Golgi-related complexes (2). The class A *vps* mutants also differ in the extent to which they mislocalize vacuolar proteins. Mutants in some complementation groups secrete close to 100% of the CPY in a precursor form, while representative alleles of 10 complementation groups mislocalize <40% of the vacuolar hydrolases (22).

In an effort to analyze further the function of the *VPS*28 gene product, we have undertaken a biochemical and molecular analysis of a *vps*28 mutant strain. This mutant contains vacuoles which are indistinguishable from those of the wild-type strain; however, it also appears to accumulate stacks of lamellae and reticular membrane arrays. These structures, which are approximately two times as prevalent in *vps*28 cells as in the parental strain, are proposed to correspond to exaggerated Golgi complexes (2). The seven mutant strains comprising the *vps*28 complementation group typically secrete 30-40% of the CPY-Inv hybrid protein. Consistent with these data, immunoprecipitation studies revealed that ~15-20% of the CPY is found at the cell surface in a precursor form (22). We report here on the modification of CPY in *vps*28 mutants and the cloning and initial characterization of the *VPS*28 gene.

MATERIALS AND METHODS

Strains, Media and Vectors. *Escherichia coli* strains MC1061 [F^- *araD139* Δ(*araABOIC-leu*)*7679* Δ*lacX74 galU galK rpsL hsdR strA*] (6) and JM101 [*supE thi* Δ(*lac-proAB*) (F' *traD36 proAB lacI*^{q} *Z M15*)] (19) were used for cloning. *E. coli* strain JF1754 (*hsdR metB leuB hisB lac gal*) (17) was used in screening plasmids pLB28-519 and pLB28-520. *Saccharomyces cerevisiae* parental strains were SEY6210 (*MAT*α *ura3-52 leu2-3,112 his3-*Δ*200 trp1-*Δ901 lys2-801 suc2-Δ9) and SEY6211 (*MAT*a *ura3-52 leu2-3,112 his3-200 trp1-*Δ*901* ade2-101 suc2-Δ9) (22). The mutant strains SEY28-2 and SEY28-7 carrying the *vps*28-2 or *vps*28-7 alleles, respectively, are isogenic with SEY6210.

Bacterial strains were grown on standard media (20). Standard YPD, SD minimal, and sporulation media for yeast were prepared as described (26).

E. coli plasmid pBluescript KS (-) is described in the Stratagene (La Jolla, CA) catalog. The yeast integrating vector pPHYI10 (*TRP1*, selectable marker) and the *E. coli*-yeast shuttle vectors pPHYC16 and pPHYC18 (*CEN4 ARS1 URA3*) will be described elsewhere (P. Herman, manuscript in preparation). The *HIS3* gene was isolated as a 1.75 kb *Bam*HI fragment from a plasmid kindly provided by E. Phizicky.

Materials. Restriction enzymes, T4 DNA ligase, and Klenow enzyme were purchased from Boehringer Mannheim Biochemicals (Indianapolis, IN). Isopropyl-β-D-thiogalactoside (I.P.T.G.) and 5-bromo-4-chloro-3-indolyl-β-D-galactoside (X-gal) were the products of United States Biochemical Corp. (Cleveland, OH). 5-Fluoroortic acid was purchased from PCR, Inc. (Gainesville, FL). Tran^{35}S label was the product of ICN Radiochemicals (Irvine, CA). Autofluor was purchased from National Diagnostics (Manville, NJ). Antisera against CPY was from Klionsky *et al.* (15). All other chemicals were purchased from Sigma (St. Louis, MO).

Enzyme Assays. Liquid assays for extracellular and total invertase activity were performed as described (13). The rapid filter assay for external invertase activity has been described (15, 22).

Genetic and DNA Manipulations. Standard recombinant DNA techniques were performed as described (16). Standard yeast genetic methods were used throughout (26). Yeast transformations were performed using the lithium acetate method of Ito *et al.* (12).

Plasmid Constructions. Plasmid pLB28-104 was constructed by cloning the 4.2 kb *Pst*I-*Kpn*I fragment (Fig. 1b) into the *Pst*I/*Kpn*I sites of the yeast integrating vector pPHYI10. The restriction fragments shown in Fig. 1b were isolated from pLB28-1 (see below) and subcloned into the appropriate restriction sites within the polylinker of the *E. coli*-yeast shuttle vector pPHYC18 to generate pLB28-40 through pLB28-47. Plasmid pLB28-418 was constructed by subcloning the 4.4 kb *Cla*I-*Pvu*II fragment (Fig. 1c) into pBluescript KS (-). Construction of pLB28-519, used in the disruption of *VPS28*, was achieved by digesting pLB28-418 with *Hind*III to remove the region shown in Fig. 1c, gel-purifying the linear DNA away from the three *Hind*III fragments, blunting the ends with Klenow enzyme, and inserting the *HIS3* gene as a blunted *Bam*HI fragment. In a similar manner, the region shown in Fig. 1c was removed by digestion with *Eco*RI and replaced with the *HIS3* gene to generate pLB28-520. In both cases, recombinant plasmids were selected directly for the presence of the *HIS3* gene in the *his*B bacterial strain JF1754 (17) on M63 media lacking histidine (20). The plasmid pCYI-433 has been described previously (13). Plasmid pLJL2 is a derivative of pSEYC306 (13) carrying a *PRC1-SUC2* fusion gene, encoding the amino terminal 95 amino acids (aa) of CPY fused to invertase, and the *LEU2* gene as a selectable marker.

Cloning of VPS28. Yeast strain SEY28-2 carrying pLJL2 was grown in SD media lacking leucine to an optical density at 600 nm of 0.5-1.0 and subcultured in YPD

for two generations. Cells were transformed with a yeast genomic library carried on the *E. coli*-yeast shuttle vector YCp50 (*CEN4 ARS1 URA3*) (23). Transformants were selected on minimal fructose media lacking uracil and leucine and screened for external invertase activity using a modification of the rapid filter assay. A solution containing sucrose, reagents which permit the detection of glucose (15) and 1.2% (final concentration) melted agar was overlaid directly on the plates and colonies were scored for color, indicating a positive reaction (external invertase activity). Transformants which failed to turn color were picked, restreaked, and tested again using the invertase filter assay. Transformants that again remained colorless were cured of the plasmid by incubation on 5-fluoroortic acid plates (5). Complementing plasmid DNA (pLB28-1) was isolated and used to retransform SEY28-2.

Immunoprecipitation. Cells were grown in SD media (26), supplemented with the appropriate amino acids. Whole cells (1.5 units at an optical density at 600 nm of 1.0) were collected by centrifugation. The cells were resuspended in 0.5 ml of the same media, and 125 μCi of Tran^{35}S label were added. Alternatively, spheroplasts were prepared as described (22) and resuspended as above. The cells or spheroplasts were labeled with shaking at 30°C and chased by the addition of methionine to a final concentration of 4 mM. The chase was terminated and cells were lysed and subjected to a single round of immunoprecipitation using antisera specific for CPY as described (7, 15).

RESULTS

Cloning and Genetic Analysis of VPS28

The *VPS28* gene was cloned from a yeast genomic library carried on the single copy vector YCp50 (*CEN4 ARS1 URA3*) (23). Because none of the *vps28* mutants exhibited a conditional-lethal phenotype such as temperature sensitivity, we devised a simple plate assay which allowed us to screen for complementation of the vacuolar protein sorting (Vps^-) defect. This screen takes advantage of a colorimetric assay for invertase activity as applied to vegetatively growing yeast colonies. Wild-type cells in which the endogenous genes encoding invertase have been deleted, but which carry a plasmid encoding an appropriate CPY-Inv fusion protein, exhibit no external invertase activity, because the hybrid protein is sequestered in the vacuole (13). In mutant cells in which the CPY-Inv fusion protein is missorted, invertase activity is detected at the cell surface (1, 22). This external invertase activity can be assayed directly by overlaying the invertase assay components on a plate of yeast colonies. Those colonies in which the CPY-Inv hybrid protein is secreted turn brown within 10 min, while control colonies exhibiting no external invertase activity remain white for at least 2 h.

This screen was employed to clone the *VPS28* gene by complementation in the *vps28* mutant SEY28-2. This strain secretes ~30-40% of the CPY-Inv hybrid protein encoded by the plasmid pLJL2. Among 12,000 transformants screened, ~75 colonies appeared to exhibit lowered levels of external invertase activity as assayed by the overlay technique (see Materials and Methods for details). These potential Suc^- colonies were picked and patched onto minimal fructose plates and screened again by filter assay for external invertase activity. One colony was found to be reproducibly Suc^-; this transformant was Suc^+ when cured of the *URA3* plasmid, indicating that the Suc^- phenotype was not simply due to reversion of the *vps28* mutation. Complementing plasmid DNA (designated pLB28-1) was

isolated from the transformant and used to transform SEY28-2 and a second *vps*28 mutant, SEY28-7. These strains were subjected to a quantitative liquid assay for external and total invertase activity; the results are shown in Table 1. These data indicate that, in the presence of the complementing plasmid, the secretion of the CPY-Inv hybrid protein by the *vps*28 mutants is reduced to close to wild-type levels.

A restriction map of the 11 kb insert in pLB28-1 is shown in Fig. 1a. Subcloning and complementation analysis revealed that the complementing activity resided on a 5.5 kb *Cla*I-*Kpn*I fragment (Fig. 1b). Further subcloning experiments, in which smaller fragments from within this *Cla*I-*Kpn*I fragment were used, gave equivocal results. While a replicating plasmid carrying the 2.6 kb *Bam*HI-*Kpn*I fragment (pLB28-47) clearly was unable to complement a *vps*28 defect, SEY28-2 carrying pLB28-45 or pLB28-46 gave rise to some yeast colonies which were Suc^+ and others which were Suc^- (Fig. 1b). The meaning of these observations is not immediately clear. However, a plasmid (pLB28-104) containing the 4.2 kb *Pst*I-*Kpn*I fragment carried on the integrating vector pPHYI10 was able to complement a *vps*28 mutation, as determined by the observation that stable integrants were Suc^- (see below). Furthermore, the 3.0 kb *Pst*I-*Pvu*II fragment carried on the *E. coli*-yeast shuttle vector pPHYC16 also appeared competent for complementation (G. Paravicini, unpublished observations). Consistent with these observations, Northern analysis revealed a single RNA species of ~1.7 kb (data not shown).

To confirm that the complementing ability of pLB28-1 was not due to suppression by another gene, we performed integrative mapping experiments with the clone. The 4.2 kb *Pst*I-*Kpn*I fragment was cloned into the integrating vector pPHYI10, which carries the selectable marker *TRP*1. The resulting plasmid (pLB28-104) (Fig. 1b) was linearized by cleavage at the unique *Bam*HI site in the

cloned DNA to facilitate homologous recombination (21) and used to transform the Trp1$^-$ strain SEY28-2 harboring the plasmid pLJL2. The transformants did not exhibit external invertase activity, indicating that the fragment used was sufficient to complement the *vps*28 defect. Two different Trp$^+$ Suc$^-$ transformants were crossed to the Trp1$^-$ *VPS*$^+$ parental strain SEY6211. Tetrad analysis of the sporulated diploids showed the expected 2:2 Trp$^-$:Trp$^+$ segregation pattern; all four spores in each of the nine asci analyzed were Suc$^-$, as assessed by the invertase filter assay. An additional 76 random spores were also examined and no Suc$^+$ segregants were uncovered. These observations indicated that the complementing clone is tightly linked to the *vps*28 mutant locus.

Disruption of VPS28

Two different constructions were used to disrupt the *VPS*28 locus using the one-step gene disruption technique of Rothstein (24). In the first construction, the 2.1 kb *Hind*III fragment shown in Fig. 1c was replaced with the *HIS*3 gene in pLB28-418 to generate plasmid pLB28-519. Similarly, the *HIS*3 gene replaced the 2.0 kb *Eco*RI fragment (indicated in Fig. 1c) in the plasmid pLB28-520. These disruptions removed two-thirds of the smallest complementing fragment, the 3.0 kb *Pst*I-*Pvu*II region. These nonreplicating plasmids were linearized to facilitate homologous recombination (21) and used to transform the His$^-$ heterozygous diploid SEY6211/SEY28-2. This diploid contains one wild-type and one mutant allele of *VPS*28 and carried the plasmid pCYI-433, which encodes a CPY-Inv fusion protein on a *URA*3 vector. Integration of the null allele at the wild-type *VPS*28 locus should uncover the Suc$^+$ phenotype of the *vps*28 mutant, while integration at the *vps*28 mutant locus should yield phenotypically wild-type diploids. As expected, if pLB28-519 or pLB28-520 had an equal chance of integrating at either chromosomal locus, 12 of 23 His$^+$ transformants examined were Suc$^-$ while 11 were Suc$^+$. Three Suc$^+$ and one Suc$^-$ transformants were chosen for further

analysis. In tetrads resulting from the Suc^+ transformants, all segregants were found to secrete the CPY-Inv hybrid protein, regardless of whether they were His^+ or His^-. The data from three representative tetrads are shown in Table 2. The level of invertase activity at the cell surface is comparable to that of the *vps*28 parental strain SEY28-2 (compare with Table 1). These observations are consistent with integration of the disruption plasmid at the wild-type ***VPS***28 chromosomal locus to generate a diploid containing two mutant *vps*28 alleles. Tetrad analysis was also performed on a Suc^- diploid transformant. Segregants from two representative tetrads were subjected to immunoprecipitation using antisera specific for CPY. These results are shown in Fig. 2. In each case, the His^+ segregants exhibited a Vps^- phenotype in which a small amount (10%) of CPY accumulated in the precursor form, while the His^- segregants were Vps^+. A third tetrad gave similar results (data not shown). As was the case for the Suc^+ transformants, the extent of the CPY processing/ missorting defect in the His^+ segregants is comparable to that observed in the original mutant strain (22). Together, these observations suggest that disruption of ***VPS***28 is not lethal and in fact, causes only a relatively minor defect in vacuolar protein localization.

vps28 Mutants Exhibit an Apparent Defect in Glycosylation

Because the gene-disruption experiments suggested that the ***VPS***28 gene product may be only indirectly involved in vacuolar protein targeting, we examined the *vps*28 mutants in more detail for any clue to the primary defect in these cells. Upon analysis of the processing of CPY in the *vps*28 mutant cells, we noticed that this protein migrated aberrantly on sodium dodecyl sulfate-polyacrylamide gels. When spheroplasts were radioactively labeled and subjected to immunoprecipitation with CPY-specific antisera, both the Golgi-modified (p2) and mature forms of CPY appeared to be larger in the *vps*28 mutant strains than in the parental strain (Fig. 3). In contrast, the ER-modified (p1) forms had the

same mobility in the wild-type and mutant cells. These observations suggest that the oligosaccharide processing of CPY which takes place in the Golgi may be defective in the *vps*28 mutant strains.

DISCUSSION

We have previously described the isolation of mutants defective in vacuolar protein processing and delivery (1, 22). We have now employed a novel screen to clone the gene defined by one *v*acuolar *p*rotein *s*orting mutant, *vps*28. Like mutants in several other *vps* complementation groups, *vps*28 strains contain morphologically normal-looking (class A) vacuoles and mislocalize only a small fraction of the vacuolar hydrolases CPY, PrA, and PrB (2, 22). These "weak" class A *vps* mutants might represent functions that only indirectly affect vacuolar protein sorting. Alternatively, the genes defined by these mutants might be essential for growth; in this case, mutations which drastically affect gene product function might be expected to lead to lethality and would never be seen in a selection such as ours. Gene disruption should allow one to distinguish between these two possibilities. Disruption of *VPS*28 is not a lethal event, but results in a vacuolar protein targeting defect which is comparable to that of the original mutants (~30% secretion of a CPY-Inv hybrid protein and ~10-15% mislocalization of CPY) (Table 2, Fig. 2). These findings indicate that the *VPS*28 gene product makes only a minor contribution to the fidelity of vacuole protein trafficking.

One possible role for a putative Vps28p is suggested by the observation that *vps*28 mutant cells appear to accumulate structures which may correspond to exaggerated Golgi complexes (2). Perhaps the *VPS*28 gene product is involved in some aspect of transport through the Golgi complex. Since vacuolar proteins transit the Golgi en route to the vacuole, defects in Golgi processes might indirectly affect protein traffic to the vacuole. Indeed, temperature-sensitive mutants in which secretion is blocked at the level of the Golgi accumulate the precursor form of CPY at the nonpermissive temperature (27). A possible role for *VPS*28 function in a Golgi-related process is supported by the observation that the Golgi-modified precursor and mature forms of CPY found in *vps*28 cells appear to

be larger than those in a wild-type strain. These data suggest that glycosyl modification events which normally take place in the Golgi may be aberrant in *vps*28 mutants. Analysis of the oligosaccharide structure on CPY, as well as on secreted proteins such as invertase, in these strains might allow confirmation of this proposal.

At least two other mutants implicated in different aspects of the secretory pathway exhibit defects in glycoprotein processing at the level of the Golgi apparatus. Mutations in the *ERD*1 gene, required for the retention of luminal ER proteins, result in slightly increased mobilities for the Golgi-modified (p2) and mature forms of CPY. In addition, *erd*1 mutants appear to missort a small fraction of the p2 CPY to the cell surface (9). Loss of *PMR*1 (also known as *SSC*1) function causes the secretion of elevated levels of some foreign proteins in yeast and suppresses the lethality of the *ypt*1-1 mutation, which blocks the secretion pathway. Strains carrying mutations in the *PMR1* gene, which encodes a protein with sequence similarity to Ca^{2+}-ATPases, secrete proteins lacking the outer chain glycosylation which normally takes place in the Golgi (25). Furthermore, Schekman and coworkers have shown that two mutations which block yeast secretion (*sec*53 and *sec*59) cause primary defects in the glycosylation of secretory proteins. The *SEC*53 gene product is a cytoplasmic protein required for the assembly of N-linked carbohydrate precursors (3, 14), while the *SEC*59 gene encodes a very hydrophobic protein that may function in mannose transfer to core oligosaccharides (4). Our observations are consistent with a role for a putative Vps28p in oligosaccharide modification, perhaps at the level of the Golgi. Further characterization of the *VPS*28 gene and gene product will be required to determine the function and location of the protein, as well as its contribution to vacuolar protein delivery.

ACKNOWLEDGEMENTS

We would like to thank Raffi Aroian for the YCp50 library DNA and for preliminary work on the invertase overlay assay.

LITERATURE CITED

1. Bankaitis, V. A., L. M. Johnson, and S. D. Emr. 1986. Isolation of yeast mutants defective in protein targeting to the vacuole. Proc. Natl. Acad. Sci. USA 83:9075-9079.

2. Banta, L. M., J. S. Robinson, D. J. Klionsky, and S. D. Emr. 1988. Organelle assembly in yeast: Characterization of yeast mutants defective in vacuole biogenesis and protein sorting. J. Cell Biol. 107:1369-1383.

3. Bernstein, M., W. Hoffman, G. Ammerer, and R. Schekman. 1985. Characterization of a gene product (Sec35p) required for protein assembly in the yeast endoplasmic reticulum. J. Cell. Biol. 101:2374-2382.

4. Bernstein, M., F. Kepes, and R. Schekman. 1989. *SEC59* encodes a membrane protein required for core glycosylation in *Saccharomyces cerevisiae*. Mol. Cell. Biol. 9:1191-1199.

5. Boeke, J. D., F. Lacroute, and G. R. Fink. 1987. 5-Fluoroortic acid as a selective agent in yeast molecular genetics. Meth. Enzymol. 154:164-175.

6. Casadaban, M. J., and S. N. Cohen. 1980. Analysis of gene control signals by DNA fusion and cloning in *E. coli*. J. Mol. Biol. 138:179-207.

7. Eakle, K. A., M. Bernstein, and S. D. Emr. 1988. Characterization of a component of the yeast secretion machinery: Identification of the *SEC18* gene product. Mol. Cell. Biol. 8:4098-4109.

8. Farquhar, M. G. 1985. Progress in unraveling pathways of Golgi traffic. Ann. Rev. Cell Biol. 1:447-488.

9. Hardwick, K. G., M. J. Lewis, J. Semenza, N. Dean, and H. R. B. Pelham. 1990. *ERD1*, a yeast gene required for the retention of luminal endoplasmic reticulum proteins, affects glycoprotein processing in the Golgi apparatus. EMBO J. 9:623-630.

10. Hasilik, A., and W. Tanner. 1978. Biosynthesis of the vacuolar yeast glycoprotein carboxypeptidase Y. Conversion of precursor into the enzyme. Eur. J. Biochem. 85:599-608.

11. Hemmings, B. A., G. S. Zubenko, A. Hasilik, and E. W. Jones. 1981. Mutant defective in processing of an enzyme located in the lysosome-like vacuole of *Saccharomyces cerevisiae*. Proc. Natl. Acad. Sci. USA 78:435-439.

12. Ito, H., Y. Fukada, K. Murata, and A. Kimura. 1983. Transformation of intact yeast cells treated with alkali cations. J. Bacteriol. 153:163-168.

13. Johnson, L. M., V. A. Bankaitis, and S. D. Emr. 1987. Distinct sequence determinants direct intracellular sorting and modification of a yeast vacuolar protease. Cell 48:875-885.

14. Kepes, F., and R. Schekman. 1988. The yeast *SEC53* gene encodes phosphomannomutase. J. Biol. Chem. 263:9155-9161.

15. Klionsky, D. J., L. M. Banta, and S. D. Emr. 1988. Intracellular sorting and processing of a yeast vacuolar hydrolase: Proteinase A propeptide contains vacuolar targeting information. Mol. Cell. Biol. 8:2105-2116.

16. Maniatis, T. E., F. Fritsch, and J. Sambrook. 1982. Molecular cloning: A laboratory manual. Cold Spring Harbor Laboratory, Cold Spring Harbor, N.Y.

17. McNeil, J. B. and J. D. Friesen. 1981. Expression of the herpes simplex virus thymidine kinase gene in *Saccharomyces cerevisiae*. Mol. Gen. Genet. 184:386-393.

18. Mechler, B., M. Muller, H. Muller, M. Meusdoerffer, and D. H. Wolf. 1982. *In vivo* biosynthesis of the vacuolar proteinases A and B in the yeast *Saccharomyces cerevisiae*. J. Biol. Chem. 257:11203-11206.

19. Messing, J. 1979. Recombinant DNA technical bulletin. National Institutes of Health Publication No. 79-99. 2:43-48.

20. Miller, J. 1972. Experiments in molecular genetics. Cold Spring Harbor Laboratory, Cold Spring Harbor, N.Y.

21. Orr-Weaver, T. L., J. W. Szostak, and R. J. Rothstein. 1981. Yeast transformation: A model system for the study of recombination. Proc. Natl. Acad. Sci. USA 78:6354-6358.

22. Robinson, J. S., D. J. Klionsky, L. M. Banta, and S. D. Emr. 1988. Protein sorting in *Saccharomyces cerevisiae*: Isolation and mutants defective in the delivery and processing of multiple vacuolar hydrolases. Mol. Cell. Biol. 8:4936-4948.

23. Rose, M. D., P. Novick, J. H. Thomas, D. Botstein, and G. R. Fink. 1987. A *Saccharomyces cerevisiae* genomic plasmid bank based on a centromere-containing shuttle vector. Gene 60:237-243.

24. Rothstein, R. J. 1983. One step gene disruption in yeast. Meth. Enzymol. 101:202-211.

25. Rudolph, H. K., A. Antebi, G. R. Fink, C. M. Buckley, T. E. Dorman, J. LeVitre, L. S. Davidow, J. Mao, and D. T. Moir. 1989. The yeast secretory pathway is perturbed by mutations in *PMR1*, a member of a Ca^{2+}-ATPase family. Cell 58:133-145.

26. Sherman, F., G. R. Fink, and C. W. Lawrence. 1979. Methods in yeast genetics: A laboratory manual. Cold Spring Harbor Laboratory, Cold Spring Harbor, N.Y.

27. Stevens, T., B. Esmon, and R. Schekman. 1982. Early stages in the yeast secretory pathway are required for transport of carboxypeptidase Y to the vacuole. Cell 30:439-448.

28. Valls, L. A., C. P. Hunter, J. H. Rothman, and T. H. Stevens. 1987. Protein sorting in yeast: The localization determinant of yeast vacuolar carboxypeptidase Y resides in the propeptide. Cell 48:887-897.

Table 1. Complementation of the Suc^+ phenotype of *vps28* mutant strains SEY28-2 and SEY28-7 by the complementing plasmid pLB28-1. All strains carried the plasmid pLJL2, which encodes a CPY-Inv fusion protein. Intact cells were assayed for external invertase activity and lysed cells were assayed for total invertase activity. The percentage external invertase activity was calculated for each strain.

Strain	Complementing Plasmid	CPY-Inv Activity Secreted
SEY28-2 (*vps28*)	-	42%
	+	18%
SEY28-7 (*vps28*)	-	33%
	+	11%
SEY6210 (wild-type)	-	9%

Table 2. Secretion of a CPY-Inv hybrid protein by segregants from diploid transformants carrying a *HIS3* disruption of the *VPS28* gene. The segregants in Tetrad I arose from a heterozygous diploid (SEY28-2/6211) transformed with the plasmid pLB28-520; for Tetrads II and III, the diploid was transformed with pLB28-519. The percentage of the CPY-Inv hybrid protein (expressed from the plasmid pCYI-433) secreted was determined as described in the legend to Table 1. The His phenotype of each segregant is indicated.

Tetrad	Segregant	His Phenotype	CPY-Inv Activity Secreted
I	A	-	42%
	B	+	26%
	C	+	29%
	D	-	31%
II	A	-	25%
	B	+	30%
	C	-	24%
	D	+	28%
III	A	-	26%
	B	-	22%
	C	+	26%
	D	+	28%

Figure 1. (A) Restriction map of the entire 11 kb insert in the complementing plasmid pLB28-1. Restriction site abbreviations: B, *Bam*HI; C, *Cla*I; K, *Kpn*I; P, *Pst*I; Pv, *Pvu*II. (B) Complementation analysis of *VPS28* subclones. Restriction fragments were cloned into pPHYC18 (*CEN4 ARS1 URA3*) to generate plasmids pLB28-40, pLB28-45, pLB28-46, and pLB28-47. Plasmid pLB28-104 carried the indicated fragment in the integrating vector pPHYI10. The *Pst*I-*Pvu*II fragment was cloned into pPHYC16 (*CEN4 ARS1 URA3*). Each of the plasmids was transformed into SEY28-2 carrying pLJL2 and transformants were scored by invertase filter assay for secretion of the CPY-Inv hybrid protein. A plus sign indicates complementation (i.e., the transformants were Suc^-); a minus sign means lack of complementation (Suc^+ transformants). A +/- indicates that some yeast transformants were reproducibly Suc^- and others were Suc^+. (C) Constructions used in the disruption of *VPS28*. The *Cla*I-*Pvu*II insert in the nonreplicating plasmid pLB28-418 is shown. Plasmids pLB28-519 and pLB28-520, in which the *HIS3* gene replaced the indicated portions of the *VPS28* gene, were used to generate *vps28* null mutants as described in the text. Additional restriction site abbreviations: H, *Hind*III; R, *Eco*RI.

A:

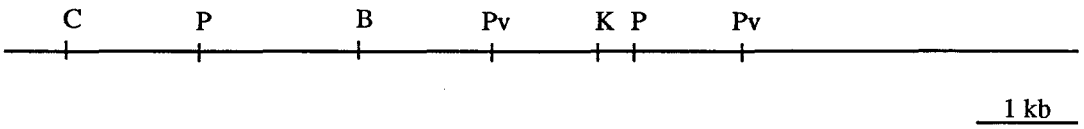

B:

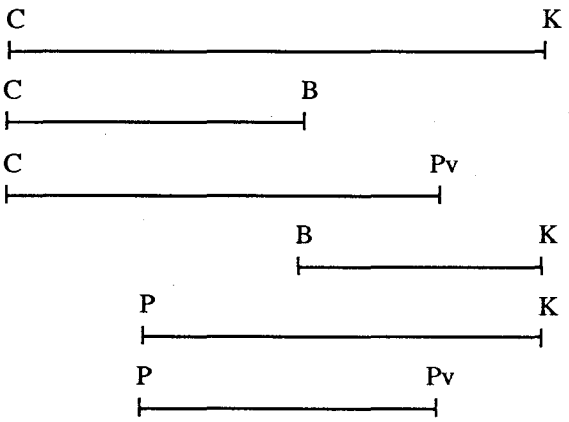

pLB28-40	+
pLB28-45	+/-
pLB28-46	+/-
pLB28-47	-
pLB28-104	+
	+

C:

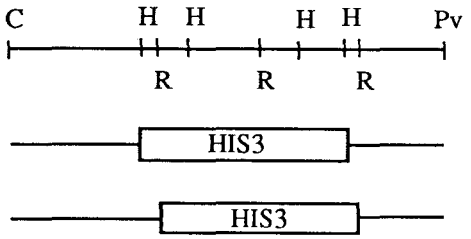

pLB28-418

pLB28-519 (Δ28)

pLB28-520 (Δ28)

Figure 2. Processing of CPY in segregants from a heterozygous diploid (SEY28-2/6211) in which the plasmid pLB28-520 was stably integrated. Whole cells were labeled with Tran^{35}S-label for 20 min at 30°C, chased for 30 min by the addition of 4 mM methionine, and subjected to immunoprecipitation with CPY-specific antisera. The His phenotype of each segregant and migration positions of the mature (m) and Golgi-modified precursor (pro) forms of CPY are shown.

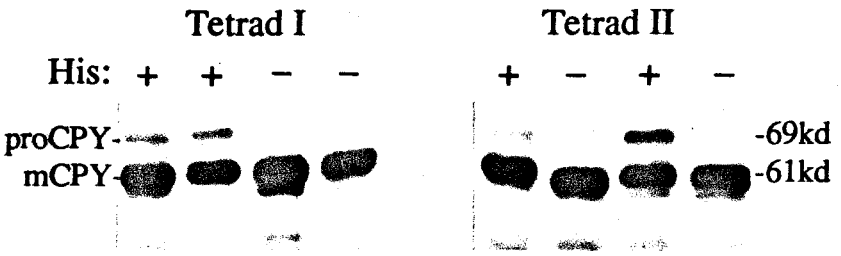
Tetrad I
Tetrad II
His: + + − − + − + −
proCPY-
mCPY-
-69kd
-61kd

Figure 3. Migration of precursor and mature forms of CPY in wild-type and *vps*28 mutant strains. Spheroplasts were labeled for 5 min at 30°C with Tran^{35}S-label and chased for 30 sec by the addition of 5 mM methionine and 5 mM cysteine. The labeled spheroplasts were placed on ice, washed three times in buffer containing 1 M sorbitol/150 mM potassium acetate/5 mM magnesium acetate/20 mM HEPES-KOH pH 6.8, and chased for 0 or 60 min, as indicated, at 25°C in the same buffer containing 5% glucose. The samples were then subjected to immunoprecipitation with CPY-specific antisera. The isogenic strains used were: wild-type (wt), SEY6210, and *vps*28, SEY28-2. The migration positions of the ER-modified (p1), Golgi-modified (p2), and mature (m) forms of CPY in wild-type cells are indicated.

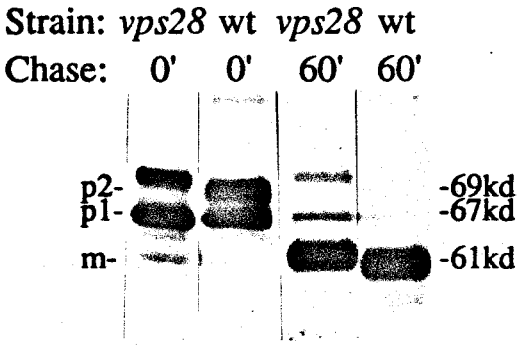
Strain: vps28 wt vps28 wt
Chase: 0' 0' 60' 60'
p2-
p1-
m-
-69kd
-67kd
-61kd

Appendix A

Intracellular Sorting and Processing of a Yeast Vacuolar Hydrolase: Proteinase A Propeptide Contains Vacuolar Targeting Information

Daniel J. Klionsky, Lois M. Banta, and Scott D. Emr

Molecular and Cellular Biology **8**:2105-2116 (1988)

MOLECULAR AND CELLULAR BIOLOGY, May 1988, p. 2105–2116 Vol. 8, No. 5
0270-7306/88/052105-12$02.00/0

Intracellular Sorting and Processing of a Yeast Vacuolar Hydrolase: Proteinase A Propeptide Contains Vacuolar Targeting Information

DANIEL J. KLIONSKY, LOIS M. BANTA, AND SCOTT D. EMR*

Division of Biology, 147-75, California Institute of Technology, Pasadena, California 91125

Received 26 October 1987/Accepted 11 February 1988

An inactive precursor form of proteinase A (PrA) transits through the early secretory pathway before final vacuolar delivery. We used gene fusions between the gene coding for PrA (*PEP4*) and the gene coding for the secretory enzyme invertase (*SUC2*) to identify vacuolar protein-sorting information in the PrA precursor. We found that the 76-amino-acid preprosegment of PrA contains at least two sorting signals: an amino-terminal signal peptide that is cleaved from the protein at the level of the endoplasmic reticulum followed by the prosegment which functions as a vacuolar protein-sorting signal. PrA-invertase hybrid proteins that carried this sequence information were accurately sorted to the yeast vacuole as determined by cell fractionation and immunolocalization studies. Hybrid proteins lacking all or a portion of the PrA prosegment were secreted from the cell. Our gene fusion data together with an analysis of the wild-type PrA protein indicated that N-linked carbohydrate modifications are not required for vacuolar sorting of this protein. Furthermore, results obtained with a set of deletion mutations constructed in the PrA prosegment indicated that this sequence also contributes to proper folding of this polypeptide into a stable transit-competent molecule.

The secretory pathway in eucaryotic cells mediates the sorting and modification of an array of intracellular and extracellular proteins. Proteins which are synthesized at the level of the endoplasmic reticulum (ER) are either secreted from the cell or specifically retained in distinct subcellular locations such as the ER, Golgi complex, lysosome, or plasma membrane. In the yeast *Saccharomyces cerevisiae*, proteins destined for delivery to the lysosomelike vacuole also traverse a portion of the secretory pathway. Delivery of enzymes to the vacuole provides a useful system to study protein targeting; vacuolar proteins must be sorted from other secretory proteins during transit through the ER and Golgi complex. Proteins or peptides that lack any apparent delivery signals other than an amino-terminal signal peptide can be secreted from yeast and mammalian cells (21, 24, 55, 59). This suggests that secretion occurs by a default mechanism. Proteins which are diverted from the secretory pathway to other cellular destinations therefore must contain active sorting information in their amino acid sequence or in their structure that is recognized during transit through the cell. We are interested in identifying the sorting information that is present in vacuolar proteins.

The vacuole of *S. cerevisiae* is a lysosomelike organelle in that it contains a number of soluble hydrolytic glycoprotein enzymes (27, 60). These include proteinase A (PrA), proteinase B (PrB), carboxypeptidase Y (CPY), repressible alkaline phosphatase, and RNase. PrA, PrB, and CPY have been shown to be synthesized as inactive proenzyme precursors (17, 29). These hydrolases are mannoproteins and initially undergo dolichol-mediated core glycosylation in the ER (18, 62). Subsequently, additional carbohydrate modifications take place in the Golgi complex. Sorting of vacuolar proteins is thought to take place on the *trans* side of the Golgi complex (12, 21, 51). The presence of a receptor carrier has not been directly demonstrated for any of the vacuolar proteins, although some evidence suggests that a receptor-mediated pathway exists (44, 52). Just before or upon arrival in the vacuole, the CPY, PrA, and PrB proenzymes are processed to their mature forms. Maturation is dependent on a functional *PEP4* gene product (PrA) (19, 31). The activation of both proPrA and proCPY requires the removal of an amino-terminal propeptide segment (1, 19). The regulation of the maturation process is not fully understood, but it may involve a mechanism which is initiated by autocatalysis of proPrA (31, 61). The *PEP4* gene of yeasts was cloned by complementation in *pep4* mutant yeasts (1, 61). Sequence analysis indicates that PrA has extensive homology to aspartyl proteases (61). Initial studies of PrA showed that it contains two N-linked glycosidic side chains (29) and is synthesized as an inactive precursor of 405 amino acids. The signal peptide and propeptide regions make up the N-terminal 76 amino acids of preproPrA. The protein (p1 form) undergoes further carbohydrate modification in the Golgi complex to produce a higher-molecular-weight form (p2) with an apparent size of 48,000 to 52,000 daltons (1, 29, 61, 62). Upon delivery to the vacuole, an N-terminal propeptide is cleaved to generate the mature 329-amino-acid enzyme, which together with its two N-linked oligosaccharide side chains has an apparent molecular weight of 42,000.

At present little is known about the factors required for delivery of proteins to the vacuole. Unlike the targeting of many mammalian lysosomal enzymes (50), delivery to the vacuole has not been shown to be dependent on a specific glycosyl modification of the protein. In the presence of tunicamycin, a drug that blocks the synthesis of high-mannose core oligosaccharides (26), proCPY and alkaline phosphatase are delivered to the vacuole and matured (7, 38, 48, 51). This indicates that sorting of proenzymes to the vacuole may occur via direct recognition of an amino acid sequence or conformational feature of the polypeptide. For CPY, it has been shown that a determinant which allows targeting of proCPY to the vacuole resides within the N-terminal propeptide (21, 55). Since many of the vacuolar proteases are synthesized as inactive precursors, the propeptide on other vacuolar enzymes also may contain vacuolar sorting information which allows for efficient vacuolar delivery in addition to maintaining the hydrolases in an inactive state before their arrival in the vacuole. The vacuo-

* Corresponding author.

lar proteins for which sequence information is available do not show any obvious sequence homology. As a result, it has not been feasible to identify vacuolar targeting signals by directly mutating suspected sequences.

As an alternative approach to identifying the vacuolar sorting information in the *PEP4* gene product, we constructed fusions of the *PEP4* gene to the *SUC2* gene (which codes for secreted invertase) of yeasts. We found that the propeptide region of PrA contains information which is sufficient to divert delivery of the normally secreted enzyme invertase to the vacuole. This indicates that vacuolar targeting information resides within the propeptide of the precursor protein. We also examined proteolytic and glycosyl processing of the wild-type PrA protein. We found that maturation of preproPrA involves the removal of an N-terminal signal peptide at the level of the ER. The two N-linked core oligosaccharides that are added in the ER are processed and extended with α-1→3-mannose linkages in the Golgi complex. After delivery to the vacuole, the propeptide segment is cleaved to yield the mature, enzymatically active PrA. The half-time for this maturation process is approximately 6 min. In addition, we showed that delivery of PrA to the vacuole is not dependent on glycosyl modification of the protein. Finally, oligonucleotide-directed mutagenesis of the PrA propeptide revealed that an intact propeptide is critical for maintaining stability of the protein and efficient transit through the secretory pathway.

MATERIALS AND METHODS

Strains and media. *Escherichia coli* strains used in this study were MC1061 F⁻ *hsdR hsdM*⁺ *araD139* (*araABOIC-leu*)*7679* (*lac*)*X74 galU galK rpsL* (6) and JM101 F′ *traD36 lacI*ᵠ*ZΔM15 proAB Δ*(*lac-pro*) *supE thi* (33). Yeast strains used were SEY2101 *MAT***a** *ura3-52 leu2-3,112 suc2-Δ9 ade2-1* (10), SEY2101-Δ*pep4* (SEY2101.1 in reference 3) *MAT***a** *ura3-52 leu2-3,112 suc2-Δ9 ade2-1 Δpep4::LEU2*, and SEY2108 *MAT***a** *ura3-52 leu2-3,112 suc2-Δ9 Δprc1::LEU2* (3). Standard methods (46, 49) were used to construct yeast strains SEY5187 *MAT***a** *sec18-1 suc2-Δ9 leu2-3,112 ura3-52*, DKY6182 *MAT***a** *sec18-1 ura3-52 ade2-1 Δpep4::LEU2*, and DKY6224 *MAT***a** *ura3-52 trp1-Δ901 his3-Δ200 leu2-3,112 ade2-101 SUC2-Δ9 Δpep4::LEU2*. Strain RDM50-94C *MAT***a** *sec62-1 leu2-3,112 his4 ura3-52* was supplied by Raymond Deshaies and Randy Schekman.

Standard yeast (49) and *E. coli* (33) media were used and supplemented as needed. The minimal medium of Wickerham (58) was modified as described previously (21). Bromocresol purple indicator plates were used as described previously (3, 49).

Reagents. Zymolyase-100T (Kirin Brewery Co.) was obtained from Seikagako Kogyo Co. (Tokyo, Japan), lyticase was from Enzogenetics, endoglycosidase H was from New England Nuclear Corp. (Boston, Mass.), papain was from Worthington Diagnostics (Freehold, N.J.), invertase and CPY were from Boehringer Mannheim Biochemicals (Indianapolis, Ind.), and proteinase A and β-glucuronidase were from Sigma Chemical Co. (St. Louis, Mo.). DNA restriction and modifying enzymes were from New England BioLabs, Inc. (Beverly, Mass.). $Na_2{}^{35}SO_4$ was from ICN Pharmaceuticals Inc. (Irvine, Calif.), and Autofluor was from National Diagnostics. All other chemicals were purchased from Sigma. PrB antiserum was a gift from Charles Moehle and Elizabeth Jones, and antiserum to α-1→3-mannose linkages was a gift from Randy Schekman. Fluorescein isothiocyanate-conjugated affinity-purified Fab fragments of antisera directed against rabbit Fab fragments were from Jackson Immunoresearch Laboratories.

Antisera to PrA, CPY, and invertase. To produce antisera to PrA, CPY, and invertase, commercially purified proteins were deglycosylated with endoglycosidase H and purified by sodium dodecyl sulfate (SDS)-polyacrylamide gel electrophoresis. Proteins were visualized by Coomassie blue staining, and deglycosylated protein bands were excised from the gel. Homogenized gel slices were mixed with Freund adjuvant and injected (150 μg of protein) into New Zealand White rabbits. Antisera were collected after multiple secondary injections (75 μg).

Plasmid constructions. The *SUC2* fusion vector pSEYC306 was constructed as described previously (21). The vector pSEYC306 was restricted with the enzymes *Nru*I and *Pvu*II and then ligated to construct the fusion vector pSEYC308. This deletion removed an approximately 0.6-kilobase fragment of DNA which includes a *Sal*I site and maps distal to the *SUC2* gene. The pSEYC308 vector then contained a unique *Sal*I site in the polylinker region 5′ of the *SUC2* sequence. Both of these vectors contained sequences that allow for stable maintenance in both *E. coli* (Amp′, ColE1 *ori*) and yeasts (*URA3 CEN4 ARS1*).

A 4.5-kilobase *Bam*HI fragment containing the entire *PEP4* gene cloned into the plasmid YEp13 (M80-*PEP4*) was supplied by Gustav Ammerer. The *PEP4-SUC2* gene fusions were constructed as follows. Oligonucleotide-directed mutagenesis was used to insert *Hin*dIII restriction sites immediately after the coding sequence for preproPrA amino acids 23, 39, 61, 76, and 90. *Bam*HI-*Hin*dIII fragments derived from the mutated *PEP4* genes were then cloned into the *Bam*HI-*Hin*dIII sites of pSEYC306 to generate the plasmids pP4I-23, pP4I-39, pP4I-61, pP4I-76, and pP4I-90. The insertion of *Hin*dIII sites did not result in any alterations of the PrA protein sequence of the final fusion constructs. The naturally occurring *Hin*dIII site at amino acid 137 was used to construct the plasmid pP4I-137. Oligonucleotide-directed mutagenesis was used to insert a *Sal*I site after amino acid 404 of PrA, and the resulting *Bam*HI-*Sal*I fragment was cloned into the *Bam*HI-*Sal*I sites of pSEYC308 to construct the plasmid pP4I-404. In this construct, the terminal amino acid of PrA, residue 405, was changed from Ile to Met. For all fusion constructs, the designated name indicates the number of wild-type amino acids from PrA which precede the fusion joint. A single-copy wild-type *PEP4* plasmid was constructed by moving a 4.5-kilobase *Bam*HI-*Sal*I fragment from the plasmid M80-*PEP4* into pSEYC306. This plasmid was designated pSEYC306-*PEP4*. A *PEP4* deletion of the coding sequence for amino acid residues 24 to 76 (Δ24-76) was constructed in two steps. The *Hin*dIII-*Ava*I fragment from pSEYC306-*PEP4* was ligated into the *Hin*dIII-*Sal*I sites of pP4I-23. The resulting construct, Δ24-137, was digested with *Hin*dIII and treated with bacterial alkaline phosphatase. The *Hin*dIII fragment from the *PEP4* gene which had been mutagenized to insert a *Hin*dIII site after amino acid 76 was ligated into the Δ24-137 construct and screened for the correct orientation. This construct, PrAΔpro, is deleted for amino acids 24 to 76 of preproPrA and contains two amino acid substitutions at positions 77 (Gly to Ala) and 78 (Gly to Cys). The deletion Δ61-76 was constructed in an analogous manner starting with the plasmid pP4I-61.

Site-specific mutagenesis. Oligonucleotide-directed mutagenesis was performed as described previously (21, 35). All mutagenesis was performed on subclones of the appropriate plasmids in M13mp8. Restriction enzyme digestion or DNA

sequencing or both were used to confirm the presence of mutations in positive plaques (47).

Assays. Invertase assays were done as described previously (11). For filter invertase assays, strains were grown on minimal fructose plates with the appropriate supplements. To test for secreted invertase activity, we replica plated intact colonies onto Whatman no. 1 filter paper which had been presaturated with sucrose and reagents which permit the detection of glucose (0.1 M sodium acetate [pH 5.1], 0.12 M sucrose, 0.4 mM *N*-ethylmaleimide, 0.01 mg of horseradish peroxidase per ml, 8 U of glucose oxidase per ml, 0.6 mg of *O*-dianisidine per ml). To score total invertase activity, we permeabilized cells by exposure to chloroform vapor for 5 min before replica plating.

The isolation of purified vacuoles and assays for the marker enzymes α-mannosidase, α-glucosidase, and NAD PH cytochrome *c* reductase were performed as described previously (3, 14, 25, 39).

Immunofluorescence microscopy. Fab fragments were prepared from an immunoglobulin G fraction of PrA antiserum as described previously (28). Cells (15 ml) were prepared and stained as described before (8), using a 1:30 dilution of anti-PrA Fab fragments and a 1:50 dilution of fluorescein isothiocyanate-conjugated Fab fragments (goat) directed against Fab fragments of rabbit immunoglobulin G. Cells were viewed with a Zeiss microscope with epifluorescence and Nomarski optics.

Immunoprecipitation. Cells were grown to the mid-logarithmic phase in Wickerham minimal proline medium plus 0.1 mM $MgSO_4$. Two units of cells at an optical density at 600 nm of 1.0 were centrifuged, washed twice with water, and suspended in 0.25 ml of the above medium lacking $MgSO_4$. After incubation for 30 to 60 min at the appropriate temperature, bovine serum albumin (final concentration 2 mg/ml) and 250 μCi of carrier-free $Na_2{}^{35}SO_4$ were added. Cells were incubated for 5 to 10 min, and the chase was initiated by the addition of $MgSO_4$ to 50 mM final concentration. The chase was terminated by the addition of trichloroacetic acid (TCA) to 5% final concentration. Precipitates were collected by centrifugation in a microcentrifuge and washed twice with acetone. Dried pellets were suspended in 50 μl of resuspension buffer (50 mM Tris hydrochloride [pH 7.5], 1 mM EDTA, 1% SDS). Cells were lysed in the presence of glass beads (0.5 mm) with a Scientific Products vortex mixer (1 min) followed by boiling for 4 min. The lysate was diluted by the addition of 1 ml of IP buffer (0.5% Tween 20, 50 mM Tris hydrochloride (pH 7.5), 150 mM NaCl, 0.1 mM EDTA), centrifuged, and transferred to a new tube. Antisera (1 to 10 μl) and bovine serum albumin (2 mg/ml, final concentration) were added, and the samples were gently agitated at 4°C for 2 h. Immunoprecipitates were collected by the addition of 50 to 75 μl of a 3.6% (wt/vol) suspension of protein A-Sepharose CL-4B beads followed by gentle agitation at 4°C (1 h). The beads were collected by centrifugation in a microcentrifuge for 1 min. The beads then were washed twice with IP buffer and once with 1% β-mercaptoethanol. Resuspension buffer was added (50 μl), followed by boiling for 4 min. The released antigen was diluted with 1 ml of IP buffer, and a second immunoprecipitation was performed. The final pellet was suspended in 30 μl of 2× SDS sample buffer and boiled 4 min. Samples (20 μl) were loaded onto a 9% polyacrylamide-SDS gel. After electrophoresis, gels were fixed and treated with Autofluor.

RESULTS

***PEP4-SUC2* gene fusions.** The *SUC2* gene product, invertase, is an easily assayable glycoprotein enzyme which is competent for delivery through the secretory pathway (5, 12). Invertase normally resides in the yeast periplasm where it catalyzes the hydrolysis of extracellular sucrose, the first step in sucrose metabolism. Together, these properties make invertase a useful biochemical marker enzyme in gene fusion studies when analyzing protein sorting through the yeast secretory pathway. Plasmid vectors that permit the construction of gene fusions to *SUC2* have been described (10, 21; Materials and Methods). We used these vectors to construct seven *PEP4-SUC2* gene fusions containing different-sized amino-terminal coding segments from the *PEP4* gene fused to a constant fragment of the *SUC2* gene (Fig. 1). Each of these gene fusions directed the synthesis of PrA-invertase hybrid proteins that exhibited invertase activity in yeasts (Fig. 2 and 3). The apparent molecular weight of each of the hybrid proteins synthesized in the presence of tunicamycin was consistent with that expected from the deduced amino acid sequence of each of the *PEP4-SUC2* hybrid gene constructs (Fig. 2). The unglycosylated hybrid proteins ranged in size from approximately 60,000 to 100,000 daltons. This analysis of the hybrid proteins as well as quantitative invertase assays indicated that each of the gene fusions directed the synthesis of similar levels of hybrid protein (Fig. 3).

Localization of hybrid proteins. The invertase activity associated with each of the hybrid proteins served as a convenient marker to detect the cellular location of these hybrid proteins. Since sucrose is unable to cross the plasma membrane, the growth phenotype of a strain utilizing sucrose as its sole fermentable carbon source provides an indication as to the cellular distribution of the invertase activity of that strain. The parental strain SEY2108 is deleted for the chromosomal *SUC* loci and therefore is unable to utilize sucrose as a carbon source. Because this strain lacks endogenous invertase, any invertase activity detected in the strain when it is harboring the different *PEP4-SUC2* gene fusions must be due to expression from the gene fusions. Strains expressing fusion proteins with 23, 39, or 61 amino acids of preproPrA fused to a functional invertase protein had Suc^+ phenotypes, indicating that a significant amount of the hybrid protein was secreted from these cells. In contrast, when *PEP4-SUC2* fusions containing the coding information for 90, 137, or 404 amino acids of preproPrA were analyzed in this way, the cells showed a Suc^- phenotype, indicating that these hybrid proteins were being retained within the cell. The PrA-Inv76 fusion (N-terminal 76 amino acids of preproPrA fused to invertase) had an intermediate growth phenotype on sucrose. Cells with this fusion grew on sucrose but did so much more slowly than those harboring shorter *PEP4-SUC2* gene fusions. Growth on sucrose was very sensitive to even small amounts of invertase enzyme activity at the cell surface, but this assay was limited to assessing only the steady-state level of secreted hybrid protein. The poor growth of cells with the PrA-Inv76 fusion on sucrose plates indicated a low level of secretion of this hybrid protein.

A steady-state analysis of hybrid protein secretion was also done with filter invertase assays of intact and chloroform-permeabilized cells (Fig. 3). Strain SEY2108 harboring each of the different *PEP4-SUC2* gene fusions was patched onto a minimal fructose master plate. After incubation at 30°C, filter invertase assays were performed as described in

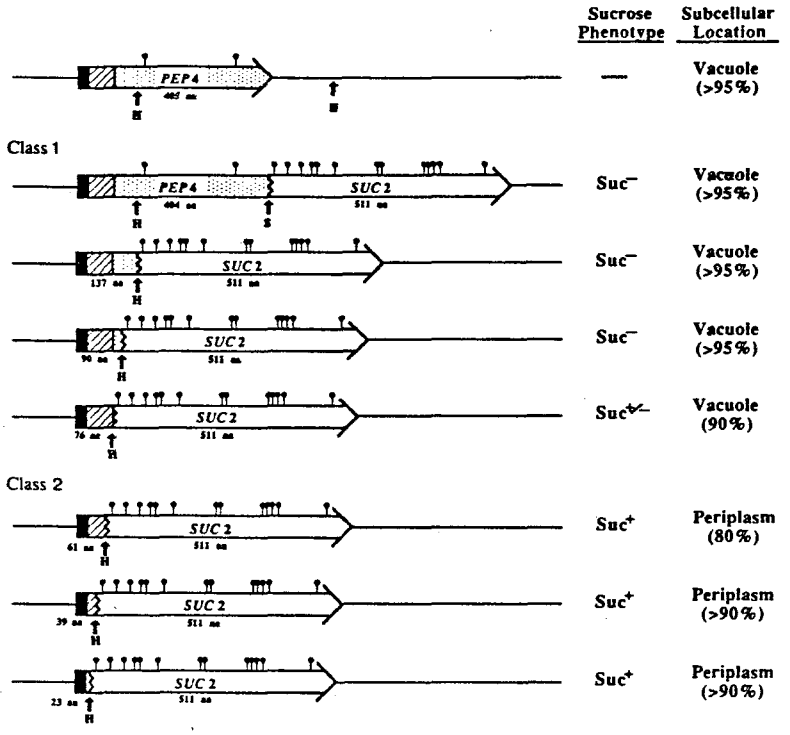

FIG. 1. *PEP4-SUC2* gene fusions. Two classes of *PEP4-SUC2* gene fusions are shown. The *PEP4* gene is divided into the coding regions for the presumed signal peptide (solid box), the propeptide (hatched box), and the mature PrA enzyme (stippled box). The *SUC2* gene is indicated by the open box. The approximate positions of the two asparagine-linked core oligosaccharides as determined from the amino acid sequence of the PrA protein (1, 61) and the 13 potential sites for core oligosaccharide addition on invertase are indicated above the *PEP4* and *SUC2* genes, respectively. The growth phenotype on sucrose of a yeast strain deleted for its normal *SUC* loci and harboring each of the indicated gene constructs on a low-copy (*CEN4-ARS1*) yeast plasmid vector is shown. Cofractionation of the *PEP4* gene product and the hybrid protein products of each of the *PEP4-SUC2* gene fusions with isolated vacuoles is as indicated. aa, Amino acids; H, *Hin*dIII; S, *Sal*I.

Materials and Methods. Assays with intact cells detected only the invertase activity that was associated with hybrid proteins which were secreted from the cell. Permeabilization of the cells by exposure to chloroform vapor enables the detection of internal invertase activity in addition to any which has been secreted. The parental strain SEY2108 (P) is deleted for its chromosomal *SUC* loci and served as a negative control (Fig. 3). Strains expressing the PrA-Inv23, -39, or -61 hybrid proteins tested strongly positive for invertase activity when intact cells were assayed, indicating secretion of substantial amounts of the hybrid proteins (Fig. 3). In contrast, the PrA-Inv76 fusion only gave a very weak signal when intact cells were examined. This is similar to the result seen with growth phenotypes on sucrose indicator plates and suggests that this hybrid protein is mostly retained within the cell. The PrA-Inv fusions with 90, 137, or 404 amino acids of preproPrA were negative for secreted invertase activity as determined by the filter assay. All the fusions expressed levels of total invertase activity similar to those seen with the chloroform-permeabilized cells. Differences in secretion of the hybrid proteins, then, are not the result of differences in their level of expression.

Invertase enzyme assays were performed on intact as well as detergent-permeabilized yeast cells to quantitate more carefully the amount of the hybrid proteins that is secreted. Invertase assays with detergent-lysed cells permit a measure

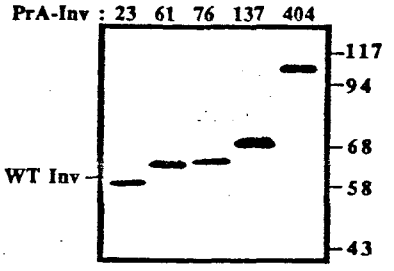

FIG. 2. Immunoprecipitation of unglycosylated PrA-Inv hybrid proteins. Immunoprecipitations of strain SEY2101-Δ*pep4* expressing the indicated hybrid proteins were done as described in Materials and Methods with the following modifications. Tunicamycin (final concentration of 20 μg/ml) was added to inhibit glycosylation 15 min before the addition of $Na_2{}^{35}SO_4$. Labeling was allowed to continue for 5 min followed by a 15-min chase. Invertase antiserum was used to precipitate the hybrid proteins. Radiolabeled proteins were analyzed by SDS-polyacrylamide gel electrophoresis and autoradiography. The number of amino acids of preproPrA fused to invertase is indicated above each lane. The position of protein standards (molecular weight × 10^3) and the migration position of unglycosylated wild-type invertase (WT Inv) are indicated.

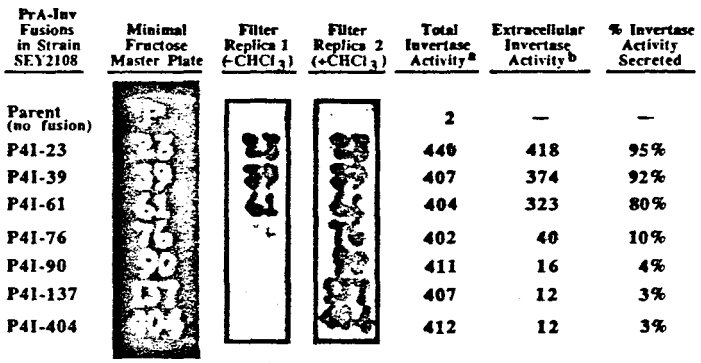

PrA-Inv Fusions in Strain SEY2108	Minimal Fructose Master Plate	Filter Replica 1 (−$CHCl_3$)	Filter Replica 2 (+$CHCl_3$)	Total Invertase Activity[a]	Extracellular Invertase Activity[b]	% Invertase Activity Secreted
Parent (no fusion)				2	—	—
P4I-23				440	418	95%
P4I-39				407	374	92%
P4I-61				404	323	80%
P4I-76				402	40	10%
P4I-90				411	16	4%
P4I-137				407	12	3%
P4I-404				412	12	3%

FIG. 3. Cellular distribution of preproPrA-Inv hybrid proteins. Strain SEY2108 harboring the indicated *PEP4-SUC2* fusion plasmids was inoculated onto a minimal fructose master plate in patterns denoting the number of amino acids of preproPrA that was fused to invertase in each case. Invertase filter assays were performed as described in Materials and Methods, using filter replicas of the master plate before (filter 1) and after (filter 2) chloroform vapor permeabilization of the yeast cells. Quantitative liquid invertase assays were done on the same strains grown in yeast nitrogen base minimal medium (Difco Laboratories) supplemented with 2% glucose. Invertase activity is expressed as nanomoles of glucose released per minute per unit of cells at an optical density of 600 nm. The percent secreted invertase activity was calculated by subtracting the background (SEY2108, no fusion plasmid) and then calculating (extracellular activity/total activity) × 100.

of the total cellular enzyme activity. Since yeast cells do not transport the invertase substrate, sucrose, across the plasma membrane, enzyme assays with whole yeast cells (as in the filter assay) detect only the invertase activity that has been secreted from the cell (37). The *PEP4-SUC2* fusions could be grouped into two classes based on the location of the invertase activity associated with the hybrid proteins. The class 1 fusions (containing 76 or more amino acids of preproPrA) represented those for which the majority of the invertase activity (>90%) remained within the cell (Fig. 1 and 3). It should be noted that the PrA-Inv76 fusion contains the entire PrA signal sequence and propeptide region but none of the mature polypeptide. In contrast, *PEP4-SUC2* gene fusions expressing hybrid proteins that contained 23, 39, or 61 amino acids of preproPrA (class 2) secreted 65 to 95% of the hybrid proteins from the cell as determined by the invertase assays. This activity was primarily localized to the periplasm.

To determine more accurately the location of the invertase activity, we fractionated cells containing the various hybrid proteins on discontinuous Ficoll step-density gradients (3). The isolated fractions were assayed along with the crude cell extract for the following enzyme activities: α-mannosidase (vacuole membrane marker), invertase (hybrid protein), NADPH cytochrome *c* reductase (ER membrane marker), and α-glucosidase (cytoplasmic marker). The percent recovery of each of these enzyme activities in the vacuole-enriched fraction is indicated in Fig. 4. Based on both protein and marker enzyme recoveries, this fractionation procedure gives an approximately 50-fold purification of vacuolar enzymes (22). In all cases, 30 to 40% of the α-mannosidase activity was recovered in the vacuole-enriched fraction compared with 4 to 6% of the NADPH cytochrome *c* reductase and 1 to 2% of the α-glucosidase. The invertase activity derived from the PrA-Inv23 and PrA-Inv39 fusions did not cofractionate with the α-mannosidase activity. This was expected since these proteins were secreted from the cell (Fig. 3). Fusions of 90, 137, or 404 amino acids showed nearly quantitative cofractionation of the invertase and α-mannosidase activities, indicating that these hybrid proteins are efficiently targeted to the vacuole. The PrA-Inv61 and PrA-Inv76 hybrid proteins resulted in approximately 10 and 65%, respectively, of the invertase activity being targeted to the vacuole. When vacuoles were isolated after a 1-h chase in the presence of cycloheximide (100 μg/ml, final concentration), the PrA-Inv61 and PrA-Inv76 hybrid proteins showed approximately 20 and 90%, respectively, of the invertase activity (after correcting for recoveries) in the vacuole (data not shown). While there was an increase in the level of the PrA-Inv61 hybrid protein in the

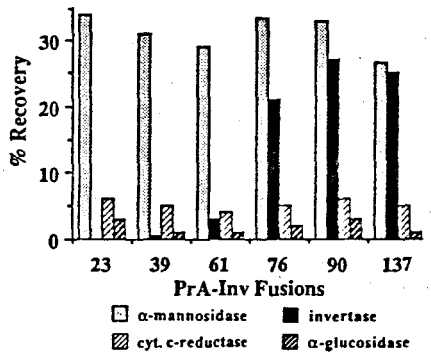

FIG. 4. Vacuole fractionation data for PrA-Inv hybrid proteins. Yeast strain SEY2108 harboring the indicated PrA-Inv fusion vectors was subjected to enzymatic digestion of the cell wall followed by mild lysis in the presence of DEAE-dextran. The resulting crude extract was fractionated on a discontinuous Ficoll step gradient. The crude extract and the gradient fraction enriched for intact vacuoles were assayed to determine the percent recovery of α-mannosidase (vacuole membrane), invertase (PrA-invertase), α-glucosidase (cytoplasm), and NADPH cytochrome *c* reductase (ER). The percent recovery for each of these enzymes was determined by dividing the total enzyme activity recovered in the vacuole-enriched fraction by the total activity loaded on the gradient. The invertase activity associated with the PrA-Inv76 hybrid protein showed approximately 65% cofractionation with α-mannosidase activity as presented in the figure. This hybrid protein showed approximately 90% cofractionation when cycloheximide (100 μg/ml, final concentration) was added 1 h before harvesting the cells (see text). Results for PrA-Inv404 are not shown but were essentially the same as those shown for PrA-Inv137.

vacuole under these conditions, the majority of this protein was still secreted from the cell. In contrast, the percentage of the PrA-Inv76 hybrid protein in the vacuole after the chase was essentially the same as that of the larger hybrid proteins. The PrA-Inv76 hybrid protein apparently is delivered to the vacuole at a slightly slower rate. These results indicate that the N-terminal 76 amino acids of preproPrA contain sufficient information to direct invertase to the yeast vacuole.

We also analyzed the subcellular localization of the hybrid proteins by immunofluorescent staining. Strain DKY6224 (*Δpep4*) containing no plasmid or containing the PrA-Inv404 fusion plasmid was converted to spheroplasts and fixed with formaldehyde (8). The hybrid proteins were then detected with Fab fragments of PrA-specific antiserum (28). Cells expressing the PrA-Inv404 hybrid protein exhibited fluorescence in the region corresponding to the vacuole, as determined by Nomarski optics (Fig. 5). Although not all the cells showed the same intensity of fluorescent staining, in every case the fluorescence was associated with the vacuole. This confirms the results obtained with the fractionation data, which indicated that the PrA-Inv404 hybrid protein is localized to the vacuole.

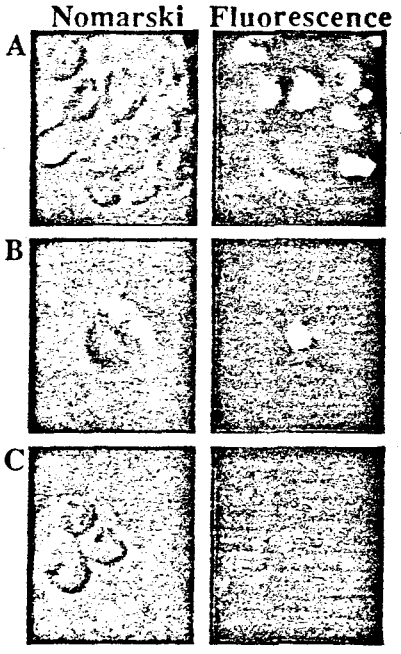

FIG. 5. Immunofluorescence detection of hybrid proteins. Strain DKY6224 without a plasmid or with the PrA-Inv404 fusion plasmid was subjected to limited enzymatic digestion of the cell wall and fixed in formaldehyde. Cells were stained with Fab fragments from PrA-specific antiserum and fluorescein isothiocyanate-conjugated second antibody as described in Materials and Methods. Cells were examined by Nomarski optics and fluorescence microscopy as indicated. The vacuoles correspond to the indentations within the cells when viewed by Nomarski optics. The identification of the vacuole was confirmed by immunofluorescence detection of wild-type CPY by using Fab fragments from CPY-specific antisera and by staining nonfixed cells with lucifer yellow, fluorescein isothiocyanate, and quinacrine (41, 43, 57; data not shown). (A and B) Strain DKY6224 (*Δpep4*) expressing the PrA-Inv404 hybrid protein. (C) Strain DKY6224 (*Δpep4*) without a plasmid. Magnification, ×300.

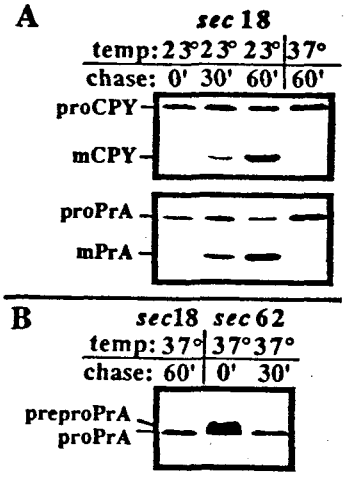

FIG. 6. Processing of wild-type PrA in *sec* mutant yeasts. Temperature-sensitive *sec18* (SEY5187) (A) or *sec18* and *sec62* (RDM50-94C) mutant strains (B) were grown to the mid-log phase at 23°C. Tunicamycin was added (final concentration, 20 μg/ml), and the cultures were shifted to 37°C for 20 min as indicated. Both strains were labeled for 10 min, and the chase was then initiated by the addition of 50 mM $MgSO_4$. The chase was stopped at the indicated times by the addition of TCA. Double immunoprecipitations were done with CPY and PrA antisera as described in Materials and Methods. The predicted locations for unglycosylated precursor and mature CPY and PrA proteins are indicated.

Processing of PrA. Our gene fusion results indicated that the 76-amino-acid prepropeptide sequence of PrA contains at least two protein-sorting signals: a signal which allows translocation across the ER membrane and a signal that directs subsequent sorting to the vacuole. The efficient secretion of the PrA-Inv23 hybrid protein indicated that the N-terminal 23 amino acids of preproPrA are able to functionally replace the normal 19-amino-acid signal peptide of invertase which is deleted from all the gene fusion constructs and is essential for ER targeting and translocation of wild-type invertase (22, 40). This hybrid protein, however, lacked sufficient information for vacuolar sorting. Therefore, additional sequences distal to the signal sequence must be required to direct efficient delivery to the vacuole. It is possible that the N-terminal signal peptide not only directs ER targeting but also directly contributes to the final targeting of PrA to the vacuole. Sequences which are involved in vacuolar targeting would presumably have to remain associated with the protein until sorting takes place, and data suggest that sorting of vacuolar proteins occurs in the Golgi complex (21, 51). To analyze the compartmental organization of PrA maturation, we used the yeast *sec* mutants. A signal sequence cleavage site is predicted to be present between amino acids 22 and 23 of preproPrA based on the rules of von Heijne (56). To determine whether the prepro-PrA signal peptide is cleaved, we analyzed PrA processing in the temperature-sensitive yeast secretory mutants with mutations in *SEC62* and *SEC18*. *sec62* cells are defective in protein translocation across the ER membrane (9), and *sec18* cells are blocked in protein transit out of the ER at the nonpermissive temperature (36). Both strains were labeled in the presence of tunicamycin to block Asn-linked carbohydrate addition. This permits direct comparison between the

unglycosylated ER-translocated (*sec18*) and nontranslocated (*sec62*) PrA proteins. The *sec62* mutation does not cause a complete block in ER translocation (9), and both preproPrA and proPrA could be seen after pulse-labeling for 10 min (Fig. 6). Comparison of the PrA protein immunoprecipitated from the *sec62* and *sec18* strains labeled at the nonpermissive temperature indicated that the signal peptide on the wild-type PrA protein is cleaved from preproPrA and that this cleavage occurs in the ER (Fig. 6).

A similar analysis was done to determine whether the signal peptide was removed from the PrA-Inv hybrid proteins. The shortest PrA-Inv fusion contains the N-terminal 23 amino acids of preproPrA. The secretion of this hybrid protein from the cell (Fig. 3) indicated the presence of a functional signal sequence. The PrA-Inv23 hybrid protein immunoprecipitated from a *sec18* strain labeled in the presence of tunicamycin at the nonpermissive temperature comigrated with normally processed *SUC2*-encoded invertase and not with unprocessed invertase (data not shown). This indicated that a signal peptide cleavage site maps within the N-terminal 23 amino acids of preproPrA, consistent with the predicted location for such a site. Molecular weight determinations on other fusion proteins indicated that the signal peptide is cleaved from each of the hybrid proteins. In both wild-type and hybrid proteins then, the PrA signal peptide apparently is cleaved at the level of the ER.

Our mapping studies of the preproPrA vacuolar sorting signal are consistent with previous observations made with vacuolar CPY (21, 55). Both preproPrA and preproCPY contain vacuolar sorting information in their propeptide sequences. No obvious sequence homology is observed, however, when comparing the propeptide of proPrA with that of proCPY. One explanation for this would be that PrA and CPY sort to the vacuole by independent mechanisms. If independent pathways are utilized, they may be reflected in different rates for maturation of proPrA and proCPY. To address this question, we carefully analyzed the processing kinetics of the intact wild-type PrA and CPY proteins. Pulse-chase labeling of yeast cells followed by immunoprecipitation with antisera directed against PrA and CPY showed a half-time of approximately 6 min for the processing of proPrA to the mature enzyme (Fig. 7). This paralleled almost exactly the observed rate for maturation of proCPY and is consistent with previously reported processing kinetics for CPY (16, 17).

In addition, we determined whether glycosyl modification of PrA was required for the sorting of this enzyme to the vacuole, a requirement not observed with CPY (48). Yeast cells were labeled with $Na_2{}^{35}SO_4$ for 10 min in the presence of tunicamycin. During a chase period, PrA was converted to a stable protein that migrated as expected for unglycosylated mature PrA, indicating arrival in the vacuole (Fig. 6). The rate of processing of PrA occurred with kinetics which were similar to those observed for CPY (Fig. 6). This indicates that targeting of PrA to the vacuole as well as processing to the mature form (29) are not dependent on carbohydrate addition. This agrees with our observation that PrA-Inv fusions containing 76 to 137 amino acids of PrA, while lacking sites for core oligosaccharide addition on the PrA portion of the protein, are competent for efficient targeting to the vacuole.

Deletions in PrA. To confirm the role of the amino-terminal portion of proPrA in directing the vacuolar localization of PrA and to define more precisely the location of the targeting signal within the propeptide region, we constructed internal deletions in the propeptide segment of the wild-type PrA protein. Initially, we deleted the coding sequence for the entire propeptide segment (amino acids 24 to 76). This deletion construct, PrAΔpro (Δ24-76), was introduced into yeast strain SEY2101-Δ*pep4*, which is deleted for the genomic copy of the *PEP4* gene. A pulse-chase analysis was utilized to follow the transit of the PrAΔpro polypeptide. We found that deletion of the entire prosequence resulted in degradation of approximately 95% of the protein during a 90-min chase period (Fig. 7). To determine whether this degradation occurs in the ER, we used the *sec18* mutant yeast strain DKY6182, deleted for the chromosomal *PEP4* locus, to analyze the stability of the PrAΔpro protein. PrAΔpro immunoprecipitated from strain DKY6182 at the nonpermissive temperature appeared to be stable during a 2-h chase. Degradation of this protein, then, may not occur in the ER, or at least not before the *sec18* block. Interestingly, the small amount of PrAΔpro which was stable (<5%) in strain SEY2101-Δ*pep4* underwent conversion to a higher-molecular-weight form that comigrated with wild-type mature PrA (Fig. 7). We believe this represents conversion of the PrAΔpro protein from a p1 to a p2 form corresponding to a Golgi-specific glycosyl modification of the deleted protein. To further analyze the transit of PrAΔpro, the protein present after 5 and 90 min of chase was first immunoprecipitated with PrA-specific antiserum, followed by a second immunoprecipitation with antiserum that specifically recognizes α-1→3-mannose linkages that are added to core oligosaccharides in the Golgi complex (2, 15). Accordingly, p2 and mature forms of CPY and PrA but not the p1 form should be recognized by this antiserum. As expected, when

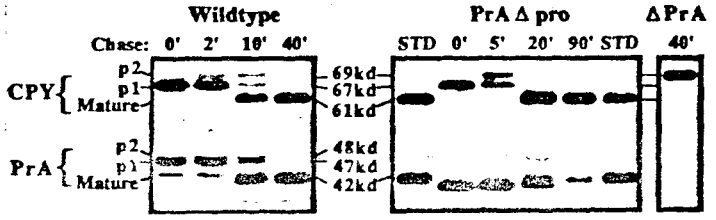

FIG. 7. Processing kinetics of wild-type PrA and PrA deleted for amino acids 24 to 76 (PrAΔpro). Strain SEY2101-Δ*pep4* containing no plasmid (ΔPrA) or containing plasmids which express wild-type PrA or PrAΔpro was labeled at 30°C for 5 min and chased for the indicated times ('. minutes). Additional time points were taken for wild-type PrA to allow a more accurate determination of the half-time for processing (data not shown). Double immunoprecipitations were performed with CPY and PrA antiserum. Lanes designated as standards (STD) are equivalent to the 40-min chase point in the wild-type control experiment and mark the position of mature CPY and PrA. The approximate molecular sizes of the different forms of CPY and PrA are indicated (kd, kilodaltons). The band seen at the 0- and 2-min time points that migrates at a position on the gel slightly above mature PrA is presumably unglycosylated preproPrA. The disappearance of this band during the chase can clearly be seen when additional time points are analyzed.

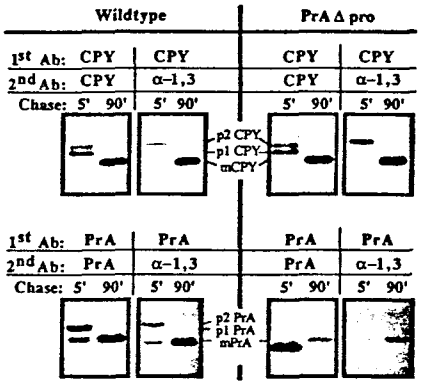

FIG. 8. Immunoprecipitation of CPY, PrA, and PrAΔpro with α-1→3-mannose-specific antiserum. Samples were prepared as described in the legend to Fig. 7. The first immunoprecipitations were done with CPY or PrA antiserum as indicated. A second immunoprecipitation was done with CPY, PrA, or α-1→3-mannose antiserum as indicated. Ab, Antibody; ', minutes.

cells were labeled for 5 min followed by a 5-min chase, all the p2 and mature PrA and CPY were immunoprecipitated with the α-1→3-mannose-specific antiserum, indicating that these forms of the proteins were modified by the Golgi-specific α-1→3-mannosyl transferase (Fig. 8). When PrAΔpro was analyzed with the α-1→3-mannose-specific antiserum, the large amount of protein which was present after 5 min of chase was not immunoprecipitated. In contrast, the small amount of PrAΔpro which was stable after a 90-min chase was precipitated under the same conditions. At least some fraction of this deleted protein appeared to undergo glycosyl processing in the Golgi complex. However, this processing was much slower than that seen for the wild-type preproPrA protein; it took approximately 10 times longer to process PrAΔpro compared with wild-type preproPrA. The instability of the PrAΔpro mutant protein has thus far prevented us from directly determining the cellular location of this protein by cell fractionation. Indirect evidence suggests, however, that at least some fraction of the p2 form of PrAΔpro is delivered to the vacuole. Maturation of proCPY is dependent on an active *PEP4* gene product (27, 60). Strain SEY2101-Δ*pep4*, which is deleted for the chromosomal *PEP4* locus, accumulated CPY as the p2 form in the vacuole, indicating the requirement for a functional PrA enzyme in the maturation of this protein (Fig. 7). When this strain, which lacks wild-type PrA, expressed the PrAΔpro protein, proCPY was processed to the mature enzyme with normal kinetics (Fig. 7). Importantly, analysis of CPY processing in a *sec18* mutant strain suggests that the maturation of CPY, which is dependent on PrA or PrAΔpro, cannot occur in the ER (data not shown). This may be due to a requirement for the lower pH of the vacuole or for additional vacuolar components for PrA activity (31, 61). This observation, along with the kinetics of CPY processing, suggests that at least some of the small amount of stable PrAΔpro is targeted to the vacuole.

The instability of the PrAΔpro protein may result from the extensive nature of the Δ24-76 deletion. To avoid this potential problem, we constructed two smaller deletions in the PrA propeptide; one removed the coding sequence for amino acids 23 to 39 and the second deleted amino acids 61 to 76 of preproPrA. Based on the results from the fusion proteins, the Δ23-39 mutation was expected to remove information that was not part of the preproPrA vacuolar sorting signal, while the Δ61-76 mutation was expected to inactivate the vacuolar targeting signal. Surprisingly, we found that each of these deletion constructs directed the synthesis of unstable polypeptides, as was observed with the PrAΔpro mutant. Less than 10% of these mutated proteins were present after a 5-min labeling and 60-min chase, similar to the result for PrAΔpro. In both cases, however, the small amount of immunoprecipitable protein which was stable appeared to migrate on an SDS gel at the position of mature PrA, suggesting that the remaining propeptide was removed (data not shown). In addition, CPY was processed with normal kinetics.

The instability of each of the mutant preproPrA proteins indicated that the wild-type propeptide may influence the folding and final structure of PrA. Deletions in the propeptide may prevent the mutated proteins from attaining the native protease-resistant conformation. This aberrant folding also appears to interfere with transit of proPrA from the

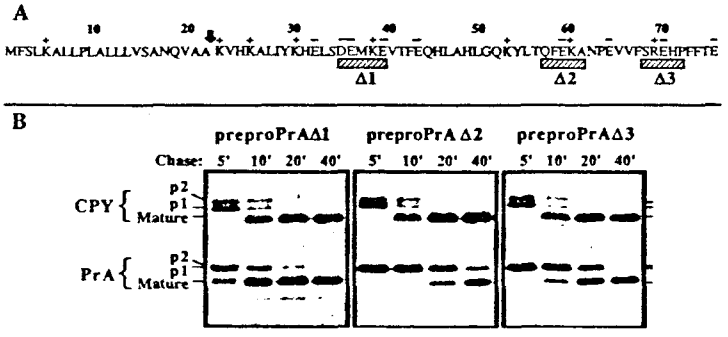

FIG. 9. Deletions in the propeptide affect the kinetics of PrA delivery to the vacuole. (A) Amino acid sequence of the PrA prepropeptide. The arrow above the sequence indicates the predicted site for signal peptide cleavage. The regions which have been deleted individually in the constructs preproPrAΔ1, -Δ2, and -Δ3 are as indicated. (B) Strain SEY2101-Δ*pep4* expressing the indicated preproPrA constructs was labeled at 30°C for 5 min with $Na_2{}^{35}SO_4$. Chase was initiated by the addition of $MgSO_4$ (50 mM final concentration), and samples were TCA precipitated at the indicated time points. Double immunoprecipitations were done with CPY and PrA antiserum. The positions of the different processed forms of the proteins are indicated. ', minutes.

ER to the Golgi complex. This early sorting-transit defect prevented us from analyzing the subsequent vacuolar sorting decision in the Golgi complex. In a final attempt to overcome the instability problem, we constructed a set of three deletions that removed the coding information for only five amino acids each (Fig. 9). These proteins were designated preproPrAΔ1 (deleted for amino acids 36 to 40), -Δ2 (amino acids 57 to 61 deleted) and -Δ3 (amino acids 68 to 72 deleted). Proteins with these deletions did not show the instability seen with larger deletions (Fig. 9). The processing kinetics of these proteins were analyzed by pulse-labeling cells harboring these constructs and immunoprecipitating at various points during a chase period (Fig. 9). PreproPrAΔ1 showed maturation kinetics which were indistinguishable from those of the wild-type protein (Fig. 9). Based on our results with the *PEP4-SUC2* fusions, this deletion was predicted to be located outside the region containing vacuolar sorting information. Both preproPrAΔ2 and -Δ3 showed significant kinetic delays in processing of PrA from the p1 to the p2 form, although both constructs were delivered to the vacuole as evidenced by the processing of the p2 form to the mature enzyme (Fig. 9). These two proteins had alterations in the propeptide which were more distal to the NH_2 terminus than preproPrAΔ1 and showed a two- to fourfold delay in conversion of preproPrA to the mature enzyme. PrA was not detected in the periplasm or medium for any of the deleted preproPrA constructs.

Glycosylation of hybrid proteins. All vacuolar proteins that were characterized are mannoproteins and undergo only limited glycosyl processing before delivery to the vacuole. As predicted from the preproPrA protein sequence, Asn-linked core oligosaccharides are added in the ER at two sites, corresponding to preproPrA residues Asn-144 and Asn-345. During transit through the ER and Golgi complex, the core groups are trimmed and then extended, resulting in a final glycosidic side chain containing 10 to 18 mannose residues (53, 54). This is contrasted with the secreted enzymes invertase or acid phosphatase which undergo extensive glycosyl processing in the Golgi complex; as many as 50 to 100 mannose residues are added to most of the 9 to 12 core oligosaccharides present on invertase, resulting in a hyperglycosylated protein with extensive outer chain carbohydrate (2, 54). This heterogeneous mixture of hyperglycosylated invertase molecules migrates as a high-molecular-weight smear on SDS-polyacrylamide gels owing to the variable length of the outer mannose chains that are added to the core oligosaccharides. In contrast, the limited extension of oligosaccharide side chains on vacuolar proteins like PrA and CPY resulted in a distinctly different SDS-gel pattern. These proteins migrated as discrete species on polyacrylamide gels (Fig. 7). The factors which control the extent of carbohydrate modification are not known. It is possible that a *cis*-acting regulatory determinant present in vacuolar proteins limits outer chain addition (21). Alternatively, vacuolar and secretory proteins may traverse separate and distinct compartments in the Golgi complex such that vacuolar proteins are not accessible to those enzymes which are responsible for outer chain elongation. To address this question, we examined the carbohydrate modification of the *PEP4-SUC2* hybrid proteins (Fig. 10). The PrA-Inv hybrid proteins contained all the oligosaccharide addition sites present in wild-type invertase. With the exception of PrA-Inv404, they did not contain either of the PrA oligosaccharide addition sites. Immunoprecipitation of the hybrid proteins in the presence of tunicamycin showed the apparent molecular weight of the proteins without carbohydrates (Fig. 2). In a *sec18* mutant strain at the nonpermissive temperature, the hybrid proteins accumulated as core oligosaccharide-modified forms in the ER (Fig. 10). The apparent molecular weight corresponded to the molecular weight of the polypeptide plus the addition of core oligosaccharides at most of the predicted tripeptide (Asn-X-Ser/Thr) addition sites. When the hybrid proteins were immunoprecipitated from wild-type yeasts, all but one showed the migration pattern normally seen with wild-type invertase (Fig. 10). The PrA-Inv404 hybrid protein migrated as a narrow smear even after a 2-h chase. While there was some smearing in the migration pattern of the PrA-Inv404 hybrid protein, the apparent molecular weight was smaller than that of the shorter fusion proteins. This suggests that the PrA-Inv404 protein is not elongated with outer chain mannose to the same extent as the other hybrid proteins. Since there is some heterogeneity in the length of the carbohydrate chains on proteins such as CPY which have few glycosylation sites and undergo relatively limited mannose addition (54), this could account for the smearing seen with PrA-Inv404; even small differences in the number of mannoses added to each core oligosaccharide could give rise to a fairly heterogeneous population of glycoslyated proteins owing to the large number of glycosylation sites which are present on the invertase portion of the hybrid protein. All the PrA-Inv hybrid proteins with the exception of PrA-Inv404 were apparently hyperglycosylated independent of their final subcellular destination. Since they undergo outer chain carbohydrate elongation, they must enter the Golgi compartments containing the mannosyl transferases responsible for this type of modification. The sorting of PrA from other secretory proteins then apparently occurs after this point in the Golgi complex.

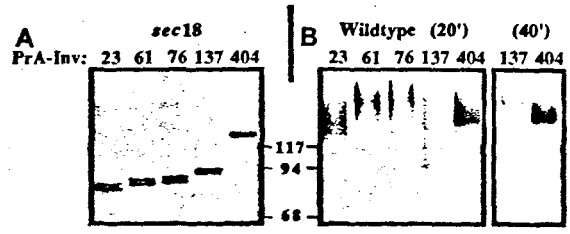

FIG. 10. Glycosyl modifications of PrA-Inv hybrid proteins. Immunoprecipitations of PrA-Inv hybrid proteins in a *sec18* mutant (SEY5187) and a wild-type strain were done as described in Materials and Methods. *sec18* cells expressing the indicated hybrid proteins were grown to the mid-log phase at 23°C and shifted to 37°C for 15 min. Cells were labeled for 15 min, and the entire cultures were then precipitated with TCA (A). Wild-type cells expressing the indicated hybrid proteins were grown at 30°C and labeled for 10 min before initiation of the chase. Samples were removed and TCA precipitated after 20 and 40 min of chase (B). Double immunoprecipitations with invertase antiserum were performed as described in Materials and Methods. The positions of protein standards (molecular sizes in kilodaltons) are indicated, and the number of amino acids of preproPrA fused to invertase for each of the hybrid proteins is shown above each lane.

DISCUSSION

Recent studies of CPY have provided important information on certain aspects of protein targeting to the vacuole (21, 55). PreproCPY contains vacuolar sorting information at the NH_2 terminus of the propeptide. Several questions about the sorting signal are immediately evident. Is it a general rule that the targeting information of vacuolar proteins is in the

propeptide region of the protein? Do the vacuolar sorting signals exhibit common structural features? To begin to address these questions, we extended the *SUC2* gene fusion approach to the study of another vacuolar enzyme, PrA. This study indicated that the NH_2-terminal 76 amino acids of preproPrA, comprising the signal peptide and propeptide region, contain information which is sufficient to direct the normally secreted enzyme invertase to the vacuole. The invertase activity derived from PrA-Inv hybrid proteins containing 76 or more amino acids of preproPrA fused to intact invertase was associated primarily with a purified vacuole fraction (Fig. 4). The presence of the hybrid proteins in the vacuole was confirmed by immunofluorescent staining of a yeast strain harboring the PrA-Inv404 hybrid protein (Fig. 5). Shorter PrA-Inv hybrid proteins, PrA-Inv23, PrA-Inv39, and PrA-Inv61, were secreted from the cell (Fig. 3). Taken together, the vacuolar delivery of PrA-Inv76 and the secretion of PrA-Inv61 suggest that the information directing vacuolar sorting of proPrA is located between amino acid residues 61 and 76. We cannot rule out the possibility, however, that targeting information precedes amino acid 61 but is not presented in the proper structural context to allow efficient recognition and subsequent vacuolar delivery of the PrA-Inv61 fusion protein.

The N terminus of preproPrA is predicted to have a signal sequence that is cleaved between amino acids 22 and 23 and is responsible for directing the protein to the ER and for initiating translocation into the ER lumen. The PrA-Inv23 hybrid protein was glycosylated and secreted from the cell (Fig. 3 and 10). This indicates the presence of a functional signal sequence within the N-terminal 23 amino acids of preproPrA. Analysis of preproPrA and the PrA-Inv23 hybrid protein in wild type and in *sec18* and *sec62* mutant yeasts indicated that the signal peptide is cleaved from preproPrA at the level of the ER (Fig. 6). This is similar to the result seen with CPY (4, 21). The signal peptide, then, does not appear to play a role in vacuolar targeting beyond directing the initial translocation into the ER. Vacuolar sorting information present in the PrA propeptide presumably resides within amino acids 23 to 76.

We attempted to identify common features between the vacuolar sorting information contained in proPrA and proCPY. Both proteins contain vacuolar sorting information in the propeptide region. This information is sufficient to direct the delivery of the normally secreted enzyme invertase to the vacuole. The vacuolar sorting signal in PrA appears, however, to map more distal to the N terminus than was observed for preproCPY (21). The difference in location of the vacuolar sorting information between preproPrA and preproCPY is underlined by the observation that the preproPrAΔ1 construct was sorted to the vacuole as efficiently as the wild-type protein. A corresponding deletion in preproCPY would presumably result in a significant level of missorting (21, 55). Several pieces of data indicate that PrA and CPY share similar pathways for vacuolar delivery. The proPrA and proCPY proteins exhibit similar processing and transport kinetics. The half-time for processing to the mature forms of both enzymes is approximately 6 min (Fig. 7). Since cleavage of the propeptide is an indication of vacuolar delivery, both PrA and CPY appear to transit through the secretory pathway at similar rates. In addition, targeting of PrA to the vacuole does not require the addition of carbohydrates. The protein synthesized in the presence of tunicamycin is processed to the mature enzyme (Fig. 6). This is identical to the results found for CPY and alkaline phosphatase (7, 38, 48, 51) (Fig. 6). Finally, an analysis of protein sorting in yeast *vpt* and *vpl* mutants which missort and secrete certain vacuolar proteins indicates that both PrA and CPY utilize a common protein-sorting apparatus (45; unpublished data). We compared the amino acid sequences of preproPrA and preproCPY but were unable to identify any significant sequence homology in their vacuolar sorting signals. Since secondary or tertiary structural information may play a critical role in the sorting process, it may be difficult to define common features of the sorting signal based on an analysis of only two proteins. Significant sequence homology, for example, is also lacking among signal peptides that direct protein translocation into the ER as well as among signals that direct protein importation into mitochondria. Another possibility is that PrA and CPY contain distinct vacuolar targeting information even though they share a common delivery pathway. We have begun to analyze the location of the targeting signals in the vacuolar enzymes alkaline phosphatase and PrB (23, 34) to compare a larger set of vacuolar sorting signals. This may allow us to detect conformational similarities as well as potential sequence biases in the overall amino acid composition of these vacuolar protein sorting signals. At present, we have not detected any obvious primary sequence homologies among this set of vacuolar proteins. Continued analysis of these and other vacuolar enzymes coupled with a more detailed analysis of the targeting signals in both PrA and CPY should provide further insight into the nature of the vacuolar sorting information.

We attempted to analyze further the role of the propeptide region by deleting part or all of this segment from the wild-type PrA protein. Deletions of 15 or more amino acids in the propeptide region led to a dramatic instability in PrA (Fig. 7). Crystallographic studies of pepsinogen and its proteolytic product pepsin, an aspartyl protease that has homology to PrA, indicate that significant conformational changes occur upon activation of the zymogen (20). One major role of the PrA propeptide may be to participate in the folding of the nascent proPrA polypeptide or to stabilize the conformation of the zymogen through interactions between the propeptide and mature portions of the enzyme. Deletion of the PrA propeptide, Δ24-76, appears to destabilize mature PrA such that most of the protein is degraded. A small fraction of the PrAΔpro polypeptides, however, must properly fold into the active enzyme since proCPY is still matured in a PrA-dependent process (Fig. 7). We also analyzed processing of PrB, another *PEP4*-dependent maturation event. We found that PrB also is processed to its mature form by the PrAΔpro protein (unpublished observations). A relatively small amount of PrAΔpro appears to be sufficient to allow efficient processing of at least these two vacuolar proteins. Since the signal peptide is apparently removed from PrAΔpro in the ER (Fig. 7), any of the PrAΔpro protein which was delivered to the vacuole would essentially be mature PrA. This protein is presumably stable in the vacuole. The small amount that is not degraded goes on to be processed in the Golgi complex by an α-1→3-mannosyl transferase (Fig. 8) and finally is delivered to the vacuole. The propeptide therefore appears to play a role in maintaining PrA in a conformation that is competent for transit out of the ER.

While some fraction of PrAΔpro is apparently delivered to the vacuole, it is not clear how this result should be interpreted with regard to vacuolar protein sorting. The small amount of PrAΔpro which could be vacuolar (the amount which is stable), as well as the kinetics of transit, indicate that targeting of this mutant protein is a very

inefficient process and may occur by an alternative sorting mechanism. This could be the result of deleting the vacuolar sorting signal which is present in the propeptide or it could be due to gross misfolding of the protein. At present, we cannot rule out the possibility that a second sorting signal is present in mature PrA. If such a signal exists, its physiological role relative to the propeptide vacuolar targeting signal is not clear. Redundancy in targeting signals, however, does appear to be a common feature of proteins destined for several other intracellular organelle targets (3a, 13, 42).

Interestingly, none of the deletions in the propeptide appeared to affect propeptide processing (Fig. 9). Indeed, a deletion of amino acids 61 to 76 of preproPrA caused most of the protein to be unstable, but the small fraction of stable molecules underwent proteolytic processing to a form of the enzyme that was indistinguishable on SDS gels from the wild-type mature enzyme (data not shown). This suggests that information on the amino-terminal side of the propeptide cleavage site is not required for removal of the propeptide. Cleavage of the propeptide, then, may not be determined by recognition of a specific cleavage site but rather by the tertiary structure of the mature portion of the enzyme. The facts that CPY can be activated by trypsin (17), that it may be a substrate for cleavage by both PrA and PrB (31), that PrA can activate CPY and PrB as well as undergo autocatalysis (19, 30, 61, 62), and that there is no sequence homology among propeptide processing sites suggest that accessibility of the propeptide is the important factor in determining the cleavage site. At present, it is not known whether removal of the propeptide occurs by a single specific endoproteolytic event or by a more nonspecific proteolysis of an exposed propeptide segment. Recent evidence, however, suggests that removal of the CPY propeptide involves at least two cleavage events (31).

We showed that targeting of wild-type PrA to the vacuole does not require the addition of carbohydrates. Similarly, the PrA-Inv76, -90, and -137 hybrid proteins were efficiently delivered to the vacuole even though they lack both of the PrA Asn-linked oligosaccharide addition sites (Fig. 1 and 4). The function of carbohydrates on vacuolar proteins is not known. The carbohydrate side chains on vacuolar proteins undergo limited mannosyl modification, but the factors controlling the extent of mannose addition are not understood. The final cellular destination does not seem to influence the extent of glycosylation, and hyperglycosylated hybrid proteins are not excluded from entering the vacuole (21) (Fig. 4 and 9). All the PrA-Inv hybrid proteins except PrA-Inv404 appeared to undergo extensive glycosyl modification (Fig. 10). PrA-Inv137 showed a kinetic delay in glycosyl modification; however, it did become hyperglycosylated like wild-type invertase. Therefore, in addition to providing information on vacuolar protein sorting signals, further analysis of other hybrid proteins also should prove useful in defining the factors involved in the regulation of glycosyl modification on vacuolar enzymes.

ACKNOWLEDGMENTS

We thank John DeModena for technical assistance, Michael W. Clark for advice on immunofluorescence techniques, and David Bedwell for critically reading the manuscript and helpful advice.

This study was supported by Public Health Service grant GM 32703 from the National Institutes of Health to S.D.E. D.J.K. was supported by a research fellowship from the Helen Hay Whitney Foundation, and L.M.B. was supported by a graduate fellowship from the National Science Foundation.

LITERATURE CITED

1. **Ammerer, G., C. P. Hunter, J. H. Rothman, G. C. Saari, L. A. Valls, and T. H. Stevens.** 1986. *PEP4* gene of *Saccharomyces cerevisiae* encodes proteinase A, a vacuolar enzyme required for processing of vacuolar precursors. Mol. Cell. Biol. **6**:2490–2499.
2. **Ballou, C.** 1982. Yeast cell wall and cell surface, p. 335–360. *In* J. Strathern, F. Jones, and T. Broach (ed.), The molecular biology of the yeast *Saccharomyces*: metabolism and gene expression. Cold Spring Harbor Laboratory, Cold Spring Harbor, N.Y.
3. **Bankaitis, V. A., L. M. Johnson, and S. D. Emr.** 1986. Isolation of yeast mutants defective in protein targeting to the vacuole. Proc. Natl. Acad. Sci. USA **83**:9075–9079.

3a. **Bedwell, D. M., D. J. Klionsky, and S. D. Emr.** 1987. The yeast F_1-ATPase β subunit precursor contains functionally redundant mitochondrial protein import information. Mol. Cell. Biol. **7**:4038–4047.

4. **Blachly-Dyson, E., and T. H. Stevens.** 1987. Yeast carboxypeptidase Y can be translocated and glycosylated without its amino-terminal signal sequence. J. Cell. Biol. **104**:1183–1191.
5. **Burger, M., E. Bacon, and J. Bacon.** 1961. Some observations on the form and location of invertase in the yeast cell. Biochem. J. **78**:504–511.
6. **Casadaban, M. J., and S. N. Cohen.** 1980. Analysis of gene control signals by DNA fusion and cloning in *Escherichia coli*. J. Mol. Biol. **138**:179–207.
7. **Clark, D. W., J. S. Tkacz, and J. O. Lampen.** 1982. Asparagine-linked carbohydrate does not determine the cellular location of yeast vacuolar nonspecific alkaline phosphatase. J. Bacteriol. **152**:865–873.
8. **Clark, M. W., and J. Abelson.** 1987. The subnuclear localization of tRNA ligase in yeast. J. Cell Biol. **105**:1515–1526.
9. **Deshaies, R. J., and R. Schekman.** 1987. A yeast mutant defective at an early stage in import of secretory protein precursors into the endoplasmic reticulum. J. Cell Biol. **105**: 633–645.
10. **Emr, S. D., R. Schekman, M. C. Flessel, and J. Thorner.** 1983. An MFα1-SUC2 (α-factor-invertase) gene fusion for study of protein localization and gene expression in yeast. Proc. Natl. Acad. Sci. USA **80**:7080–7084.
11. **Goldstein, A., and J. O. Lampen.** 1975. β-D-Fructofuranoside fructohydrolase from yeast. Methods Enzymol. **42**:504–511.
12. **Griffiths, F., and K. Simons.** 1986. The *trans* Golgi network: sorting at the exit site of the Golgi complex. Science **234**:438–443.
13. **Hall, M. N., and A. D. Johnson.** 1987. Homeo domain of the yeast repressor α2 is a sequence-specific DNA-binding domain but is not sufficient for repression. Science **237**:1007–1012.
14. **Halvorson, H. O., and L. Ellias.** 1958. The purification and properties of an α-glucosidase of *Saccharomyces italicus* Y1225. Biochim. Biophys. Acta **30**:28–40.
15. **Haselbeck, A., and R. Schekman.** 1986. Interorganelle transfer and glycosylation of yeast invertase *in vitro*. Proc. Natl. Acad. Sci. USA **83**:2017–2021.
16. **Hasilik, A., and W. Tanner.** 1976. Biosynthesis of carboxypeptidase Y in yeast. Evidence for a precursor form of the glycoprotein. Biochem. Biophys. Res. Commun. **72**:1430–1436.
17. **Hasilik, A., and W. Tanner.** 1978. Biosynthesis of the vacuolar yeast glycoprotein carboxypeptidase Y. Conversion of precursor into the enzyme. Eur. J. Biochem. **85**:599–608.
18. **Hasilik, A., and W. Tanner.** 1978. Carbohydrate moiety of carboxypeptidase Y and perturbation of its synthesis. Eur. J. Biochem. **91**:567–575.
19. **Hemmings, B. A., G. S. Zubenko, A. Hasilik, and E. W. Jones.** 1981. Mutant defective in processing of an enzyme located in the lysosome-like vacuole of *Saccharomyces cerevisiae*. Proc. Natl. Acad. Sci. USA **78**:435–439.
20. **James, M. N. G., and A. R. Sielecki.** 1986. Molecular structure of an aspartic proteinase zymogen, porcine pepsinogen, at 1.8 Å resolution. Nature (London) **319**:33–38.
21. **Johnson, L. M., V. A. Bankaitis, and S. D. Emr.** 1987. Distinct sequence determinants direct intracellular sorting and modifica-

tion of a yeast vacuolar protease. Cell **48**:875–885.
22. **Kaiser, C. A., and D. Botstein.** 1986. Secretion-defective mutations in the signal sequence for *Saccharomyces cerevisiae* invertase. Mol. Cell. Biol. **6**:2382–2391.
23. **Kaneko, Y., Y. Tamai, A. Toh-e, and Y. Oshima.** 1985. Transcriptional and posttranscriptional control of *PHO8* expression by *PHO* regulatory genes in *Saccharomyces cerevisiae*. Mol. Cell. Biol. **5**:248–252.
24. **Kelly, R. B.** 1985. Pathways of protein secretion in euckaryotes. Science **230**:25–32.
25. **Kubota, S., Y. Yoshida, H. Kumaoka, and A. Furumichi.** 1977. Studies on the microsomal electron-transport system of anaerobically grown yeast. J. Biochem. **81**:197–206.
26. **Kuo, S. C., and J. O. Lampen.** 1974. Tunicamycin, inhibitor of yeast glycoprotein synthesis. Biochem. Biophys. Res. Commun. **58**:287–295.
27. **Lenney, J., P. Matile, A. Wiemken, M. Schellenberg, and J. Meyer.** 1974. Activities and cellular localization of yeast proteinases and their inhibitors. Biochem. Biophys. Res. Commun. **60**:1378–1383.
28. **Mage, M. G.** 1980. Preparation of Fab fragments from IgG's of different animal species. Methods Enzymol. **70**:142–150.
29. **Mechler, B., M. Müller, H. Müller, F. Meussdoerffer, and D. H. Wolf.** 1982. *In vivo* biosynthesis of the vacuolar proteinases A and B in the yeast *Saccharomyces cerevisiae*. J. Biol. Chem. **257**:11203–11206.
30. **Mechler, B., M. Müller, H. Müller, and D. Wolf.** 1982. *In vivo* biosynthesis of vacuolar proteinases in proteinase mutants of *Saccharomyces cerevisiae*. Biochem. Biophys. Res. Commun. **107**:770–778.
31. **Mechler, B., H. Müller, and D. H. Wolf.** 1987. Maturation of vacuolar (lysosomal) enzymes in yeast: proteinase yscA and proteinase yscB are catalysts of the processing and activation event of carboxypeptidase yscY. EMBO J. **6**:2157–2163.
32. **Messing, J., and J. Vieira.** 1982. A new pair of M13 vectors for selecting either DNA strand of double-digest restriction fragments. Gene **19**:269–276.
33. **Miller, J.** 1972. Experiments in molecular genetics. Cold Spring Harbor Laboratory, Cold Spring Harbor, N.Y.
34. **Moehle, C. M., M. W. Aynardi, M. R. Kolodny, F. J. Park, and E. W. Jones.** 1987. Protease B of *Saccharomyces cerevisiae*: isolation and regulation of the *PRB1* structural gene. Genetics **115**:255–263.
35. **Neuman, A. J., R.-J. Lin, S.-C. Cheng, and J. Abelson.** 1985. Molecular consequences of specific intron mutations on yeast mRNA splicing *in vivo* and *in vitro*. Cell **42**:335–344.
36. **Novick, P., C. Field, and R. Schekman.** 1980. Identification of 23 complementation groups required for post-translational events in the yeast secretory pathway. Cell **21**:205–215.
37. **Novick, P., and R. Schekman.** 1979. Secretion and cell surface growth are blocked in a temperature-sensitive mutant of *Saccharomyces cerevisiae*. Proc. Natl. Acad. Sci. USA **76**:1858–1862.
38. **Onishi, H. R., J. S. Tkacz, and J. O. Lampen.** 1979. Glycoprotein nature of yeast alkaline phosphatase. J. Biol. Chem. **254**: 11943–11952.
39. **Opheim, D. J.** 1978. α-D-Mannosidase of *Saccharomyces cerevisiae* characterization and modulation of activity. Biochim. Biophys. Acta **524**:121–130.
40. **Perlman, D., P. Raney, and H. O. Halvorson.** 1986. Mutations affecting the signal sequence alter synthesis and secretion of yeast invertase. Proc. Natl. Acad. Sci. USA **83**:5033–5037.
41. **Preston, R. A., R. F. Murphy, and E. W. Jones.** 1987. Apparent endocytosis of fluorescein isothiocyanate-conjugated dextran by *Saccharomyces cerevisiae* reflects uptake of low molecular weight impurities, not dextran. J. Cell Biol. **105**:1981–1987.
42. **Richardson, W. D., B. L. Roberts, and A. E. Smith.** 1986. Nuclear location signals in polyoma virus large-T. Cell **44**:77–85.
43. **Riezman, H.** 1985. Endocytosis in yeast: several of the yeast secretory mutants are defective in endocytosis. Cell **40**:1001–1009.
44. **Rothman, J. H., C. P. Hunter, L. A. Valls, and T. H. Stevens.** 1986. Overproduction-induced mislocalization of a yeast vacuolar protein allows isolation of its structural gene. Proc. Natl. Acad. Sci. USA **83**:3248–3252.
45. **Rothman, J. H., and T. H. Stevens.** 1986. Protein sorting in yeast: mutants defective in vacuole biogenesis mislocalize vacuolar proteins into the late secretory pathway. Cell **47**:1041–1051.
46. **Rothstein, R. J.** 1983. One-step gene disruption in yeast. Methods Enzymol. **101**:202–212.
47. **Sanger, F., F. Nicklen, and A. R. Coulson.** 1977. DNA sequencing with chain-terminating inhibitors. Proc. Natl. Acad. Sci. USA **74**:5463–5467.
48. **Schwaiger, H., A. Hasilik, K. von Figura, A. Wiemken, and W. Tanner.** 1982. Carbohydrate-free carboxypeptidase Y is transferred into the lysosome-like yeast vacuole. Biochem. Biophys. Res. Commun. **104**:950–956.
49. **Sherman, F., G. R. Fink, and C. W. Lawrence.** 1979. Methods in yeast genetics: a laboratory manual. Cold Spring Harbor Laboratory, Cold Spring Harbor, N.Y.
50. **Sly, W. S., and H. D. Fischer.** 1982. The phosphomannosyl recognition system for intracellular and intercellular transport of lysosomal enzymes. J. Cell. Biochem. **18**:67–85.
51. **Stevens, T., B. Esmon, and R. Schekman.** 1982. Early stages in the yeast secretory pathway are required for transport of carboxypeptidase Y to the vacuole. Cell **30**:439–448.
52. **Stevens, T. H., J. H. Rothman, G. S. Payne, and R. Schekman.** 1986. Gene dosage-dependent secretion of yeast vacuolar carboxypeptidase Y. J. Cell Biol. **102**:1551–1557.
53. **Trimble, R. B., and F. Maley.** 1977. The use of endo-β-*N*-acetylglucosaminidase H in characterizing the structure and function of glycoproteins. Biochem. Biophys. Res. Commun. **78**:935–944.
54. **Trimble, R. B., F. Maley, and F. K. Chu.** 1983. Glycoprotein biosynthesis in yeast. Protein conformation affects processing of high mannose oligosaccharides on carboxypeptidase Y and invertase. J. Biol. Chem. **258**:2562–2567.
55. **Valls, L. A., C. P. Hunter, J. H. Rothman, and T. H. Stevens.** 1987. Protein sorting in yeast: the localization determinant of yeast vacuolar carboxypeptidase Y resides in the propeptide. Cell **48**:887–897.
56. **von Heijne, G.** 1986. A new method for predicting signal sequence cleavage sites. Nucleic Acids Res. **14**:4683–4690.
57. **Weisman, L. S., R. Bacallao, and W. Wickner.** 1987. Multiple methods of visualizing the yeast vacuole permit evaluation of its morphology and inheritance during the cell cycle. J. Cell Biol. **105**:1539–1547.
58. **Wickerham, L. J.** 1946. A critical evaluation of the nitrogen assimilation tests commonly used in the classification of yeasts. J. Bacteriol. **52**:293–301.
59. **Wieland, F. T., M. L. Gleason, T. A. Serafini, and J. E. Rothman.** 1987. The rate of bulk flow from the endoplasmic reticulum to the cell surface. Cell **50**:289–300.
60. **Wiemken, A., M. Schellenberg, and K. Urech.** 1979. Vacuoles: the sole compartments of digestive enzymes in yeast (*Saccharomyces cerevisiae*)? Arch. Microbiol. **123**:23–35.
61. **Woolford, C. A., L. B. Daniels, F. J. Park, E. W. Jones, J. N. van Arsdell, and M. A. Innis.** 1986. The *PEP4* gene encodes an aspartyl protease implicated in the posttranslational regulation of *Saccharomyces cerevisiae* vacuolar hydrolases. Mol. Cell. Biol. **6**:2500–2510.
62. **Zubenko, G. S., F. J. Park, and E. W. Jones.** 1983. Mutations in *PEP4* locus of *Saccharomyces cerevisiae* block final step in maturation of two vacuolar hydrolases. Proc. Natl. Acad. Sci. USA **80**:510–514.

Appendix B

An Open Reading Frame of Unknown Function
Shares Sequence Similarity with Yeast
Sec18p and Porcine Valosin-Containing Protein

Sequence analysis of *VPS33* (see Chapter 4) revealed an open reading frame (UORF) 5' of the *VPS33* gene. Figure 1a shows the position of this UORF, for which we have only partial (carboxy-terminal) sequence data, relative to the *VPS33* ORF. The sequence of the UORF is given in Fig. 2. A search for sequence homology using the GENEMBL data bank and the TFASTA algorithm (4) revealed that the predicted amino acid (aa) sequence shares significant similarity (46% identity over 110 aa) with the porcine valosin-containing protein (VCP) (3). Since the homology with VCP starts already with the first residue of the UORF for which we have sequence data, additional sequencing in the 5' direction might be expected to reveal continued homology with VCP. Valosin was originally identified as a putative biologically active peptide from pig intestine. A cDNA encoding an unexpectedly large valosin-containing protein was isolated and was found to lack features common to other biologically active peptide precursors. The valosin-specific mRNA occurs in almost every porcine tissue tested; on the basis of these inconsistencies, the authors concluded that valosin is likely to be a protein degradation product and does not occur *in vivo* (3).

A number of other proteins have very recently been shown to contain sequence similarity with VCP. These include the yeast Sec18p (1), its mammalian equivalent NSF (8), a putative yeast protein, Sug1p, involved in transcription (J. Swaffield, personal communication), and the apparent *Xenopus* homolog of VCP (5). Comparison of the aa sequences of these proteins with the UORF reveals a highly conserved motif of ~70 aa; this domain is present twice in VCP (Fig. 3). The significance of this homology is not clear at the present, although it could define a structural motif. Mutagenesis of this region in the *SEC18* gene, for example, might confirm the functional importance of this domain.

Gene disruption of the UORF was performed as depicted in Fig. 1b. A 500 bp region adjacent to the UORF was deleted and replaced with the *HIS3* gene, and

the resulting construction was used to transform the *his3*-Δ200 diploid SEY6210/SEY6211. Tetrad analysis of all 13 asci examined from three different His^+ diploid transformants gave rise to 2 viable and 2 dead spores; all live segregants were His^-. These results suggest that disruption of the UORF results in lethality, and that the function encoded by the UORF is essential for cell growth.

ACKNOWLEDGEMENTS

We would like to thank J.-M. Peters and J. Swaffield for communicating results prior to publication, and K. Eakle for pointing out the similarity between Sec18p and the UORF.

LITERATURE CITED

1. Eakle, K. A., M. Bernstein, and S. D. Emr. 1988. Characterization of a component of the yeast secretion machinery: Identification of the *SEC*18 gene product. Mol. Cell. Biol. 8:4098-4109.

2. Ito, H., Y. Fukada, K. Murata, and A. Kimura. 1983. Transformation of intact yeast cells treated with alkali cations. J. Bacteriol. 153:163-168.

3. Koller, K. J. and M. J. Brownstein. 1987. Use of a cDNA to identify a supposed precursor protein containing valosin. Nature 325:542-545.

4. Pearson, W. R., and D. J. Lipman. 1988. Improved tools for biological sequence analysis. Proc. Natl. Acad. Sci. USA 85:2444-2448.

5. Peters, J.-M., M. J. Walsh, and W. W. Francke. 1990. An abundant and ubiquitous homo-oligomeric ring-shaped ATPase particle related to the putative vesicle fusion proteins Sec18p and NSF. EMBO J., in press.

6. Rothstein, R. J. 1983. One step gene disruption in yeast. Meth. Enzymol. 101:202-211.

7. Wada, Y., K. Kitamoto, T. Kanbe, K. Tanaka, and Y. Anraku. 1990. *SLP*1 gene of *Saccharomyces cerevisiae* is essential for vacuolar morphogenesis and function. Mol. Cell Biol. 10:2214-2223.

8. Wilson, D. W., C. A. Wilcox, G. C. Flynn, E. Chen, W.-J. Kuang, W. J. Henzel, M. R. Block, A. Ullrich, and J. E. Rothman. 1989. A fusion protein required for vesicle-mediated transport in both mammalian cells and yeast. Nature 339:355-359.

Figure 1. (A) The relative positions of *VPS33* and the UORF are shown with a restriction map of the corresponding region of the *VPS33* complementing clone pLB33-6 (see Chapter 4). There are 241 bp between the stop codon of the UORF and the start codon of *VPS33*. (B) Disruption of the UORF using one-step gene disruption (6). The *Xba*I-*Eco*RI fragment indicated was subcloned into the nonreplicating vector pBluescript KS(-) (Stratagene). The 500 bp *Pst*I fragment was deleted and replaced with the *HIS3* gene to construct pLB33-013. This plasmid was linearized by digestion with *Eco*RI and *Xba*I and used to transform the diploid SEY6210/SEY6211 using the lithium acetate method of Ito (2).

A:

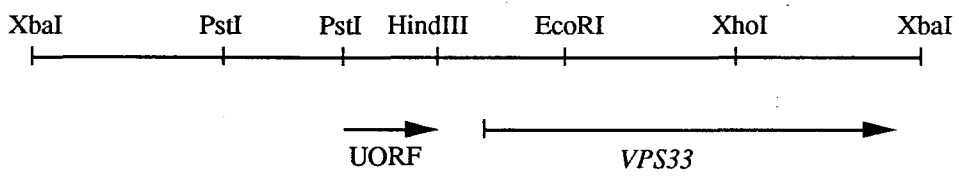
XbaI
PstI
PstI
HindIII
EcoRI
XhoI
XbaI
UORF
VPS33

B:

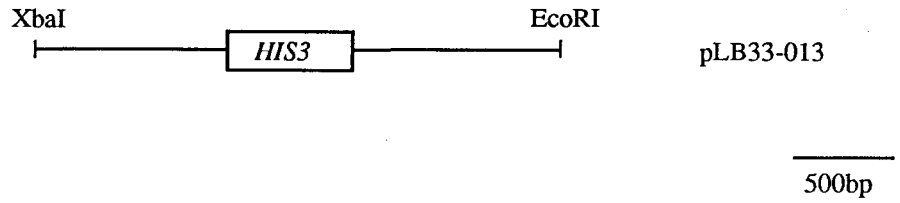
XbaI
HIS3
EcoRI
pLB33-013
500bp

Figure 2. Partial sequence of the UORF. The nucleotide sequence and the deduced aa sequence are shown. Putative transcription termination sequences are underlined. Sequence similarity with VCP (3) is confined to the amino-terminal 110 aa. The sequence shown was compiled from our sequence data and that of the *SLP*1 gene (7), which is identical to *VPS33*.

1 GCA GCT AAT CAC GTG CTC ACA TCT TTA CTC AAT GAG ATT GAT GGT GTT GAA GAG TTA AAG
Ala Ala Asn His Val Leu Thr Ser Leu Leu Asn Glu Ile Asp Gly Val Glu Glu Leu Lys

61 GGT GTA GTT ATT GTA GCG GCG ACG AAT AGA CCT GAT GAA ATA GAT GCT GCT CTT CTA AGG
Gly Val Val Ile Val Ala Ala Thr Asn Arg Pro Asp Glu Ile Asp Ala Ala Leu Leu Arg

121 CCT GGT AGG TTA GAT AGA CAC ATT TAC GTT GGC CCT CCA GAC GTA AAC GCC CGC TTG GAA
Pro Gly Arg Leu Asp Arg His Ile Tyr Val Gly Pro Pro Asp Val Asn Ala Arg Leu Glu

181 ATC TTA AAG AAG TGC ACA AAG AAA TTT AAT ACA GAA GAG TCT GGA GTC GAT CTT CAT GAA
Ile Leu Lys Lys Cys Thr Lys Lys Phe Asn Thr Glu Glu Ser Gly Val Asp Leu His Glu

241 TTG GCA GAC CGT ACA GAA GGT TAT TCC GGA GCT GAA GTT GTG CTG CTT TGT CAA GAA GCG
Leu Ala Asp Arg Thr Glu Gly Tyr Ser Gly Ala Glu Val Val Leu Leu Cys Gln Glu Ala

301 GGC TTG GCT GCC ATA ATG GAA GAT TTA GAT GTC GCA AAA GTG GAA TTA CGT CAT TTT GAG
Gly Leu Ala Ala Ile Met Glu Asp Leu Asp Val Ala Lys Val Glu Leu Arg His Phe Glu

361 AAA GCT TTT AAA GGA ATT GCT AGG GGC ATT ACT CCA GAA ATG CTC TCT TAT TAT GAA GAG
Lys Ala Phe Lys Gly Ile Ala Arg Gly Ile Thr Pro Glu Met Leu Ser Tyr Tyr Glu Glu

421 TTT GCT CTA AGA AGC GGT TCA TCT TCG TAA GCTTGTTCATAGTCAATTCTTTTCCTTTGTGTGCTC
Phe Ala Leu Arg Ser Gly Ser Ser Ser END

486 AATAATAGTAGATAGAAATTATACTGAACTCCGGTCATTTTGTATAATATATTAATCACTTCACACGAAC

Figure 3. A conserved domain is shared by the UORF, Sec18p, NSF, VCP and Sug1p. The indicated regions of VCP (3), the *Xenopus laevis* VCP homolog, X.l.p97, (5), Sec18p (1), NSF (8), the UORF and Sug1p (J. Swaffield, personal communication) are aligned. Note that VCP has two regions containing this conserved domain. A consensus sequence, consisting of any residue common to at least four of the seven proteins at a given position, is shown. Amino acids matching the consensus sequence are in bold face; in addition, there are many conservative substitutions.

```
          CONSENSUS:      D R V   N Q L L     M D G   -     K N V   I I G A T N R P D   I D
VCP       (320-354):  V E R R I V S Q L L T L M D G L K Q R A H V I V M A A T N R P N S I D
VCP       (596-630):  A A D R V I N Q I L T E M D G M S T K K N V F I I G A T N R P D I I D
X.l.p97   (154-188):  A A D R V I N Q I L T E M D G M S I K K N V F I I G A T N R P D I I D
Sec18p    (366-399):  V G D N V V N Q L L A K M D - V D Q L N N I L V I G M T N R K D L I D
NSF       (354-388):  V H D T V V N Q L L S K I D G V E Q L N N I L V I G M T N R P D L I D
UORF        (1-35):   A A N H V L T S L L N E I D G V E E L K G V V I V A A T N R P D E I D
Sug1p     (267-301):  E V Q R T M L E L L N Q L D G F E T S K N I K I I M A T N R L D I L D

          CONSENSUS:  P A L L R P G R L D     I   I   L P D E K   R L   I L + I   T + K M
VCP       (355-389):  P A L R R F G R F D R E V D I G I P D A T G R L E I L Q I H T K N M K
VCP       (631-665):  P A I L R P G R L D Q L I Y I P L P D E K S R V A I L K A N L R K S P
X.l.p97   (189-323):  P A I L R P G R L D Q L I Y I P L P D E K S R M A I L K A N L R K S P
Sec18p    (400-434):  S A L L R P G R F E V Q V E I H L P D E K G R L Q I F D I Q T K K M R
NSF       (389-423):  E A L L R P G R L E V K M E I G L P D E K G R L Q I L H I H T A R M R
UORF        (36-70):  A A L L R P G R L D R H I Y V G P P D V N A R L E I L K K C T K K F N
Sug1p     (302-335):  P A L L R P G R I D R K I E F - P P S V A A R A E I L R I H S R K M N
```